Міністерство освіти і науки України

Національний університет
«Полтавська політехніка імені Юрія Кондратюка»

Ministry of Education and Science of Ukraine

National University «Yuri Kondratyuk Poltava Polytechnic»

ЗБІРНИК НАУКОВИХ ПРАЦЬ

ГАЛУЗЕВЕ МАШИНОБУДУВАННЯ,
БУДІВНИЦТВО

Випуск 1 (56)′ 2021

ACADEMIC JOURNAL

INDUSTRIAL MACHINE BUILDING,
CIVIL ENGINEERING

Issue 1 (56)′ 2021

Полтава – 2021

Poltava – 2021











www.znp.nupp.edu.ua
http://journals.nupp.edu.ua/znp

Збірник наукових праць. Галузеве машинобудування, будівництво / Національний університет «Полтавська політехніка імені Юрія Кондратюка»

Збірник наукових праць видається з 1999 р., періодичність – двічі на рік.

Засновник і видавець – Національний університет «Полтавська політехніка імені Юрія Кондратюка».

Свідоцтво про державну реєстрацію КВ 24621-14561ПР від 14.12.2020 р.

Збірник наукових праць уключений до переліку наукових фахових видань (категорія Б), у яких можуть публікуватися результати дисертаційних робіт (Наказ МОН України №1218 від 07.11.2018 року).

Збірник наукових праць рекомендовано до опублікування вченою радою Національного університету «Полтавська політехніка імені Юрія Кондратюка» протокол №2 від 02.09.2021 р.

У збірнику представлені результати наукових і науково-технічних розробок у галузі машинобудування, автомобільного транспорту та механізації будівельних робіт; із проектування, зведення, експлуатації та реконструкції будівельних конструкцій, будівель і споруд; їх основ та фундаментів; будівельної фізики та енергоефективності будівель і споруд.

Призначений для наукових й інженерно-технічних працівників, аспірантів і магістрів.

Адреса видавця та редакції – Національний університет «Полтавська політехніка імені Юрія Кондратюка»
Науково-дослідницька частина, к. 320Ф, Першотравневий проспект, 24, м. Полтава, 36011.
тел.: (05322) 29875; e-mail: v171@pntu.edu.ua; www.pntu.edu.ua
Макет та тиражування виконано у поліграфічному центрі
Національного університету «Полтавська політехніка імені Юрія Кондратюка»,
Першотравневий проспект, 24, м. Полтава, 36011.
Свідоцтво про внесення суб'єкта видавничої справи до державного реєстру видавців,
виготівників і розповсюджувачів видавничої продукції (ДК № 3130 від 06.03.2008 р.).
Комп'ютерна верстка – В.В. Ільченко. Коректори – Я.В. Новічкова, Л.А. Клочко.
Підписано до друку 03.09.2021 р.
Папір ксерокс. Друк різограф. Формат 60x80 1/8. Ум. друк. арк. – 16,74.
Тираж 300 прим.

Academic journal. Industrial Machine Building, Civil Engineering / National University «Yuri Kondratyuk Poltava Polytechnic»

Academic journal was founded in 1999, the publication frequency of the journal is twice a year.
Founder and Publisher is National University «Yuri Kondratyuk Poltava Polytechnic».
State Registration Certificate КВ 24621-14561ПР dated 14.12.2020.
Academic journal is included into the list of specialized academic publications where graduated thesis results could be presented (Order of Department of Education and Science of Ukraine № 1218 dated 07.11.2018).
Academic journal was recommended for publication by the Academic Board of National University «Yuri Kondratyuk Poltava Polytechnic», transactions №2 of 02.09.2021.
The results of scientific and scientific-technical developments in the sphere of mechanical engineering, automobile transport and mechanization of construction works; designing, erection, operation and reconstruction of structural steels, buildings and structures; its bases and foundations; building physics and energy efficiency of buildings and structures are presented in the collection.
Academic journal is designed for researchers and technologists, postgraduates and senior students.

Address of Publisher and Editorial Board − National University «Yuri Kondratyuk Poltava Polytechnic»,
Research Centre, room 320-F, Pershotravnevyi Avenue, 24, Poltava, 36011, Ukraine.
tel.: (05322) 29875; e-mail: v171@pntu.edu.ua; www.pntu.edu.ua
Layout and printing made in the printing center of National University «Yuri Kondratyuk Poltava Polytechnic»,
Pershotravnevyi Avenue, 24, Poltava, 36011, Ukraine.
Registration certificate of publishing subject in the State Register of Publishers Manufacturers and Distributors of publishing products (ДК № 3130 from 06.03.2008).
Desktop Publishing – V. Ilchenko. Corrections − Y. Novichkova, L. Klochko.
Authorize for printing 03.09.2021.
Paper copier. Print rizograf. Format 60x80 1/8. Conventionally printed sheets – 16,74.
Circulation 300 copies.

Збірник наукових праць. Галузеве машинобудування, будівництво
Academic journal. Industrial Machine Building, Civil Engineering

http://journals.nupp.edu.ua/znp
https://doi.org/10.26906/znp.2021.56.2491

UDC 666.97.035

Theoretical determination of the law of motion of vibrating plate at surface compaction of polymer concrete

Maslov Alexandr[1], Savielov Dmitry[2*], Vakulenko Roman[3]

[1] Kremenchuk Mykhailo Ostrohradskyi National University https://orcid.org/0000-0002-8860-2035
[2] Kremenchuk Mykhailo Ostrohradskyi National University https://orcid.org/0000-0002-5170-9621
[3] Kremenchuk Mykhailo Ostrohradskyi National University https://orcid.org/0000-0002-8845-962X
*Corresponding author E-mail: dvsavelov@gmail.com

To theoretically determine the law of motion of a vibrating plate with polymer concrete, the dynamic system "vibration plate - polymer concrete" was researched. The compacted polymer concrete in it is presented as a system with distributed parameters, which takes into account the action of elastic and dissipative resistance forces from polymer concrete at its surface compaction. In accordance with the accepted rheological model of polymer concrete, a partial derivative ratio between stress and deformation is proposed for conditions of a uniaxial stress state. A vibration wave equation describing the motion of the compacted polymer concrete was created. Its solution enables the determination of the law of propagation of elastic-viscous deformation waves in polymer concrete.

Key words: vibrating plate, polymer concrete, vibrations, deformation.

Теоретичне визначення закону руху вібраційної плити при поверхневому ущільненні полімерного бетону

Маслов О.Г.[1], Савєлов Д.В.[2*], Вакуленко Р.А.[3]

[1] Кременчуцький національний університет імені Михайла Остроградського
[2] Кременчуцький національний університет імені Михайла Остроградського
[3] Кременчуцький національний університет імені Михайла Остроградського
*Адреса для листування E-mail: dvsavelov@gmail.com

Для теоретичного визначення закону руху поверхневого вібраційного робочого органу з полімерним бетоном виконано дослідження динамічної системи «вібраційна плита – полімерний бетон». У даній динамічній системі ущільнюваний полімерний бетон уявлений у вигляді системи з розподіленими параметрами, яка враховує дію пружних і дисипативних сил опору, що діють з боку полімерного бетону при його деформуванні у формі на жорсткій основі. Відповідно до прийнятої реологічної моделі полімерного бетону для умов одноосного напруженого стану запропонована залежність у приватних похідних між напруженням і деформацією полімерного бетону, характер якої залежить від динамічного модуля пружної деформації, динамічного модуля пружної деформації Максвелла та коефіцієнта динамічної в'язкості. Складено хвильове рівняння коливань, яке описує поширення пружно-в'язких хвиль деформації у полімерному бетоні, що деформується поверхневим вібраційним робочим органом, розв'язання якого дозволило визначити: закономірність поширення пружно-в'язких хвиль деформації у полімерному бетоні, що ущільнюється, а також теоретичні вирази для чисельного визначення наведених коефіцієнтів жорсткості та дисипативного опору полімерного бетону, приєднаної маси; закон руху і амплітуду коливань вібраційної плити, а також закономірності руху поверхневого шару полімерного бетону. Отримані теоретичні залежності дозволяють обґрунтовано визначити раціональні параметри вібраційного робочого органу залежно від фізико-механічних властивостей полімерного бетону, що ущільнюється, а отримані результати можуть надалі використовуватися для проведення теоретичних досліджень для аналітичного визначення закону зміни напружень, що виникають в ущільнюваному шарі полімерного бетону при вібраційному ущільненні, а також при аналізі та синтезі отриманого віброударного режиму роботи вібраційної плити.

Ключові слова: вібраційна плита, полімерний бетон, коливання, деформація.

Introduction

At surface compaction of polymer concrete by a vibration method, the vibrating plate of the working body interacts with the compacted medium. At the same time, the physical and mechanical characteristics of the compacted polymer concrete have a significant impact on the behavior of the dynamic system of vibration equipment and the choice of its main operating parameters. Determination of the physical and mechanical characteristics of the compacted polymer concrete will make it possible to establish a rational law of motion of a vibrating plate interacting with polymer concrete, to assess the operating modes of a vibrating plate, to correctly select the technological parameters of vibration action, the use of which will ensure effective compaction of polymer concrete.

Review of the research sources and publications

At present, research has been carried out on the process of vibration compaction of polymer concrete on a vibrating plate with vertically directed vibrations [1-5]. In papers [1, 2], a mathematical model of a dynamic system of a vibrating plate interacting with polymer concrete was created. As a result of the research, analytical expressions were obtained to determine the dynamic moduli of elastic deformation and the coefficient of dynamic viscosity of polymer concrete [3, 4], the law of motion of the movable frame of the vibrating plate and polymer concrete, depending on its physical and mechanical characteristics, the amplitude and frequency of forced vibrations and the height of the compacted layers. In paper [5], the design scheme of the dynamic system "vibrating working body - polymer concrete" is substantiated.

For the effective operation of vibration compaction equipment, it is necessary to accurately determine its main parameters and modes of vibration action, depending on the physical and mechanical characteristics of the compacted medium, which can be represented by various types of rheological models [6-9]. In [1-5], the physical and mechanical characteristics of polymer concrete compacted by vibration load are presented by the Zener rheological model, which, along with reversible and irreversible deformation, describes reversible highly elastic deformation, which is most clearly manifested in media containing polymers [10-12]. At the same time, for the most accurate description, polymer concrete is presented in the form of a system with distributed parameters, taking into account its elastic and viscous properties.

Definition of unsolved aspects of the problem

All these results were obtained to determine the rational parameters of vibration areas and cannot be applied to surface vibration compactors of polymer concrete.

Therefore, carrying out further theoretical research aimed at accurately determining the law of motion of vibration equipment for surface compaction of polymer concrete, determining the modes of vibration impact depending on the physical and mechanical characteristics of the compacted material and the size of the products is a very topical task.

Problem statement

The purpose of this research is to theoretically determine the law of motion of the vibrating plate of the working body during surface compaction of polymer concrete.

Basic material and results

Determining theoretically the resistance forces acting during surface compaction in the vertical direction from the polymer concrete on the vibrating plate, let us consider the design scheme of the dynamic system "vibrating plate - polymer concrete", in which polymer concrete is presented in the form of a system with distributed parameters [4] (Fig. 1).

In the operating mode, the vibration plate 3 of the working body, which is suspended on elastic shock absorbers 2 to the support frame 1, is subjected to the disturbance in the form of a vertically directed harmonic force $Q \sin \omega t$. As a result, vibrating plate 3 vibrates in the vertical plane and vibrates the polymer concrete 5 in the mold 4. With this interaction, a stress state occurs in the deformable layer of polymer concrete 5.

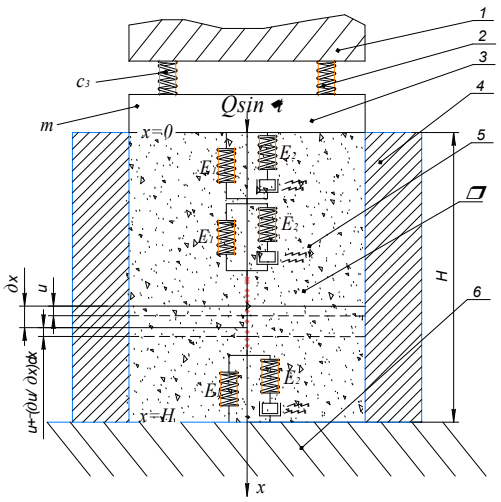

Figure 1 – Design diagram of the dynamic system "vibration plate - polymer concrete":
1 – support frame; 2 – elastic shock absorber; 3 – vibrating plate; 4 – mold; 5 – polymer concrete; 6 – base

In accordance with the proposed rheological model of polymer concrete [6], the relationship between stress and deformation in polymer concrete has the form [1]:

$$\sigma(x,t) = E_1 \frac{\partial u(x,t)}{\partial x} + \eta \cdot \left(\frac{E_1 + E_2}{E_2} \right) \frac{\partial^2 u(x,t)}{\partial x \partial t} - \left(\frac{\eta \cdot \rho}{E_2} \right) \frac{\partial^3 u(x,t)}{\partial t^3} \quad (1)$$

where $\sigma(x,t)$ – stresses arising in the compacted layer of polymer concrete;
u and x – Euler and Lagrangian coordinates;
E_1 and E_2 – dynamic modulus of elastic deformation of polymer concrete;
η – dynamic viscosity coefficient taking into account internal friction in polymer concrete;
ω – forced angular frequency; t – current time.

Functional values of dynamic modules E_1, E_2 and η based on the paper [4] can be found due to the following expressions:

$$E_1 = E_{01} \cdot \left[1 + \mu \cdot \left((\rho - \rho_0) / (\rho_k - \rho) \right)^z \right], \quad (2)$$

$$E_2 = E_{02} \cdot \left[1 + \mu \cdot \left((\rho - \rho_0) / (\rho_k - \rho) \right)^z \right], \quad (3)$$

$$\eta = H_1 \cdot \sqrt{(E_1 + E_2)\rho} \ , \quad (4)$$

where E_{01} and E_{02} – dynamic modulus of elastic deformation of uncompacted polymer concrete at an initial density ρ_0 (E_{01} =3.12 MPa, E_{02} = 4.28 MPa);
μ and z – experimental coefficients taken accordingly 3.5 and 3;
ρ – the current value of the polymer concrete density corresponding to the applied dynamic load P, kg/m^3;
ρ_0 – initial density of polymer concrete, kg/m^3;
ρ_k – density of polymer concrete mixture under load P_k = 40 MPa;
H_1 –reduced thickness of the compacted layer of polymer concrete, taken depending on the vibration direction and the ratio between the wavelength of the disturbance and the layer thickness [4].

Vibrations of polymer concrete layer in the direction of the coordinate x in time t will be of the form [1, 2]:

$$\frac{\partial \sigma(x,t)}{\partial x} = \rho \frac{\partial^2 u(x,t)}{\partial t^2} \ , \quad (5)$$

where ρ – polymer concrete density.

Substituting expression (1) into (5), we obtain the differential equation of motion of the compacted polymer concrete in the form [1]:

$$\frac{\partial^2 u(x,t)}{\partial x^2} + \eta \cdot \left(\frac{E_1 + E_2}{E_1 \cdot E_2} \right) \cdot \frac{\partial^3 u(x,t)}{\partial x^2 \partial t} - \left(\frac{\eta \cdot \rho}{E_1 \cdot E_2} \right) \cdot \frac{\partial^3 u(x,t)}{\partial t^3} = \left(\frac{\rho}{E_1} \right) \cdot \frac{\partial^2 u(x,t)}{\partial t^2} \ , \quad (6)$$

To solve the wave equation of vibrations (6), we use the following boundary conditions resulting from the design scheme in Fig. 1:
at x = 0:

$$-m \frac{\partial^2 u(0,t)}{\partial t^2} - c_3 u(0,t) + E_1 F \frac{\partial u(0,t)}{\partial x} + \left(\frac{E_1 + E_2}{E_2} \right) \times \eta F \frac{\partial^2 u(0,t)}{\partial x \partial t} - \left(\frac{\eta \rho F}{E_2} \right) \frac{\partial^3 u(0,t)}{\partial t^3} = -Q \sin(\omega t) \quad (7)$$

at $x = H$:

$$u(H,t) = 0 \ , \quad (8)$$

where m – vibrating plate mass;
c_3 – coefficient of stiffness of elastic shock absorbers in the vertical direction in the vibrating plate suspension;
F – vibrating plate bearing surface area;
Q – disturbing force amplitude;
H – height of the compacted layer of polymer concrete.

Boundary condition (7) describes the interaction of the vibrating plate with the surface of the compacted polymer concrete. Boundary condition (8) indicates that the displacement of the compacted layer of polymer concrete at a distance H from the surface of the vibrating plate is zero.

We represent the solution to equation (6) in the form of the imaginary part of the complex number [1]:

$$u(x,t) = u(x) \cdot e^{i\omega \cdot t} \ , \quad (9)$$

where $u(x)$ – complex vibration amplitude meeting the boundary conditions for the design diagram shown in Fig. 1.

Using the technique described in [1], we find a solution to equation (6) in the complex form:

$$u(x,t) = \left[B \cdot e^{-(ik+\alpha) \cdot x} + D \cdot e^{(ik+\alpha) \cdot x} \right] \cdot e^{i\omega \cdot t} \ , \quad (10)$$

where B and D – integration constants (complex amplitudes) determined by boundary conditions (7) and (8).

The functional values of coefficients α and k are determined in [1].

To determine integration constants B and D we substitute expression (10) into the boundary condition (8) and, after transforming, we find the relation between the complex amplitudes in the form:

$$B = -D \cdot \frac{e^{(ik+\alpha) \cdot H}}{e^{-(ik+\alpha) \cdot H}} \ . \quad (11)$$

Substituting the found value B from relation (11) into expression (10), we find a solution to equation (6) in the form:

$$u(x,t) = D \left[\frac{-e^{(ik+\alpha) \cdot (H-x)} + e^{-(ik+\alpha) \cdot (H-x)}}{e^{-(ik+\alpha) \cdot H}} \right] e^{i\omega \cdot t} . \quad (12)$$

Substitute expression (12) into the boundary condition (7). Based on (9) expression $Q \sin \omega t$ in boundary condition (7) can be represented as the imaginary part of a complex function, namely $Q \sin \omega t = Q\, e^{i\omega t}$. After the transformations, we get the following expression:

$$2D \cdot \left\{ sh\left[(ik+\alpha) H \right] \cdot \left(c_3 - m\omega^2 - \frac{i\omega^3 \rho F}{E^2} \right) - ch\left[(ik+\alpha) H \right] (ik+\alpha) F \left(E_1 + i\omega\eta \left(\frac{E_1 + E_2}{E_2} \right) \right) \right\} = Q \cdot e^{-(ik+\alpha) H} \quad (13)$$

Transforming expression (13), we determine the integration constant D in the following form:

$$D = \frac{Q \cdot e^{-(ik+\alpha) H}}{2sh\left[(ik+\alpha) H \right] (c_3 + c_n - (m + m_n)\omega^2 + i\omega b_n)} \quad (14)$$

where c_n – reduced coefficient of compacted polymer concrete stiffness;
m_n – the reduced mass of compacted polymer concrete;
b_n – reduced coefficient of dissipative resistance of compacted polymer concrete:

$$c_n = F\left[\left(E_1\alpha\right)sh\left(2\alpha H\right)+\left(E_1k+\eta\omega\alpha\left(\frac{E_1+E_2}{E_2}\right)\right)\sin\left(2kH\right)\right]/\left[ch\left(2\alpha H\right)-\cos\left(2kH\right)\right]; \quad (15)$$

$$m_n = Fk\eta\left(\frac{E_1+E_2}{E_2}\right)sh\left(2\alpha H\right)/\omega\cdot\left[ch\left(2\alpha H\right)-\cos\left(2kH\right)\right] \quad (16)$$

$$b_n = \frac{1}{\omega}\left(\frac{F\left[\left(E_1k+\eta\omega\alpha\left(\left(E_1+E_2\right)/E_2\right)\right)sh\left(2\alpha H\right)-\left(E_1\alpha-\omega\eta k\left(\left(E_1+E_2\right)/E_2\right)\right)\sin\left(2kH\right)\right]}{\left[ch\left(2\alpha H\right)-\cos\left(2kH\right)\right]}-\frac{F\omega^3\rho}{E_2}\right). \quad (17)$$

It follows from expressions (15) – (17) that numerical values of coefficients c_n, b_n and m_n will depend on the area of the supporting surface F of the vibrating plate; dynamic modulus of elastic deformation of polymer concrete E_1 and E_2; dynamic viscosity coefficient η; angular frequency of forced vibrations ω; the height of the compacted layer of polymer concrete H, vibration absorption coefficient α and wave number k. Substituting the value of integration constant D from (14) into expression (11), we determine integration constant B:

$$B = -\frac{Qe^{(ik+\alpha)H}}{2sh\left[(ik+\alpha)H\right]}\times \times\frac{Qe^{(ik+\alpha)H}}{\left(c_3+c_n-(m+m_n)\omega^2+i\omega b_n\right)}. \quad (18)$$

Substituting the found integration constants (14) and (18) into dependence (10), we find in the complex form the solution to the wave equation of vibrations (6), meeting the boundary conditions (7) and (8):

$$u(x,t) = \frac{Qsh\left[(ik+\alpha)(H-x)\right]e^{i\omega\cdot t}}{sh\left[(ik+\alpha)H\right]}\times \times\frac{Qsh\left[(ik+\alpha)(H-x)\right]e^{i\omega\cdot t}}{\left(c_3+c_n-(m+m_n)\omega^2+i\omega b_n\right)} \quad (19)$$

Multiply the numerator and denominator of expression (19) by a complex number $(c_3+c_n-(m+m_n)\omega^2-i\omega b_n)$, after performing the decomposition of expressions $sh[(ik+\alpha)(H-x)]$ in the numerator and $sh[(ik+\alpha)H]$ in the denominator, and, separating the imaginary part of the complex function from the obtained expression, we get a solution to the wave equation of oscillations (6) meeting the boundary conditions (7) and (8) in the following form:

$$u(x,t) = \frac{A}{\sqrt{\left(sh\alpha H\cos kH\right)^2+\left(ch\alpha H\sin kH\right)^2}}\times \times[sh\left[\alpha(H-x)\right]\cos\left[k(H-x)\right]\sin\left(\omega t-\theta\right)+ + ch\left[\alpha(H-x)\right]\sin\left[k(H-x)\right]\cos\left(\omega t-\theta\right)] \quad (20)$$

where A – amplitude of forced vibrations of the vibrating plate and the upper layer of polymer concrete:

$$A = \frac{Q}{\sqrt{\left[c_3+c_n-(m+m_n)\omega^2\right]^2+\omega^2b_n^2}}; \quad (21)$$

$$\theta = \varphi_1+\varphi_2; \quad (22)$$

$$\varphi_1 = arctg\left(\frac{\omega\cdot b_n}{c_3+c_n-(m+m_n)\omega^2}\right); \quad (23)$$

$$\varphi_2 = arctg\left(cth(\alpha H)\cdot tg(kH)\right). \quad (24)$$

Expression (20) describes the law of the polymer concrete motion compacted by a vibrating plate of the researched dynamic system "vibrating plate - polymer concrete" in the direction of the coordinate x depending on the angular frequency of forced vibrations ω, the amplitude of the disturbing force Q, the thickness of the compacted layer H and the current time value t.

At $x = 0$ expression (20) describes the law of the vibrating plate motion of the surface vibrating working body in the form:

$$u(0,t) = A\cdot\sin(\omega t-\varphi_1). \quad (25)$$

Taking into account the physical and mechanical characteristics of the compacted polymer concrete makes it possible to quite accurately determine the law of motion of the vibrating plate and select the modes of vibration action, which ensure the most effective compaction of polymer concrete. The obtained expressions (15)-(17) enable the determination of the physical and mechanical characteristics of polymer concrete in its model representation, which can be used in the research of complex dynamic systems.

Specific reduced weight m_{ny}, as well as specific reduced coefficients of resistance b_{ny} and rigidity c_{ny} of polymer concrete at vibrations of the movable frame of the vibrating platform in the vertical direction is determined by dividing m_n, b_n and c_n by the area F of the base of the molded product:

$$m_{ny} = \frac{m_n}{F}; \quad b_{ny} = \frac{b_n}{F}; \quad c_{ny} = \frac{c_n}{F}. \quad (26)$$

The theoretical provisions were tested on a laboratory vibrating working body with the following main parameters: the mass of the vibrating plate m = 75 kg; disturbing force amplitude Q =4415 N; forced angular frequency ω = 293 rad/s; stiffness of elastic shock absorbers c_3 = 470880 N/m; the amplitude of vibrations of the movable frame of the vibrating plate in idle mode A_{xx} = 0.68 mm.

This vibrating working body was used to compact polymer concrete in a mold being the size in plan 0.2×0.4 m^2, of the following structural composition [13]: crushed granite fraction 5-20 (50 % of the total volume of the mixture), river sand with a fineness module M_k = 1.8 (22-27 %); marshal with fraction 0.05 mm (10-15 %); polyester resin Filabond 2000 PA (5 %); hardener MEKP-HA-2 (0,5…1 %).

Height H of the compacted layer was taken equal to 50, 60, 80, 100, 120, and 150 mm.

Figs. 4 and 5 show the change in the coefficients of specific reduced stiffness c_{ny} and dissipative resistance b_{ny} of polymer concrete with vertical vibrations of a vibrating plate depending on the relative density ε and the height of the compacted layer H.

The obtained data analysis reveals that the specific reduced stiffness coefficients significantly depend on the compacted layer height H and relative density ε of the polymer concrete. In this case, the specific reduced coefficient of dissipative resistance b_{ny} at surface compaction significantly depends on the relative density ε of polymer concrete and to a lesser extent depends on the height of the compacted layer H.

Fig. 6 shows the change in the vibration amplitude of the vibrating plate A depending on the relative density ε and the compacted layer height H.

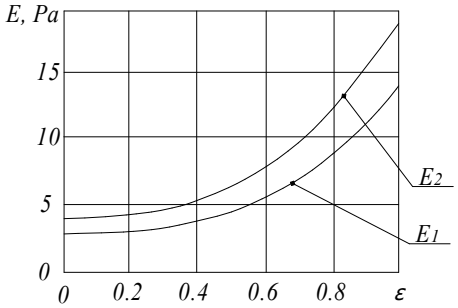

Figure 2 – Change in dynamic moduli of elastic deformation of polymer concrete E_1 and E_2 depending on the relative density ε

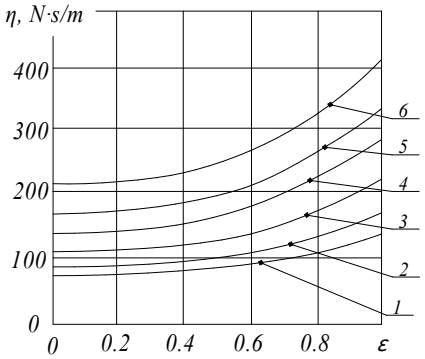

Figure 3 – Change in the coefficient of dynamic viscosity η depending on the relative density ε and the height of the compacted layer H:
1 – at H =50 mm; 2 – at H =60 mm;
3 – at H =80 mm; 4 – at H =100 mm;
5 – at H =120 mm; 6 – at H =150 mm

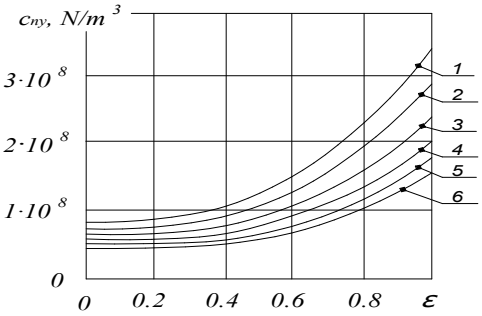

Figure 4 – Change in the specific reduced stiffness coefficient c_{ny} of polymer concrete depending on the relative density ε and the compacted layer height H:
1 – at H =50 mm; 2 – at H =60 mm;
3 – at H =80 mm; 4 – at H =100 mm;
5 – at H =120 mm; 6 – at H =150 mm

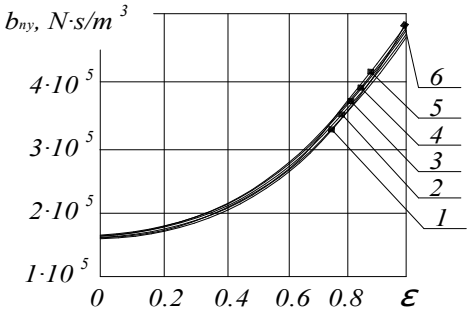

Figure 5 – Change in the specific reduced coefficient of dissipative resistance b_{ny} of polymer concrete depending on the relative density ε and of the compacted layer height H:
1 – at H =50 mm; 2 – at H =60 mm;
3 – at H =80 mm; 4 – at H =100 mm;
5 – at H =120 mm; 6 – at H =150 mm

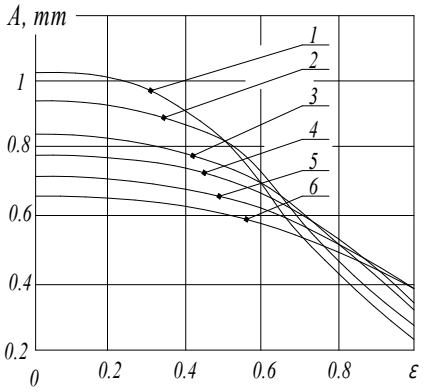

Figure 6 – Change in vibration amplitude A of a vibrating plate depending on the relative density ε and the compacted layer height H:
1 – at H =50 mm; 2 – at H =60 mm;
3 – at H =80 mm; 4 – at H =100 mm;
5 – at H =120 mm; 6 – at H =150 mm

Curves in Fig. 6 show that the physical and mechanical characteristics of polymer concrete and the compacted layer height H have a significant effect on the vibration amplitude A of the vibrating plate.

With an increase in the thickness of the compacted layer H from 50 to 150 mm and the relative density ε of polymer concrete, the vibration amplitude of the vibrating plate decreases.

At the very beginning of the vibration compaction process with the values of the layer heights H 50 and 60 mm and relative density ε from 0 to 0.5 there is a decrease in the vibration amplitude A of the vibrating plate, respectively, from 1.01 to 0.82 mm and from 0.93 to 0.82 mm. With a further increase in the relative density ε from 0.5 to 1 there is a significant decrease in the vibration amplitude A of the vibrating plate, respectively, to 0.23 and 0.27 mm.

During vibration compaction of polymer concrete of the specified composition with a layer thickness of 80, 100, 120, and 150 mm at a relative density ε from 0 to 0.5, a smoother decrease in the vibration amplitude of the vibration plate occurs. For the specified values ε the vibration amplitude changes from 0.83 to 0.76 mm at thickness H = 80 mm; from 0.77 to 0.71 mm – at H =100 mm; from 0.72 to 0.67 mm at H =120 mm and from 0.66 to 0.62 mm at H =150 mm. With a further increase in the relative density ε from 0.5 to 1 there is a significant decrease in the vibration amplitude A of the vibrating plate to 0.39 ... 0.33 mm.

The obtained results make it possible to conclude that at the very beginning of the vibration compaction process at a relative density ε from 0 to 0.5 vibrating plate works in vibration mode. When this operating mode is implemented, the vibrating plate does not detach from the surface of the compacted layer of polymer concrete.

With a further increase in the relative density ε from 0.5 to 1 the dynamic system goes into the vibration-impact operation mode, in which the vibrating plate breaks off from the surface of the compacted layer of polymer concrete and moves in the air until the next impact. In this case, it is advisable to further research the discrete vibroimpact mode of operation of the vibrating plate interacting with the compacted plate, represented by the found physical and mechanical characteristics.

Thus, based on the study of the propagation of deformation waves in compacted polymer concrete, presented in the form of a system with distributed parameters, theoretical expressions were obtained to determine the physical and mechanical characteristics of the compacted medium (polymer concrete): stiffness and dissipative resistance coefficients. These coefficients make it possible to accurately determine the main parameters of the vibrating working body for surface compaction of polymer concrete, take them into account in the expression to establish the law of motion, and determine rational modes of vibration impact on polymer concrete, depending on the type of polymer concrete and its relative density, the height of the compacted layer, the vibration frequency and the amplitude of the disturbing force.

Conclusions

A physical and mechanical model has been developed as a result of theoretical research of the dynamic system "vibrating plate - polymer concrete". Polymer concrete is presented in it as a system with distributed parameters. The model enables rather accurate determination of elastic and dissipative forces acting from polymer concrete on a vertical vibrating plate moving in the vertical plane. The law of the vibrating plate motion of the working body is established depending on the found physical and mechanical characteristics of the compacted polymer concrete, the angular frequency of forced vibrations, and the thickness of the compacted layer.

The obtained theoretical expressions make it possible to reasonably choose the rational parameters of the working body for surface vibration compaction of polymer concrete.

The found results can be used in theoretical research on the analytical determination of the law of change in stresses arising in the compacted layer of polymer concrete, as well as in the analysis and synthesis of the obtained vibro-shock operation mode of the vibrating plate.

References

1. Маслов А.Г., Савелов Д.В. (2020). Теоретическое определение закона движения подвижной рамы виброплощадки с полимерным бетоном при его уплотнении. *Вісник Кременчуцького національного університету ім. М. Остроградського*, 4/2020 (123), 84-90 https://doi.org/10.30929/1995-0519.2020.4.84-90

2. Маслов О.Г., Савєлов Д.В. (2021). Теоретичні дослідження напружено-деформованого стану ущільнюваного середовища динамічної системи «вібромайданчик – полімерний бетон». *Вісник Кременчуцького національного університету ім. М. Остроградського*, 1/2021 (126), 92-97 https://doi.org/10.30929/1995-0519.2021.1.92-97

1. Maslov A.H., Savelov D.V. (2020). Theoretical definition of the law of motion for mobile frame of a vibrating platform with polymer concrete when compacting it. *Bulletin of Kremenchuk Mykhailo Ostrohradskyi National University*, 4/2020 (123), 84-90 https://doi.org/10.30929/1995-0519.2020.4.84-90

2. Maslov A.H., Savelov D.V. (2021). Theoretical studies of the strain-deformed state of the compacted medium of the dynamic system “vibrating platform-polymer concrete”. *Bulletin of Kremenchuk Mykhailo Ostrohradskyi National University*, 1/2021 (126), 92-97 https://doi.org/10.30929/1995-0519.2021.1.92-97

3. Маслов О.Г., Савєлов Д.В., Пузир Р.Г. (2020). Дослідження взаємодії рухомої рами вібраційного майданчика з полімерним бетоном при його модельному уявленні. *Збірник наукових праць III Міжнародної конференції «Building innovations-2020»,* 127-130

4. Маслов А.Г., Савелов Д.В. (2020). Реологические характеристики полимерного бетона. *Збірник наукових праць VII Міжнародної конференції "Сучасні тенденції розвитку машинобудування та транспорту"*, 167-169

5. Савелов Д.В. (2019). Разработка теории взаимодействия поверхностного вибрационного рабочего органа с полимерным бетоном при его модельном представлении. *Вісник Кременчуцького національного університету ім. М. Остроградського*, 6/2019 (119), 126-132 https://doi.org/10.30929/1995-0519.2019.6.126-132

6. Juradin S., Baloević G., Harapin A. (2014). Impact of Vibrations on the Final Characteristics of Normal and Self-compacting Concrete. *Journal of Materials Research*, 17(1), 178-185

7. Sudarshan N. M., Chandrashekar Rao T. (2017). Vibration Impact on Fresh Concrete of Conventional and UHPFRC. *Int. Journal of Applied Engineering Research*, 12, 1683-1690

8. Koh H. B., Yeoh D., Shahidan S. (2017). Effect of revibration on the compressive strength and surface hardness of concrete. *IOP Conf. Series: Materials Science and Engineering*, 271, 012057, 1-6

9. Gutierrez J., Ruiz E., Trochu F. (2013). High-frequency vibrations on the compaction of dry fibrous reinforcements. *Journal of Advanced Composite Materials*, 22(1), 13–27

10. Маслов А.Г., Савелов Д.В. (2019). Реологическая модель вибрирующего полимерного бетона. *Вісник Кременчуцького національного університету ім. М. Остроградського*, 5/2019 (118), 135-141 https://doi.org/10.30929/1995-0519.2019.5.135-141

11. Бобрышев А.Н., Воронов П.В., Галимов Э.Р., Лахно А.В., Абдуллин И.А. (2014). Кинетические модели релаксации напряжений в композитах. *Вестник Технологического университета*, 17/2014 (14), 431-434

12. Bogomolov V., Zhdanyuk V., Tsynka P. (2016). Viscoelastic structural model of asphalt concrete. *Автомобильный транспорт*, 2016, 117-123

13. Маслов А.Г., Савелов Д.В. (2018). Разработка структурного состава полимерного бетона. *Вісник Кременчуцького національного університету ім. М. Остроградського*, 4/2018 (111), 94-99 https://doi.org/10.30929/1995-0519.2018.4.94-99

3. Maslov A.H., Savelov D.V., Puzyr R.G. (2021). Investigation of the interaction of the movable frame of a vibrating platform with polymer concrete in its model representation. *Collection of scientific papers III International conference «Building innovations-2020»*, 127-130

4. Maslov A.H., Savelov D.V. (020). Rheological characteristics of polymer concrete. *Collection of scientific papers VII International Conference "Current trends in the development of machinery and transport"*, 167-169

5. Savielov D.V. (2019). Development of interaction surface selective working body with polymer concrete during its modeling theory. *Bulletin of Kremenchuk Mykhailo Ostrohradskyi National University*, 9/2019 (119), 126-132 https://doi.org/10.30929/1995-0519.2019.6.126-132

6. Juradin S., Baloević G., Harapin A. (2014). Impact of Vibrations on the Final Characteristics of Normal and Self-compacting Concrete. *Journal of Materials Research*, 17(1), 178-185

7. Sudarshan N. M., Chandrashekar Rao T. (2017). Vibration Impact on Fresh Concrete of Conventional and UHP-FRC. *Int. Journal of Applied Engineering Research*, 12, 1683-1690

8. Koh H. B., Yeoh D., Shahidan S. (2017). Effect of revibration on the compressive strength and surface hardness of concrete. *IOP Conf. Series: Materials Science and Engineering*, 271, 012057, 1-6

9. Gutierrez J., Ruiz E., Trochu F. (2013). High-frequency vibrations on the compaction of dry fibrous reinforcements. *Journal of Advanced Composite Materials*, 22(1), 13–27

10. Maslov A.H., Savelov D.V. (2019). Rheological model of vibrating polymer concrete. *Bulletin of Kremenchuk Mykhailo Ostrohradskyi National University*, 5/2019 (118), 135-141 https://doi.org/10.30929/1995-0519.2019.5.135-141

11. Bobryshev A.N., Voronov P.V., Galimov E.R., Lakhno A.V., Abdullin I.A. (2014). Kinetic models of stress relaxation in composites. *Bulletin of Technological University,* 17/2014 (14), 431-434

12. Bogomolov V., Zhdanyuk V., Tsynka P. (2016). Viscoelastic structural model of asphalt concrete. *Автомобильный транспорт*, 2016, 117-123

13. Maslov A.H., Savelov D.V. Development of the structural composition of polymer concrete. *Bulletin of Kremenchuk Mykhailo Ostrohradskyi National University*, 4/2018 (111), 94-99 https://doi.org/10.30929/1995-0519.2018.4.94-99

Збірник наукових праць. Галузеве машинобудування, будівництво
Academic journal. Industrial Machine Building, Civil Engineering

http://journals.nupp.edu.ua/znp
https://doi.org/10.26906/znp.2021.56.2492

UDC 666.97.003.16

The influence of the lever fixturing of the vibration exciter on the overall efficiency of concrete-mix vibration

Korobko Bogdan[1]*, Korotych Yuriy[2]

[1] National University «Yuri Kondratyuk Poltava Polytechnic» https://orcid.org/0000-0002-9086-3904
[2] National University «Yuri Kondratyuk Poltava Polytechnic» https://orcid.org/0000-0002-1961-5318
*Corresponding author E-mail: korobko@pntu.edu.ua

The article presents the design of the compaction table with the option of fixing the vibration exciter on the lever, providing that there is free space under it (when fixing the compaction table on the supporting structure above the floor line). The authors have conducted research on a specially created research model, aimed at determining the dependence of the amplitude of vibration on the lever length, on which the vibration exciter is fixed, and on the load on the moving member of the compaction table. A research model of the compaction table with lever fixturing of the vibration exciter was created in order to conduct research and obtain measurement results. The results of the conducted research have shown that with increasing the length of the lever, on which the vibration exciter is fixed, the values of the shock pulses acting on the vibratory plate increase accordingly, and the increase in the load leads to the decrease in the magnitude of the shock pulses. The obtained results provide an opportunity to reduce energy consumption in production and to continue further research in this study area.

Keywords: concrete mixture, resilient support, spatial vibrations, vibration exciter, vibration amplitude, vibration compaction, vibration platform

Вплив важільного закріплення віброзбуджувача на загальну ефективність віброущільнення

Коробко Б.О.[1]*, Коротич Ю.Ю.[2]

[1] Національний університет «Полтавська політехніка імені Юрія Кондратюка»
[2] Національний університет «Полтавська політехніка імені Юрія Кондратюка»
*Адреса для листування E-mail: korobko@pntu.edu.ua

У статті розглянута конструкція вібростолу, у якого за наявності вільного простору під ним (при закріпленні вібростолу на каркасі вище площини підлоги) виникає можливість закріплення віброзбуджувача на важелі. Важіль з віброзбуджувачем закріплюється вертикально під віброплитою по центру знизу. Приводиться опис роботи вібростолу при дії на нього важільного закріплення віброзбуджувача. Надані кінематична схема вібростолу з важільним закріпленням віброзбуджувача та розрахункова схема визначення віброколивань на віброплиті. Дана конструкція вібростолу була створена у вигляді дослідної моделі. На ній за допомогою вимірювального обладнання проведені дослідження, метою яких було виявлення впливу важільного закріплення віброзбуджувача на віброущільнення, а саме існування залежності амплітуди віброколивань від довжини важеля, на якому закріплений віброзбуджувач, та від навантаження на рухому частину вібростолу Довжина важіля під час експерименту змінювалася поступово від 0 до 150 мм, а навантаження також збільшувалось поступово від 0 до 0,36 кг при постійній довжині важіля 150 мм. На базі результатів дослідів та отриманих показників побудовані графіки залежності величини ударних імпульсів від довжини важеля та від навантаження на вібростіл. Результати проведених досліджень показують, що при збільшенні довжини важіля, на якому закріплюється віброзбуджувач, відповідно збільшуються значення ударних імпульсів, що діють на віброплиту, а збільшення навантаження на віброплиту приводить до зменшення величини ударних імпульсів. Отримані результати вказують на те, що за рахунок покращення віброущільнення від зміни амплітуди є можливість заощадити енерговитрати при виробництві. Дані результати також дають перспективу для проведення подальших досліджень у напрямку покращення енергоефективності та загальної ефективності віброущільнення.

Ключові слова: амплітуда віброколивань, бетонна суміш, віброзбуджувач, вібростіл, віброущільнення, просторові коливання, пружня опора

Introduction

Concrete mix compaction is one of the most responsible operations in the manufacture of concrete and reinforced concrete products. As far as concrete-mix vibration is widely used in the construction industry, the process of its application has been considered by a number of authors [1-5]. In other words, it can be said that the manufacture of construction products without vibration compaction is not carried out at all [6,7]. Therefore, the manufacturing application of the design of the vibratory compactor, which, at limited metal intensity has the appropriate characteristics of vibration compaction, is an urgent challenge [8]. The ability of the vibratory compactor to transmit the appropriate level of vibration compaction to the concrete product without significantly complicating its design is closely related to the reduction in the time of vibration compaction. With the increase in electricity prices, reducing the operating time of the electrical part of the device leads to electricity savings. Therefore, the creation of an energy-saving vibratory compactor is the task that must be solved, first of all in order to reduce the cost of concrete products.

Review of the research sources and publications

The manufacture of concrete and concrete products is regulated by standard specifications and engineering standards [9-13]. Compaction tables for paving flags are widely used in the production of small-scale concrete products [14]. The structure consists of movable and immovable frames. The immovable frame serves as the basis of the vibration exciter. The movable frame is installed on an immovable frame through vibration-damping springs. A mechanical vibration exciter, the axis of rotation of which is located parallel to the plane surface of the frame, is rigidly mounted directly to the lower plane of the movable frame. Plastic molds, preliminarily filled with concrete, are installed on the upper plane of the movable frame. Plastic molds are made with a profile, which is provided to future products. When the vibration exciter is brought into action, the vibrational oscillations from it are transmitted directly to the plastic molds, in which concrete-mix vibration takes place. The movable frame is held due to vibration-damping springs, which transmit gravitational forces to the immovable frame.

There is also a vibration machine for the formation of small-scale concrete and reinforced concrete products [15]. In design, it coincides with the previous model [14], but the axis of rotation of the vibration exciter is located at an angle of 30 degrees to the plane of the movable frame. Such location of the axis of the vibration exciter allows changing the direction vector of vibration oscillations pertaining to the plane of reinforced concrete products, which improves the conditions of their vibration compaction. However, direction change of vibration does not allow to reduce the energy consumption of the vibration compaction process.

Definition of unsolved aspects of the problem

One of the main problems in mechanical engineering, which constantly needs to be solved or improved, is the problem of energy conservation [16].

Vibration-damping springs reduce the amplitude of vibration oscillations, especially in the area of their location. This requires increasing the power of the vibration exciter to achieve the required values of vibration oscillations [17].

Problem statement

The main task is to create conditions for increasing the amplitude of vibration vibrations without significantly complicating the design of the compaction table in order to improve the compaction of construction mixes and reduce energy consumption.

For this purpose, the authors offer the effective model of a compaction table with lever fixturing of the vibrating exciter in free space under a vibrating plate. It is necessary to conduct research on a specially created bench tester and then to estimate the efficiency of the offered installation (model) based on the obtained research results.

The purpose of this study is to identify the dependence of the amplitude of vibration on the length of the lever, on which the vibration exciter is installed.

It is assumed that with increasing the lever length, the amplitude of vibration will increase.

It is also necessary to confirm the effectiveness of the proposed design of the compaction table depending on the load level. It is planned to conduct the study of the load capacity of the structure, which would determine the dependence of the amplitude of vibration oscillations on the load on the moving part of the compaction table.

Basic material and results

The formulated problem is solved due to the lever fixturing of the vibration exciter 3 relative to the vibroplate 1 (see Fig. 1).

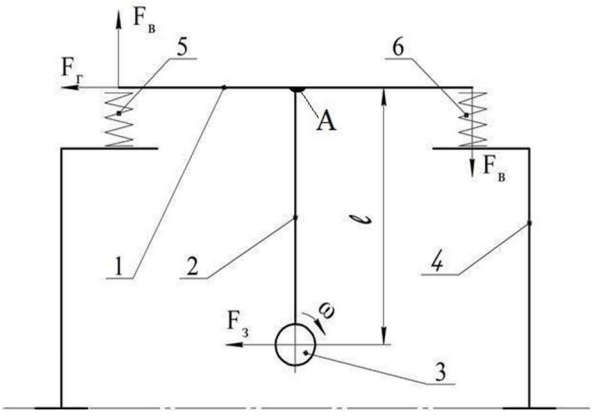

Figure 1 – Kinematic scheme of the compaction table with lever fixturing of the vibration exciter

Vibroplate 1 is fixed on the elastic supports 5 and 6. Under the bottom of the compaction table, in its middle (point A), lever 2 is rigidly fixed at the angle of 90 degrees. The lever length ℓ is determined by the height of frame 4 of the compaction table, and the increase in its length ℓ may affect the change of the amplitude of vibration. The operation of the compaction table with the lever fixturing of the vibration exciter is as follows. The vibration exciter is an electric motor with an eccentrically fixed load. When the electric motor shaft of the vibration exciter rotates, the vibrating exciting force is directed in the radial direction and changes it circlewise within 360 degrees. For example, let us consider the instantaneous horizontal direction which is shown in Fig.1. We present the compaction table with the lever as a braced structure. The vibration direction on the vibroplate 1 at the anchorage point of the fixturing of the elastic support 5 is as follows. The horizontal component Fг is transmitted from the horizontal force of the vibration exciter F3. But, in addition to the horizontal component Fг, there is a vertical component Fв, whose operation is conditioned by the lever fixturing of the vibration exciter. When considering the rotation of the vibroplatform with the lever with respect to the point "A", the horizontal force of the vibration exciter Fз tries to rotate the vibroplate with respect to the point "A" and causes the occurrence of the specified vertical force component Fв, the value of which increases with increasing the length ℓ of the lever 2. The joint action of forces Fв and Fг in general, through the single-sided support of the vibration exciter, significantly increases the value of vibration not only for the horizontal direction of the Fз force but also for all 360 degrees of direction.

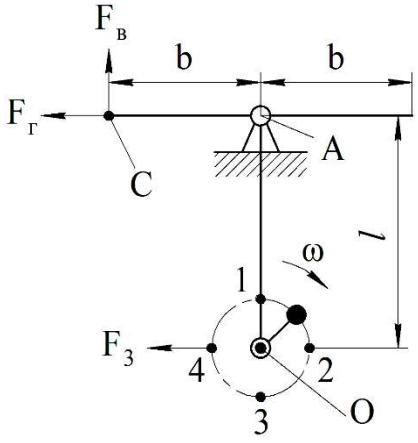

Figure 2 – Calculation scheme for determining vibration oscillations on the vibroplate

The compaction table with the lever fixturing of the vibration exciter, which contains the vibroplate (1), elastic supports (5,6), the frame of the compaction table (4), the vibration exciter (3), is characterized by the availability of the lever (2), which is rigidly fixed to the vibroplate (1). The vibration exciter (3) is fixed on the lever (2), the lever fixturing of the vibration exciter (3) causes an increase in the component values of vibration oscillations on the entire plane of the vibroplate (1).

Let us consider the relationship between the exciting force of the vibration exciter Fз (see Fig. 2) and the values of vibrations on the vibratory plate in the place of fixing the spring-controlled vibration-damping spring – the point "C".

Let's say that the vibroplate with a lever is a braced structure. The vibroplate on the perimeter is in resting contact upon flexible supports and has the possibility of free motion in any direction. Put the case that the specified braced structure conditionally rotates with respect to the point of attachment of the lever to the vibroplate (point "A"). Therefore, we have indicated the point "A" as an instantaneous fulcrum point (Fig. 2). The axis of the vibration exciter is located parallel to the plane of the vibroplate and is defined by the point "O". When it rotates with an angular velocity ω, the centrifugal exciting force Fз arises. In Figure 2, some points of the gravitational center of the unbalanced load of the vibration exciter are marked as 1-4. The instantaneous exciting force Fз is applied at these points. For example, let us consider the instantaneous position of the gravitational center of the vibration exciter at point "4". In this position, the action of the exciting force Fз causes a burst of the vertical component of the force Fв over the flexible support at the point "C". Its value can be determined by the formula through the ratio of the length of the fastening levers:

$$F_в = F_z \cdot l/b \; ; \qquad (1)$$

From the analysis of formula (1) it is apparent that with increasing lever l length, the vertical component of the force Fв increases in direct proportion. Assuming the actual size of the experimental vibration exciter, namely: l = 0; 0.025; 0.05; 0.075; 0.1; 0.125; 0.15 m (seven variable sizes); b = 0.2 m; F_z = 0.64 H, we have constructed a theoretical graph of the change in the values of shock pulses depending on the lever length of the vibration exciter (see Figure 6). In this graph, we have presented not the values of the vertical component of $F_в$ force, but the values of shock pulses in the dimension of decibels (dB) caused by the Fв force. The change of the values of the dimension of the force "H" into the dimension of the shock pulses "dB" was carried out based on table 6 [18]. We need a dependency graph in the specified dimension to further compare the theoretical values of vibration pulses with their practical measurements.

An experimental model of a compaction table with a lever fixturing of a vibration exciter was created in order to conduct research and obtain measurement results (see Fig. 3, 4).

The experimental model is a compaction table with a reduced scale of 1:10. The vibroplate is placed on the metal frame with four frame legs by means of elastic supports. Below it, in the center, we have rigidly fixed the vertical lever, to which we have connected a vibration exciter, which is an electric motor with an eccentrically fixed load. The lever length can vary within 0; 50; 100; 150mm. The vibration exciter is actuated by an electric power supply.

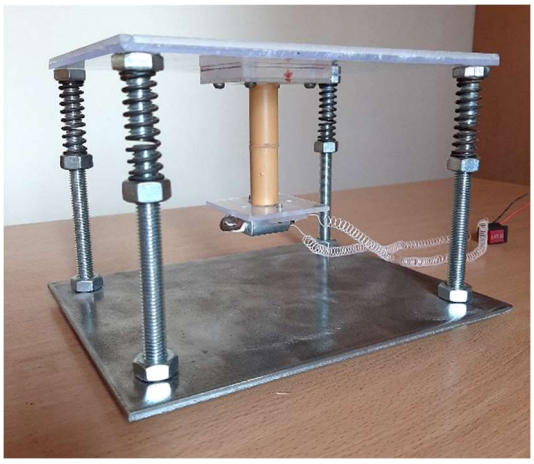

Figure 3 – An experimental model of a compaction table with a lever fixturing of a vibration exciter

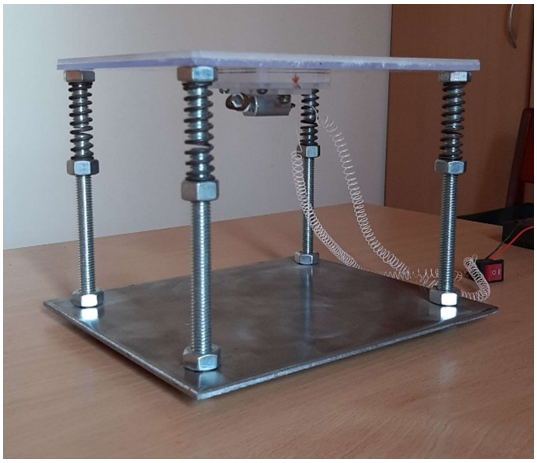

Figure 4 – An experimental model of a compaction table with leverless fixturing of the vibration exciter

The ISP-1 vibrometer (see Fig. 5) was used for measurements, with the help of which we obtained the values of shock pulses (dB) at the test points of the experimental model of the compaction table.

Figure 5 – The ISP-1 vibrometer for measuring the values of shock pulses (dB) at the test points of the experimental model of the compaction table

In the first study, the measurements were performed as follows.

The place for measurements was chosen on the upper plane of the compaction table, at the point above the vibration-damping spring. At the beginning of the study, the vibration exciter was fixed leverless (l = 0), it was actuated and the obtained indicators of shock pulses in dB were taken. Then the lever length varied in the above-mentioned ranges from 0 to 150 mm and the appropriate experimental parameters were received as well.

Based on the results of the carried experiment and the obtained indicators, we constructed a graph of the dependence of the magnitude of shock pulses on the length of the lever, on which the vibration exciter is fixed (Fig. 6).

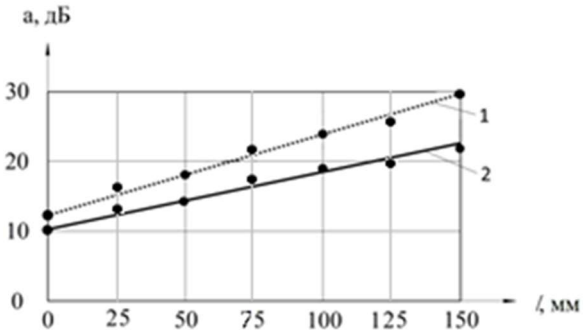

Figure 6 – Value change graph of shock pulses *a* (dB) depending on the lever length, fixturing the vibration exciter l (mm), relationships ratio:
1 - theoretical, 2 - experimental

From the analysis of the ratio, presented in Figure 6, the following conclusions can be drawn. The lever location of the vibration exciter confidently increases pulse amplitude, which is confirmed both theoretically and practically. The discrepancy between theoretical and practical results, in our opinion, is due to the fact that the theoretical curve has been obtained without reference to the weight of the vibroplate and has higher values than the experimental one. This encourages us to develop a theoretical model that would take into account the weight of the vibroplate.

In the second study, we considered the dependence of the vibration oscillations amplitude on the load on the moving part of the compaction table at the optimal lever length l = 150 mm. The load was gradually increased, changing the weight of the moving part of the compaction table. The weight of the moving part of the compaction table was increased by placing additional loading weighing 0.12; 0.24 and 0.36 kg. Values indicators of shock pulses were measured, as in the first study, on the upper plane of the compaction table at the point above the vibration-damping spring (Fig. 7).

Based on the obtained results, we constructed the graph of values' variance of shock pulses depending on the load on the moving part of the compaction table (Fig. 8).

Figure 7 – Experimental model of a compaction table with lever fixturing of the vibration exciter under load

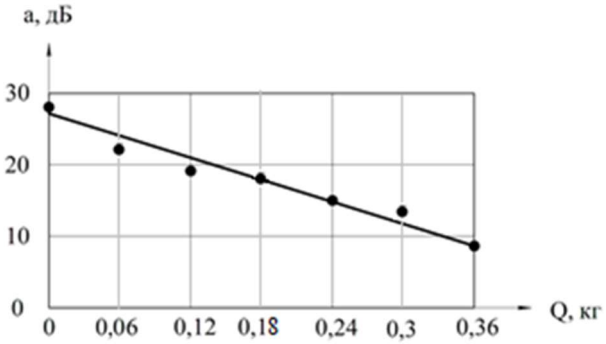

Figure 8 – Value change graph of shock pulses *a* (dB) depending on the load on the compaction table weighing Q (kg)

Conclusions

The results of the research show that with increasing the length of the lever on which the vibration exciter is attached, the values of the shock pulses acting on the vibro plate increase accordingly. That is, without changing the electric driving power, it is possible to increase the amplitude of vibration with the length of the lever for fixturing the vibration exciter.

It has been confirmed that increasing the load on the moving part of the compaction table leads to a decrease in the current amplitude of vibration oscillations. This factor must be taken into account in the production of concrete products, assigning operational and technological parameters of the proposed design of the compaction table.

Having considered the advantages of the proposed compaction table design, we found out the vibration exciter can be fixed on the lever when there is free space under it (when fixing the compaction table on the frame above the floor plane). The lever fixturing of the vibration exciter allows increasing the amplitude of vibration oscillations on the compaction table with a slight increase in steel intensity. This has got a positive effect on improving the quality of vibration compaction of concrete products with an overall reduction in energy consumption.

References

1. Juradian S., Baloevic G. & Harapin A. (2014). Impact of vibrations on the final characteristics of normal and self compacting concrete. *Mat. Res*. [online], 17(1), 178-185 https://doi.org/10.1590/S1516-14392013005000201

2. Shigeyuki D., Goryozono Y. & Hashimoto S. (2012). Study on consolidation of concrete with vibration. *Physics Procedia*, 25, 325-332 https://doi.org/10.1016/j.phpro.2012.03.091

3. Murhy W.E. (1964). A survey of Past-War British Research on the Vibration of concrete. *Technical Report*, 9, 110-117

4. Сівко В.Й., Кузьмінець М.П. (2012). Оцінка впливу робочого середовища на режими коливань вібраційних машин. *Теорія і практика будівництва*, 10, 3-5

5. Davies R.D. (1951). Some experiments on the compaction of concrete by vibration. *Magazine of Concrete Research*, 8, 14-17

6. Нестеренко М.П., Білецький В.С., Семко О.В. (2017). Оцінка конструктивно-технологічних параметрів та експлуатаційних якостей вібраційних машин для формування залізобетонних виробів. *Збірник наукових праць. Галузеве машинобудування, будівництво*, 1(43), 231-237

7. Назаренко І.І. (2007). *Вібраційні машини і процеси будівельної індустрії*. Київ: КНУБА

1. Juradian S., Baloevic G. & Harapin A. (2014). Impact of vibrations on the final characteristics of normal and self compacting concrete. *Mat. Res*. [online], 17(1), 178-185 https://doi.org/10.1590/S1516-14392013005000201

2. Shigeyuki D., Goryozono Y. & Hashimoto S. (2012). Study on consolidation of concrete with vibration. *Physics Procedia*, 25, 325-332 https://doi.org/10.1016/j.phpro.2012.03.091

3. Murhy W.E. (1964). A survey of Past-War British Research on the Vibration of concrete. *Technical Report*, 9, 110-117

4. Sivko V.Y., Kuzminets M.P. (2012). Estimation of influence of the working environment on vibration modes modes of vibrating machines. *The Theory and practice of construction*, 10, 3-5.

5. Davies R.D. (1951). Some experiments on the compaction of concrete by vibration. *Magazine of Concrete Research*, 8, 14-17

6. Nesterenko M.P., Biletsky V.S., Semko O.V. (2017). Estimation of constructive-technological parameters and operational qualities of vibrating machines for the formation of reinforced concrete products. *Collection of research papers. Industrial Machine Building, Civil Engineering*, 1 (43), 231-237

7. Nazarenko I.I. (2007). *Vibration machines and the processes of the construction industry*. Kyiv: KNUCA

8. Назаренко І.І. (2010). *Прикладні задачі теорії вібраційних систем*. – Київ: Слово
9. Jamrozy Z. (2000). *Beton i jego technologie*. Warszawa: Wydawnictvo naukove pwn
10. ДСТУ Б В.2.7-23-95. (1996). *Будівельні розчини. Загальні технічні умови*. Київ: Держбуд України

11. ДСТУ Б В.2.7-96-2000. (2010). *Суміші бетонні. Технічні умови*. Київ: Держбуд України

12. ДБН В.2.8-3-95. (1995). *Будівельна техніка, оснастка, інвентар та інструмент. Технічна експлуатація будівельних машин*. Київ: Держбуд України

13. ДСТУ Б В.2.7-114-2002. (2002). *Будівельні матеріали. Суміші бетонні. Методи випробувань*. Київ: Держбуд України
14. Вібростіл для тротуарної плитки [Електронний ресурс]. – Режим доступу: http://remoo.ru
15. Нестеренко М.П., Скляренко Т.О. (2011). Патент на корисну модель № 63973 Україна, B28B7/24. *Віброустановка для формування малогабаритних бетонних і залізобетонних виробів*
16. Нестеренко М.П. (2017). Прогресивний розвиток вібраційних установок з просторовими коливаннями для формування залізобетонних виробів. *Збірник науковихпраць. Галузеве машинобудування, будівництво*, 2(44), 16-23
17. Свідерський А.Т., Делембовський М.М. (2010). Критерії оцінки якості віброплощадок. *Техніка будівництва*, 24, 24-27
18. [Електронний ресурс]. – Режим доступу: http://docs.cntd.ru/document/1200031406

19. Nazarenko I., Ruchynskyi M. & Delembovskyi M. (2018). The basic parameters of vibration settings for sealing horizontal surfaces *International Journal of Engineering & Technology (UAE)*, 7(3.2), 255-259. http://dx.doi.org/10.14419/ijet.v7i3.2.14415

8. Nazarenko I.I. (2010). *Applied problems of the theory of vibration systems*. Kyiv: Word.
9. Jamrozy Z. (2000). *Beton i jego technologie*. – Warszawa: Wydawnictvo naukove pwn
10. DSTU B B.2.7-23-95. (1996). *Building solutions. General technical conditions*. Kyiv: State Construction Committee of Ukraine
11. DSTU B B.2.7-96-2000. (2010). *Concrete mixes. Specifications*. Kyiv: State Construction Committee of Ukraine
12. DBN B.2.8-3-95. (1995). *Construction machinery, equipment, fittings and tools. Technical operation of construction machines*. Kyiv: State Construction Committee of Ukraine
13. DSTU B B.2.7-114-2002. (2002). *Building materials. Concrete mixes. Test methods*. Kyiv: State Construction Committee of Ukraine
14. Compaction table for paving flags [Electronic resource]. - Access mode: http://remoo.ru
15. Nesterenko M.P., Sklyarenko T.O. (2011). Useful model patent № 63973 Ukraine, B28B7 / 24. *Vibration unit for the formation of small concrete and reinforced concrete products*
16. Nesterenko M.P. (2017). Progressive development of vibration installations with spatial oscillations for the formation of reinforced concrete products. *Collection of research papers. Industrial Machine Building, Civil Engineering*, 2 (44), 16-23
17. Svidersky A.T., Delembovsky M.M. (2010). Criteria for assessing the quality of vibrating platforms. *Structural Engineering,* 24, 24-27
18. [Electronic resource]. - Access mode: http://docs.cntd.ru/document/1200031406

19. Nazarenko I., Ruchynskyi M. & Delembovskyi M. (2018). The basic parameters of vibration settings for sealing horizontal surfaces *International Journal of Engineering & Technology (UAE)*, 7(3.2), 255-259. http://dx.doi.org/10.14419/ijet.v7i3.2.14415

Збірник наукових праць. Галузеве машинобудування, будівництво
Academic journal. Industrial Machine Building, Civil Engineering

http://journals.nupp.edu.ua/znp
https://doi.org/10.26906/znp.2021.56.2493

UDK 624.042.42

Development of crane load codes on the basis of experimental research

Pichugin Sergii[1*]

[1] National University «Yuri Kondratyuk Poltava Polytechnic» https://orcid.org/0000-0001-8505-2130
*Corresponding author E-mail: pichugin.sf@gmail.com

The buildings and structures reliability and safety largely depend on a proper understanding of the nature and quantitative description and rationing of loads on building structures, including crane loads. Most of the parameters of the crane load codes have a probabilistic nature and require the use of statistical methods to substantiate them. These methods are constantly changing and evolving together with the regular revision of building design codes. Analysis of domestic codes' evolution of crane load together with their statistical substantiation is an urgent task, which is this article's purpose. Since the late 1930s, leading construction research institutes and universities have conducted research on crane loads, which results have been consistently incorporated into design codes. Giving an overall assessment of Ukrainian crane loads standards, it should be emphasized that they are compiled on a modern methodological basis, close to European standards Eurocode, based on representative statistics, more differentiated, and have a scientific probabilistic nature.

Keywords: building design codes, bridge crane, overhead crane, crane load, normative load, design load

Розвиток норм кранових навантажень на основі експериментальних досліджень

Пічугін С.Ф.[1*]

[1]Національний університет «Полтавська політехніка імені Юрія Кондратюка»
*Адреса для листування E-mail: pichugin.sf@gmail.com

Забезпечення надійності та безаварійності будівель і споруд у великій мірі залежить від правильного розуміння природи і кількісного опису та нормування навантажень на будівельні конструкції, в тому числі кранових навантажень. Ці навантаження на виробничі споруди мають досить складну фізичну природу і мінливий характер, що вимагають знання конструктивних відмінностей мостових та підвісних кранів, кінематичних та динамічних процесів, що реалізуються при роботі кранів, особливостей технологічних процесів, що відбуваються у виробничих цехах, які обслуговуються підйомними кранами. Такі особливості у певній мірі відображаються в розділах норм проектування будівельних конструкцій, що містять нормативи кранового навантаження. Більшість параметрів норм кранового навантаження мають імовірнісну природу і вимагає для свого обґрунтування застосування статистичних методів. Ці методи постійно змінювалися і розвивалися разом з регулярним переглядом норм будівельного проектування. Тому аналіз еволюції вітчизняних норм кранового навантаження разом з їх статистичними обґрунтуванням є актуальною задачею. Матеріали, присвячені крановим навантаженням, опубліковані в різних науково-технічних журналах, збірниках статей, матеріалах конференцій. Стаття містить систематизований огляд норм проєктування та публікацій по проблемі кранового навантаження за 90-річний період з 30-х років XX століття до теперішнього часу. Головна увага приділяється аналізу тенденцій розвитку норм проектування конструкцій в частині змін розрахункових коефіцієнтів, призначення нормативних і розрахункових значень кранового навантаження і залучення до цього дослідних статистичних даних. Відзначається високий науковий рівень вітчизняних норм ДБН В.1.2-2006 «Навантаження і впливи», які мають сучасний імовірнісний базис і асоціюються з нормами Єврокод. Виділяються наукові результати, що можуть бути включеними в наступні норми кранового навантаження.

Ключові слова: норми будівельного проєктування, мостовий кран, підвісний кран, кранове навантаження, нормативне навантаження, розрахункове навантаження

Introduction

Lifting and transport machines are indispensable elements of any sphere of the economy. The technological process of most manufacturing enterprises is associated with the need to mechanize operations for vertical and horizontal goods transportation with a wide range of weight. This mechanization, along with other vehicles, is carried out by means of a bridge (support) and overhead cranes, which are special devices that move with loads along and across the shop. Ensuring the reliability and safety of buildings and structures largely depends on a proper understanding of the nature and quantitative description and rationing of loads on building structures, including crane loads. Loads from cranes can be significant; they have a variable dynamic nature and have a significant force on the structure of industrial buildings. These features are reflected in the sections of building structure design codes that contain codes for crane load. Most of the crane load code parameters are probabilistic in nature and require the use of statistical methods to substantiate them. These methods are constantly changing and evolving together with the regular review of building design standards. Analysis of the evolution of domestic codes of crane load together with their statistical substantiation is an urgent task.

Review of research sources and publications

With approval the first domestic building codes, which included the section of crane loads, related publications of the 30s of builders and crane operators [1]. Subsequently, active studies of bridge cranes loads were performed in TSNIPS [2]. This process was intensified with the preparation of structural calculations for the limit states method. In the postwar years, the study of crane loads was restored by TSNISK [3-6]. In the 60-80s, a comprehensive study of crane loads was performed by the Test Station of the Moscow Civil Engineering Institute (MIBI) [7-29]. Since the '70s, research on crane loads has been conducted at the Poltava Civil Engineering Institute (now the National University "Yuri Kondratyuk Poltava Polytechnic") [30-40]. The conducted researches promoted regular revision of loading codes and improvement of crane loads rationing. Beginning in the 1990s, design codes were developed by individual countries that were formerly part of the USSR. In this regard, probabilistic studies of crane loads were intensified in Ukraine, which resulted in the relevant section of DBN B.1.2-2006 "Loading and effects". In the following years, the study of crane loads continued along with the justification and refinement of the calculated coefficients of design standards [41-43].

Definition of unsolved aspects of the problem

Field studies of bridge loads and overhead cranes have been performed for many years on a large scale, creating a significant array of statistical information. However, there is no common information database for this data. Some of them have been published in various scientific and technical journals, collections of articles, conference proceedings. Access to these publications is difficult, as the translation into electronic form has taken place only for publications published after 2000. The results of crane loads studies are partially included in the design codes, but several reasonable proposals remain outside the current regulations. There is no analysis of trends in crane codes and the allocation of further development issues of this important load rationing.

Problem statement is a systematic review of research results and scientific publications on the problem of crane loads for the 90-year period from the 30s of the twentieth century to the present. It is emphasized that these loads on buildings have a complex physical nature and changeable character. The main focus is on identifying the relationship between the crane loads and developing the results of experimental studies of these loads. Aspects of probabilistic substantiation of calculated coefficients, assignment of normative and calculated values of crane load are emphasized. Scientific results that can be included in subsequent editions of crane load standards are highlighted.

Basic material and results

The beginning of domestic standardization of crane loads was laid in 1930, when the "Uniform codes of construction design" were introduced. Given that at that time the relevant experimental work was not carried out in the USSR, the basis of the adopted codes were foreign standards, the work of crane operators, and reference books, for example [1]. There are the horizontal loads transmitted from the cranes to the crane tracks and directed along with the building and were defined as

$$H = 0.1\, P\, n\,, \qquad (1)$$

where P - the calculated vertical pressure on the crane wheel;

n - the number of brake crane wheels located on the beam.

Formula (1) is obtained based on the law of friction $F = f N$, ie the friction force is equal to the normal pressure N multiplied by the coefficient of friction between the rails and wheels of the crane f, equal to 0.1.

In the late 1930s, a leading construction research organization, the Central Research Institute of Industrial Structures (CNIPS), organized large-scale field studies of the actual operation and bridge crane loads on steel frames of industrial buildings. The employees of TsNIPS N.E. Romanov tested 60, 125, and 220-ton foundry cranes [2]. Transverse loads when passing cranes past the measuring range were of different nature, but in all cases, they significantly exceeded the forces from the braking of the truck.

In 1940, the standard OST 90057-40 "Payloads" was adopted, in which crane loads were specified. In addition to the previous requirements, it emphasized that the transverse force should depend on the type of load suspension. For cranes with flexible suspension, this force was taken equal to 0.05 of the sum of load capacity and weight of the trolley, and for cranes with rigid suspension twice as much - 0.1 of the same sum.

Thus, the braking force transmitted to the crane wheel with a flexible suspension of the load was defined as

$$T_k = \frac{0{,}05}{n_0}(Q_t + Q) \ , \qquad (2)$$

where Q_t is the weight of the crane trolley;
Q – load capacity of the crane;
n_0 – the number of wheels on each side of the crane bridge.

In 1942, instead of OST 90057-40, the state standard GOST 1645-42 was issued. In addition to the previous requirements, it specifies that when calculating crane structures, the vertical load is taken from the actual number of cranes, but not more than two cranes approaching for joint work in each span of the building and on each tier. In multi-span stores, the possibility of placing cranes in one line in adjacent spans is taken into account.

In the pre-war and first post-war years, the Gipromez Institute under the leadership of O.I. Kikin (later doctor of technical sciences) carried out large-scale studies of the operation mode and loads of bridge cranes in the shop of metallurgical production. O.I. Kikin divided the horizontal transverse loads of overhead cranes on the *lateral forces* arising from the movement of cranes on tracks, and the *braking forces* caused by braking of trolleys of overhead cranes. The measured lateral forces were significantly (up to 3… 5 times) more than the loads from trolley braking. The obtained results were used in the preparation of TU 104-53 "Technical conditions for the design of steel structures of buildings of metallurgical plants with a heavy mode of operation." They introduced lateral forces, which, however, it was recommended to take into account only for individual structures and components by multiplying the standard braking forces by an increase factor equal to 1.1 ... 2.5, when calculating the upper belts of crane girders and brake structures, and a coefficient equal to 2.2 ... 5.0, when calculating the attachment of the brake structures of the crane girders to the columns. This approach was selective and did not take into account the lateral forces when calculating the transverse frames. These coefficients then passed to NiTU 121-55 "Codes and technical conditions for the design of steel structures."
In the 50s of the last century, studies of the lateral bridge cranes were continued in the TsNIPS under the leadership of M.F. Barstein [3]. As a normative load, it was proposed to take the lateral forces arising from the movement of the wheel crane with normal factory tolerances, with crane rails, concluded with the usual installation deviations. In this case, the formula of lateral forces, taking into account the pseudo-slip and the skew angle of the wheel 0.001 was as follows:

$$H = 1{,}5\sqrt{F_{\max} \cdot d} \ \text{(kgs)}, \qquad (3)$$

where d is the diameter of the crane wheel.

The values calculated by the formula (3) were close to the results calculated by the formula $H = 0.1\ F_{max}$ that M.F. Barstein recommended determining the lateral forces.

The first edition of the State building codes and rules of SNiP II-B.1-54 "Loading and effects" kept the general recommendations of the previous codes concerning bridge cranes loadings, having noted that "... the influence of crane distortions has to be considered according to special codes and technical conditions". In connection with the transition to the method of calculating structures for limit states, for crane load, an overload factor of 1.3 was introduced.

Study of the lateral forces of bridge cranes continued, beginning in 1954, at the Institute VNIIPTMASH under the leadership of V.P. Balashov [4]. The research included a theoretical part, an experimental test, and concerned four-wheel and multi-wheel cranes with wheels on rolling bearings with central and separate drives. The design case was considered to be the skew of the crane during its movement, which is caused by numerous factors, among which the difference in diameters and skew of the wheel axes, as well as the displacement of the crane tracks in the horizontal and vertical planes. The work developed an idea of the mechanical nature of the lateral crane forces, but the derived formulas were not included in the codes due to their cumbersomeness.

A number of experimental studies of crane loads were conducted at the TsNIISK in 1954-1955 under the leadership of A.Kh. Khokharin [5]. The experiments were performed on an experimental frame equipped with a 10 tons capacity bridge crane, as well as in existing shops. Studies have confirmed that the main case of force interaction of the crane with the crane tracks should be considered the case of the crane skew with the contact of the wheel flanges. Based on the above experimental studies, a calculated formula for the lateral force transmitting the crane wheel was proposed:

$$T = \alpha\beta \frac{L_{cr}}{B} F_{\max} \ , \qquad (4)$$

where F_{max} is the maximum vertical pressure of the wheel;
L_{cr} – crane span;
B – crane base;
β – coefficient that takes into account the ratio of the stiffness of the crane bridge and the transverse stiffness of the shop frame;
α – coefficient taken depending on the load capacity of the crane and the mode of shop operation within 0.01 … 0.03 for the calculation of brake trusses and upper belts of crane girders and twice as much - for the calculation of fastening of brake trusses to crane girders and columns, rails to crane beam.

In the late '50s of last century, there was the first publication on the statistical study of crane loads, in which A.A. Bat (TsNIISK) cited the results of field studies of the crane girders load regime [6]. The research was carried out in 1956 - 1958 in 25 operating shops of 4 metallurgical factories, in total more than 8 thousand cycles of crane girders loading were recorded. The obtained experimental statistics on the mode of crane girders op-

eration allowed to develop their calculation for endurance and gave an idea of the statistical variability of vertical crane loads.

In the 50-80s of the last century, the study of bridge crane loads was actively carried out at the Moscow Civil Engineering Institute (MISI) at the Test Station of the Department of Metal Structures. The results of these studies are summarized in collective monographs [7, 8], in which the author of this article took part. The first large-scale statistical study of vertical bridge cranes loads was conducted in the late 50s of the last century by B.N. Koshutin [9]. Observations were conducted in 23 spans of shops for various purposes. 52 experimental distribution polygons were obtained, which included 65535 cases of vertical loads on the columns and crane girders.

The polygons turned out to be symmetrical, single-vertex, and were reasonably replaced by curves of normal law. Developing a probabilistic approach to determining the overload factor, B.N. Koshutin drew attention to the misconception of the 50s of last century that the design load should be at a distance of three or four standards from the center of the distribution curve, ie the probability of exceeding it should not be more than $1.3 \cdot 10^{-3}$ or $3.1 \cdot 10^{-5}$. If we take into account that the vertical crane load can act on the columns, according to the obtained experimental data, $N = (0.6 \ldots 0.5)\ 10^6$ times during the 20-year service life, it becomes obvious that the above probabilities do not provide sufficient provision for the crane loads normalization. In view of this, the following expression was proposed for the overload factor

$$n = \left[1{,}1\left(\overline{X} + \beta\hat{X}\right) + 0{,}1\frac{F_K}{F_{M1}} \right] \frac{F_{M!}}{F_{M2}}, \qquad (5)$$

where $\overline{X}$ and $\hat{X}$ are the experimental average statistical value and standard;

F_K – load on the column from the weight of the bridge;

F_{M1} and F_{M2} - load on the column, respectively, from one and two cranes;

β – the number of standards corresponding to the probability of exceeding the design load F_R, $V = (F \geq F_R) = 1/N$, where N is the number of loads during the service life.

Based on the conducted statistical research the differentiated values (accepted with a stock) of overload coefficients of vertical crane loading of 1.0 … 1.2 were offered.

A.A. Bat and B.N. Koshutin in 1958 conducted a joint study of vertical crane loads at the Dniprospetsstal plant in the rolling shop and the pouring span of the electric steel shop [10]. Both methods gave the following main results, which coincide:

• distribution curves of vertical loads on columns have an approximately symmetrical look with the most probable size of 0,35 … 0,60 from standard loading of one crane without dynamic factor;

• cases of complete convergence of two cranes are rare and do not have a noticeable effect on the appearance of load distribution curves;

• the overload factor for the crane load can be reduced from 1.3 to 1.2.

In 1962 the second edition of SNiP II-A.11-62 "Loading and effects" was published. In a publication [11], the drafters list the new aspects of the publication related to crane loads. The value of the overload factor has been reduced from 1.3 to 1.2 for vertical and horizontal loads from cranes with a capacity of 5 tons and more (than taking into account the above results of statistical studies). This version of SNiP, as before, distanced itself from the specifics in determining the lateral forces of bridge cranes: "Horizontal transverse loads arising from the movement of the crane due to its skew and non-parallel crane tracks should be determined and taken into account in the calculation in accordance with the provisions of the design codes of structures of buildings and structures for various purposes." According to this installation, for steel structures, the coefficients α_1 and α_2 taking into account the action of lateral forces on individual structures and assemblies were preserved.

In the same years, the MIBI Test Station actively studied the lateral forces of bridge cranes. Chronologically, the first studies were realized by I.B. Izosimov at the Cherepovets Metallurgical Plant [12]. Four-wheel cranes on rolling bearings were investigated in order to identify the factors influencing the lateral forces. Noting the number of factors influencing the lateral forces, and the difficulty of taking them into account by calculation, it was decided to determine the lateral force as a function of the vertical pressure on the wheel:

$$H_k = f_p F_k, \qquad (6)$$

where H_k and F_k – respectively, the lateral and vertical load on the wheel;

f_p – the coefficient of proportionality, called the "realized friction coefficient of the transverse slip", which must be determined according to field tests.

The latter term cannot be considered successful, because f_p is essentially a generalization that establishes the relationship between horizontal and vertical loads. Setting the task in this form oversimplifies the problem, while making it difficult to assign f_p. The experimental values of the realized coefficients of friction were summarized in graphs of their dependence on the vertical pressure on the wheel and described by power functions. Received by I.V. Izosimov empirical dependences for the lateral forces cannot be considered sufficiently substantiated due to the insufficiency of the original statistical material and the depersonalization of a number of factors.

More profound field studies of the transverse loads of bridge cranes were conducted by A.V. Figarovsky (MISI, Test Station), with whom the author has long and fruitfully collaborated in joint work. In 1962-1963 years in one of the machine-building plant shops, it was conducted experimental force effects studies of a four-wheeled bridge crane of medium mode with a separate drive, with a capacity of 15/3 ts [13,14]. Simultaneous measurements of vertical and horizontal crane loads were performed. The used integrated methodology was

a significant step forward in comparison with the crane loads studies of previous years, it was unique in its complexity and thoroughness of preparation and application. Based on the tests, A.V. Figarovsky derived the formula for the values of the largest lateral forces on the wheels of four-wheeled cranes:

$$H_к = 0{,}1F_{\max} + \alpha(F_{\max} - F_{\min})\frac{L_{cr}}{B}, \qquad (7)$$

where F_{max} and F_{min} – the average pressure of the wheels, respectively, more or less loaded side of the crane;

α – coefficient equal to 0.01 for cranes with a separate drive of the movement mechanism and 0.03 – for cranes with a central drive.

In the above formula, the first term gives the transverse force from the skew of the wheel, the second - the horizontal component on the wheel flange, which limits the bridge skew. On other wheels can act only friction forces, approximately equal $0.1F$. This formula provides a fairly close coincidence with the experimental values.

A.V. Figarovsky also conducted a comprehensive field experiment in the pouring span of the open-hearth shop of the metallurgical plant [15]. A multi-wheeled foundry crane with a capacity of 175 tons with a central drive was tested. Unlike a four-wheel crane, a multi-wheel crane is less prone to skew and tends to keep the initial angle of skew constant. This is due to the smaller ratio of the crane span to its base and the presence on each side of the bridge balancing carts that allow some rotation in the vertical plane. Lubrication of the side surface of the rail head significantly (1.7 ... 2.0 times) reduced the magnitude of the lateral forces and their dynamics. The magnitude and nature of changes in the lateral forces of multi-wheel cranes are significantly affected by deviations in track width that exceed the total clearances of the flanges. It was found that in places of narrowing and widening of the track, the lateral forces increase by 2.0 ... 2.5 times.

In 1963-1965 years in the laboratory of dynamics of CNDIBK the researches of lateral forces were carried out by A.N. Zubkov under the direction of M.F. Barstein [16]. The theoretical development of the question was based on the idea of the bridge crane movement on the crane track, which has random deviations in the horizontal plane. The continuous contact of the rail with the flange of one wheel or with the flanges of two wheels located on one end beam was considered. Differential equations of crane motion were formed, and it was considered that the track deviation in the horizontal plane is a stationary normal process, the correlation functions of which were calculated from the materials of a geodetic survey of crane tracks in existing shops. Based on the research, a formula to determine the calculated values of the transverse forces acting on the wheels of the crane when limiting the skew by the flanges of the wheels on one side of the crane was proposed:

$$R = 15(\alpha\frac{L_{cr}}{b} \pm \beta)\sqrt{F} \ \text{(in kgf)}, \qquad (8)$$

where L_{cr} – the crane flight;

b is the distance between the end crane wheels;

F – average vertical wheel pressure;

α, β – coefficients accepted for four-wheel, eight-wheel, and sixteen-wheel cranes equal to [0,4, 0,8, 1,6] and [1, 3, 7].

In the same years, probabilistic studies of bridge crane loads were carried out at the MISI Test Station. The first attempt to obtain and process statistical data on horizontal loads of bridge cranes was made by B.N. Koshutin in the open-hearth shop of the Cherepovets Metallurgical Plant [17]. Lateral forces were recorded on the columns in the normal operation of the shop in the pouring and furnace spans. The experimental values of the overload coefficient had a large variance, and for the furnace, span exceeded the normative value equal to 1.2 (according to the variant SNiP valid at the time of testing).

In 1964-1966 years S.F. Pichugin conducted complex field studies of vertical and horizontal loads of bridge cranes for various purposes [13, 15, 18]. Statistical material was collected as a result of continuous registration of crane loads of normal operation in existing shops. Crane loads were presented in the form of random variables. The following features of statistical distributions of crane loadings were revealed:

- rapid stabilization, i.e. detection of these distributions taking into account the relatively small amount of statistical material, further increase of which does not change the picture either qualitatively or quantitatively;
- reasonable opportunity of applying the normal law to describe the ordinate distributions of vertical and horizontal crane load is substantiated;
- close connection of cranes work and crane loadings with the production technology of shops in which cranes are operated, stability of trajectories of movement of cranes and trolleys, the technological features influence on probabilistic characteristics of crane loadings (actual location of crane work areas, unequal loading of different rows structures, restriction of crane trolleys approach);
- a specific feature of some crane loads with flexible suspension (for example, foundries), which consists in the allocation in their distributions of the extreme "tail" parts, corresponding to operations with loads close to the load capacity; these parts should be considered separately [19,20].

Based on the analysis of statistical distributions of lateral crane loads for different purposes for 14 spans of 12 shops of three metallurgical plants, formulas were proposed to determine the normative values of these loads and the values of the overload coefficients of lateral bridge cranes forces.

In 1967-1968 years, the MISI Test Station (Y.S. Kunin) carried out large-scale field measurements of crane loads in the shops of metallurgical plants. The main results of this work are presented in a publication [21], which illustrates the transition from the representation of crane loads in the form of random variables to a probabilistic model of random processes. It was confirmed that crane loads are normal stationary random processes of ergodic nature. The obtained statistical data allowed estimating the overload factor of

the vertical crane load based on the theory of random processes outliers

$$n = \overline{X} + \gamma\hat{X} \ , \qquad (9)$$

where $\overline{X}$ and $\hat{X}$ – mathematical expectation and standard,

γ – the number of standards, which is determined taking into account the accepted service life of the structure and the specified probability of not exceeding $[P(T)]$ or exceeding $[Q]$ the calculated value of the crane load:

$$\gamma(T) = \sqrt{2\ln\frac{T\cdot\overline{n}_0}{-\ln[P(T)]}} = \sqrt{2\ln\frac{\omega T}{2\pi[Q(T)]}} \ , \qquad (10)$$

Here, on the left part, a variant of the formula is given, in which the frequency characteristic includes the average number $\overline{n}_0$ of excess of the average level per unit time; the left part of the formula includes the effective frequency of the crane load – this option was used in further crane loads studies.

According to the formula (9), the overload coefficient n = 0.45 … 1.08 for the service life T = 50 years and the probability of trouble-free operation $[P(T)]$ = 0.999 was obtained, which in all cases turned out to be less than the normative one.

Operators and researchers, including those mentioned above, have repeatedly noted that the actual vertical pressures on individual wheels of bridge cranes can differ significantly from the passport values. Such differences are called "uneven pressure of crane wheels". It is known that the bridge crane is a redundant spatial system that has fairly high rigidity in the vertical direction. Therefore, for example, a real 4-wheel crane while driving on real roads at certain times can rely on the rails at three or even two points (located on the diagonal of the bridge). As a result, the load on the wheels of bridge cranes can change both upwards and downwards. The non-uniformity of wheel pressures was studied in detail by V.N. Val (MISI, 1966-1969) [22], who used the method of weighing in tests of 26 cranes with a capacity of 5 ... 225 tons. He proposed to take into account the increase in wheel pressure of the bridge crane by the *coefficient of non-uniformity*

$$n_н = 1 + \Delta F / F_n \ , \qquad (11)$$

where ΔF – increase in wheel pressure;

F_n – maximum normative wheel pressure.

Based on the performed research, values of coefficient of non-uniformity of pressures on separate wheels of cranes were received in the range 1.3 ... 1.1 for cranes with a loading capacity of 5 ... 200 ts.

Another source of increasing the pressure of individual crane wheels is their dynamic nature, which is taken into account by the local dynamic coefficient $k_{d,loc}$, which depends on the stiffness of the crane girders, the speed of the cranes, and especially on the condition of the crane tracks. Experimentally obtained values $k_{d,loc}$ = 1.0 ... 1.5 depends on the type of load suspension and lifting capacity of cranes.

Taking into account the above values of the non-uniformity coefficient of pressure on the wheel n_n and the local dynamic coefficient $k_{d,loc}$, V.N. Val proposed (not yet implemented) to increase the total coefficient to the following values: γ_{f1} = 1.8 – for cranes with rigid suspension; γ_{f1} = 1.5 for cranes with the flexible suspension of heavy rate (groups of modes 7K and 8K); γ_{f1} = 1.3 for other cranes [22].

The next statistical research stage of the MISI Test Station was the study in 1970-1973 combinations of vertical crane loads by A.T. Yakovenko [23]. Statistical data were obtained for vertical loads of 17 cranes operating in 7 spans of metallurgical plants. The actual combination coefficients of crane loads were determined by a formula suitable for any random loads:

$$\psi = \left[S_\Sigma\right] \Big/ \sum_{i=1}^{n}\left[S_i\right] \ , \qquad (12)$$

where $\sum_{i=1}^{n}\left[S_i\right]$ – the sum of loads (efforts) at unfavorable loading of a line of influence by the approached cranes provided that pressures of separate wheels of each crane can be exceeded with probability $Q(T)$;

$\left[S_\Sigma\right]$ – design load (effort) taking into account the actual random process of crane load, which is determined from the condition of the same probability of exceeding the service life $Q(T)$ according to formulas (9) and (10).

Of the thus obtained combination coefficients, the largest was the experimental values for cranes of groups of modes 8K (ψ = 0.75 … 0.85), which regularly lift loads close to the nominal and have high speeds. Slightly smaller, within ψ = 0.58 … 0.73, the obtained composition coefficients for cranes of groups of modes 7K. The lowest values ψ = 0.38 … 0.40 were observed in cranes of groups of modes 4K… 6K. These cranes are less loaded, rarely lift loads close to the nominal, approach relatively rarely.

In 1974 the next edition of SNiP II-6-74 "Loading and effects" was published in which the load codes of overhead cranes were combined with the load standards from overhead cranes. Long-term loads (without experimental justification) included the load from one crane, multiplied by 0.6 for cranes of medium mode and by 0.8 for cranes of heavy and very heavy modes. Taking into account large-scale studies of crane loads conducted in the '60s and '70s at MISI (as described above), the overload factor for loads of all cranes was assumed to be 1.2. For the first time, a scale of lowering combination coefficients for vertical loads from two and four cranes in the range of 0.70 ... 0.95, depending on the modes of operation of the cranes, was included. A lateral force standard equal to 0.1 of the normative vertical load on the wheel was introduced for each running wheel. However, as before, it was inconsistently regulated that "... this load should be taken into account when calculating only the beams of crane tracks and their attachments to columns in buildings with cranes of very heavy mode, with foundries and other cranes of the heavy mode of metallurgical production." For the endurance calculation of crane track beams, it

was indicated that the normative load from one crane should be multiplied by a factor of 0.6 for cranes of medium mode and a factor of 0.8 for cranes of heavy and very heavy modes.

In the 70's the Dnepropetrovsk Institute of Railway Engineers (DIIT, Yu.A. Zdanevych [24]) continued a study initiated earlier by a number of researchers to assess the impact on the crane load of the technological process features. The recommendation to reduce the overload factor to $n = 1.1$ was substantiated for the payload of steel ladles (taking into account the wear of the lining) in determining the vertical loads of foundry cranes. For an open-hearth shop with 10 furnaces with a capacity of 220 ... 450 t, the following composition coefficients for vertical crane loads in the interval $\psi = 0.70 \ldots 0.90$ were substantiated.

In the same period, the features of the technological process of rolling shops were also identified by S.A. Nischeta (MISI Test Station) during experimental studies on seven heavy-duty bridge cranes with a capacity of 10 ... 20 tons with a flexible suspension traverse and a separate drive [25]. The obtained experimental statistics, together with the results of previous studies [8, 21], as well as the provisions of the design standards of bridge cranes [26], allowed the recommendation to reduce the overload factor of the crane load to $n = 1,1$.

The maximum values of horizontal loads that exceeded the braking forces by 2.5 ... 3.0 times were obtained. Based on these data, the following formula of lateral force on the wheel of a crane with a separate drive was proposed

$$H_k^n = 0,04 \frac{L_{cr}}{B} F_{\max}^n, \qquad (13)$$

S.A. Nischeta also studied the coefficients of forces composition from vertical crane loads for crane girders and columns of the extreme and middle rows by statistical modeling (Monte Carlo). Coefficients of the combination of vertical crane influences on columns from two bridge cranes located on one crane way, and four cranes - on different ways, were defined by the formula

$$\psi = S / \left(n S_i^n \right), \qquad (14)$$

where S is the value of the vertical loads on the column from two or four bridge cranes, corresponding to the probability of realization $P = 0.95$ per time $T = 40$ years;

nS_i^n – the sum of the products of the loads on the column from each of the "k" cranes wheels (with unfavorable loading of the influence line of the crane girders support reactions) on the corresponding actual values (for each of the spans) of the overload coefficients n.

It was found that the combination coefficients significantly depend on the line length of corresponding force influence and the ratio of the crane span to its base.

The dependence on the length of the working area and the structure position (column, crane beam) is also noted. The actual combination coefficients obtained in the range $\psi = 0.60 \ldots 0.95$ were lower (especially taking into account the four cranes) than those set in the SNiP, which indicates that under operating conditions, the maximum convergence of two (and even more so four) cranes with a maximum load is an exceptional phenomenon. Therefore, there was (and now is) the possibility of differentiation and further reduction of the crane load combination coefficients.

In the following years, a number of changes in the part of crane loads were introduced in SNiP II-6-74 [27], which were included in SNiP 2.01.07-85 "Loading and effects", which came out after 11 years. Based on statistical data obtained by A.A. Bat, the long-term parts of the loads from the bridge and overhead cranes were reduced: from 0.6 to 0.5 from one medium mode crane and from 0.8 to 0.7 from a heavy and very heavy mode crane. It was indicated that instead of taking into account two cranes, the check of deflections of crane track beams should be performed from one crane - on the basis of research by M.Ya. Kouzin (MISI [28]).

The reliability factor for the load (which replaced the former overload factor) for crane loads began to be taken equal to $\gamma_f = 1.10$ (justification is given above). A long-overdue addition was made - the coefficient of increase of concentrated load on a single wheel of the bridge crane was transferred from SNiP for steel structures to SNiP for loads in the range $\gamma_{f1} = 1.10 \ldots 1.60$ depending on the groups of operation modes of cranes and cargo suspension. The scope of the lateral force standard, which is caused by the skew of bridge cranes and non-parallelism of crane tracks, was slightly changed – now it concerning the calculation of durability and stability of crane tracks beams and their fastenings to columns in buildings with cranes of operating modes groups 7K, 8K.

The latest field tests, aimed at a study of crane loads, were conducted by V.A. Plotnikov in the 90s of the twentieth century in the shops of the Magnitogorsk Metallurgical Plant [29]. Experimental values of lateral forces from multi-wheel cranes in all cases did not exceed the normative values according to SNIP 2.01.07-85. This work significantly supplemented the idea of the nature and magnitude of the lateral forces of multi-wheel cranes. However, the probabilistic coefficients remained undefined in the proposed formulas, and no comparison of the obtained theoretical formulas with experimental data was performed. Investigation of horizontal loads of four-wheel cranes V.A. Plotnikov performed on an open scrap yard overpass. It was found that the values of the experimental loads correspond quite closely to the values determined by the formula (13), proposed by S.A. Nischeta for overhead cranes of industrial buildings.

Researchers, designers, and operators have identified significant shortcomings of SNiP 2.01.07-85 in terms of crane loads normalization.

1. Double approach to determining the horizontal transverse effects of the bridge and overhead cranes. On the one hand, when calculating the transverse frames of buildings and beams of crane tracks, it is proposed to take into account the load caused by trolley

braking - the transverse braking force. On the other hand, when calculating the strength and stability of crane track beams and their attachments to columns in buildings with cranes of operating modes 7K, 8K, it is proposed to take into account much larger lateral forces directed across the crane track and caused by skew electric cranes and non-parallel crane tracks.

2. Lack of explicit connection of the crane load standard with the period of its recurrence, which does not allow to take into account the service life of buildings.

3. Disadvantages in the rationing of the reduced component of the crane load, which refers to long-term loads and is also intended for the calculation of structures for endurance.

With the collapse of the USSR, the new states had the opportunity to move away from the rude Soviet rationing and develop their own, more adequate codes for crane loads. Further development of crane codes in the CIS was realized in the form of national codes of individual states.

Russia has followed the path of gradual development of SNiP. The Code of Rules of SP 20.13330.2011 "Loading and effects" and the updated version of SNiP 2.01.07-85* were developed. They do not differ in principle from the previous version of SNiP 2.01.07-85 and include the following changes:

• the multiplier of 0.1 is replaced by 0.2 for determination of the lateral loads;

• the coefficient of reliability on loading is increased to $\gamma_f = 1.2$ for cranes of all groups of operating modes;

• the increased factor taking into account local and dynamic action of vertical loading from one wheel of the crane, to $\gamma_f = 1.2 \ldots 1.8$ (in accordance with the above recommendations of V.N. Val).

Ukrainian specialists, in contrast to Russian standards developers, have prepared the State Codes of Ukraine DBN B.1.2:2006 "Loading and effects", conceptually different from SNiP in terms of crane loads. The publication of these codes was preceded by the systematization of the results of many years of work in the field of crane loads, described above, by the combined efforts of MISI (B.N. Koshutin, Y.S. Kunin) and PoltISI (National University "Yuri Kondratyuk Poltava Polytechnic", V.A. Pashinsky, S.F. Pichugin) [30, 31].

83 processes of crane loading were generalized, from which 8 concerned cranes with a rigid suspension of cargo, and the rest - to cranes with a flexible suspension with a loading capacity of 5 ... 650 ts of various groups of operating modes. As a result, a generalized probabilistic model of vertical crane load in the form of a normal stationary random process was created. Determined with the necessary security, the mathematical expectation $\overline{X}$, standard $\hat{X}$ and effective frequency ω fully described this random process. Mathematical models of crane loads such as absolute maxima of random processes, a scheme of independent tests, a discrete representation, extremes, and a correlated random sequence of overloads have also been developed [32]. This allowed the development of the combining random loads issue, including the participation of crane loads [33-35].

Codes DBN B.1.2-2: 2006 for loads, including crane loads, are conceptually built similarly to European standards Eurocode [36]. They are based on the characteristic values of loads (previously they were called normative). The calculated values of loads are determined by multiplying the characteristic values by the coefficient of reliability for the load, which depends on the type of load. DBN considers crane load as a variable load with four calculated values of the vertical component: limit F_m, operational F_e, cyclic F_c and quasi-constant F_c [37,38]:

$$F_m = \gamma_{fm}\psi F_0 \ , \quad F_e = \gamma_{fe}F_{01} \ , \\ F_c = \gamma_{fc}F_{01} \ , \quad F_p = \gamma_{fp}F_{01} \ , \tag{15}$$

where F_{01}, F_0 – the characteristic values of the vertical load, respectively, from one or two of the most unfavorable for the impact of cranes (determined similarly to the normative load according to SNiP);

ψ – composition coefficient of crane loads, which passed in the range of 0.70 ... 0.95 from the previous codes.

The reliability coefficient of the crane load limit value γ_{fm} was determined, according to the general concept of DBN, depending on the average return period of load *T*. Its maximum value was taken equal $\gamma_{fm} = 1.1$ based on the statistical results of a number of researchers, discussed above. This coefficient corresponds to the base return period $T = 50$ years and does not change with increasing *T* due to the small variability of the crane load maxima. For units with a service life of fewer than 50 years, reduced reliability coefficients in the range of 0.97 ... 1.10, determined by the formula

$$\gamma_{fm}(T) = \frac{1 + V\gamma(T)}{1 + V\gamma(T = 50\,years)}, \tag{16}$$

where $V = \hat{X}/\overline{X}$ is the coefficient of crane load variation;

$\gamma(T)$ – normalized deviation from the mathematical expectation of the maximum calculated value of the crane load at a given probability of its exceeding *Q(T),* determined by the formula (10).

The reliability coefficient of the operational design value of the crane load was assumed to be equal $\gamma_{fe} = 1$. Thus, for the calculations of structures at the second limit state (deflections, displacements, etc.), the characteristic load from one crane is used, based on the operating experience, which shows the validity of such SNiP recommendation.

The cyclic design value of the vertical crane load, which is used in the calculations of crane structures for endurance, was included in the DBN at the suggestion of V.A. Pashinsky [39]. Since the real crane load processes are random and therefore cannot be directly included in endurance calculations, the cyclic design value is determined based on a schematic load process of the simplest type – a harmonic process with a given frequency equivalent to the actual load process. The cyclic calculated value characterizes the "average" load

mode and therefore should not depend on the service life of the object. In DBN the cyclic design value is presented in the unified form of the product of characteristic vertical loading from one crane and reliability coefficients $\gamma_{c\,max}$, $\gamma_{c\,min}$. The duration of the cyclic load is taken into account by the number of cycles (per day) n_c = 270…820 depending on the groups of modes of crane operation.

The quasi-constant design value of the vertical crane load, adopted in the calculations, which takes into account long processes in structural materials (creep, etc.), is proposed to be equal to the vertical load of one crane without load (empty) F_{01}^{II} with the introduction of the reliability coefficient $\gamma_{fp} = F_{01}^{II} / F_{01}$ in formula (15).

In the development of DBN in terms of horizontal crane loads, it was taken into account the main provisions relating to the actual nature and magnitude of the lateral forces of bridge cranes. For these loads, the characteristic values were the values of loads from two cranes H_0 or one crane H_{01} which are determined differently for four-wheel and multi-wheel cranes.

For four-wheel cranes, the lateral force from one crane is determined by the formula (7) proposed by A.V. Figarovsky. The lateral forces H_{01} calculated by this formula can be applied:

• to the wheels of one side of the crane and directed in different directions (inside or outside the considered span of the building), which corresponds to the limitation of the skew of the crane wheels of one side;

• to the wheels on the crane diagonally and also directed in different directions (inside or outside the considered span of the building), which corresponds to the case of limiting the skew of the crane by wheels located on the diagonal of the crane.

At the same time to other wheels the forces $0.1F_{\max}^{n}\left(0.1F_{\min}^{n}\right)$, directed in the most unfavorable direction (inside or outside of the considered run) are applied.

For multi-wheel cranes, a new lateral force standard has been introduced based on the results of many years of testing such cranes. The characteristic value of the lateral force on the wheel of multi-wheeled cranes with the flexible suspension of the load H_k^n is taken equal to 0.1 of the vertical load on the wheel, calculated at the location in the middle of the bridge of the trolley with a load equal to the passport capacity of the crane. For multi-wheel cranes with rigid suspension, the load H_k^n is assumed to be equal to 0.1 of the maximum vertical load on the wheel.

When determining the characteristic values H_k^n, it is taken into account that the lateral forces from the two multi-wheel cranes are transmitted to both sides of the crane track. On each side of the crane, the lateral forces have one direction - outwards or inwards, on different tracks, they are directed in opposite directions (both inwards or both outwards). On one of the tracks, the full lateral force is accepted, on the other track, half of the lateral force is accepted. In contrast to the SNiP, the above-mentioned lateral forces of bridge cranes are proposed to be taken into account when calculating the strength and stability of beams of crane tracks, frames, columns, and foundations.

The assumption of vertical loads reduction from cranes with constant restrictions of wheelchair approximations introduced by the DBN is based on a fairly representative experimental and statistical material [40] and makes it possible to take into account the reduction factors K_y = 0.94 … 0.76.

Giving a general assessment of the Ukrainian code DBN B.1.2-2006 "Loading and effects" in terms of crane load, it should be emphasized that they are compiled on a modern methodological basis, close to European codes Eurocode [36], based on representative statistics, more differentiated and have scientific probabilistic substantiation, more deeply developed than in the codes of previous years

An analysis of the consequences of the implementation of the recommendations of DBN B.1.2-2: 2006 "Loading and effects" in terms of bridge cranes loads were carried out [41]. The excess of horizontal loads on the wheel of four-wheel bridge cranes, determined by DBN, is up to 1.3… 9.6 times, compared with the loads calculated in accordance with SNiP. In the transition to determining the force of four-wheel bridge cranes by DBN, bending moments in the columns of the transverse frames of single-story industrial buildings from the lateral forces increase 1.9… 6.9 times, compared with the forces from the braking forces of SNiP. Bending moments in the structures of crane girders increase 1.2… 7.8 times. As a result, there is a slight increase in material consumption of crane girders, which averages 1.1%, as well as an increase in material consumption of up to 24% of crane parts of columns of buildings equipped with four-wheeled cranes.

Under the action of multi-wheel bridge cranes, the load on the wheel according to DBN exceeds the load according to SNiP by 1.3… 1.7 times. It was found that the bending moments in the transverse frames increase by 1.1… 1.2 times and up to 1.6 times in the crane girders.

Based on inspections of the load-bearing capacity of structures, it was found that in the case of equipping buildings with multi-wheeled bridge cranes, the transition to determining the loads according to DBN does not increase the cost of materials for crane girders and columns.

To neutralize the consequences of the introduction into the practice of design codes, it is recommended to use such a reserve of steel frames as its spatial operation. It is established that taking into account the effect of spatial work when calculating the transverse frames on the crane loads according to DBN B.1.2-2: 2006 allows to approximate the results of calculations of frames for loading according to SNiP 2.01.07-85 and to avoid additional costs of materials.

As can be seen from the above, the study of crane loads on the structures of industrial buildings has a long history, and most of the work performed on this topic is based on the results of field observations in industrial

buildings with the most intensive work of cranes. Numerical statistical modeling was also used in some studies. However, the computational capabilities of the time were limited, and the number of randomized trials in each task was relatively small. In view of these circumstances, A.V. Perelmuter performed a statistical study of crane loads, which involved modern computational capabilities [42] and methods of mathematical modeling [43]. As a result, it was clearly shown that the values of crane loads and combination coefficients of these loads, presented in the design codes, are somewhat overstated. Therefore, it is relevant and real in the current conditions to perform research aimed at clarifying the codes of crane loads, using modern methods of statistical modeling.

Conclusions

It is shown that during the last ninety years the domestic codes of building structures design in terms of crane loads normalization have undergone significant changes and expanded their statistical bases. There is a high scientific level of domestic codes DBN B.1.2-2006 "Loading and effects", which have a modern statistical basis, are associated with Eurocode and provide the required level of building structures reliability. The modified account of bridge cranes lateral forces is developed and included in these codes; the substantiation of normative (characteristic) and design values of crane loading is developed. For further research such tasks are allocated: the further statistical analysis of random crane loadings combinations, in-depth consideration of the physical nature of crane loads, an estimation of the technological processes' influence on bridge crane loading.

References

1. Левенсонъ А.А. (1905). *Справочная книга для архитекторовъ, механиковъ и студентовъ* («HÜTTE»). Часть I. – Москва: Товарищество СКОРОПЕЧ

2. Романов Н.Е. (1938). Исследование поперечных горизонтальных крановых нагрузок кольцом. *Исследование действительной работы стальных конструкций промышленных зданий*, 164-175

3. Барштейн М.Ф. (1951). Экспериментальное определение горизонтальных поперечных сил, возникающих при движении мостовых кранов прокатного цеха завода «Азовсталь». *Труды института ЦНИИПС*,16-51

4. Балашов В.П. (1957). Поперечные силы при движении мостовых кранов с центральным приводом механизма передвижения. *Сборник научных трудов ВНИИПТМАШ*, №18, 24-59

5. Хохарин А.Х. (1961). О боковых воздействиях мостовых кранов на каркас промышленного здания. *Промышленное строительство*, № 9, 38-45

6. Бать А.А. (1959). О расчете на выносливость. *Строительная механика и расчет сооружений*, №5, 24-28

7. Кикин, А.И., Васильев А.А., Кошутин Б.Н. (1969). *Повышение долговечности конструкций промышленных зданий*. Москва: Стройиздат

8. Кикин А.И., Васильев А.А., Кошутин Б.Н., Уваров Б.Ю., Вольберг Ю.Л. (1984). *Повышение долговечности конструкций промышленных зданий*. Москва: Стройиздат

9. Кошутин Б.Н. (1966). Статистическое определение коэффициентов перегрузки вертикальных крановых нагрузок. *Металлические конструкции (Работа школы Н.С. Стрелецкого)*. Москва: Стройиздат, 195-210

10. Бать А.А., Кошутин Б.Н. (1960). Статистическое изучение крановых нагрузок. *Строительная механика и расчет сооружений*, №2, 1-5

11. Клепиков Л.В., Отставнов В.А. (1962). Определение нагрузок при расчете строительных конструкций. *Строительная механика и расчет сооружений*, №5, 39-45

12. Кикин А.И., Изосимов И.В. (1966). Изучение факторов, влияющих на величины боковых сил мостовых кранов в цехах металлургического завода. *Известия вузов. Строительство и архитектура*, №12, 1-8

13. Изосимов И.В., Фигаровский А.В., Пичугин С.Ф., Валь В.Н. (1966). Исследование силовых воздействий мостовых кранов. *Металлические конструкции (Работа школы профессора Н.С. Стрелецкого)*. Москва: Стройиздат, 164-176

1. Levenson A.A. (1905). *Reference book for architects, mechanics and students ("HÜTTE") Part I.* Moscow: SKOROPECH Partnership

2. Romanov N.E. (1938). Investigation of transverse horizontal crane loads by a ring. *Research of the actual work of steel structures of industrial buildings,* 164-175

3. Barshtein M.F. (1951). Experimental determination of horizontal shear forces arising from the movement of overhead cranes in the rolling shop of the Azovstal plant. *Proceedings of the Institute TsNIIPS*, 16-51

4. Balashov V.P. (1957). Cross forces during the movement of bridge cranes with a central drive of the movement mechanism. *Collection of scientific works of VNIIPTMASH*, 18, 24-59

5. Khokharin A.Kh. (1961). On the lateral loads of bridge cranes on the frame of an industrial building. *Industrial construction*, 9, 38-45.

6. Bat A.A. (1959). On the calculation of endurance. *Building mechanics and calculation of structures*, 5, 24-28.

7. Kikin A.I., Vasiliev A.A., Koshutin B.N. (1969). *Increasing the durability of industrial buildings structures.* Moscow: Stroyizdat

8. Kikin A.I., Vasiliev A.A., Koshutin B.N., Uvarov B.Yu., Volberg Yu.L. (1984). *Increasing the durability of industrial buildings*. Moscow: Stroyizdat

9. Koshutin B.N. (1966). Statistical determination of the overload coefficients of vertical crane loads. *Metal structures (Work of the school of N.S. Streletsky)*. Moscow: Stroyizdat, 195-210

10. Bat A.A., Koshutin B.N. (1960). Statistical study of crane loads. *Building mechanics and calculation of structures*, 2, 1-5

11. Klepikov L.V., Otstavnov, V.A. (1962). Determination of loads in the calculation of building structures. *Building mechanics and calculation of structures*, 5, 39-45

12. Kikin A.I., Izosimov I.V. (1966). Study of the factors affecting the magnitude of the lateral forces of overhead cranes in the shops of a metallurgical plant. *Izvestiya vuzov. Construction and architecture,* 12, 1-8

13. Izosimov I.V., Figarovsky A.V., Pichugin S.F., Val V.N. (1966). Investigation of the power effects of bridge cranes. *Metal structures (Work of the school of NS Streletsky)*. Moscow: Stroyizdat, 164-176

14. Фигаровский, А.В. (1970). Исследование боковых сил четырехколесных кранов с гибким подвесом груза. *Металлические конструкции: Сборник трудов*, № 85, 41-52

15. Кикин А.И., Фигаровский А.В., Пичугин С.Ф. (1967). Экспериментальные данные о поперечных горизонтальных силах от разливочных кранов. *Промышленное строительство*, №12, 8-13

16. Барштейн М.Ф., Зубков А.Н. (1966). Статистический анализ боковых сил, возникающих при движении мостового крана. *Строительная механика и расчет сооружений*. №2

17. Кошутин Б.Н. (1963). О коэффициенте перегрузки боковых сил от мостовых кранов. *Методика определения нагрузок на здания и сооружения: Сборник статей ЦНИИСК*, 81-88

18. Пичугин С.Ф. (1970). Результаты статистического экспериментального исследования горизонтальных и вертикальных нагрузок мостовых кранов на. конструкции промышленных зданий. *Исследование и расчет стр. конструкций: Сб. научных трудов МГМИ*, 59, 8-16

19. Пичугин С.Ф. (1972). К исследованию крайних частей статистических распределений (на примере нагрузок мостовых кранов). *Проблемы надежности в строительном проектировании*, 169-175

20. Пичугин С.Ф., Леванин Ю.П. (1974). Результаты экспериментального изучения вертикальных нагрузок мостовых кранов на колонны мартеновских цехов. *Известия вузов. Строительство и архитектура*, №12, 31-35

21. Кунин Ю.С., Эглескалн Ю.С. (1969). Исследование статистических свойств режимов нагружения подкрановых конструкций. *Промышленное строительство*, №9, 36-39

22. Валь В.Н., Эглескалн Ю.С. (1969). Влияние дефектов подкрановых путей на силовые воздействия мостовых кранов. *Промышленное строительство*, №4, 36-38

23. Васильев А.А., Кунин Ю.С., Яковенко А.Т. (1974). Об уточнении расчетных вертикальных нагрузок от мостовых кранов. *Промышленное строительство*, №6, 31-33

24. Зданевич Ю.А. (1974). О некоторых резервах нагрузок на подкрановые конструкции действующих сталеплавильных цехов. *Труды ДИИТ*, 159

25. Кошутин Б.Н. Кунин Ю.С., Нищета С.А. (1979). Исследование вертикальных и горизонтальных воздействий от мостовых кранов методом статистического моделирования. *Облегченные конструкции покрытий зданий*, 195-199

26. Бать А.А. (1969). О согласовании норм нагрузок для расчета кранов и подкрановых конструкций. *Промышленное строительство, 10,* 46-47

27. Отставнов В.А., Бать А.А., Клепиков Л.В. (1983). О новых дополнениях и изменениях главы СНиП II-6-74 «Нагрузки и воздействия». *Промышленное строительство*, №9, 9-10

28. Кунин Ю.С., Кузин Н.Я. (1972). О нагрузках при расчёте жёсткости подкрановых балок, *Промышленное строительство*, 6, 26-27

29. Плотников В.А. (1990). Исследование горизонтальных силовых воздействий от мостовых кранов. *Межвузовский сборник научных трудов*, 122-125

30. Кошутин Б.Н., Кунин Ю.С., Пашинский В.А. (1985). Обобщенная математическая модель вертикальной крановой нагрузки. *Вопросы надежности железобетонных конструкций*, 40-51

31. Pichugin S. (1998). Analysis of bridge crane loads on industrial buildings. *XLIV Konferencja Naukowa KILiW PAN i KN PZITB. Poznan-Krynica*, 172-179

14. Figarovsky A.V. (1970). Study of the lateral forces of four-wheel cranes with flexible load suspension. *Metal structures: Collection of works of MISI*, 85, 41-52

15. Kikin A.I., Figarovsky A.V., Pichugin S.F. (1967). Experimental data on transverse horizontal forces from casting cranes. *Industrial construction*, 12, 8-13

16. Barshtein M.F., Zubkov A.N. (1966). Statistical analysis of lateral forces arising from the movement of an overhead crane. *Building mechanics and calculation of structures*, 2

17. Koshutin B.N. (1963). On the coefficient of overload of lateral forces from bridge cranes. *Methodology for determining loads on buildings and structures: Collection of articles of TSNIISK*, 81-88

18. Pichugin S.F. (1970). The results of a statistical experimental study of horizontal and vertical loads of overhead cranes on. structures of industrial buildings. *Research and Calculation of Structural Structures: Collection of Scientific Papers of MGMI*, 59, 8-16

19. Pichugin S.F. (1972). On the study of the extreme parts of statistical distributions (for example, the loads of overhead cranes). *Problems of reliability in construction design*, 169-175

20. Pichugin S.F., Levanin Yu.P. (1974). Results of experimental study of vertical loads of overhead cranes on columns of open-hearth shops. *Izvestiya vuzov. Construction and architecture*, 12, 31-35

21. Kunin Yu.S., Egleskaln Yu.S. (1969). Study of the statistical properties of loading modes for crane structures. *Industrial construction*, 9, 36-39

22. Val V.N., Egleskaln Yu.S. (1969). The influence of crane runway defects on the power effects of bridge cranes. *Industrial construction*, 4, 36-38

23. Vasiliev A.A., Kunin Yu.S., Yakovenko A.T. (1974). On the clarification of the calculated vertical loads from bridge cranes. *Industrial construction*, 6, 31-33

24. Zdanevich, Yu.A. (1974). On some reserves of loads on crane structures of operating steel-making shops. *Proceedings of DIIT*, 159

25. Koshutin, B.N., Kunin, Yu.S., Nyscheta, S.A. (1979). Investigation of vertical and horizontal impacts from overhead cranes by the method of statistical modeling. *Lightweight Building Coating Structures*, 195-199

26. Bat, A.A. (1969). About coordination of codes of loads for calculation of cranes and crane structures. *Industrial construction, 10,* 46-47

27. Oststavnov V.A., Bat A.A., Klepikov L.V. (1983). On new additions and changes to the chapter of SNiP II-6-74 "Loads and loadings". *Industrial construction*, 9, 9-10

28. Kunin Yu.S.. Kuzin N.Ya. (1972). About loads when calculating the rigidity of crane beams. *Industrial construction*, 6, 26-27

29. Plotnikov V.A. (1990). Investigation of horizontal force effects from bridge cranes. *Interuniversity collection of scientific papers*, 122-125

30. Koshutin B.N., Kunin Yu.S., Pashinsky V.A. (1985). Generalized mathematical model of vertical crane load, *Questions of the reliability of reinforced concrete structures,* 40-51

31. Pichugin S. (1998). Analysis of bridge crane loads on industrial buildings. *XLIV Konferencja Naukowa KILiW PAN i KN PZITB. Poznan-Krynica*, 172-179

32. Пичугин С.Ф. (1995). Вероятностное представление нагрузок, действующих на строительные конструкции. *Известия вузов. Строительство*, №4, 12-18

33. Пичугин С.Ф., Пашинский В.А. (1982). Методика вычисления коэффициентов сочетаний нагрузок. *Вопросы надежности железобетонных конструкций*, 94-97

34. Пичугин С.Ф. (1995). Вероятностный расчет стальных элементов на совместное действие нагрузок. *Известия вузов. Строительство*, 5,6, 23-29.

35. Pichugin S. (1995). Reliability estimation of steel elements under variable loads. *XLI Konferencia Naukowa KILIW PAN i KN PZITB, Krakow-Krynica,* 151-156

36. Eurocode 1 EN 1991-3.: Actions on structures – Part 3: Actions induced by cranes and machinery. – Brussels: CEN, Sep. 2006. – 42 p.

37. Pichugin S.F. (1994). Calculation coefficients of design codes based on the analysis of the reliability of steel structures. *Construction of Ukraine*, 1, 18-20

38. Пічугін С.Ф. (2007). Кранові навантаження в ДБН В.1.2-2:2006 «Навантаження і впливи». *Будівельні конструкції: Збірник наукових праць*, 67, 691-702

39. Пашинський В.А. (1999). Циклічні розрахункові значення навантажень на будівельні конструкції. *Вибрации в технике и технологиях*, №2, 15-17

40. Pichugin S. (1997). Probabilistic description of crane load on building structures. *XLIII Konferencja Naukowa KILiW PAN i KN PZITB, Poznan-Krynica,* 171-178

41. Pichugin S., Patenko Iu., Maslova S. (2018). Comparative analysis of loads from the travelling cranes of different producers. *International Journal of Engineering &Technology*. 7 (3.2), 36-39

42. Perelmuter A.V. (2017). Statistical simulation of crane loads and calculated force combinations. *International Journal for Computational Civil and Structural Engineering,* 13(2), 136-144

43. Pasternak H., Rozmarynowski B., Wen Y.-K. (1996). Crane load modeling. *Structural Safety,* 17, 205-224

32. Pichugin S.F. (1995). Probabilistic representation of loads acting on building structures. *Izvestiya vuzov. Construction*, 4, 12-18

33. Pichugin S.F., Pashinsky V.A. (1982). Methodology for calculating the coefficients of combinations of loads. *Questions of the reliability of reinforced concrete structures*, 94-97

34. Pichugin S.F. (1995). Probabilistic calculation of steel elements for joint action of loads. *Izvestiya vuzov. Construction*, 5,6, 23-29

35. Pichugin S. (1995). Reliability estimation of steel elements under variable loads. *XLI Konferencia Naukowa KILIW PAN i KN PZITB, Krakow-Krynica,* 151-156

36. *Eurocode 1 EN 1991-3.: Actions on structures – Part 3: Actions induced by cranes and machinery.* (2006). Brussels: CEN, Sep.

37. Pichugin S.F. (1994). Calculation coefficients of design codes based on the analysis of the reliability of steel structures. *Construction of Ukraine*, 1, 18-20

38. Pichugin S.F. (2007). Crane loads in DBN B.1.2-2: 2006 "Loads and iloadings". *Building constructions: Collection of scientific works of NDIBK*, 67, 691-702

39. Pashinsky V.A. (1999). Cyclic calculated values of loads on building structures. *Vibrations in technology and technology*, 2, 15-17

40. Pichugin S. (1997). Probabilistic description of crane load on building structures. *XLIII Konferencja Naukowa KILiW PAN i KN PZITB, Poznan-Krynica,* 171-178

41. Pichugin S., Patenko Iu., Maslova S. (2018). Comparative analysis of loads from the travelling cranes of different producers. *International Journal of Engineering &Technology*. 7 (3.2), 36-39

42. Perelmuter A.V. (2017). Statistical simulation of crane loads and calculated force combinations. *International Journal for Computational Civil and Structural Engineering,* 13(2), 136-144

43. Pasternak H., Rozmarynowski B., Wen Y.-K. (1996). Crane load modeling. *Structural Safety,* 17, 205-224

Збірник наукових праць. Галузеве машинобудування, будівництво
Academic journal. Industrial Machine Building, Civil Engineering
http://journals.nupp.edu.ua/znp
https://doi.org/10.26906/znp.2021.56.2504

UDC 624.072.233

Optimization of the double-span purlins design sketch in a framework with portal frames through the rafter stays application

Hudz Serhii[1]*, Ichanska Natalia[2], Rendyuk Serhii[3], Molchanov Petro[4]

[1] National University «Yuri Kondratyuk Poltava Polytechnic»; https://orcid.org/0000-0002-4764-8635
[2] National University «Yuri Kondratyuk Poltava Polytechnic»; https://orcid.org/0000-0001-5963-9288
[3] National University «Yuri Kondratyuk Poltava Polytechnic»; https://orcid.org/0000-0003-1593-7632
[4] National University «Yuri Kondratyuk Poltava Polytechnic»; https://orcid.org/0000-0001-5335-4281
*Corresponding author E-mail: goods.sergiy@gmail.com

Secondary structures, such as rafter stays, attached to the load-bearing element increase its stiffness, change its sketch and lead to a redistribution of internal forces. The influence of rafter stays on the bearing capacity of the frame elements was analyzed. A number of measures are considered to ensure the spatial stability of the linear elements of frame buildings, which lead to a decrease in the metal consumption of steel purlins. Based on the analysis of internal forces, the peculiarities of the working conditions of the beam were identified and described. It is proposed to increase material savings through detailed calculation. A comparison of design results is presented in software for calculating building models with portal frames

Keywords: design sketch, framework, internal forces redistribution, metal consumption, purlin, rafter stay

Оптимізація розрахункової схеми двопролітних прогонів у каркасній системі з портальними рамами із застосуванням в'язевих підкосів

Гудзь С.А.[1]*, Ічанська Н.В.[2], Рендюк С.П. [3], Молчанов П.О.[4]

[1, 2, 3, 4] Національний університет «Полтавська політехніка імені Юрія Кондратюка»
*Адреса для листування E-mail: goods.sergiy@gmail.com

Приєднані до несучого елемента (основної балки або колони рамного каркасу) різного роду другорядні конструкції, такі як встановлені планомірно в'язеві підкоси, збільшують його жорсткість, змінюють його розрахункову схему і призводять до перерозподілу внутрішніх зусиль. Проаналізовано вплив розкріплення в'язевими підкосами на несучу здатність елементів каркасу із використанням математичних методів. Розглянуто ряд заходів для забезпечення просторової стійкості лінійних несучих елементів каркасних будівель, що призводять до зменшення металоємності сталевих прогонів покриття для типового каркасу. На основі аналізу внутрішніх зусиль було виявлено та описано особливості умов роботи балки. Розкрито переваги та недоліки конструктивних рішень відповідно до принципів простоти та ефективності. Запропоновано збільшити економію матеріалу за допомогою детального розрахунку. Вирішення задачі в системі комп'ютерної алгебри wxMaxima за розрахунковою моделлю показало суттєве зменшення внутрішніх зусиль, яке має високу збіжність із результатами розрахунку моделі методом скінченних елементів. Варто звернути увагу на значний перерозподіл зусиль, а саме згинальних моментів, у прогоні. Зменшення максимального розрахункового згинального моменту в ньому може досягати 20% при середній жорсткості опор, що суттєво впливає на загальну металоємність несучих елементів каркасу (до 15%). Наведено порівняння результатів розрахунку із використанням спеціалізованого програмного забезпечення для аналізу моделей будівель із портальними рамами (Consteel). Урахування факторів, що характеризують особливості роботи прогонів покриття позитивно відображається на рівні використання і запасу міцності матеріалу. В'язеві підкоси можуть не тільки виконувати свою безпосередню функцію, але й ефективно використовуватися для підкріплення прогонів, таким чином змінюючи їх розрахункову схему, зменшуючи витрати сталі, що є позитивним чинником

Ключові слова: розрахункова схема, рамний каркас, перерозподіл зусиль, металоємність, прогін, в'язевий підкіс

Introduction

One of the major structural components in the system of the building with a steel framework is the purlin. Purlins make a considerable part of the mass of load-carrying structures (Fig. 1). Roofing purlins of solid cross-section make up an average of 10 - 15% of the mass of the building, walls - 15 - 25% depending on the building ratio of dimensions.

Figure 1 – General view of a steel framework and purlins

As structural steel for frame buildings is a significant share in the total energy-intensive production of steel, the solution of the problem of reducing the metal consumption of load-bearing elements through optimization of the design sketch is an urgent scientific and technical problem that requires the construction of an analytical model.

Conventional mathematical models in general do not characterize all the behaviour features of the structure in the building framework, especially with significant stiffness of the connected elements. In such cases, the modelling often has little in common with the actual processes, does not correspond to the real picture of the stress-strain state, and needs refinement to adequately reflect the using ratio of the cross-section by stress required to ensure the reliability and stability of the structure as a whole.

We will analyse and identify ways to solve the problem of determining the bearing capacity of elements that are prone to lateral-torsional buckling. The tendency of the element to instability occurs due to insufficient restraining of the attached structures. These structures reduce the design length of the element and increase its overall stability. Stabilization can also take place through the arrangement of structural parts: stiffeners, rafter stays, the protrusions of the beams in the supporting areas, and the adjacency of the columns in the supports. Effective restraint should be provided for members carrying either a bending moment or bending moment and axial force by lateral restraint to both flanges. This may be provided by lateral restraint to one flange and a stiff torsional restraint to the cross-section preventing the lateral displacement of the compression flange relative to the tension flange, see Figure 2.

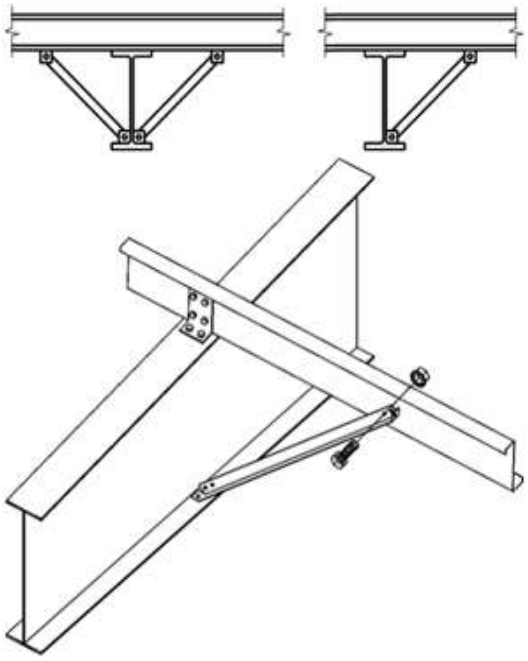

Figure 2 – The rafter-purlin-rafter stay system with double side rafter stays and one-side rafter stay; 3D-view of the typical stiff torsional restraint

Review of the research sources and publications

The articles [1 – 4] are devoted to the advanced design and geometrical optimization of steel portal frames. The papers [5, 6] present the influence of the diaphragm effect on the behaviour of pitched roof portal frames. The purpose of the research is to make a comparison between the simplified design model of a portal frame, where the supports simulating the purlins are considered with infinite axial stiffness, and a portal frame design model where the calculated stiffness of the cladding for the lateral supports is introduced manually.

Despite the leading role of purlin in the structure of roofing, conditions of its work and behaviour under loading remain low-investigated owing to the trouble of their description at difficult resistance, which the publication [7] confirms and demands careful research.

Rational designing, the detailed analysis of boundary conditions of restraining, internal forces and stresses with additional taking note of functioning features with

reliably attached enclosing structures allows to reach a significant reduction of steel costs both for purlins in particular, and on cross frames, in general, that is described in the article [8]. A mass of purlins depends mainly on their bearing capacity and also with an increase in their span - on rigidity. With an increase in the step of frames steel expenses on them decrease, however, a mass of purlins grows that has a negative effect on the total mass of the framework. The solution to the problem of high metal consumption of the building is an optimization of the static purlins sketch. Application of effective cross-sections and design sketches of roofing elements leads to a decrease in design internal forces and deformations and consequently, to a reduction of material consumptions by designs in general.

In the article [9] we can find the answer to the question of how efficient is the lateral support of rafters by stays. In single-storey steel buildings, the problem of how to stabilize long-span carrying structures occurs very often. Economic aspects are decisive for the choice of the possible bracing system. The arrangement of stays along the girder has a high degree of effectiveness. The paper [10] presents the influence of purlin-to-beam connection stiffness, allowing the development of the stress skin action, in the case of roof shear panels attached to pitched portal frames. The main purpose of this work is to separate the purlin-to-beam connection flexibility from the equivalent model and to evaluate the impact on frame lateral deformation and stability expressed by the load multiplication factor α_{cr} when purlin to rafter connection stiffness varies from flexible to a stiff one.

In combined steel structures and cross frames of the solid constant or variable cross-section for the purpose of ensuring effective work of purlins, it is possible to use the additional effect of supporting rigid rafter stays between them and the bottom flange of the frame rafter [11, 12]. They are established for flange restraining out of the frame plane from the lateral displacement and torsion and also play the role of vertical bracings, which due to the small height of the solid rafter are almost impossible to arrange. At the same time, the design sketch of purlin changes and reduction of bending moment in it can reach 20%.

Definition of unsolved aspects of the problem

In the case of evenly distributed load on the supported by rafter stays purlin, reduction of bending moment due to the presence of additional intermediate flexible supports is taken into account approximately by the introduction of a reduction factor that depends only on the ratio of edge minor spans and the total span of the single-span purlin and does not depend on the level of supports stiffness, so the development of a universal accurate method of determining the bending moment is an unsolved problem.

Problem statement

Optimization of the load-bearing elements design sketch through using a clarification analytical model of their boundary conditions is one way of solving the urgent scientific and technical problem of reducing metal consumption for frame buildings. The use of welded, built-up, spatial cross-sections of purlins or roof systems without purlins solves this problem partially too, however, complicates the process of production and mounting that by a significant number of structural components plays an essential role in their choice. In the case of the use of easy thin-walled cold-formed profiles, the material is distributed on cross-section not absolutely rationally; some of its parts are conditionally excluded from work because of excessive sensitivity to loss of local stability, forming effective design geometrical properties of the incomplete cross-section. Besides, their efficiency decreases due to the impossibility of accounting for the plastic stage of material work. The need for the creation of additional stiffeners by means of bending of the sheet makes cross-section not so simple, and its identical thickness in flanges and web of profile causes lowering of the geometrical properties important at bending. The last one partially is eliminated thanks to providing continuity of purlins which is reached by blousing one purlin of Z-shaped form on another on a certain area on both sides from intermediate support or installation of pads, similar in form. In spite of the fact that in this sketch the bigger basic bending moment is perceived by the doubled cross-section, and the span bending moment decreases, the single-span sketch of such profiles is simpler and cheaper in mounting. Therefore, we will concentrate attention further on the purlins made of rolled profiles (channels and I-beams).

Basic material and results

For a decrease in a mass of purlins and avoidance of rather a difficult assembly joint, it is reasonable to use the continuous sketch of work in both planes without a local increase in the cross-section over support, which, usually, is carried out in the form of the double-span sketch on 6 meters that is caused by dimensions of cargo transport in Ukraine for delivery of structures to a construction site. The maximum transport length is 15 meters in the European Union, thus the maximum span is 7.5 meters. The positive property of double-span purlins in comparison with single-span is their deformability lowered by 2.5 times that on condition of the defining serviceability limit state at rather a small loading can lead to preservation of about 35% of the metal mass. However, the bending moment over average support in the double-span sketch exceeds the maximum span bending moment by almost 80%. That does it determinative and predetermines excess stocks of purlins bearing capacity in the span. When using channels there is a possibility of the creation of a compound I-section in middle support areas at different spatial orientations of profiles that leads to an increase in bearing capacity, torsional stiffness, and stability of purlins.

A double-span system of purlins arrangement in a framework (Fig. 3) is a relatively stiff system intended for use as brickwork restraints. The advantage of its use is a reduced number of erection components.

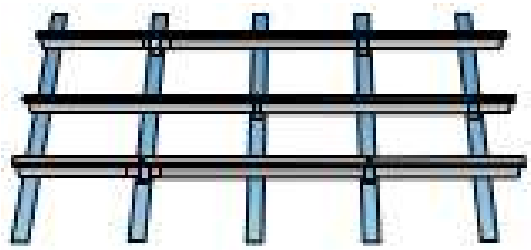

Figure 3 – Double-span system of purlins arrangement in a framework

However, at double-span purlins, there is big unevenness of edge and middle support reactions and, respectively, a difference of load on cross frames. At their consecutive arrangement, the frames located under the middle support of double-span purlins perceive loading nearly 70% more than adjacent frames. It leads to excessive consumption of steel on frames or the need for the production of cross frames with different cross-sections depending on the load on them. At alternate order of purlins arrangement, loads on each frame approximately are levelled to allow designing easier identical frames, but there is a need for developing separately edge single-span purlins of identical height. It is reached due to reduction of edge steps of frames and, respectively, the span of edge purlin approximately for 20%; reduction at the possibility of edge purlins step; selection of the cross-section of edge purlin with the following profile number of identical height according to assortment; for it is used increased strength steel or regulation of rafter stays stiffness.

On condition of the establishment of the rigid rafter, working for compression and tension in two places from frame cross-section, they can be executed from rolled equal angles with stiffeners or with short local connectors (Fig. 4).

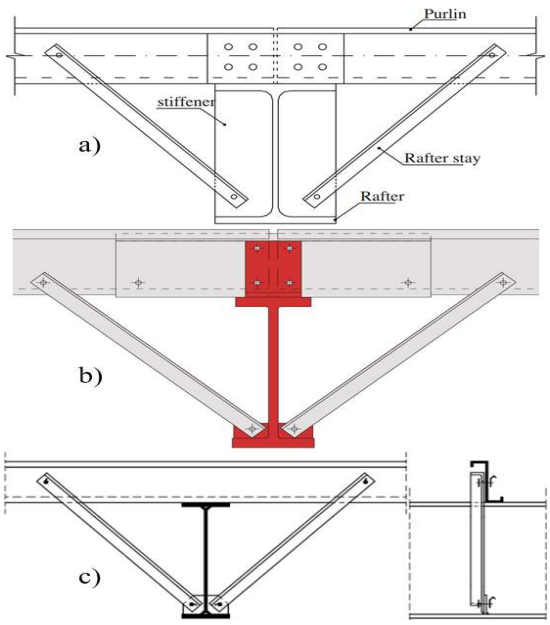

Figure 4 – Torsional restraint of a rafter with a lower flange in compression through rafter-stays
a) with stiffeners; b) with short local connectors

It is possible to execute the calculation of the purlins supported with rafter stays according to the rules of building mechanics [13]. But rafter stays need to be considered in that case as the flexible displaced supports. To do this, we must first determine the stiffness of the rafter according to the principle of virtual forces according to the scheme in Figure 5.

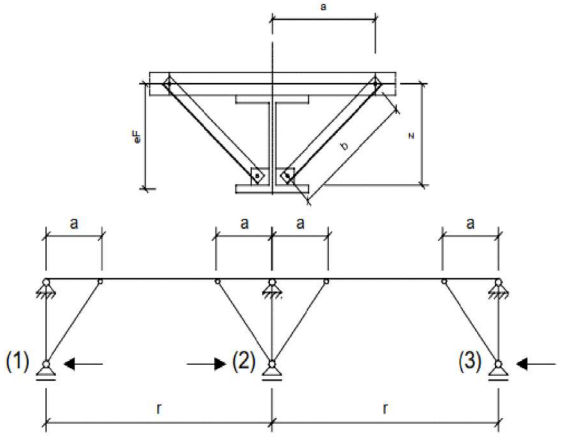

Figure 5 – Restraining of steel linear load-bearing elements by means of rafter stays and the simplified design sketch

Virtual forces are applied in the direction of the accepted displacements of the rafter lower flange, which are calculated, in this case, using the equations:

$$f_M = \int_0^l \frac{M_F M_V}{EI} dx \ ; \qquad (1)$$

$$f_N = \int_0^l \frac{N_F N_V}{EA_S} dx \ ; \qquad (2)$$

where M_F, N_F – bending moment and longitudinal force from the external load;
M_V, N_V – bending moment and longitudinal force from virtual forces;
EI, EA_S – stiffness of the purlin cross-section in bending and stiffness of the rafter stay cross-section in tension-compression.

Given the dimensions taken in Figure 5, after integration the displacements will be equal to:

$$f_M = \frac{\left(-\frac{4}{3}a + r\right)\frac{e_F^{\,2}}{4}}{EI} \ ; \qquad (3)$$

$$f_N = \frac{2b\left(\frac{b}{z}\frac{e_F}{2a}\right)^2}{EA_S} \ . \qquad (4)$$

The total stiffness of the rafter stays as pliable supports is inversely proportional to the total displacement of the rafter lower flange, and their pliability is the inverse value of the stiffness:

$$C = \frac{1}{f_M + f_N} \ ; \qquad (5)$$

$$K = \frac{1}{C} \ . \qquad (6)$$

Therefore, we will consider spans, geometrical properties of cross-sections, and elastic properties of supports (stiffness) known. For the unknowns, we will take the supporting bending moments. As the basic system, we will accept the beam divided by hinges into a row of single-span beams. In the basic system, it is possible to construct the plots of the bending moments caused by unit values of unknowns and the plot of the bending moments from the external load.

The canonical equation for the n-th (middle) support of double-span purlin will look like this:

$$M_{n-2}\delta_{n,n-2} + M_{n-1}\delta_{n,n-1} + M_n\delta_{n,n} + \\ + M_{n+1}\delta_{n,n+1} + M_{n+2}\delta_{n,n+2} + \Delta_{nF} = 0 \quad (7)$$

where M_{n-2}, M_{n-1}, M_n, M_{n+1}, M_{n+2} – unknown bending moments;

$\delta_{n,n-2}$, $\delta_{n,n-1}$, $\delta_{n,n}$, $\delta_{n,n+1}$, $\delta_{n,n+2}$ – coefficients of the canonical equation;

Δ_{nF} – a free member of the canonical equation.

The number of equations (7) will be equal to the number of unknowns. In the matrix notation, the system of canonical equations for all five intermediate supports will look like $M\delta = \Delta$, where the vector M, the matrix δ and vector Δ will be written in the form:

$$M = \begin{pmatrix} M_{n-2} \\ M_{n-1} \\ M_n \\ M_{n+1} \\ M_{n+2} \end{pmatrix}; \quad (8)$$

$$\delta = \begin{pmatrix} \delta_{n-2,n-2} & \delta_{n-2,n-1} & \delta_{n-2,n} & \delta_{n-2,n+1} & \delta_{n-2,n+2} \\ \delta_{n-1,n-2} & \delta_{n-1,n-1} & \delta_{n-1,n} & \delta_{n-1,n+1} & \delta_{n-1,n+2} \\ \delta_{n,n-2} & \delta_{n,n-1} & \delta_{n,n} & \delta_{n,n+1} & \delta_{n,n+2} \\ \delta_{n+1,n-2} & \delta_{n+1,n-1} & \delta_{n+1,n} & \delta_{n+1,n+1} & \delta_{n+1,n+2} \\ \delta_{n+2,n-2} & \delta_{n+2,n-1} & \delta_{n+2,n} & \delta_{n+2,n+1} & \delta_{n+2,n+2} \end{pmatrix} \quad (9)$$

$$\Delta = \begin{pmatrix} -\Delta_{n-2,F} \\ -\Delta_{n-1,F} \\ -\Delta_{n,F} \\ -\Delta_{n+1,F} \\ -\Delta_{n+2,F} \end{pmatrix}. \quad (10)$$

The solution of the system can be obtained by the matrix method using the inverse matrix. To express the coefficients, it is necessary to consider the bending moments and the reactions in the supports:

$$\delta_{n,n-2} = \delta_{n-2,n} = \frac{K_{n-1}}{l_{n-1}l_n}; \quad (11)$$

$$\delta_{n,n-1} = \delta_{n-1,n} = \frac{l_n}{6EI} - \frac{K_{n-1}}{l_n}\left(\frac{1}{l_{n-1}} + \frac{1}{l_n}\right); \quad (12)$$

$$\delta_{n,n} = \frac{l_n}{3EI} + \frac{l_{n+1}}{3EI} + \frac{K_{n-1}}{l_n^2} + \frac{K_{n+1}}{l_{n+1}^2}; \quad (13)$$

$$\delta_{n,n+1} = \delta_{n+1,n} = \frac{l_{n+1}}{6EI} - \frac{K_{n+1}}{l_{n+1}}\left(\frac{1}{l_{n+1}} + \frac{1}{l_{n+2}}\right); \quad (14)$$

$$\delta_{n,n+2} = \delta_{n+2,n} = \frac{K_{n+1}}{l_{n+1}l_{n+2}}; \quad (15)$$

$$\delta_{n-1,n-2} = \delta_{n-2,n-1} = \frac{l_{n-1}}{6EI} - \\ - \frac{K_{n-2}}{l_{n-1}}\left(\frac{1}{l_{n-2}} + \frac{1}{l_{n-1}}\right) - \frac{K_{n-1}}{l_{n-1}}\left(\frac{1}{l_{n-1}} + \frac{1}{l_n}\right) \quad (16)$$

$$\delta_{n-1,n-1} = \frac{l_{n-1}}{3EI} + \frac{l_n}{3EI} + \frac{K_{n-2}}{l_{n-1}^2} + K_{n-1}\left(\frac{1}{l_{n-1}} + \frac{1}{l_n}\right)^2 \quad (17)$$

$$\delta_{n-1,n+1} = \delta_{n-1,n+2} = \delta_{n-2,n+1} = \delta_{n-2,n+2} = \\ = \delta_{n+1,n-2} = \delta_{n+1,n-1} = \delta_{n+2,n-2} = \delta_{n+2,n-1} = 0; \quad (18)$$

$$\delta_{n-2,n-2} = \frac{l_{n-2}}{3EI} + \frac{l_{n-1}}{3EI} + \frac{K_{n-1}}{l_{n-1}^2} + K_{n-2}\left(\frac{1}{l_{n-2}} + \frac{1}{l_{n-1}}\right)^2 \quad (19)$$

$$\delta_{n+1,n+1} = \frac{l_{n+1}}{3EI} + \frac{l_{n+2}}{3EI} + \frac{K_{n+2}}{l_{n+2}^2} + K_{n+1}\left(\frac{1}{l_{n+1}} + \frac{1}{l_{n+2}}\right)^2 \quad (20)$$

$$\delta_{n+1,n+2} = \delta_{n+2,n+1} = \frac{l_{n+2}}{6EI} - \\ - \frac{K_{n+1}}{l_{n+2}}\left(\frac{1}{l_{n+1}} + \frac{1}{l_{n+2}}\right) - \frac{K_{n+2}}{l_{n+2}}\left(\frac{1}{l_{n+2}} + \frac{1}{l_{n+3}}\right) \quad (21)$$

$$\delta_{n+2,n+2} = \frac{l_{n+2}}{3EI} + \frac{l_{n+3}}{3EI} + \frac{K_{n+1}}{l_{n+2}^2} + K_{n+2}\left(\frac{1}{l_{n+2}} + \frac{1}{l_{n+3}}\right)^2 \quad (22)$$

The free members of the canonical equations system will be equal to the following expressions:

$$\Delta_{n,F} = \frac{B_{n,F}}{EI} + \frac{A_{n+1,F}}{EI} + \frac{K_{n-1}}{l_n}R_{n-1} + \frac{K_{n+1}}{l_{n+1}}R_{n+1}; \quad (23)$$

$$\Delta_{n-2,F} = \frac{B_{n-2,F}}{EI} + \frac{A_{n-1,F}}{EI} - \\ - K_{n-2}\left(\frac{1}{l_{n-2}} + \frac{1}{l_{n-1}}\right)R_{n-2} + \frac{K_{n-1}}{l_{n-1}}R_{n-1} \quad (24)$$

$$\Delta_{n+2,F} = \frac{B_{n+2,F}}{EI} + \frac{A_{n+3,F}}{EI} + \\ + \frac{K_{n+1}}{l_{n+2}}R_{n+1} - K_{n+2}\left(\frac{1}{l_{n+2}} + \frac{1}{l_{n+3}}\right)R_{n+2} \quad (25)$$

$$\Delta_{n-1,F} = \frac{B_{n-1,F}}{EI} + \frac{A_{n,F}}{EI} + \\ + \frac{K_{n-2}}{l_{n-1}}R_{n-2} - K_{n-1}\left(\frac{1}{l_{n-1}} + \frac{1}{l_n}\right)R_{n-1} \quad (26)$$

$$\Delta_{n+1,F} = \frac{B_{n+1,F}}{EI} + \frac{A_{n+2,F}}{EI} - \\ - K_{n+1}\left(\frac{1}{l_{n+1}} + \frac{1}{l_{n+2}}\right)R_{n+1} + \frac{K_{n+2}}{l_{n+2}}R_{n+2} \quad (27)$$

To find fictitious reactions, it is necessary to build a plot of bending moments in the basic system from a given load. The constructed plot should be taken as a fictitious load. From this load, fictitious reactions are found by the formulas (we can use ready formulas to determine fictitious reactions [13, p. 208]):

$$B_{n,F} = A_{n,F} = \frac{ql_n^3}{24}; \quad (28)$$

$$B_{n-2,F} = A_{n-2,F} = \frac{ql_{n-2}^3}{24}; \quad (29)$$

$$B_{n-1,F} = A_{n-1,F} = \frac{ql_{n-1}^3}{24}; \quad (30)$$

$$B_{n+1,F} = A_{n+1,F} = \frac{ql_{n+1}^3}{24}; \quad (31)$$

$$B_{n+2,F} = A_{n+2,F} = \frac{ql_{n+2}^3}{24}; \quad (32)$$

$$A_{n+3,F} = \frac{ql_{n+3}^3}{24}; \quad (33)$$

$$R_{n-1} = \frac{ql_{n-1}}{2} + \frac{ql_n}{2}; \quad (34)$$

$$R_n = \frac{ql_n}{2} + \frac{ql_{n+1}}{2}; \quad (35)$$

$$R_{n+1} = \frac{ql_{n+1}}{2} + \frac{ql_{n+2}}{2}; \quad (36)$$

$$R_{n-2} = \frac{ql_{n-2}}{2} + \frac{ql_{n-1}}{2}; \quad (37)$$

$$R_{n+2} = \frac{ql_{n+2}}{2} + \frac{ql_{n+3}}{2}. \quad (38)$$

Taking the supports at the location of the rafters absolutely rigid, the pliability of them will be equal to zero:

$$K_{n-3} = K_n = K_{n+3} = 0. \quad (39)$$

The wxMaxima computer algebra system was used to find the solutions of the system. Solving the problem in this software according to the calculation model showed a significant reduction of the maximum design bending moment in the double-span purlin. It can reach 20% at standard span (6 m = 1 m + 4 m + 1 m) and average stiffness of supports with rafter stays (1.0 – 1.2 kN/mm) that essentially influences the general metal consumption of load-bearing elements of a framework (to 15%). The calculation of the model by the finite element method in software Consteel showed high convergence of the results, which does not exceed 0.3% in the direction of increasing reliability (Fig. 6). It was also found the optimal angle of rafter stay inclination relative to the vertical, which is about 30°. When it increases to 45°, a slightly smaller bending moment is obtained, but the rafter stays length increases, which significantly affects the total cost of metal.

Conclusions

Rafter stays can not only perform the direct function but also be used effectively for the restraining of purlins, thus changing their design sketch and reducing the use ratio of cross-section and steel costs, which is a positive factor in reducing the metal consumption of load-bearing elements in a framework with portal frames.

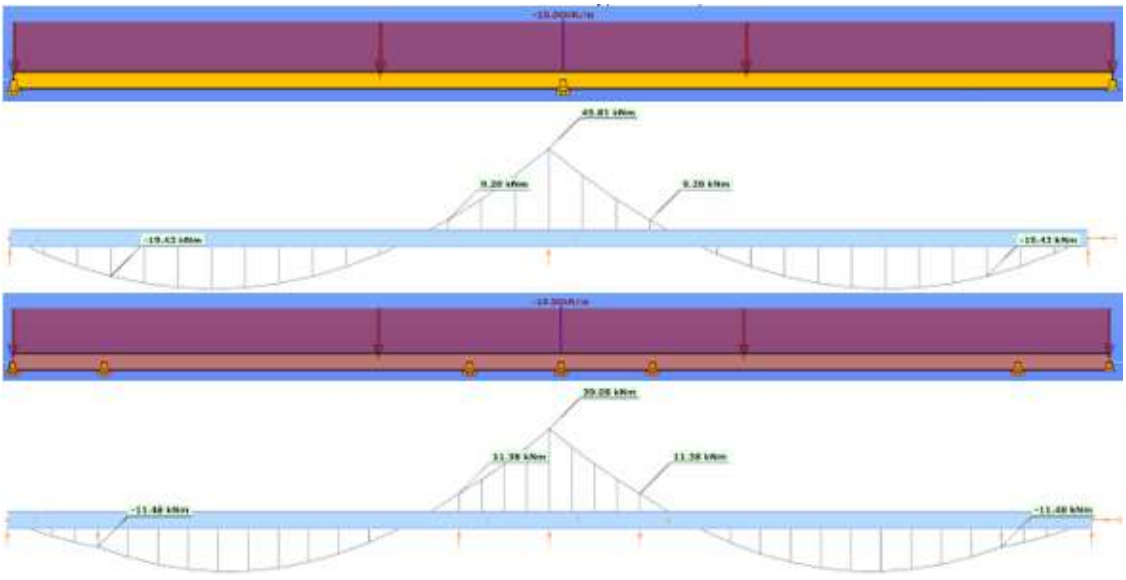

Figure 6 – Design sketches of double-span purlin without rafter stays and with them; comparison of bending moment values on plots in software Consteel

References

1. Hernández S., Fontán A.N., Perezzán J.C., Loscos P. (2005). Design optimization of steel portal frames. *Advances in Engineering Software*, 36(9), 626-633
http://dx.doi.org/10.1016/j.advengsoft.2005.03.006

2. Shah S.N.R., Aslam M., Sulong N.H.R. (2016). Geometrically optimum design of steel portal frames. *University of Engineering and Technology Taxila. Technical Journal*, 21(4), 24-30

3. Hradil P., Mielonen M. Fülöp L. (2010). Advanced design and optimization of steel portal frames. *Journal of Structural Mechanics*, 43(1), 44-60

4. Saka M.P. (2003). Optimum design of pitched roof steel frames with haunched rafters by genetic algorithm. *Computers & Structures*, 81(18-19), 1967-1978
http://dx.doi.org/10.1016/S0045-7949(03)00216-5

5. Nagy Zs., Pop A., Moiș I., Ballok R. (2016). Stressed skin effect on the elastic buckling of pitched roof portal frames. *In Structures*, 8, 227-244
http://dx.doi.org/10.1016/j.istruc.2016.05.001

6. Wrzesien A.M., Lim J.B.P., Xu Y., IMacLeod.A., Lawson R.M. (2015). Effect of Stressed Skin Action on the Behaviour of Cold-Formed Steel Portal Frames. Engineering *Structures*, 105, 123-136
http://dx.doi.org/10.1016/j.engstruct.2015.09.026

7. Hudz S., Storozhenko L., Gasii G., Hasii O. (2020). Features of Operation and Design of Steel Sloping Roof Purlins. *Lecture Notes in Civil Engineering*, 73, 65-73
https://doi.org/10.1007/978-3-030-42939-3_8

8. Гудзь С.А., Гасій Г.М., Дарієнко В.В. (2020). Розвинена модель розрахунку сталевих розкріплених елементів на стійкість при сумісній дії поперечного згину та кручення. *Сучасні будівельні конструкції з металу та деревини*, 24, 43-52
https://doi.org/10.31650/2707-3068-2020-24-43-52

9. Pasternak H., Hannebauer D. (2001). Wie wirkungsvoll sind Flanschstreben bei der Stabilisierung von Riegeln? *Bauingenieur*,76.10, 444-447

10. Nagy Zs., Moiș I., Pop A., Dező A. (2018). The influence of purlin-to-beam connection stiffness in stress skin action on portal frames. *ICTWS 2018*, Lisbon, Portugal

11. Gogol M., Zygun A., Maksiuta N. (2018). New effective combined steel structures. *International Journal of Engineering and Technology*, 7 (3.2), 343-348
https://doi.org/10.14419/ijet.v7i3.2.14432

12. Катюшин В.В. (2005). *Здания с каркасами из стальных рам переменного сечения (расчет, проектирование, строительство)*. Москва: Издательство «Стройиздат

13. Чихладзе Е.Д. (2002). *Будівельна механіка*. Харків: УкрДАЗТ

1. Hernández S., Fontán A.N., Perezzán J.C., Loscos P. (2005). Design optimization of steel portal frames. *Advances in Engineering Software*, 36(9), 626-633
http://dx.doi.org/10.1016/j.advengsoft.2005.03.006

2. Shah S.N.R., Aslam M., Sulong N.H.R. (2016). Geometrically optimum design of steel portal frames. *University of Engineering and Technology Taxila. Technical Journal*, 21(4), 24-30

3. Hradil P., Mielonen M. Fülöp L. (2010). Advanced design and optimization of steel portal frames. *Journal of Structural Mechanics*, 43(1), 44-60

4. Saka M.P. (2003). Optimum design of pitched roof steel frames with haunched rafters by genetic algorithm. *Computers & Structures*, 81(18-19), 1967-1978
http://dx.doi.org/10.1016/S0045-7949(03)00216-5

5. Nagy Zs., Pop A., Moiș I., Ballok R. (2016). Stressed skin effect on the elastic buckling of pitched roof portal frames. *In Structures*, 8, 227-244
http://dx.doi.org/10.1016/j.istruc.2016.05.001

6. Wrzesien A.M., Lim J.B.P., Xu Y., IMacLeod.A., Lawson R.M. (2015). Effect of Stressed Skin Action on the Behaviour of Cold-Formed Steel Portal Frames. *Engineering Structures*, 105, 123-136
http://dx.doi.org/10.1016/j.engstruct.2015.09.026

7. Hudz S., Storozhenko L., Gasii G., Hasii O. (2020). Features of Operation and Design of Steel Sloping Roof Purlins. *Lecture Notes in Civil Engineering*, 73, 65-73
https://doi.org/10.1007/978-3-030-42939-3_8

8. Hudz S.A., Gasii G.M., Darienko V.V. (2020). Developed model for calculating steel restrained elements for stability under the combined action of transverse bending and torsion. *Modern building structures made of metal and wood*, 24, 43-52
https://doi.org/10.31650/2707-3068-2020-24-43-52

9. Pasternak H., Hannebauer D. (2001). Wie wirkungsvoll sind Flanschstreben bei der Stabilisierung von Riegeln? *Bauingenieur*,76.10, 444-447

10. Nagy Zs., Moiș I., Pop A., Dező A. (2018). The influence of purlin-to-beam connection stiffness in stress skin action on portal frames. *ICTWS 2018*, Lisbon, Portugal

11. Gogol M., Zygun A., Maksiuta N. (2018). New effective combined steel structures. *International Journal of Engineering and Technology*, 7 (3.2), 343-348
https://doi.org/10.14419/ijet.v7i3.2.14432

12. Katyushin V.V. (2005). Buildings with frameworks made of steel frames of variable cross-section (calculation, design, construction). Moscow: Publishing house «Stroyizdat»

13. Chikhladze E.D. (2002). *Building mechanics*. Kharkiv: UkrDAZT

Збірник наукових праць. Галузеве машинобудування, будівництво
Academic journal. Industrial Machine Building, Civil Engineering
http://journals.nupp.edu.ua/znp
https://doi.org/10.26906/znp.2021.56.2505

UDC 69.002.5

Structural analysis of vibration platform for panel units forming and consideration of its utilizing options

Nazarenko Ivan[1]*, Diachenko Oleksandr[2], Pryhotskyi Vasyl[3], Nesterenko Mykola[4]

[1] Kyiv National University of Construction and Architecture https://orcid.org/0000-0002-1888-3687
[2] Kyiv National University of Construction and Architecture https://orcid.org/0000-0001-8199-2504
[3] Kyiv National University of Construction and Architecture https://orcid.org/0000-0002-7741-838X
[4] National University «Yuri Kondratyuk Poltava Polytechnic» https://orcid.org/0000-0002-4073-1233
*Адреса для листування E-mail: i_nazar@i.ua

The review of the utilizing directions of the shakers of various designs for consolidation of concrete mixtures at the production of flat panel elements is executed. The major limitations and advantages of certain designs of shakers are analyzed, the main production technologies of flat reinforced concrete units in which their use is most reasonable. The evaluation of prospects for the equipment of different designs to be quickly adjusted to the production program changes is made. The main idea in the production of flat panel elements on vibrating pads using Industry 4.0 technologies is to use the latest information technology and automation and that business and engineering processes are deeply integrated.

Keywords: readjustment, pallet, vibration platform, technology, volume consolidation.

Аналіз конструкцій віброустановок панельних елементів та напрямків їх використання

Назаренко І.І.[1]*, Дьяченко О.С.[2], Пригоцький В.В.[3], Нестеренко М.М.[4]

[1] Київський національний університет будівництва та архітектури
[2] Київський національний університет будівництва та архітектури
[3] Київський національний університет будівництва та архітектури
[4] Національний університет «Полтавська політехніка імені Юрія Кондратюка»
*Адреса для листування E-mail: i_nazar@i.ua

Виконано аналіз напрямків використання різних конструкцій вібромайданчиків для ущільнення бетонних сумішей при виробництві плоских панельних елементів із можливим застосуванням сучасних технологій індустрії 4.0 для підвищення загальної ефективності будівництва. Проаналізовано основні недоліки і переваги тих чи інших конструкцій вібромайданчиків, виявлені основні технології виробництва плоских залізобетонних виробів, у яких їх використання є найбільш доцільним. Виконано оцінку і виявлено можливості обладнання різних конструкцій бути швидко переналагодженими під зміни виробничої програми. Встановлено, що у переважній більшості у технології збірного залізобетону використовують малорухомі бетонні суміші з яких у результаті виробляють потрібні як за конфігурацією так і за належною якістю поверхонь суцільні (одношарові) панельні залізобетонні елементи, які відповідають необхідним вимогам по міцності, водонепроникності, морозостійкості і при цьому з належною якістю поверхонь. Останні десятиліття все більшого використання набувають різного роду багатошарові панельні елементи, які складаються з шарів залізобетону, розділеного різними за складом ізолювальними матеріалами. У обох випадках суміш, яка завантажена у форму, вимагає додаткового ущільнення для зменшення кількості повітря і витіснення зайвої рідини. Найбільш розповсюдженим методом ущільнення є об'ємний метод з використанням вібраційної дії на оброблюване середовище, для чого зазвичай використовують вібраційні майданчики різних конструкцій. Встановлено, що основна ідея при виробництві плоских панельних елементів на вібромайданчиках із застосуванням технологій індустрії 4.0 полягає в тому, щоб використовувати новітні інформаційні технології та автоматизацію, щоб бізнес-процеси та інженерні процеси були глибоко інтегровані. Завдяки цьому виробництво працюватиме гнучким, ефективним та екологічно чистим способом із постійно високою якістю та низькою вартістю.

Ключові слова: переналагодження, палета, віброустановка, технологія, об`ємне ущільнення.

Introduction

Nowadays, the selection and use of equipment that would best meet the technological production scheme of flat reinforced concrete products is an increasingly important task. At the same time, the most responsible process is the consolidation of concrete mixtures on shakers, vibrating tables, which should ensure high productivity and product quality. In addition, such equipment should provide opportunities for rapid readjustment of production lines depending on market needs.

Review of the research sources and publications

In times of increasing use of the monolithic-frame method of building construction, the technology of manufacturing precast reinforced concrete structures seems to have lost its relevance. However, it opens a new milestone in the form of the use of precast units in monolithic technology, various types of floors, cabins, which can accelerate the construction rate by reducing the number of concrete works on the construction site [1]. The costs of materials used in the reinforcement of units in the factory are much lower [2]. Also, this technology does not lose its relevance in the construction of low-rise buildings for both private and non-residential use. The most common method of compacting concrete mix in factory production conditions is the three-dimensional vibration method of forming [3].

Definition of unsolved aspects of the problem

The equipment used in compaction has a wide range of both design and manufacturing technology of products in which it is advisable to use, which causes problems in choosing both equipment [4] and technological parameters of the compaction process [8].

Problem statement

The work aims to review the designs of vibrating equipment for volumetric compaction of concrete mixtures and to analyze the production technologies in which their use is most appropriate.

To achieve this goal it is necessary to solve the following tasks:

– to inspect the most common designs of vibrating equipment for forming and compacting flat reinforced concrete units;

– analyze their advantages and limitations;

– assess the possibilities of different designs of vibration equipment for rapid readjustment, depending on changes in the production program.

Basic material and results

The vast majority of precast reinforced concrete technology uses low-density concrete mixtures, which result in manufacturing the continuous (single layer) reinforced concrete panel units of the required configuration and proper surface which meet the necessary criteria of strength, water- and frost resistance having an independent surface quality

In recent decades, various types of multilayer panel elements, which consist of layers of reinforced concrete separated by insulating materials of different compositions, have become increasingly used.

In both cases, the mixture, which is loaded into the mold, requires additional compaction to reduce the amount of air and displace excess fluid [7]. The most common method of compaction is the three-dimensional method with the use of vibration action on the treated medium, which usually uses vibrating pads of different designs.

In the production of solid reinforced concrete units in the conditions of flow-aggregate and conveyor technology, the most common at present are vibrating stationary platforms of frame or block construction with removable forms (Fig. 1) [2].

Figure 1 – Vibration platform for compaction of concrete mix in removable forms

The following technological and operational requirements are set for them: achieving the required degree of compaction of the concrete mixture throughout the unit, high productivity, reliability, as well as durability of equipment and compliance with sanitary and hygienic standards, ease of maintenance.

Vibration platforms of the frame type have been used in the twentieth century for a long time. They became most widespread due to developments and research at Poltava Civil Engineering Institute in 1972 and were mostly used for compaction of large concrete products weighing 10-50 tons, with low noise, oscillations mainly in the horizontal plane, and operation at low oscillation frequency 24 Hz.

We will consider designs of frame vibrating platforms in more detail by the example of the VPG 1,5x12 vibrating platform which scheme is shown in fig.2.

Vibrating platform HSV 1.5×12 consists of a movable frame 1, which is welded from channels and steel sheet, in the middle part there is a ledge 2 for rigid mounting unbalanced vibrator excitation of circular action with a vertical shaft (vibrator) 3, the movable frame rests on eight elastic rubber-metal supports mounted on the support frame 5. Rubber-metal supports work on shear and compression, providing horizontal and vertical components of vibration.

The electric motor 6 is mounted on the lower support frame and transmits rotation using a V-belt transmission to the vibrator pulley. The mold with the concrete mixture is fixed on a movable frame between the rigid stops 7.

The simplicity of a design allows to reach low noise level in workplaces, has high reliability and efficiency of compaction.

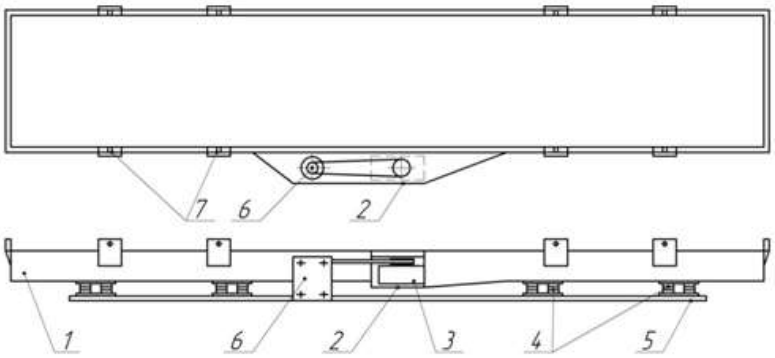

Figure 2 – VPG 1,5×12 vibrating platform scheme

The simplicity of a design allows to reach low noise level in workplaces, has high reliability and efficiency of compaction.

The disadvantage of frame vibrating tables is the high metal capacity of the structure, due to the requirements for rigidity of the structure, which must be kept under high loads, transmit vibrations from one vibrator and distribute them evenly over the whole area of the mixture.

The blocked vibrating tables were another development area for compaction of concrete mixtures with vibration or shock-vibration action on the mix. Serial block vibrating tables such as SMZh-187 and SMZh-200 were proposed in the late 50s of the last century at the VNDI Buddormash. These vibrating tables were generating vertical harmonic frequency oscillations up to 50 Hz. The concrete`s mixture form is mounted on a frame with electromagnetic grips. The scheme of construction of the vibrating table SMZh-187 is presented in Fig.3.

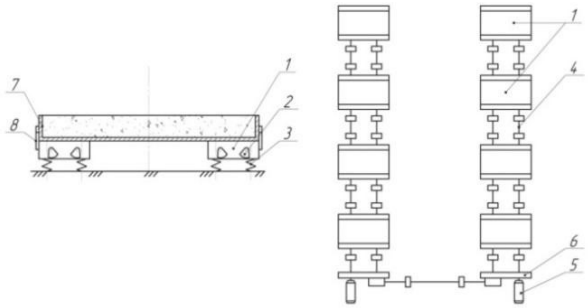

Figure 3 – Scheme of the vibrating table SMZh-187

The SMZh-187 vibrating tables consist of eight vibrating blocks 1 with the vibrators 2 mounted on them, generating vertical fluctuations.

Vibrating blocks rest on the elastic pile 3, which is mounted on the foundation. The vibrators of all four vibrating blocks are interconnected by cardan shafts 4, and they provide synchronous operation. The drive of the vibrating table consists of two motors 5, which are connected to the vibrators by synchronizers 6 and cardan shafts. The form with the concrete mixture 7 is fixed with the help of electromagnetic grips 8.

Low-frequency vibrating tables with vertical oscillations freely mounted on them through elastic gaskets forms have also become quite common in reinforced concrete plants due to high efficiency in the compaction of mixtures. The low-frequency vibrating tables include the shock-vibration platform UVP-10 (Fig. 4), developed based on the design of the vibrating table SMZh-187A.

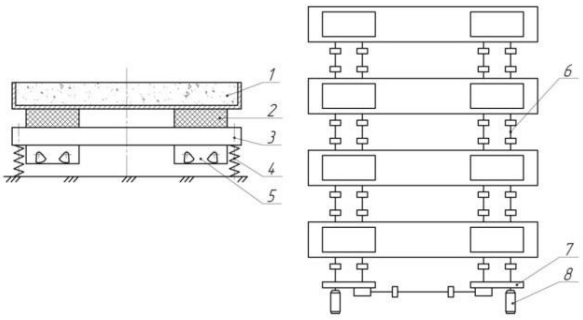

Figure 4 – Scheme of shock-vibration table UVP-10

It consists of four vibrating blocks 3 with vibrators 5 connected to them from below, which create vertical oscillations. The frame of each vibrating block rests on elastic support elements 4 mounted on the foundation. The vibrators of all four vibrating blocks are interconnected by cardan shafts 6 due to their synchronous operation is provided. The drive of the vibrating table consists of two motors 8, of which there are synchronizers-frames 7 and cardan shafts are connected to the vibrating frames.

The main difference is that between the mold with mixture 1 and the vibrating block table 3, elastic rubber elements 2 are established, which allows implementing the shock-vibration mode of the site. The shock-vibration mode of work increases compaction efficiency, and rubber elements reduce the noise load in the workshop.

The block design of vibrating tables, in general, allows adjusting them to a certain type-size of the product, which is planned for production on the production line, by changing the number of vibrating blocks. This, in turn, reduces the company`s costs when changing the production program, changing the size of products, and more.

Among the disadvantages of block vibrating tables there may be noted lower, compared to the frame, reliability due to the high number of components: gearboxes-synchronizers, elastic supports, card shafts, due to which such structures create high noise levels in the workplace.

There are constructions of tables in which the frame with vibration exciters of oscillations is at the same time a pallet (form) for concrete mix (Fig. 5), sometimes they are called stationary vibrating tables.

Figure 5 – The vibrating table with mounted exciters of oscillations

The scheme of this table is presented in Fig.6. It consists of a frame 1, which is mounted on elastic piles 2. The installation is actuated by excited oscillations 3, which are mounted asymmetrically on the structure`s frame [5]. The structure`s frame is directly and is a pallet (form) on which to perform compaction of concrete mixtures 4. The dimensions of the future product are formed due to removable magnetic boards and partitions in the plan. On such vibrating tables, they perform laying of reinforcing structures, concrete mix, sealing, and partial steaming of the product, thanks to the heating registers established under the table. After the product has gained sufficient strength, it is removed from the vibrating table and transported to the steaming rooms for final aging.

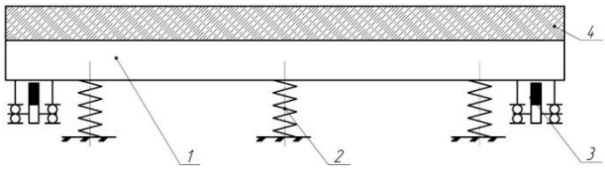

Figure 6 – Scheme of a vibrating table with mounted exciters of oscillations

These vibrating tables have advantages such as reducing the metal content of the structure due to the uniform installation of mounted vibrators along the contour of the frame, which reduces its stiffness and increases the uniformity of oscillation amplitudes over the area of the forming surface and energy transfer. Product`s different sizes compaction is due to the use of the magnetic boards and partitions.

The disadvantage is the lower productivity due to the lack of removable forms, due to such tables being used in the stand technology of small and medium-scale production of flat reinforced concrete products.

Recently, the use of multi-layered elements as prefabricated units, which are several materials connected in one panel, is becoming more and more common.

These include the following types of products (Fig.7-9):

- double wall (Fig. 7, a), consisting of two parallel prefabricated reinforced concrete slabs with a thickness of at least 50 mm, interconnected by lattice trusses at some distance, resulting in an air layer appear, which allows reducing thermal conductivity;
- double wall with additional intermediate insulation with foam (Fig. 7, b), which serves to further reduce the thermal conductivity of the panel for use in cold regions;
- wall sandwich panel (Fig. 8, a), which consists of an outer massive reinforced concrete part and smooth inner slab, the space between which is filled with insulating material;
- facade walls (sandwich panels) (Fig. 8, b), which differ from the previous type of panels in that the outer (front) part is provided with various design solutions, such as washing, grinding, or polishing and the use of matrices and facing materials for decoration;
- walls made of light concrete (Fig. 9), with or without decoration of the front sides.

Figure 7 – Multilayer thin-walled elements:
a – with an air layer;
b – with an air layer and foam

Figure 8 – Sandwich panels with a heat-insulating layer:
a – without external decoration;
b – with external decoration

Figure 9 – Solid slabs of lightweight concrete

Using prefabricated multilayer slabs (panels) enables operating all the advantages of precast concrete technology. It significantly reduces the time of building concrete work on the construction site and reduces their cost, also creating residential and non-residential buildings that will comply with modern technical solutions for energy efficiency.

As you can see from the above elements, the finished panels vary in type, form and size. From this, we can conclude that they require the use of appropriate production technologies and equipment that will allow without significant readjustments of production lines to perform their production.

A large number of companies around the world specialize in the development of such equipment, including Ebawe, Avermann, Weckenmann.

The main requirement for more flexibility and productivity of the technological line is using fully standardized variable forms, the so-called "forming pallets" (Fig. 10).

Figure 10 – Molding pallet for the production of panels

Such pallets pass through all processes at the production of prefabricated elements and are used both at the bench and on aggregate-current technology. The dimensions of the future product in the plan are formed due to removable magnetic boards and partitions.

To complete the compaction of mixtures in pallets, the vibrating units are used (Fig. 11), in which all the elements inherent in conventional vibrating tables are separate nodes. They are connected only by an installed molding pallet.

a) b)

Figure 11 – Vibrating structures for mixtures compaction in molding pallets of different manufacturers:
a) Ebawe; b) Weckenmann

In this case, such structures can perform seals in the vertical or horizontal directions and simultaneously in both directions.

The schematic diagram of this vibrating structure type is shown in Fig.12 and consists of mounted on the foundation of elastic supports 1, vibrating blocks 2, vibroisolating from the foundation by elastic elements 3. The elastic supports and vibrating blocks have locks 4 for fixing the molding pallet 5 with concrete mixture 6 during the sealing process. The lock for the fastening of a pallet can be electromagnetic, pneumatic, or with a mechanical drive.

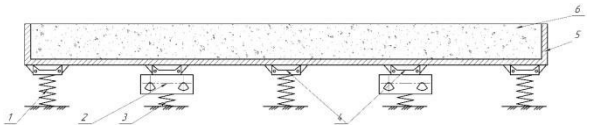

Figure 12 – Schematic diagram of a vibrating structure for vibrating molding pallets

The high reliability of the structure due to the separation of the nodes from each other [6], low noise, high performance, the ability to change the direction of oscillations, and vibration frequency during operation are among the advantages. It makes it possible to perform compaction of elements with different characteristics and enables flexible and logistical efficient organizing the production process and its quick-adjusting when changing the production program, which in today's environment is an important factor.

Among the disadvantages is the inexpediency of their use in small and medium-scale production of prefabricated structures.

Swivel (tipping) vibrating tables or tilters have become widespread (Fig. 13). They are used in the production of flat precast concrete products (single-layer, multilayer). The design of rotary tables is an improved version of the stationary vibrating table, which is additionally equipped with mechanical devices or hydraulic cylinders to move the surface from horizontal to close to vertical (about 80 degrees to horizontal).

Figure 13 –Weckenmann turntable

Moving the molding surface to an almost vertical position enables the safe removal of the element with the least risk of damage.

Therefore, the industry needs a radical change and it is the Industrie 4.0 that addresses this change. The core idea of Industrie 4.0 is to use the emerging information technologies to implement IoT and services so that business processes and engineering processes are deeply integrated making production operate in a flexible, efficient, and greenway with constantly high quality and low cost [10, 11].

Conclusions

As a result of the analysis completed, the main structures of vibrating machines for three-dimensional compaction of concrete mixtures in the production of precast reinforced concrete structures are determined. The production technologies in which they are mostly used were given. Their disadvantages and advantages in terms of logistically efficient organization of production activities are considered. It was found that in the modern realities using flat prefabricated reinforced concrete structures, it is advisable to choose such equipment in their production that will allow you to quickly readjust production depending on changes in the production program without excessive costs.

References

1. Борейко В.І., Притула М.Ю. (2011). Перспективи виробництва будівельних матеріалів в Україні. *Збірник наукових праць. Проблеми раціонального використання соціально-економічного та природно-ресурсного потенціалу регіону: фінансова політика та інвестиції*. XVII (4), 64-71

2. Назаренко І.І. (1999). *Машини для виробництва будівельних матеріалів*. Київ, КНУБА

3. Лермит Р. (2007). *Проблемы технологии бетона*: Пер. с фр. / под ред. А.Е. Десова. Москва: Изд-во ЛКИ

4. Иткин А.Ф. (2009) *Вибрационные машины для формования бетонных изделий*. Київ: «МП Леся»

5. Назаренко І.І., Дєдов О.П., Дьяченко О.С. (2018) Огляд конструкцій існуючих навісних збудників коливань та дослідження ефективності їх використання для покращення ущільнення залізобетонних виробів на вібраційних установках. *Техніка будівництва*, 39, 46-55

6. Делембовський М.М. (2021). Вплив режимів експлуатації і властивостей елементів вібромашин будівельної індустрії на процеси надійності. *Грааль науки*, 4, 209-214

7. Maslov O., Batsaikhan J., Salenko Yu. (2018). The theory of concrete mixture vibratory compacting. *International Journal of Engineering and Technology*, 7(3), 239-244

8. Pinţoi R., Barbu A.M., Ionescu A. (2020). Vibrations influence on concrete compaction. *Applied Mechanics and Materials*, 896, 355-360

9. Nesterenko M.P., Nesterenko M.M., Orysenko O.V., Sklyarenko T.O. (2019). Vibrating tables with the spatial oscillations of the moving frame technological properties for forming reinforced concrete products. *Academic Journal. Industrial Machine Building, Civil Engineering,* 2(53), 13-18
https://doi.org/10.26906/znp.2019.53.1881

10. Dallasega P., Rauch E., Linder C. (2018). Industry 4.0 as an enabler of proximity for construction supply chains: A systematic literature review. *Computers in Indust*ry, 99, 205-225
https://doi.org/10.1016/j.compind.2018.03.039

11. Wang S., Wan J., Li D., Zhang C. (2016). *Implementing* Smart Factory of Industrie 4.0: An Outlook. *International Journal of Distributed Sensor Networks,* 12, 3159805
https://doi.org/10.1155%2F2016%2F3159805

1. Borejko V. I., Prytula M.Ju. (2011). Prospects for the production of building materials in Ukraine. *Academic Journal. Problems of rational use of the socio-economic and natural resource potential of the region: financial policy and investments.* XVII (4), 64-71

2. Nazarenko I.I. (1999). *Machines for the production of building materials*. Kyiv, KNUBA

3. Lermit R. (2007). *Problems of concrete technology*: Trans. with fr. / Ed. A.E. Desov. Moscow: Publishers LKI

4. Itkin A.F. (2009) *Vibration machines for forming concrete products*. Kyiv: «MP Lesya»

5. Nazarenko I.I., Dedov O.P., Diachenko O.S. (2018) Overview of the constructions of existing hinged vibrators and the study of the efficiency of their use to improve the compacting of reinforced concrete products on vibration platforms. *Structural engineering*, 39, 46-55

6. Delembovs'kyj M.M. (2021). Influence of operating modes and properties of elements of vibrating machines of the construction industry on reliability processes. *Grail of science*, 4, 209-214

7. Maslov O., Batsaikhan J., Salenko Yu. (2018). The theory of concrete mixture vibratory compacting. *International Journal of Engineering and Technology*, 7(3), 239-244

8. Pinţoi R., Barbu A.M., Ionescu A. (2020). Vibrations influence on concrete compaction. *Applied Mechanics and Materials*, 896, 355-360

9. Nesterenko M.P., Nesterenko M.M., Orysenko O.V., Sklyarenko T.O. (2019). Vibrating tables with the spatial oscillations of the moving frame technological properties for forming reinforced concrete products. *Academic Journal. Industrial Machine Building, Civil Engineering,* 2(53), 13-18
https://doi.org/10.26906/znp.2019.53.1881

10. Dallasega P., Rauch E., Linder C. (2018). Industry 4.0 as an enabler of proximity for construction supply chains: A systematic literature review. *Computers in Indust*ry, 99, 205-225
https://doi.org/10.1016/j.compind.2018.03.039

11. Wang S., Wan J., Li D., Zhang C. (2016). *Implementing* Smart Factory of Industrie 4.0: An Outlook. *International Journal of Distributed Sensor Networks,* 12, 3159805
https://doi.org/10.1155%2F2016%2F3159805

Збірник наукових праць. Галузеве машинобудування, будівництво
Academic journal. Industrial Machine Building, Civil Engineering
http://journals.nupp.edu.ua/znp
https://doi.org/10.26906/znp.2021.56.2506

UDC 699.86:[692.52:727

Determination of optimal variant for insulation of the attic floor of the educational building

Yurin Oleg[1], Zyhun Alina[2]*, Kliepko Anastasiia[3], Mahlinza Qiniso[4]

[1] National University «Yuri Kondratyuk Poltava Polytechnic» https://orcid.org/0000-0002-9290-9048
[2] National University «Yuri Kondratyuk Poltava Polytechnic» https://orcid.org/0000-0002-1743-2294
[3] National University «Yuri Kondratyuk Poltava Polytechnic» https://orcid.org/0000-0001-7200-1510
[4] National University «Yuri Kondratyuk Poltava Polytechnic» https://orcid.org/0000-0003-2132-5755
*Corresponding author E-mail: alinazygun@gmail.com

The analysis of heat-protective properties of the existing attic floor of the educational building of National University «Yuri Kondratyuk Poltava Polytechnic» showed their non-compliance with regulatory requirements. The required thickness of the insulation in the attic floor was determined without taking into account the heat-conducting inclusions. Overlapping areas with heat-conducting inclusions reduce the reduced heat transfer resistance. In the attic floor, these are the areas where the floor adjoins the inner and outer walls. It is possible to increase the reduced heat transfer resistance due to additional insulation of external and internal walls within the cold attic. The study determined the optimal length of additional insulation for eight different options. To determine the optimal value, options for additional insulation of external and internal walls within the attic with a simultaneous reduction in the thickness of the insulation on the attic floor were considered.

Keywords: heat-conducting inclusions, insulation of cold attic walls, optimal insulation option.

Визначення оптимального варіанту утеплення горищного перекриття навчального корпусу

Юрін О.І.[1], Зигун А.Ю.[2]*, Клєпко А.В.[3], Кінісо Махлінза[4]

[1,2,3,4] Національний університет «Полтавська політехніка імені Юрія Кондратюка»
*Адреса для листування E-mail: alinazygun@gmail.com

Робота присвячена визначенню оптимального варіанту утеплення горищного перекриття навчального корпусу Національного університету «Полтавська політехніка імені Юрія Кондратюка». Аналіз теплозахисних властивостей існуючого горищного перекриття показав невідповідність їх нормативним вимогам. Була визначена необхідна товщина утеплювача у горищному перекритті без урахування теплопровідних включень. Але на теплозахисні властивості горищного перекриття значний вплив здійснюють ділянки перекриття з теплопровідними включеннями. Вони зменшують приведений опір теплопередачі. Такими ділянками у горищному перекритті є ділянки примикання перекриття до внутрішніх та зовнішніх стін. Збільшити приведений опір теплопередачі можливо за рахунок додаткового утеплення зовнішніх та внутрішніх стін у межах холодного горища. У роботі були розглянуті варіанти додаткового утеплення у межах холодного горища: зовнішньої стіни з зовнішньої сторони, зовнішньої стіни з внутрішньої сторони, зовнішньої стіни з внутрішньої та зовнішньої сторони, внутрішніх стін, зовнішньої стіни з зовнішньої сторони та внутрішніх стін, зовнішньої стіни з внутрішньої сторони та внутрішніх стін, зовнішньої стіни з обох сторін та внутрішніх стін, збільшення товщини утеплювача горищного перекриття. Були визначені оптимальні варіанти довжини додаткового утеплення ділянок з теплопровідними включеннями. За оптимальні приймалися такі довжини додаткового утеплення при яких подальше збільшення довжини утеплювача не дає істотного збільшення приведеного опору теплопередачі. Дослідження показали, що варіант підвищення товщини утеплювача на горищному перекритті до 400 мм дозволяє досягнути нормованого значення теплозахисту для горищного перекриття. Але даний варіант утеплення є економічно не доцільним так як потребує значного збільшення об'єму утеплювача. Для визначення економічно оптимального варіанта були розглянуті варіанти додаткового утеплення зовнішніх та внутрішніх стін у межах горища з одночасним зменшенням товщини утеплювача на горищному перекритті.

Ключові слова: теплопровідні включення, утеплення стін холодного горища, оптимальний варіант утеплення

Introduction

Ensuring the projected regulatory level of thermal protection of buildings is the main task of modern design and construction in Ukraine.

Heat losses through sections of walls of complex configuration are usually different from heat losses through sections accepted for thermal calculation. Areas of complex shape include nodal joints of walls with mezzanine floors, adjacency of window filling to the walls, corners of walls, etc. Such and similar nodes are «cold bridges», which significantly reduce the value of the reduced resistance to heat transfer of enclosing structures.

Additional insulation of the main field of enclosing structures is economically impractical, as it requires a significant increase in the volume of insulation. Therefore, it is necessary to find ways to insulate the nodes with heat-conducting inclusions that would bring the reduced resistance of heat transfer to the requirements of the norms.

Review of the research sources and publications

Research on building thermophysics devoted to the calculation of temperature fields of sections of external enclosing structures of complex configuration belong to such prominent scientists as K. Fokin [1], A. Lykov [2], V. Ilinskiy [3], M. Miheev [4], A. Shklover [5], A. Mogilat [6], as well as modern research H. Fareniuk [7], A. Prishchenko [8], M. Tymofieiev [9, 10], S. Fomin [11].

Definition of unsolved aspects of the problem

A significant number of works by many authors are devoted to the study of heat-protective properties of sections of external walls of complex configuration [12, 13].

The option of increasing the heat-protective properties of the cold attic floor due to additional insulation of its external and internal walls was not considered. Research in this area is relevant.

Problem statement

The aim of the work is to increase the level of thermal protection of cold roof enclosing structures by improving the thermal solutions of attic floor units with heat-conducting inclusions.

Research objectives:

– perform an analysis of the heat-protective properties of the floor of the educational building of the National University «Yuri Kondratyuk Poltava Polytechnic»;

– perform an analysis of ways to improve the heat-protective properties of the attic floor with heat-conducting inclusions. Identify a cost-effective option.

Basic material and results

Thermally conductive inclusions reduce the reduced resistance to heat transfer of enclosing structures. In the construction of the attic floor, heat-conducting inclusions are the joints between the outer and inner walls with the floor structure.

To calculate the reduced heat transfer resistance of the attic floor, it is necessary to know the values of the linear heat transfer coefficients of these heat-conducting inclusions.

Determination of linear heat transfer coefficients is performed according to the method [14,15], which involves the calculation of temperature fields of these areas.

The cold attic of the educational building of the National University «Yuri Kondratyuk Poltava Polytechnic» was accepted for research. The performed researches of the value of heat protection of the existing external enclosing constructions of the educational building do not satisfy the norms. The facades of the educational building are shown in Figure 1 and 2.

Figure 1 – The main facade of the educational building

Figure 2 – Side facade of the educational building

Areas, where the linear heat transfer coefficients were determined, are:

1. Connection of the outer wall with the construction of the attic floor (node 1);

2. Connection of the inner wall with the construction of the attic floor (node 2).

ELCUT software is used for further calculations of two-dimensional temperature fields.

To increase the heat-protective properties of the outer wall, it was proposed to insulate it with a layer of mineral wool IZOVAT, density $\rho_0 = 135$ kg/m^3 and thickness 150 mm. Insulation must be performed on the outside after removing the finishing layer from the ceramic tile, cleaning and repairing the outer surface of the wall.

Determination of the linear heat transfer coefficient of the node №1.

The calculation scheme for determining the linear coefficient of the node №1 is shown in Figure 3.

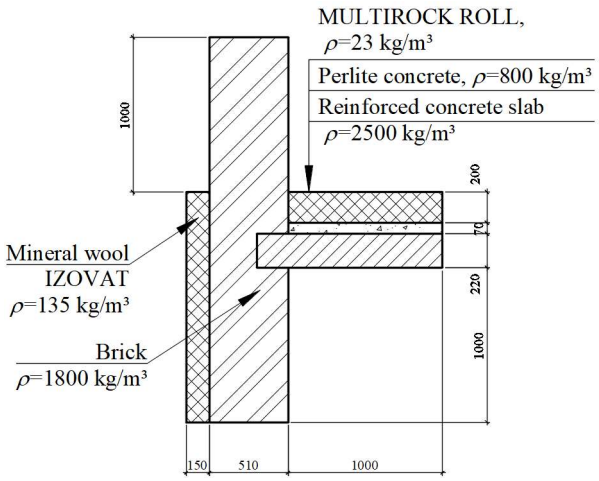

Figure 3 – Calculation scheme for determining the linear coefficient of the node №1

The calculation of the linear heat transfer coefficient is performed according to the formula:

$$k_1 = \sum L_i^{2D} - \sum_{i=1}^{j} U_i \cdot I_i =$$

$$=0.545+0.444–0,199\cdot1–0,235\cdot1=0,556 \text{ W/(m·K)}$$

where L^{2D} – linear coefficient of thermal connection, W/K, respectively in the areas of the attic floor and the outer wall is determined by formulas:

$$L_{at}^{2D} = \frac{Q_{tot.at}}{t_{in} - t_{at}} = \frac{21.101}{21-(-17.7)} = 0.545 \text{ W/K}$$

$$L_{w}^{2D} = \frac{Q_{tot.w}}{t_{in} - t_{ex}} = \frac{19.104}{21-(-22)} = 0.444 \text{ W/K}$$

where $Q_{tot.at}$, $Q_{tot.w}$ – the heat flux passing through the attic floor and the outer wall, respectively, W, is determined on the basis of the results of the calculation of the two-dimensional temperature field (Figure 4);

$Q_{tot.at} = 21.101$ W ;

$Q_{tot.w} = 19{,}104$ W

where t_{in} – temperature, °C, indoor air t_{in} =21 °C

Since the difference between the outside air temperature and the attic temperature is 0.9 of the difference between the outside air temperature and the room temperature, the attic temperature is determined by the formula:

$$t_{at} = 0.9\ (t_{ex} - t_{in}) + t_{in} =$$

$$= 0.9\ (-22 + 21) + 21 = -17{,}7\ ^{o}\text{C}$$

U_1, U_2 – heat transfer coefficients of one-dimensional fragments, W/(m²·K), respectively, the floor and the outer wall separating the studied medium is determined by formulas:

$$U_1 = \frac{1}{R_{\Sigma.at}} = \frac{1}{5.024} = 0.199 \text{ W/(m}^2\text{·K)}$$

$$U_2 = \frac{1}{R_{\Sigma.w}} = \frac{1}{4.248} = 0.235 \text{ W/(m}^2\text{·K)}$$

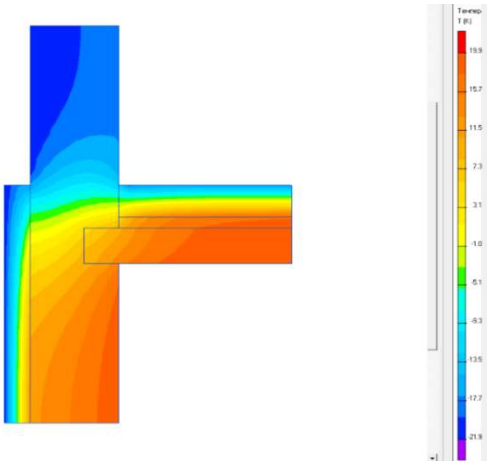

Figure 4 – Results of calculation of temperature field of node №1

where $R_{\Sigma.at}$; $R_{\Sigma.w}$ – heat transfer resistance of the thermally homogeneous part of the attic floor and the wall, respectively, (m²·K)/W, determined by formulas:

$$R_{\Sigma.at} = \frac{1}{\alpha_{in.at}} + \sum_{i=1}^{n} R_i + \frac{1}{\alpha_{ex.at}} =$$

$$= \frac{1}{\alpha_{in.at}} + \frac{\delta_1}{\lambda_{1cal}} + \frac{\delta_2}{\lambda_{2cal}} + \frac{\delta_3}{\lambda_{3cal}} + \frac{1}{\alpha_{ex.at}} =$$

$$= \frac{1}{8.7} + \frac{0.22}{2.04} + \frac{0.07}{0.33} + \frac{0.20}{0.044} + \frac{1}{12} =$$

$$=5.024 \text{ (m}^2\text{·K)/W}$$

$$R_{\Sigma.w} = \frac{1}{\alpha_{in.w}} + \frac{\delta_1}{\lambda_1} + \frac{\delta_2}{\lambda_2} + \frac{\delta_3}{\lambda_3} + \frac{\delta_4}{\lambda_4} + \frac{\delta_5}{\lambda_5} + \frac{1}{\alpha_{ex.w}} =$$

$$= \frac{1}{8.7} + \frac{0.02}{0.81} + \frac{0.51}{0.81} + \frac{0.01}{0.93} + \frac{0.15}{0.044} + \frac{0.014}{0.93} + \frac{1}{23} =$$

$$=4.248 \text{ (m}^2\text{·K)/W}$$

$\alpha_{in.at}$, $\alpha_{in.w}$ – heat transfer coefficients of internal surfaces, respectively, attic and wall, W/(m²·K), which are accepted in accordance with Annex B [14]:

$\alpha_{in.at} = 8.7$ W/(m²·K); $\alpha_{in.w} = 8.7$ W/(m²·K) ;

$\alpha_{ex.at}$, $\alpha_{ex.w}$ – heat transfer coefficients of external surfaces, respectively, attic and wall, W/(m²·K), which are accepted in accordance with Annex B [14]:

$\alpha_{ex.at} = 12$ W/(m²·K); $\alpha_{ex.w} = 23$ W/(m²·K) ;

l_1 , l_2 – lengths, respectively, of the attic and the wall, m, to which the values are applied U_1 and U_2

l_1 =1 m; l_2 =1 m

Determination of the linear heat transfer coefficient of the node №2.

The calculation scheme for determining the linear coefficient of the node №2 is shown in Figure 5.

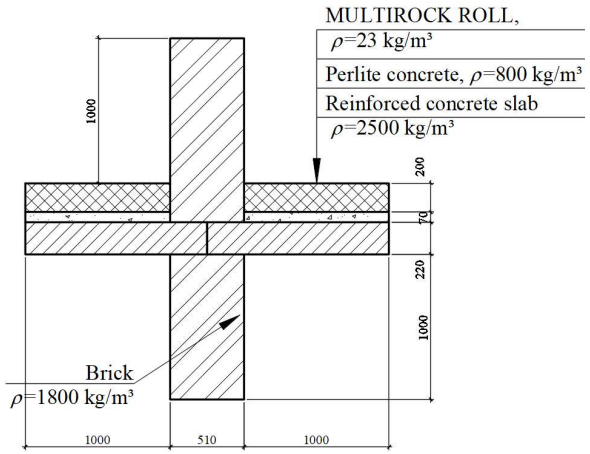

Figure 5 – Calculation scheme for determining the linear coefficient of the node №2

The calculation of the linear heat transfer coefficient is performed according to [15] according to the formula:

$$k_2 = \sum L_i^{2D} - \sum_{i=1}^{j} U_i \cdot I_i =$$

$$= 1.066 - 0{,}199 \cdot 2 = 0.668 \text{ W/(m·K)}$$

where L^{2D} – linear coefficient of thermal connection, W/K, on the site of the attic floor is determined by the formula:

$$L_{at}^{2D} = \frac{Q_{tot.at}}{t_{in} - t_{at}} = \frac{41.236}{21-(-17.7)} = 1.066 \text{ W/K}$$

where $Q_{tot.at}$, $Q_{tot.w}$ – heat flow passing through the attic floor and the outer wall, W, determined on the basis of the results of the calculation of the two-dimensional temperature field (Figure 6);

$Q_{tot.at} = 41.236$ W

where t_{in} – temperature, ºC, indoor air indoor air

t_{in} =21 ºC.

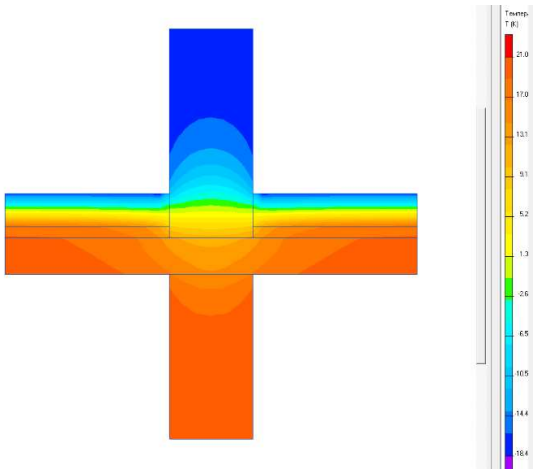

Figure 6 – Results of calculation of temperature field of node №2

Since the difference between the outside air temperature and the attic temperature is 0.9 of the difference between the outside air temperature and the room temperature, the attic temperature is determined by the formula:

$$t_{at} = 0.9\ (t_{ex} - t_{in}) + t_{in} =$$

$$= 0.9\ (-22 + 21) + 21 = -17.7 \text{ ºC}$$

U_1 – heat transfer coefficient of one-dimensional fragment, W/(m²·K), the overlap separating the studied medium is determined by the formula:

$$U_1 = \frac{1}{R_{\Sigma.at}} = \frac{1}{5.024} = 0.199 \text{ W/(m}^2\text{·K)}$$

where $R_{\Sigma.at}$ – heat transfer resistance of the thermally homogeneous part of the attic floor, (m²·K)/W, determined by the formula:

$$R_{\Sigma.at} = \frac{1}{\alpha_{in.at}} + \sum_{i=1}^{n} R_i + \frac{1}{\alpha_{ex.at}} =$$

$$= \frac{1}{\alpha_{in.at}} + \frac{\delta_1}{\lambda_{1p}} + \frac{\delta_2}{\lambda_{2p}} + \frac{\delta_3}{\lambda_{3p}} + \frac{1}{\alpha_{ex.at}} =$$

$$= \frac{1}{8.7} + \frac{0.22}{2.04} + \frac{0.07}{0.33} + \frac{0.20}{0.044} + \frac{1}{23} =$$

$$= 5.024 \text{ (m}^2\text{·K)/W}$$

l_1 – the length of the attic floor, m, to which the value is applied U_1, l_1 =1 m

Determination of the reduced heat transfer resistance of the attic floor structure

The configuration of the design area for determining the reduced resistance to heat transfer to the attic floor is shown in Figure 7.

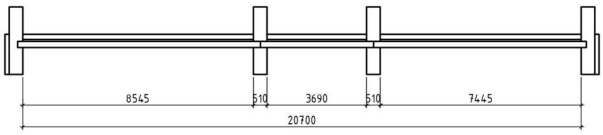

Figure 7 – Configuration of the calculation scheme for determining the reduced heat transfer resistance of the attic floor

The width of the calculated section is assumed to be 1 m.

The reduced heat transfer resistance of the attic floor is determined by the formula:

$$R_{\Sigma 1} = \frac{F_\Sigma}{\sum_{i=1}^{n} \frac{Fi}{R_{\Sigma i}} + \sum_{j=1}^{m} k_j L_j + \sum_{k=1}^{k} \varphi_k N_k} =$$

$$= \frac{F_\Sigma}{\frac{Fi}{R_\Sigma} + k_1 L_1 \times 2 + k_2 L_2 \times 2} =$$

$$= \frac{20{,}7}{\frac{19{,}68}{5{,}024} + 0{,}556 \times 1 \times 2 + 0{,}668 \times 1 \times 2} =$$

$$= 3.253 \text{ (m}^2\text{·K)/W}$$

where F_Σ – area of the enclosing structure, m^2, determined by the formula

$F_\Sigma = 20.7 \times 1 = 20.7$ m^2 ;

R_Σ – heat transfer resistance of thermally homogeneous part of the structure, (m^2·K)/W, determined by the formula:

$$R_\Sigma = \frac{1}{\alpha_{in}} + \sum_{i=1}^{n} R_i + \frac{1}{\alpha_{ex}} =$$

$$= \frac{1}{\alpha_{in}} + \frac{\delta_1}{\lambda_{1p}} + \frac{\delta_2}{\lambda_{2p}} + \frac{\delta_3}{\lambda_{3p}} + \frac{1}{\alpha_{ex}} =$$

$$= \frac{1}{8.7} + \frac{0.22}{2.04} + \frac{0.07}{0.33} + \frac{0.20}{0.044} + \frac{1}{23} =$$

$$= 5.024 \text{ (m}^2\text{·K)/W}$$

F_1 – the area of the thermally homogeneous part of the enclosing structure, m^2, determined by the formula

$F_1 = (8.545 + 3.69 + 7.445) \times 1 = 19.68$ m^2 ;

k_1 , k_2 – linear heat transfer coefficients, W/(m^2·K), respectively in the place of adjacency of the overlap structure to the outer and inner walls

$k_1 = 0.55$ W/(m^2·K) ; $k_2 = 0.668$ W/(m^2·K) ;

L_1 , L_2 – linear size (projection) of linear heat-conducting inclusions, m;

$L_1 = 1$ m, $L_2 = 1$ m.

Determine the difference between the values $R_{\Sigma 1}$ and R_Σ according to the formula:

$$n = \frac{R_{\Sigma 1}}{R_\Sigma} 100 - 100 = \frac{3.253}{5.064} 100 - 100 = 35.8\%$$

Sincen $R_{\Sigma 1} = 3.253$ (m^2·K)/W < $R_{q/min} = 4.95$ (m^2·K)/W then the heat-protective properties of the attic floor of the educational building are not sufficient.

Not taking into account heat-conducting inclusions leads to an overestimation of the actual heat transfer resistance of the attic floor of the educational building by 35.8%.

To bring the heat-protective properties of the attic floor of the educational building to the regulatory requirements, eight constructive options for insulation were considered.

Option 1. Insulation of the outer wall on its outer surface above the level of the top of the attic floor insulation.

Raising the insulation above the level of the top of the attic floor insulation was assumed to be a multiple of 200 mm. Determination of the reduced heat transfer resistance of the attic floor was performed on the basis of calculations of the temperature fields of node 1 and node 2. The temperature field of node 2 is constant.

The calculation results of the reduced resistance of heat transfer of the attic floor are shown in table 1.

Table 1 – Calculation results of the reduced heat transfer resistance of the attic floor

Increasing the length of the insulation, mm	k_1, W/(m · K)	k_2, W/(m · K)	$R_{\Sigma пр}$, m^2 · K/W	$R_{q.min}$, m^2 · K/W
0	0,556	0,668	3,253	4,95
200	0,508		3,302	
400	0,487		3,325	
600	0,477		3,335	
800	0,473		3,339	
1000	0,472		3,341	
1200	0,471		3,342	
1400	0,470		3,343	
1600	0,470		3,343	

Figure 8 shows a graph of the dependence of the reduced resistance to heat transfer of the attic floor on the increase in the length of the insulation.

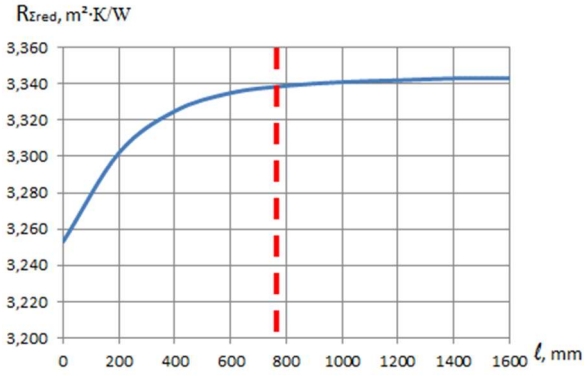

Figure 8 – The graph of the dependence of the reduced resistance of heat transfer of the attic floor on the increase in the length of the insulation.

Result for option 1.

1. Additional insulation of the outer surface of the outer wall of the cold attic does not allow to achieve the normalized value of thermal protection for the attic floor.

2. The optimal increase in the length of the insulation is 800 mm. A further increase in the length of the insulation does not significantly increase the reduced heat transfer resistance.

Option 2. Insulation of the outer wall on its inner surface above the level of the top of the attic floor insulation.

Raising the insulation above the level of the top of the attic floor insulation was taken as a multiple of 200 mm. The determination of the reduced heat transfer resistance of the attic floor was performed on the basis of calculations of the temperature fields of node 1 and node 2. The temperature field of node 2 is constant.

The calculation results of the reduced resistance of heat transfer of the attic floor are shown in table 2.

Table 2 – Calculation results of the reduced heat transfer resistance of the attic floor

Increasing the length of the insulation, mm	k_1, W/(m · K)	k_2, W/(m · K)	$R_{\Sigma пр}$, m² · K/W	$R_{q.min}$, m² · K/W
0	0,556	0,668	3,253	4,95
200	0,495		3,316	
400	0,483		3,329	
600	0,482		3,330	
800	0,483		3,329	
1000	0,483		3,329	
1200	0,483		3,329	
1400	0,484		3,328	
1600	0,484		3,328	

Figure 9 shows a graph of the dependence of the reduced resistance to heat transfer of the attic floor on the increase in the length of the insulation.

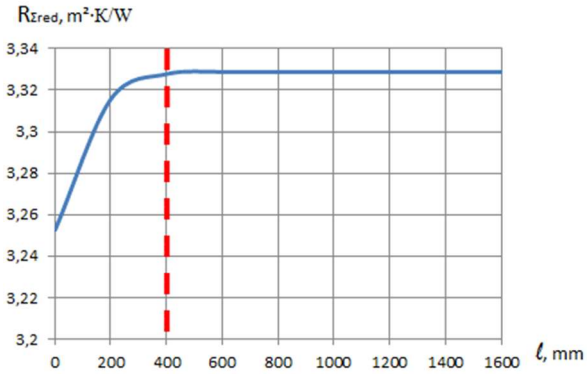

Figure 9 – The graph of the dependence of the reduced resistance of heat transfer of the attic floor on the increase in the length of the insulation

Result for option 2.

1 Additional insulation of the inner surface of the outer wall of the cold attic does not allow to achieve the normalized value of thermal protection for the attic floor.

2. The optimal increase in the length of the insulation is 400 mm.

Option 3. Insulation of the inner wall above the level of the top of the attic floor insulation.

Raising the insulation above the level of the top of the attic floor insulation was taken as a multiple of 200 mm. Determination of the reduced heat transfer resistance of the attic floor was performed on the basis of calculations of the temperature fields of node 1 and node 2. The temperature field of node 1 is constant.

The calculation results of the reduced resistance of heat transfer of the attic floor are shown in table 3.

Table 3 – Calculation results of the reduced heat transfer resistance of the attic floor

Increasing the length of the insulation, mm	k_1, W/(m · K)	k_2, W/(m · K)	$R_{\Sigma пр}$, m² · K/W	$R_{q.min}$, m² · K/W
0	0,556	0,668	3,253	4,95
200		0,492	3,443	
400		0,403	3,549	
600		0,350	3,613	
800		0,321	3,650	
1000		0,303	3,674	
1200		0,292	3,688	
1400		0,285	3,698	
1600		0,273	3,713	

Figure 10 shows a graph of the dependence of the reduced resistance to heat transfer of the attic floor on the increase in the length of the insulation.

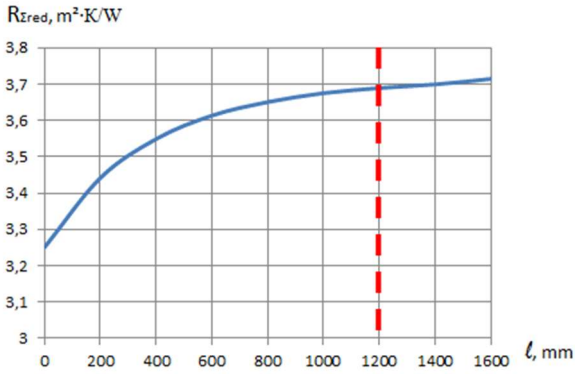

Figure 10 – The graph of the dependence of the reduced resistance of heat transfer of the attic floor on the increase in the length of the insulation

Result for option 3.

1. Additional insulation of the inner walls of the cold attic does not allow to achieve the normalized value of thermal protection for the attic floor.

2. The optimal increase in the length of the insulation is 1200 mm.

Option 4. Insulation of the outer wall on the outer and inner surface above the level of the top of the attic floor insulation.

Raising the insulation above the level of the top of the attic floor insulation was taken as a multiple of 200 mm. The determination of the reduced heat transfer resistance of the attic floor was performed on the basis of calculations of the temperature fields of node 1 and node 2. The temperature field of node 2 is constant.

The calculation results of the reduced resistance of heat transfer of the attic floor are shown in table 4

Table 4 – Calculation results of the reduced heat transfer resistance of the attic floor

Increasing the length of the insulation, mm	k_1, W/(m · K)	k_2, W/(m · K)	$R_{\Sigma пр}$, m² · K/W	$R_{q.min}$, m² · K/W
0	0,556	0,668	3,253	4,95
200	0,452		3,363	
400	0,378		3,445	
600	0,348		3,480	
800	0,329		3,503	
1000	0,317		3,516	
1200	0,310		3,525	
1400	0,305		3,531	
1600	0,294		3,545	

Figure 11 shows a graph of the dependence of the reduced resistance to heat transfer of the attic floor on the increase in the length of the insulation.

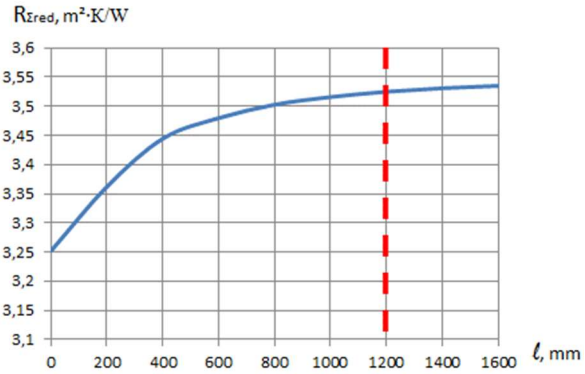

Figure 11 – The graph of the dependence of the reduced resistance of heat transfer of the attic floor on the increase in the length of the insulation

Result for option 4.

1. Additional insulation of the inner and outer surface of the outer wall of the cold attic does not allow to achieve the normalized value of thermal protection for the attic floor.

2. The optimal increase in the length of the insulation is 1200 mm.

Option 5. Insulation of the outer wall on the outside and the inner wall above the level of the top of the attic floor insulation.

Raising the insulation above the level of the top of the attic floor insulation was assumed to be a multiple of 200 mm.

The values of the linear heat transfer coefficient k_1 will be the same as in option 1, and the coefficient k_2 as in option 3.

The calculation results of the reduced resistance of heat transfer of the attic floor are shown in table 5.

Table 5 – Calculation results of the reduced heat transfer resistance of the attic floor

Increasing the length of the insulation, mm	k_1, W/(m · K)	k_2, W/(m · K)	$R_{\Sigma пр}$, m² · K/W	$R_{q.min}$, m² · K/W
0	0,556	0,668	3,253	4,95
200	0,508	0,492	3,498	
400	0,487	0,403	3,633	
600	0,477	0,350	3,716	
800	0,473	0,321	3,760	
1000	0,472	0,303	3,786	
1200	0,471	0,292	3,803	
1400	0,470	0,285	3,814	
1600	0,470	0,273	3,831	

Figure 12 shows a graph of the dependence of the reduced resistance to heat transfer of the attic floor on the increase in the length of the insulation.

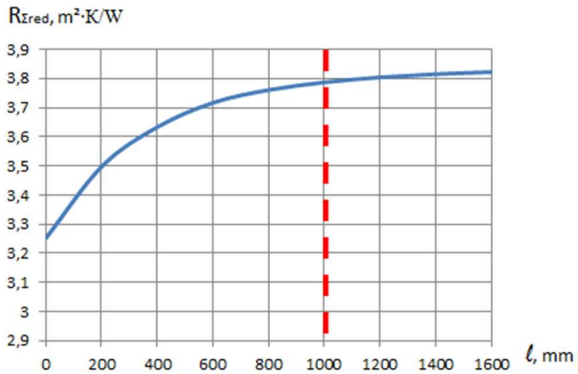

Figure 12 – The graph of the dependence of the reduced resistance of heat transfer of the attic floor on the increase in the length of the insulation

Result for option 5.

1. Additional insulation of the inner walls of the cold attic does not allow to achieve the normalized value of thermal protection for the attic floor.

2. The optimal increase in the length of the insulation is 1000 mm.

Option 6. Insulation of the outer wall from the inside and the inner wall above the level of the top of the attic floor insulation.

Raising the insulation above the level of the top of the attic floor insulation was assumed to be a multiple of 200 mm.

The values of the linear heat transfer coefficient k_1 will be the same as in option 2, and the coefficient k_2 as in option 3.

The calculation results of the reduced resistance of heat transfer of the attic floor are shown in table 6.

Table 6 – Calculation results of the reduced heat transfer resistance of the attic floor

Increasing the length of the insulation, mm	k_1, W/(m · K)	k_2, W/(m · K)	$R_{\Sigma пр}$, m² · K/W	$R_{q.min}$, m² · K/W
0	0,556	0,668	3,253	4,95
200	0,495	0,492	3,514	
400	0,483	0,403	3,638	
600	0,482	0,350	3,709	
800	0,483	0,321	3,746	
1000	0,483	0,303	3,771	
1200	0,483	0,292	3,786	
1400	0,484	0,285	3,795	
1600	0,484	0,273	3,811	

Figure 13 shows a graph of the dependence of the reduced resistance to heat transfer of the attic floor on the increase in the length of the insulation.

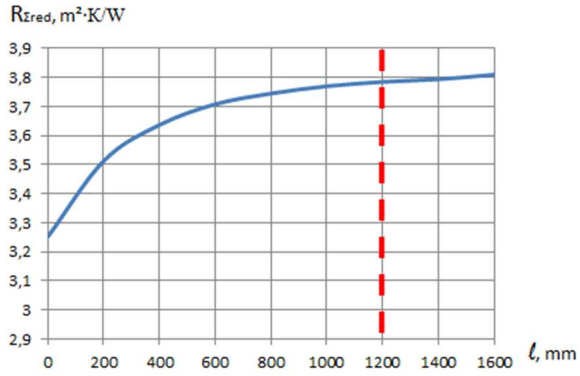

Figure 13 – The graph of the dependence of the reduced resistance of heat transfer of the attic floor on the increase in the length of the insulation

Result for option 6.

1. Additional insulation of the inner walls of the cold attic does not allow to achieve the normalized value of thermal protection for the attic floor.
2. Insulation of more than 1200 mm is inefficient.

Option 7. Insulation of the outer wall on the inside and outside and the inner wall above the level of the top of the attic floor insulation.

Insulation was taken from the same insulation as on the main wall. The thickness of the insulation was assumed to be the same (150 mm). Raising the insulation above the level of the top of the attic floor insulation was assumed to be a multiple of 200 mm.

The values of the linear heat transfer coefficient k_1 will be the same as in option 4, and the coefficient k_2 as in option 3.

The calculation results of the reduced resistance of heat transfer of the attic floor are shown in table 7.

Table 7 – Calculation results of the reduced heat transfer resistance of the attic floor

Increasing the length of the insulation, mm	k_1, W/(m · K)	k_2, W/(m · K)	$R_{\Sigma пр}$, m² · K/W	$R_{q.min}$, m² · K/W
0	0,556	0,668	3,253	4,95
200	0,452	0,492	3,566	
400	0,378	0,403	3,778	
600	0,348	0,350	3,896	
800	0,329	0,321	3,968	
1000	0,317	0,303	4,014	
1200	0,310	0,292	4,042	
1400	0,305	0,285	4,061	
1600	0,294	0,273	4,098	

Figure 14 shows a graph of the dependence of the reduced resistance to heat transfer of the attic floor on the increase in the length of the insulation.

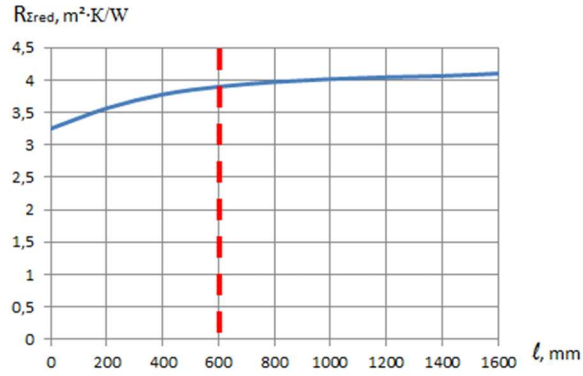

Figure 14 – The graph of the dependence of the reduced resistance of heat transfer of the attic floor on the increase in the length of the insulation

Result for option 7.

1. Additional insulation of the inner walls of the cold attic does not allow to achieve the normalized value of thermal protection for the attic floor.
2. Insulation of more than 600 mm is inefficient.

Option 8. Increasing the thickness of the attic floor insulation.

The increase in the thickness of the attic floor insulation was taken as a multiple of 20 mm.

The calculation results of the reduced resistance of heat transfer of the attic floor are shown in table 8.

Table 8 – Calculation results of the reduced heat transfer resistance of the attic floor

Increasing the length of the insulation, mm	k_1, W/(m · K)	k_2, W/(m · K)	$R_{\Sigma np}$, m² · K/W	$R_{q.min}$, m² · K/W
0	0,556	0,668	3,253	4,95
20	0,553	0.649	3.452	
40	0,549	0.630	3.648	
60	0,546	0.613	3.834	
80	0,543	0.597	4.014	
100	0,541	0.580	4.191	
120	0,539	0,566	4.359	
140	0,538	0,551	4.523	
160	0,535	0,537	4.687	
180	0,534	0,525	4.840	
200	0,533	0,511	4.994	

Figure 15 shows a graph of the dependence of the reduced resistance to heat transfer of the attic floor on the increase in the length of the insulation.

Result for option 8.

Increasing the thickness of the insulation on the attic floor by 200 mm (up to 400 mm) allows to achieve the normalized value of thermal protection for the attic floor.

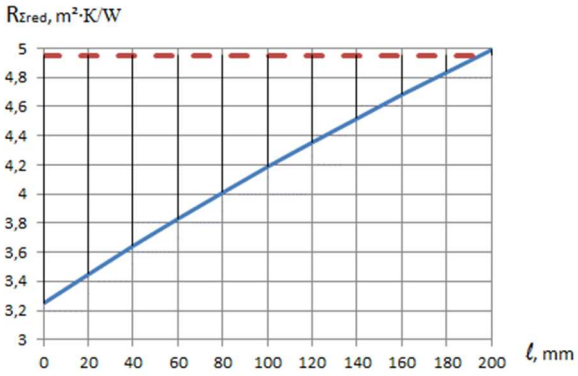

Figure 15 – The graph of the dependence of the reduced resistance of heat transfer of the attic floor on the increase in the length of the insulation

But this option of insulation is economically impractical as it requires a significant increase in the volume of insulation. It is more preferable to use the optimal options for additional insulation of external and internal walls within the mountain while reducing the thickness of the insulation on the attic floor. In this case, the reduced resistance to heat transfer of the attic transmission should be the closest in terms of the normal value.

The research results are shown in Table 9.

As can be seen from Table 9, the smallest volume of insulation equal to 7.09 m³ per meter of running floor structure is achieved by increasing by 1 m the height of insulation of the outer wall on its outer surface and insulation of internal capital walls by 1.2 m from the level of insulation attic floor.

Table 9 – The cost of additional insulation of the cold attic (per 1 m of attic width), ensuring compliance with thermal protection

Variant	Additional insulation, m³				Total amount of additional insulation
	Outer surface of the external walls	Inner surface of the external walls	Interior walls	Attic floor	
1	0,186			7,478	7,664
2		0,06		7,872	7,932
3			0,624	6,691	7,315
4	0,312	0,312		6,691	7,315
5	**0,264**		**0,528**	**6,298**	**7,09**
6		0,318	0,636	6,691	7,645
7	0,204	0,084	0,648	6,298	7,334
8				7,872	7,872

Conclusions

1. The value of thermal protection of the existing external enclosing structures of the educational building does not meet the standards.

2. Not taking into account heat-conducting inclusions leads to an overestimation of the actual resistance to heat transfer of the attic floor of the educational building by 35.8%.

3. The smallest amount of insulation of the cold attic of the educational building is 7.09 m^3 per 1 meter of the attic length. This amount of insulation is achieved when the thickness of the insulation on the attic floor is 320 mm, the height of the insulation of the outer wall along the outer surface is increased by 1 m and the surfaces of the internal capital walls are warmed to a height of 1.2 m from the bottom of the insulation of the attic floor.

References

1. Фокин К.Ф. (1973). *Строительная теплотехника ограждающих частей зданий.* Москва: Стройиздат

2. Лыков А.В. (1978). *Теория теплопроводности*. Москва: Высшая школа

3. Ильинский В.М. (1974). *Строительная теплофизика (ограждающие конструкции и микроклимат зданий)*. Москва: Высшая школа

4. Михеев М.А., Михеева И.М. (1977). *Основы теплопередачи*. Москва: Энергия

5. Шкловер А.М., Васильев Б.Ф., Ушков Ф.В. (1956). *Основы строительной теплотехники жилых и общественных зданий*. Москва: Госстройиздат

6. Могилат А.Н., Волик Г.Л., Юрин О.И. (1989). *Строительная теплофизика ограждающих конструкций зданий*. Київ, УМК ВО

7. Фаренюк Г.Г., Колесник Є.С. (2008). Визначення лінійного коефіцієнту теплопередачі термічно неоднорідних огороджувальних конструкцій. *Будівельні конструкції*, 1(28), 138-147

8. Пріщенко А.М. (2015). *Вузлові з'єднання зовнішніх стін з підвищеними теплотехнічними показниками як засіб забезпечення енергоефективності будівель* (автореф. дис. … канд. техн. наук). Київ

9. Тимофєєв М.В., Фаренюк Г.Г. (2009). *Розрахунки теплової ізоляції будівель*. Донецьк-Макіївка: Норд-Прес, ДонНАБА

10. Тимофєєв М.В., Сахновська С.О., Жмихова В.В. (2010). Математичне моделювання потрібних опорів теплопередачі елементів зовнішньої оболонки будинків. *Вісник Донбаської національної академії будівництва і архітектури,* 2(82), 32-37

11. Фомин С.Л., Фурсов Ю.В. (2007). *Особенности конструирования дополнительной теплозащиты фасадных конструкций*. Харьков: ХДТУБА АБУ, 290-294

12. Semko O., Yurin O., Avramenko Y., Skliarenko S. (2017). Thermophysical aspects of reconstruction of cold roof spaces. *MATEC Web Conferences*, 116, 02030 https://doi.org/10.1051/matecconf/201711602030

13. Yurin O., Azizova A., Galinska T. (2018). Study of heat shielding qualities of a brick wall corner with additional insulation on the brick. *MATEC Web of Conferences*, 230, 02039 https://doi.org/10.1051/matecconf/201823002039

14. ДБН В.2.6-31:2016. (2016). *Теплова ізоляція будівель*. Київ: Мінрегіон України

15. ДСТУ ISO 10211-1:2005. (2008). *Теплопровідні включення в будівельних конструкція. Обчислення теплового потоку та поверхневої температури. Частина 1. Загальні методи*. Київ: Держспоживстандарт України

1. Fokin K.F. (1973). Construction heat engineering of enclosing parts of buildings. Moscow: Stroyizdat

2. Lykov A.V. (1978). Theory of thermal conductivity. Moscow: Higher School

3. Ilyinsky V.M. (1974). Building thermal physics (enclosing structures and microclimate of buildings). Moscow: Higher School

4. Mikheev M.A., Mikheeva I.M. (1977). Fundamentals of heat transfer. Moscow: Energy

5. Shklover A.M., Vasiliev B.F., Ushkov F.V. (1956). Fundamentals of construction heat engineering of residential and public buildings. Moscow: Gosstroyizdat

6. Mogilat A.N., Volik G.L., Yurin O.I. (1989). Building thermal physics of enclosing structures of buildings. Kyiv, UMK VO

7. Farenyuk G.G., Kolesnyk E.S. (2008). Determination of linear heat transfer coefficient of thermally inhomogeneous enclosing structures. Building constructions,1(28), 138-147

8. Prishchenko A.M. (2015). Nodal connections of external walls with increased thermal performance as a means of ensuring energy efficiency of buildings (abstract of the dissertation - Candidate of Technical Sciences). Kyiv

9. Timofeev M.V., Farenyuk G.G. (2009). Calculations of thermal insulation of buildings. Donetsk-Makeyevka: Nord-Press, DonNACEA

10. Timofeev M.V., Sakhnovskaya S.O., Zhmykhova V.V. (2010). Mathematical modeling of the required heat transfer resistances of the elements of the outer shell of buildings. Bulletin of the Donbas National Academy of Civil Engineering and Architecture, 2(82), 32-37

11. Fomin S.L., Fursov Yu.V. (2007). Design features of additional thermal protection of facade structures. Kharkiv: HDTUBA ABU, 290-294

12. Semko O., Yurin O., Avramenko Y., Skliarenko S. (2017). Thermophysical aspects of reconstruction of cold roof spaces. *MATEC Web Conferences*, 116, 02030 https://doi.org/10.1051/matecconf/201711602030

13. Yurin O., Azizova A., Galinska T. (2018). Study of heat shielding qualities of a brick wall corner with additional insulation on the brick. *MATEC Web of Conferences*, 230, 02039 https://doi.org/10.1051/matecconf/201823002039

14. DBN V.2.6-31:2016. (2016). *Thermal insulation of buildings. Kyiv: Ministry of Regional Development of Ukraine*

15. DSTU ISO 10211-1:2005. (2008). Thermally conductive inclusions in building structures. Calculation of heat flux and surface temperature. Part 1. General methods. Kyiv: Derzhspozhyvstandart of Ukraine

Збірник наукових праць. Галузеве машинобудування, будівництво
Academic journal. Industrial Machine Building, Civil Engineering
http://journals.nupp.edu.ua/znp
https://doi.org/10.26906/znp.2021.56.2507

UDC 692.23:699.86

Improving the technology of replacing window frames in precast concrete walls

Pashynskyi Victor[1]*, Dzhyrma Stanislav[2], Pashynskyi Mykola[3], Nastoiashchyi Vladyslav[4]

[1] Central Ukrainian National Technical University https://orcid.org/0000-0002-5474-6399
[2] Central Ukrainian National Technical University https://orcid.org/0000-0003-2248-1653
[3] Central Ukrainian National Technical University https://orcid.org/0000-0002-2669-523X
[4] Central Ukrainian National Technical University https://orcid.org/0000-0002-8931-5097
*Corresponding author E-mail: pva.kntu@gmail.com

The constructive-technological decision of the junction design of a block frame window to an uninsulated precast concrete wall which practically excludes a possibility of condensate formation on a surface of internal window jamb is proved. The study was performed by constructing two-dimensional temperature fields in nodes of different designs and comparing the lowest temperature on the internal window jamb surface with the dew point temperature. It is established that thermal reliability can be ensured by the condensate formation criterion by insulating the exterior window jamb with mineral wool or expanded polystyrene slabs and local facade insulation in the form of an outside window casing with 50 mm thickness and 200…250 mm width. The block frame window should be installed at a distance of 60… 80 mm from the outer surface of the precast concrete wall.

Keywords: condensate, precast concrete walls, temperature regime, thermal failure, window-wall junction

Удосконалення технології заміни віконних блоків в залізобетонних панельних стінах

Пашинський В.А.[1]*, Джирма С.О.[2], Пашинський М.В.[2], Настоящий В.А[4]

[1, 2, 3, 4] Центральноукраїнський національний технічний університет
*Адреса для листування E-mail: pva.kntu@gmail.com

З метою підвищення комфортності житлових будинків другої половини 20-го століття часто здійснюється заміна дерев'яних віконних блоків на сучасні металопластикові конструкції. В зимовий період температура поверхні внутрішнього відкосу поблизу віконної коробки може опускатися нижче точки роси, що призводить до теплової відмови за критерієм утворення конденсату. Для обгрунтування надійного конструктивно-технологічного рішення вузла примикання віконних блоків до неутеплених стін з керамзитобетонних панелей побудовані та проаналізовані двомірні температурні поля у вузлах різної конструкції. Найменша температура на поверхні внутрішнього віконного відкосу порівнювалася з температурою точки роси. Показано, що на температурний режим експлуатації вузла примикання віконного блоку до стіни істотно впливає конструкція вузла та положення вікна в товщі стіни. Утеплення зовнішнього віконного відкосу та зміщення вікна всередину приміщення підвищує температуру критичної зони вузла. На прикладі поширених панельних стін з керамзитобетону товщиною 300 мм показано, що для забезпечення належного температурного режиму експлуатації вузла необхідно виконати утеплення зовнішнього віконного відкосу та локальне фасадне утеплення у вигляді обрамлення віконного прорізу шириною 200 мм або 250 мм. Віконний блок слід відповідно встановлювати на відстані 80 мм чи 60 мм від зовнішньої поверхні стінової панелі. З технологічної точки зору для утеплення краще використовувати плити з пінополістиролу, кріплення яких до стінових панелей та зовнішнє оздоблення є менш трудомістким і дешевшим порівняно з використанням плит з мінеральної вати. Локальне фасадне утеплення навкруги віконних прорізів з товщиною, яка задовольняє вимоги норм до опору теплопередачі стін, у майбутньому може стати частиною повного фасадного утеплення при термомодернізації будівлі.

Ключові слова: конденсат, панельні стіни, примикання вікон, температурний режим, теплова відмова

Introduction

A significant part of the Ukrainian cities' housing stock consists of prefabricated houses built in the second half of the 20th century. One of the main disadvantages of such buildings is the insufficient resistance to heat transfer of enclosing structures. This leads to increased heat loss and can cause discomfort when staying indoors near walls.

An additional problem of prefabricated houses is wooden casement windows. They not only wear out during long operation periods but also do not meet modern requirements for heat loss.

Complete thermal modernization of existing buildings with the installation of facade insulation is a very complex and costly measure. Therefore in practice, quite often they are limited to a half-measure in the form of replacing worn-out block frame windows with modern metal-plastic structures with sufficiently high thermal characteristics. This reduces heat loss to some extent but does not exclude the possibility of condensation on the surface of the internal window jamb.

Review of the research sources and publications

The junction between the window and wall is a zone of increased thermal conductivity. Requirements for thermal characteristics of such junctions and walls, in general, are set in DBN [1], and for European countries are covered in works [2, 3]. The main requirement for thermal reliability is the inadmissibility of condensation due to the temperature drop of the inner wall surface below the dew point temperature.

Studies of the window junctions temperature regime to the walls in the winter were carried out in [4…9], where the impact of the window position in a cavity wall was analyzed. The calculations performed in [4…6] for brick walls showed that a simple replacement of the window with a better one does not solve the condensation problem. The temperature of the internal jamb in the junction area of the block frame window to a wall may fall below the dew point at real values of outside air temperature.

In articles [4...9] it is shown that the temperature of the internal window jamb can be increased due to additional insulation or by shifting the block frame window to the inner side of the building. In [7], the example of several nodes at two positions of block frame window shows that the design of the window junction to the wall significantly affects heat loss, the position of the zero isotherms in the wall, and the possibility of condensation on the inner wall surface. There was an increase in the temperature of the inner wall surface as a result of shifting the block frame window inside the building.

The influence of the window position of the cavity wall on the temperature of the inner surface and the possibility of condensation has been studied in more detail in the works of the authors [4, 5, 6, 8].

In [4] the temperature dependence of the metal-plastic window junction critical zone to the brick wall with a thickness of 510 mm from its position was obtained. It is shown that in the conditions of Kirovograd region window installation close to the outside surface of the wall the temperature of the internal jamb is about +8 °C, and the shifting of the block frame window inside the building significantly increases the temperature at the critical jamb point. The obtained graph makes it possible to establish the position of the block frame window at which the surface temperature of the internal jamb exceeds the dew point temperature and thus avoids the condensate formation.

In the article [8] by a method similar to [4], obtained a nomogram and analytical expression that allows setting the desired position of the block frame window in the cavity of the brick wall depending on the allowable temperature of the inner wall surface in the critical zone (dew point temperature) and outside air temperature.

A detailed analysis of the window junction temperature regime to the wall of different designs was carried out in [5, 6]. In particular, the junctions to the brick and precast concrete wall are shown in Figures 1 and 2, which are taken from [5] with minor editorial changes. The designations of the node elements are given in table 1.

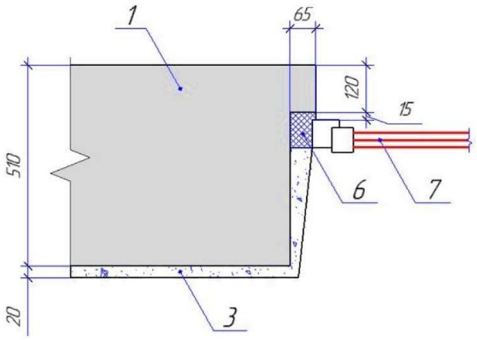

Figure 1 – The junction of the metal-plastic window to the brick wall

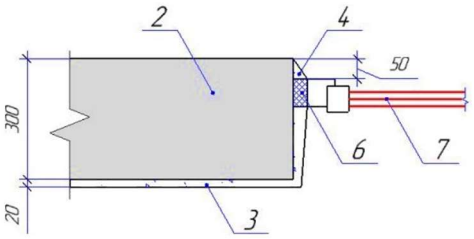

Figure 2 – The junction of the metal-plastic window to the precast concrete wall

Figures 1, 2 show the junctions at the initial design position of the block frame window. When shifting the block frame window inside the brick wall, the space between the outside casing and the window frame is filled with an effective thermal insulation material (mineral wool or polystyrene slabs). The external jamb of the precast concrete wall is made of cement-sand plaster.

The simulation results of these nodes in [5] showed that shifting the block frame window in the cavity of the brick wall inside the room by 150…170 mm from the outside casing allows raising the temperature of the critical zone to the dew point equal to 10.7 °C. In this way, thermal failure by the criterion of condensate formation can be avoided. It is impossible to achieve such

an effect in a precast concrete wall. Even with the maximum possible shift of 150 mm from the outer surface of the wall, the temperature of the critical zone on the internal jamb does not rise above 9,2°C. Articles [5, 6] show that this problem is successfully solved with proper facade insulation of brick and precast concrete walls in accordance with the requirements of [1]. Without such insulation, condensation can be formed on the surface of the internal window jamb of the precast concrete wall.

In general, works [4…9] showed that the position of the block frame window in the cavity wall can significantly affect the surface temperature of the internal window jamb and the possibility of condensation in this area.

The study of the temperature regime of enclosing structures operation can be performed using the open-source program THERM [11], which allows to build two-dimensional temperature fields for fragments of structures using the finite element method and obtain temperatures at specified critical points of the nodes.

Definition of unsolved aspects of the problem

The results of previous studies indicate the need for facade insulation to ensure the thermal reliability of the block frame window junction to the brick and precast concrete walls of residential buildings. It is possible to improve the conditions of the operating units of the insulated brick walls, provided that reinforced-plastic windows are installed with a shift inside the building. In the case of precast concrete walls, this solution does not give a positive result. The analyzed works do not contain recommendations for ensuring the thermal reliability of the block frame window junction to the precast concrete wall of residential buildings.

Problem statement

To offer a rational constructive insulation scheme and technology of the metal-plastic window junction to the uninsulated walls of prefabricated houses based on the results of temperature field analysis.

Basic material and results

The subject of the study is the junctions of metal-plastic windows to the uninsulated walls of prefabricated residential buildings. The five types of junctions are compared below:

1) the junction according to the scheme of Figure 2 at different shift values of the window inside the building;
2) the junction according to the scheme of Figure 3 with insulation of the outer jamb;
3) the junction from Figure 4 with insulation of the external jamb and local insulation of the facade in the form of an outside window casing with a width of 150 mm;
4) the same with the casing width of 200 mm;
5) the same with the casing width of 250 mm.

Insulation of the exterior window jamb and local facade insulation in the form of the outside window casing is performed by slabs made of expanded polystyrene or mineral wool, which according to [13] have sufficiently close thermal conductivity coefficients. From the technological point of view, it is more profitable to use expanded polystyrene plates which are much cheaper and can be pasted to a surface of the expanded clay precast concrete wall without the performance of labor-consuming operations on the attachment of a mineral wool plate by dowels. The use of expanded polystyrene in the form of local insulation is also permissible from the point of view of fire safety, as such a scheme of insulation does not allow the fire to spread on the surface of the facade. Constructions of window junctions to the walls are performed in accordance with the requirements of the current standard [12].

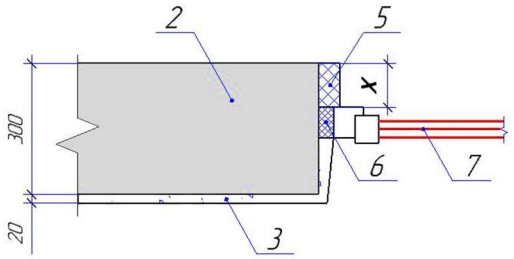

Figure 3 – The junction of a metal-plastic window to a precast concrete wall with external jamb insulation

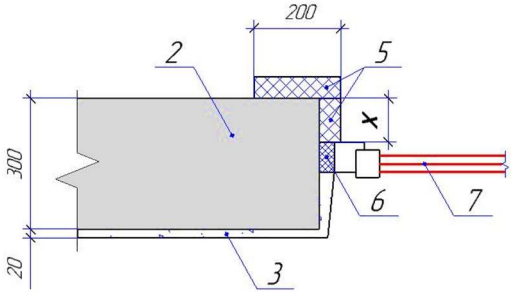

Figure 4 – The junction of a metal-plastic window to a precast concrete wall with additional local insulation of a facade

When modeling temperature fields, the values of density ρ and thermal conductivity λ of materials are taken into account, as shown in Table 1. To simulate a metal-plastic block frame window the reduced value of thermal conductivity, which is shown in table 1 is used in the program THERM [11].

The outside air temperature according to [14, 15] is assumed to be equal –24°C. For the Kirovograd region and most of the central regions of Ukraine, this value with a certain margin corresponds to the temperature of the coldest five days with a reliability level of 0.92…0.95, which is used for the design of massive walls.

At the design indoor air temperature of +20°C and relative humidity of 55%, as indicated in the standard [1] for residential premises, the dew point temperature value of +10,7°C is set according to psychrometric tables.

Table 1 – Thermal characteristics of materials

	Materials and products	ρ, kg/m^3	λ, W/(m^2·K)
1	Brickwork	1800	0,81
2	Expanded clay concrete slab	1000	0,41
3	Lime plaster	1600	0,81
4	Cement plaster	1800	0,93
5	Effective insulation	135	0,039
6	Construction foam	25	0,03
7	Block frame window	30	0,037

Simulation of the described junctions is performed in the environment of the THERM program. Junctions of types 1 and 2 are calculated at five positions of the block frame window in the cavity of the wall, which is given by the distance X from the outer edge of the wall to the outer surface of the window frame. The smallest distance X = 25 mm corresponds to the maximum possible approach of the window to the outer surface of the wall. The biggest distance X = 125 mm, taking into account the thickness of a window frame of 70 mm corresponds to the position of a window near the middle of a 300 mm wall. A further shift of the window inside the building reduces the width of the window sill too much and worsens the conditions of natural lighting. Junctions of types 3, 4, and 5 are calculated at six positions of the block frame window in a cavity of the wall. The position at a distance of X = 0 mm corresponds to the absence of an external jamb. At the same time, the joint of the block frame window with a wall is covered by local front insulation in the form of an outside window casing.

As a result of the performed calculations, the temperature fields and temperature values in the critical zone of the nodes were obtained. In all nodes, the critical zone with the minimum temperature of an internal surface of a wall is placed on a surface of an internal window jamb near a window frame. Figure 5 shows examples of temperature fields of types nodes 1, 2, and 4 with a shift of the window frame inside the building by 100 mm. The figure shows that the insulation of the exterior jamb and additional local facade insulation significantly changes the position of the isotherms in the wall thickness and increase the surface temperature of the internal window jamb. As the insulation improves, the temperature of the critical point, given in a separate window on the temperature field figures, also increases. For junctions of types 1 and 2, it is lower than the dew point temperature, which indicates the possibility of condensation. In the type 4 junction, the temperature of the critical point +11,1°C exceeds the dew point. This indicates a low probability of condensation on the surface of the internal window jamb.

The results of critical zone temperature calculations of all types of junctions at the considered positions of the block frame window are presented in table 2. Changes in these temperatures when the window frame is shifted inside the cavity of the wall are shown in Figure 6, which is made according to table 2.

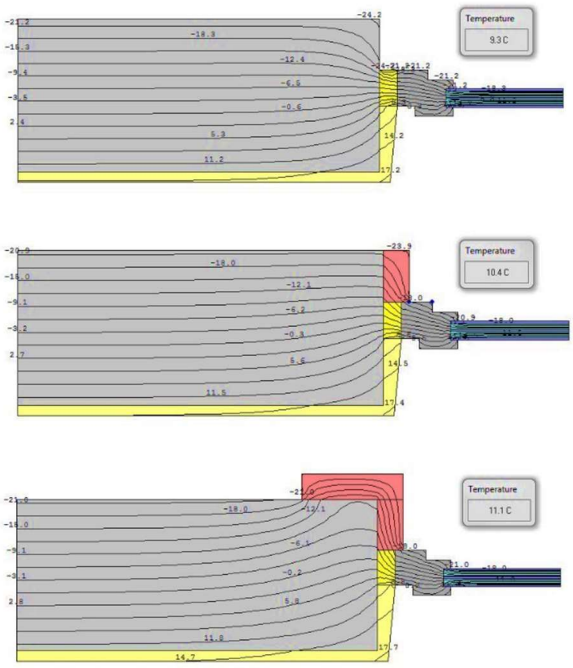

Figure 5 – Temperature fields of type 1, 2, and 4 junctions

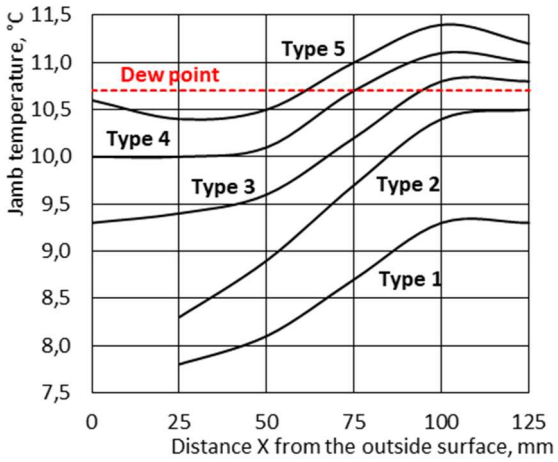

Figure 6 – Temperatures in the critical zone of the window junctions to the precast concrete wall with different schemes of additional insulation and different positions of the window frame

Table 2 – Temperatures at critical points of the junctions

X, mm	Temperatures in junctions of different types				
	1	2	3	4	5
0			9,3	10	10,6
25	7,8	8,3	9,4	10	10,4
50	8,1	8,9	9,6	10,1	10,5
75	8,7	9,7	10,2	10,7	11,0
100	9,3	10,4	10,8	11,1	11,4
125	9,3	10,5	10,8	11,00	11,2

Analysis of table 2 and figure 6 showed that the type of junction and the position of the block frame window in the wall cavity significantly affect the temperature of the internal window jamb. The conclusion about the possibility of condensation can be made by comparison with the temperature of the dew point, which is equal to +10,7°C and is shown in Figure 6 by a horizontal line.

The figure shows that the junctions of types 1 and 2 do not have a sufficient level of thermal reliability at any position of the window frame. Additional local insulation of the facade in the form of a window casing significantly increases the level of unit thermal reliability. The formation of condensate on the surface of the internal jamb becomes unlikely when shifting the window frame by about 90 mm for node type 5 and by 60 mm for node type 3.

Conclusions

1. Replacement of block frame windows with modern metal-plastic structures is often implemented in the practice of residential buildings renovation that was built in the second half of the 20th century. It does not solve the problem of energy efficiency, but to some extent increases the comfort of living in these houses.

2. The critical area with the lowest temperature of block frame windows junctions to the expanded clay precast concrete walls is the surface of the internal jamb near the window frame. When the temperature drops below the dew point temperature in this zone, thermal failure can be realized in the form of condensate formed on the jamb surface.

3. The operation temperature mode of the block frame window junction to the wall is influenced by the design of the junction and the position of the window in the cavity wall. Insulation of the external window jamb and shift of the window into the room increases the temperature of the critical area of the node.

4. In block frame window junctions to expanded clay precast concrete walls with a thickness of 300 mm without insulation of an external jamb the temperature of a critical zone does not rise above +9,3°C regardless of the window frame position. The temperature, less than the dew point +10,7°C causes the possibility of condensation.

5. In units with external jamb insulation the temperature of the critical zone can reach +10,5°C, i.e. also does not exceed the dew point and can cause condensation on the surface of the internal window jamb.

6. To ensure the proper temperature of the unit, it is necessary to perform insulation of the exterior window jamb and local insulation of the facade in the form of an outside window casing. When the width of such a frame is 150…250 mm, the corresponding shift of the block frame window inside the room by 90…60 mm increases the temperature of the inner surface of the window jamb above the dew point temperature.

7. For practical use in precast concrete walls with a thickness of 300 mm, we can recommend the design of the unit with insulation of the exterior window jamb and local insulation of the facade in the form of outside window casing with a width of 200 mm or 250 mm. The window frame should be installed at a distance of 80 mm or 60 mm from the outer surface of the wall (according to the selected width of the frame). It is better to use plates from expanded polystyrene as insulation. Attaching them to the wall and exterior decoration is less time-consuming and cheaper compared to the use of mineral wool slabs.

8. Local insulation of the facade around the outside window casing should be arranged with a thickness that meets the requirements of thermal insulation on the resistance to heat transfer of external walls according to DBN B.2.6-31: 2006. In this case, the executed local insulation will become a part of the front insulation of the building in the course of full thermal modernization in the future.

9. Further research is focused on the probabilistic assessment of thermal reliability of the block frame window junctions to the walls and other problematic units of buildings, taking into account the random nature of the influencing factors.

References

1. ДБН В.2.6-31:2006 (2016). Конструкції будинків і споруд. Теплова ізоляція будівель. Київ: Мінрегіонбуд України

2. Tsikaloudaki K., Laskos K., Bikas D. (2012). On the Establishment of Climatic Zones in Europe with Regard to the Energy Performance of Buildings. *Energies*, 5(1), 32-44 https://doi.org/10.3390/en5010032

3. The critical importance of building insulation for the environment. European insulation manufacturers association: https://www.eurima.org

4. Пашинський В.А., Настоящий В.А., Джирма С.О., Плотніков О.А., Остапчук А.С. (2017). Вплив положення віконних блоків по товщині стіни на теплотехнічні характеристики вузла їх примикання. *Sciences of Europe*, 21(3), 8-13

1. DBN V.2.6-31:2006 (2016). Constructions of houses and buildings. Thermal insulation of building. Kyiv: Ministry of Construction of Ukraine

2. Tsikaloudaki K., Laskos K., Bikas D. (2012). On the Establishment of Climatic Zones in Europe with Regard to the Energy Performance of Buildings. *Energies*, 5(1), 32-44 https://doi.org/10.3390/en5010032

3. The critical importance of building insulation for the environment. European insulation manufacturers association: https://www.eurima.org

4. Pashynskyi V.A., Nastoiashchyi V.A., Dzhyrma S.O., Plotnikov O.A., Ostapchuk A.S. (2017). The influence of the position of window blocks by the wall thickness on the thermal characteristics of their adjoining node. *Sciences of Europe*, 7, 21(3), 8-13

5. Пашинський В.А., Джирма С.О, Пашинський М.В. (2020). Теплові характеристики вузлів примикання вікон до цегляних та залізобетонних стін цивільних будівель на території Кіровоградської області. *Центральноукраїнський науковий вісник. Технічні науки*, 3(34), 200-209 https://doi.org/10.32515/2664-262X.2020.3(34).200-209
6. Pashynskyi M., Dzhyrma S., Pashynskyi V., Nastoyashchiy V. (2020). Providing the thermal reliability of window junctions during the thermal modernization of civil buildings, *Electronic Journal Osijek-e-GFOS*, 21, 45-54 https://doi.org/10.13167/2020.21.4
7. Stolarska A., Strzałkowski J. & Garbalińska H. (2018). Using CFD software for the evaluation of hygrothermal conditions at wall-window perimeters. *IOP Conference Series: Materials Science and Engineering*, 415, 1-8 https://doi:10.1088/1757-899X/415/1/012046
8. Kariuk A., Rubel V., Pashynskyi V., Dzhyrma S. (2020) Improvement of Residential Buildings Walls Operation Thermal Mode. *Proceedings of the 2nd Intern. Conf. on Building Innovations «ICBI 2019»*. Lecture Notes in Civil Engineering, 73. Springer, Cham. https://doi.org/10.1007/978-3-030-42939-3_9
9. Azmy Y., Ashmawy E. (2018). Effect of the Window Position in the Building Envelope on Energy Consumption. *Intern. J. of Engineering & Technology,* 7(3), 1861-1868 http://dx.doi.org/10.14419/ijet.v7i3.11174
10. Sierra F., Gething B., Bai J., Maksoud T. (2017). Impact of the position of the window in the reveal of a cavity wall on the heat loss and the internal surface temperature of the head of an opening with a steel lintel. *Energy and Buildings*, 142, 23-30 https://doi.org/10.1016/j.enbuild.2017.02.037
11. THERM 2.0 Program Description (1998). Berkeley CA 94720 USA
12. ДСТУ Б В.2.6-79:2009 (2013). *Конструкції будинків і споруд. Шви з'єднувальні місць примикань віконних блоків до конструкцій стін. Загальні технічні умови*. Київ: Мінрегіонбуд України
13. ДСТУ Б В.2.6-189:2013 (2013). *Методи вибору теплоізоляційного матеріалу для утеплення будівель*. Київ: Мінрегіонбуд України
14. ДСТУ-Н Б В.1.1-27:2010 (2011). *Захист від небезпечних геологічних процесів, шкідливих експлуатаційних впливів, від пожежі. Будівельна кліматологія*. Київ: Мінрегіонбуд України
15. Семко В.О., Пашинський В.А., Джирма С.О., Пашинський М.В. (2019). Температурний режим експлуатації будівель на території Кіровоградської області. *Центральноукраїнський науковий вісник. Технічні науки*, 1(32), 235-243

5. Pashynskyi V.A., Dzhyrma S.O., Pashynskyi M.V. (2020). Thermal characteristics of window junctions to brick and reinforced concrete walls of civil buildings in the Kirovohrad region. *Central Ukrainian Scientific Bulletin. Engineering sciences*, 3(34), 200-209 https://doi.org/10.32515/2664-262X.2020.3(34).200-209
6. Pashynskyi M., Dzhyrma S., Pashynskyi V., Nastoyashchiy V. (2020). Providing the thermal reliability of window junctions during the thermal modernization of civil buildings, *Electronic Journal Osijek-e-GFOS*, 21, 45-54 https://doi.org/10.13167/2020.21.4
7. Stolarska A., Strzałkowski J. & Garbalińska H. (2018). Using CFD software for the evaluation of hygrothermal conditions at wall-window perimeters. *IOP Conference Series: Materials Science and Engineering*, 415, 1-8 https://doi:10.1088/1757-899X/415/1/012046
8. Kariuk A., Rubel V., Pashynskyi V., Dzhyrma S. (2020) Improvement of Residential Buildings Walls Operation Thermal Mode. *Proceedings of the 2nd Intern. Conf. on Building Innovations «ICBI 2019»*. Lecture Notes in Civil Engineering, 73. Springer, Cham. https://doi.org/10.1007/978-3-030-42939-3_9
9. Azmy Y., Ashmawy E. (2018). Effect of the Window Position in the Building Envelope on Energy Consumption. *Intern. J. of Engineering & Technology,* 7(3), 1861-1868 http://dx.doi.org/10.14419/ijet.v7i3.11174
10. Sierra F., Gething B., Bai J., Maksoud T. (2017). Impact of the position of the window in the reveal of a cavity wall on the heat loss and the internal surface temperature of the head of an opening with a steel lintel. *Energy and Buildings*, 142, 23-30 https://doi.org/10.1016/j.enbuild.2017.02.037
11. THERM 2.0 Program Description (1998). Berkeley CA 94720 USA
12. DSTU B V.2.6-79:2009 (2013). *Construction of buildings and structures. The seams in the adjoining points of window blocks to the construction of the walls. General specification*. Kyiv: Ministry of Regional Development of Ukraine
13. DSTU B V.2.6-189:2013 (2013). *Methods of choosing of insulation material for insulation*. Kyiv: Ministry of Regional Development of Ukraine
14. DSTU-N B V.1.1-27:2010(2011). Protection against dangerous geological processes, harmful operational impacts, from fire. Building climatology. Kyiv: Ministry of Regional Development of Ukraine
15. Semko V.O., Pashynskyi V.A., Dzhyrma S.O., Pashynskyi M.V. (2019). Temperature regime of buildings operation in the Kirovohrad region. *Central Ukrainian Scientific Bulletin. Engineering sciences*, 1(32), 235-243

Збірник наукових праць. Галузеве машинобудування, будівництво
Academic journal. Industrial Machine Building, Civil Engineering

http://journals.nupp.edu.ua/znp
https://doi.org/10.26906/znp.2021.56.2508

UDK 624.012

Introduction of heat and energy-saving structures in construction as a condition of its sustainable ecological and economic development

Rohovyi Stanislav[1], Boginska Lydmila[2]*

[1.]Sumy National Agrarian University https://orcid.org/0000-0002-9431-5884
[2.]Sumy National Agrarian University https://orcid.org/0000-0001-8635-7980
*Corresponding author E-mail: Lyudmila.boginska@snau.edu.ua

The article identifies the main aspects of sustainable construction development in the implementation of the development strategy. Approaches and proposals for interrelated components of improving the efficiency of construction production, which are based on interdependent and complementary actions to achieve the competitiveness of the construction industry and are relevant to the functioning of the construction industry. Directions for improving construction production through the introduction of heat-saving structures at construction sites are proposed. The conclusions analyze the results of the construction industry. It is determined that the use of heat-saving structures, technologies, the formation and implementation on this basis of a strategy of long-term sustainable development - one of the construction priorities.

Keywords: sustainable development, construction production, heat-saving structures

Впровадження теплоенергозберігающих конструкцій в будівництво як умова його стійкого еколого-економічного розвитку

Роговий С.І.[1], Богінська Л.О.[2*]

[1, 2] Сумський національний аграрний університет
*Адреса для листування E-mail: Lyudmila.boginska@snau.edu.ua

У статті визначені основні аспекти стійкого розвитку будівництва в рамках реалізації стратегії розвитку. Розглянуто підходи і розроблено пропозиції щодо взаємопов'язаних складових підвищення ефективності будівельного виробництва, які ґрунтуються на взаємозалежних і взаємодоповнюючих діях досягнення конкурентоспроможності будівельної галузі і є актуальними для функціонування будівельного комплексу. Запропоновані напрями вдосконалення будівельного виробництва через впровадження теплоенергозберігаючих конструкцій на об'єктах будівництва. Задача, що розглядається в статті, полягає у пошуці нових підходів до вирішення еколого-економічних проблем будівельного виробництва за допомогою застосування теплоенергозберегаючих конструкцій. В роботі досліджується взаємозв'язок між випуском та виведенням на ринок теплоенергозберегаючих матеріалів й конструкцій нового покоління (коли для вироблення теплової енергії використовують поновлювані джерела енергії (енергію сонця, вітру і т.п.)), які дозволяють економити традиційні джерела теплопостачання та енергозабезпечення і еколого-економічним розвитком будівельної галузі. У висновках проаналізовано результати розвитку будівельної галузі. Визначено, що ефективне залучення природних ресурсів на інтерактивній основі, застосування теплоенергосберегаючих конструкцій, технологій, формування і реалізація на цій основі стратегії довгострокового стійкого розвитку - один з пріоритетів будівництва.

Ключові слова: стійкий розвиток, будівельне виробництво, тепло енергозберігаючі конструкції

Introduction

The construction industry is a key sector of the economy, designed to solve the most important tasks for the implementation of the socio-economic development strategy of the region and the state as a whole. The modern construction industry is forced to take into account the market instability and dynamism. For this reason, the following trend is important - any construction company needs to adapt to new economic conditions in a transient survival environment.

Construction is designed to create an artificial environment that ensures human life. Until now, the environment has been considered as a source of negative effects on the newly created man-made artificial environment. Construction as a powerful reversible factor influencing the environment has been the subject of research relatively recently. As practically necessary, certain limits of this problem are subject to study and solution (for example, waste disposal, air purification in settlements, etc.). Construction production has an anthropogenic impact on nature at all stages - from the extraction of building materials to the operation of the commissioned facilities.

Disruption of relationships within the ecosystem, the likelihood of serious consequences for a given region or area, is some negative results of construction activities. Large-scale combustion of extracted fuel leads to irreversible changes in the environment, up to changes in climatic conditions on the planet. This understanding to some extent contributes to the formation of the need for environmental safety and encourages manufacturers to develop, produce and market heat-saving materials and structures of the new generation (when renewable energy sources (solar, wind, etc.) are used to generate heat). They help to save traditional sources of heat supply and energy supply and are the main direction of ecological and economic development of the construction industry.

Review of research sources and publications

Baranovskiy V., Melnik L., Lesnoy A., Onegina V., Popova A. have analyzed in-depth theoretical and practical aspects of sustainable development in their works.

The authors of works devoted to the formation problems of the Concept of sustainable development are Vernadsky V., Girusov E., Gorshkov V., Landel M., Matrosova V., Paton B. and others.

Of the foreign specialists who dealt with sustainable development issues, it is worth noting: Mill J., Schumpeter J., Harrod R., Domar E., Solow R., Romer P., Porter M., Kotler F., Hay D., Morris D., Meadows D., Saaty T., Siegel J., Target D., Hargshoorn G., Oiken V., Plath R., Richardson Ch. and others.

The issue of using heat and energy-saving materials and structures in the production was raised in the works of Aleksandrovsky S., Bogoslovsky V., Vlasov O., Balmer R., Ilyinsky V., Gusarsky K., Srovsky S., Likova A., Lukyanova V., Koryakins A., Upenietse L., Bakhare D., Savitsky M., Semko A., Stroy A., Tabunshchikova Yu., Ushkova F., Fokin K. and others.

Definition of unsolved aspects of the problem

However, the insufficient elaboration mechanism of sustainable development of the construction complex, taking into account the involvement of innovative building materials production and heat-saving structures provides further study of this topic.

Objective of the work and research methods

The study aims to search for new approaches to solving environmental and economic problems of construction production through the introduction of heat-saving structures.

The goal was achieved by the following methods:

– theoretical studies based on modern developments of the strategy for the development of the construction industry;

– research of innovations in the field of theory and practice of creating new building structures with increased thermal efficiency;

– mathematical modeling.

Basic material and results

The efficiency of the construction complex is directly dependent on the growth in demand for construction products, work, services in the materials replacement, structures produced by more innovative ones through successful scientific and technical innovations that significantly improve, optimize construction processes and are accompanied by resource, technological, environmental, economic, budgetary effects (Fig. 1).

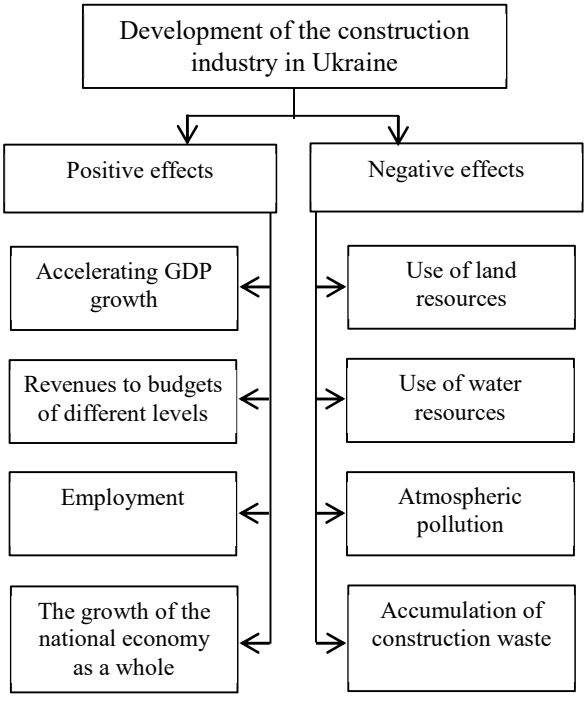

Figure 1 – The results of the construction industry

Production efficiency implies sustainable development and success in the future. The interpretation of the definition of "sustainable construction" has been in place recently. The first international conference on sustainable construction (Tampa, USA, 1994) proposed

the following definition: “Sustainable construction means the creation and responsible maintenance of a healthy artificial habitat based on the efficient use of natural resources and environmental principles.” This definition was further developed in the decisions of the Second Conference (Paris, 1997): “Sustainable construction is the support of a healthy economy in order to ensure a quality of life while protecting human life and the environment; minimization of damage caused to self-healing of the environment, human health, biological diversity; optimal use of non-renewable resources and constant use of renewable resources” [8].

In modern economic conditions, the main emphasis shifts from solving problems identified by the analysis of the optimal use of resources available to the construction company, the problems of existing production situations, to find ways to solve them (Fig. 2).

Relevant in today's conditions is the search and approval of new approaches to sustainable development, taking into account the current and future state of environmental resources, which should be reflected in the mechanisms for the implementation of the country's resource and environmental policy.

Energy and resource-saving are the general directions of the technical policy of Ukraine in the field of construction and a prerequisite for its sustainable development [6].

Development is a multi-criteria, complex process that illuminates the individual characteristics of each enterprise and depends on its strategic goals. Only managed development can be sustainable. The sustainable development of an enterprise is a full-fledged reflection of its competitiveness in market conditions. Under these conditions, it is important to draw up an expert assessment of the development of a particular construction company (Figure 3).

Environmental friendliness in construction is achieved through the introduction of heat-saving structures and technologies. Control and management of energy-saving and heat saving in the construction industry must be carried out both at the state level and at the level of individual enterprises, as well as at all building life cycle stages.

It is expedient to reduce energy costs in construction by applying the latest technologies of thermal renovation of buildings by increasing the thermal insulation capacity of the enclosing structures of construction objects. The choice of thermal insulation materials takes into account the natural and climatic conditions of the construction area, architectural and structural solutions of buildings in accordance with environmental and economic monitoring.

For a long time, the issue of energy savings in construction, as well as in the national economy as a whole, was not given the necessary attention. According to the standards in force in Ukraine, the resistance to heat transfer of building envelopes was reduced compared to European standards on the walls - 1.2-3.5 times, on the floor and ceiling - 2 times, on the windows - 1.3 times. As a result, we have significant costs of fuel and energy resources in the operation of housing [8].

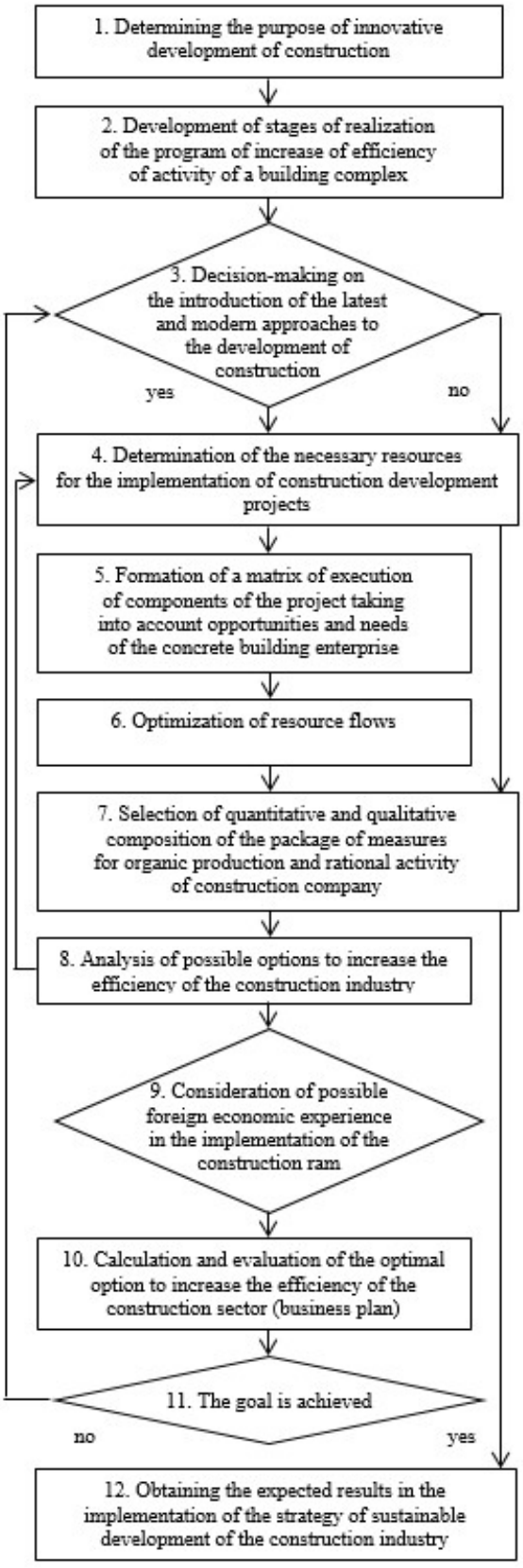

Figure 2 – Algorithm of the construction development program
(*developed by the author*)

In this algorithm, an important link is the definition of indicators for assessing the state and development prospects of business entities, competitiveness.

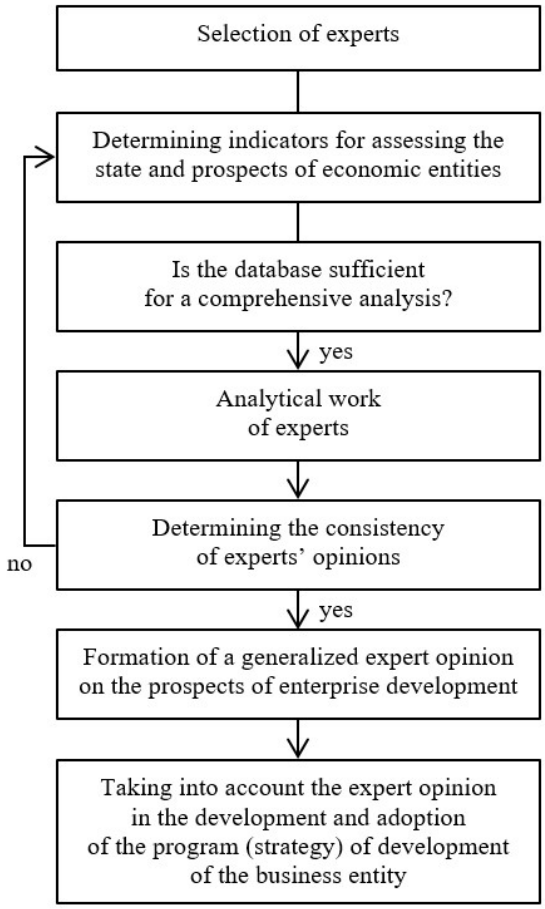

Figure 3. Algorithm of expert assessment of the business entity development (construction company)
(*developed by the author*)

Modern building codes in European countries set energy consumption at 80-100 kWh / m^2 per year. In the new generation of houses that are designed and built according to the concept of Passive House, the level of energy consumption can be reduced to 15-30 kWh / m^2 per year, depending on the region of construction. The determining factor that allows providing such a standard is the use of effective thermal insulation in building structures [7, 11].

Based on the accumulated experience of design organizations in Ukraine [5], analysis of the principles of ensuring the energy efficiency of buildings adopted in European countries, where problems connected with heat and energy saving is given priority values, developed Ukrainian building codes DBN B.2.6-31: 2006 "Thermal insulation of buildings". These rules provide:

– an increase of the minimum level of thermal protection enclosing structures of residential and office buildings on average by 15-40% for exterior walls, 20-25% for coatings, 20% for windows;

– standard indicators of the maximum permissible values of heat loss for heating buildings;

– introduction of energy certification of buildings for new construction and reconstruction;

– introduction of norms for indicators of thermal reliability of heat-insulating shells of buildings and structures [4].

It should be noted that the reserves of fuel energy resources (natural gas, oil, coal) are limited. The ways to solve the problems of preserving and restoring the ecological balance of natural and anthropogenic life systems are as follows:

– formation of scientific foundations for rational resource and energy consumption in urban planning, taking into account regional differences;

– formation of the scientific foundations of the "city - building – structure" model;

– development of a regulatory and legal framework for heat and power saving;

– implementation of new promising low-cost technologies with two to four times lower heat and energy consumption;

– implementation of constructive and architectural solutions of increased energy efficiency under construction and reconstruction.

For the competent decision of this problem, it is necessary to carry out complex inspections of a building heat-insulating cover for the definition of places of the greatest heat losses and ways of their reduction.

This work should include acquaintance with the design documentation for the construction site, conducting an estimated assessment of heat loss, and, if necessary, conducting instrumental studies of thermal insulation of fences.

Numerous and intensive researches are carried out in our country and abroad, directed basically on the search of easy and heat-and-energy protecting designs differing in low complexity of erection, durability, and maintainability.

Such close attention to the design of effective enclosing structures is explained, on the one hand, by the important place they occupy in the structure of the building, and on the other hand - by the role, they play in solving the problem of saving fuel and energy resources.

Foreign and domestic experience and accumulated knowledge suggest that the implementation of heat-efficient construction should move towards reducing heat loss of the building, efficient use, and production of energy.

To assess the effectiveness of the work done to reduce the building heat loss, the efficient use of energy in it and its efficient production, the European Association "Active House" proposes to use three main criteria:

– comfortable living (healthy lifestyle);

– energy (energy balance of the building - the total amount of energy generated and consumed by the house should ultimately make up a positive energy balance)

– environment (the effect of the building's impact on the environment should be minimal) [5].

The introduction of heat and energy-saving technologies is a today requirement. It is estimated that the heat cost and energy saving is recouped in two to three years.

Heat and energy saving in an apartment building is, first of all, reducing heat losses by insulating walls, floors, ceilings, windows,s, and doors.

According to the rating "Ukrainian Energy Index – 2011", the energy efficiency of the Ukrainian economy is 52% of the EU level [1].

Improving energy efficiency to European levels will save approximately € 11.8 billion annually.

The main priority in solving this problem is the thermal modernization of buildings. Saving energy resources as a result of thermal modernization is several times higher than the savings from improving the means of generating heat. At the same time, thermal modernization of buildings leads to a decrease in heat losses in boiler houses and heating networks, as it reduces the required volumes of produced and transported heat carriers.

Ukraine must comply with EU directives on energy efficiency, in particular, Directive 2010/31 / EU on the energy performance of buildings and Directive 2006/32 / EU on the efficiency of the energy end-use and services. Obviously, no modernization of the means of generating and transporting heat can and closely compare in efficiency with thermal modernization at the consumer [2, 12].

Thermal modernization of external walls with the protection of heat-insulating material from external influences with a protective and decorative plaster layer has the following disadvantages:

– seasonality of work performance;

– unacceptable to apply plaster in direct sunlight, rain, and strong wind;

– the system fragility;

– the need for the device of expansion joints 6 mm wide, which compensate for the deformation of the plaster layers from fluctuations in temperature and humidity;

– increased requirements for the vapor permeability of the outer layers of additional insulation while maintaining their ability to provide protective functions;

– rapid contamination of the facade;

– increased requirements for the rigidity of heat-insulating dowels, which leads to the formation of cracks and destruction of the outer decorative and protective layer;

– impossibility to conduct operational control over the state of the heat-insulating material;

– the high operational cost of the system [9, 13].

The most expensive measure in the thermal modernization of the building is the insulation of enclosing structures. The estimated payback period of this measure is from 7-8 years when using heat-insulating materials of Ukrainian production, and from 12 years - when using imported materials. However, by warming the greatest energy-saving effect is reached.

In this case, the insulation of the building is inevitably accompanied by its overhaul, which in turn increases the service life of the building, the degree of its comfort.

Therefore, when calculating the payback, it is necessary to take into account these advantages of thermal modernization, which will significantly increase the economic attractiveness of such projects [10, 14].

In the initial phase of a construction project, it is useful to be able to assess the performance of a future facility. An integral part of one-time and operating costs are the costs of the construction part of the building. It is important to note that this part of the cost is not involved in the technological process, so its minimization is very useful.

Conclusions

The model of sustainable development is implemented in the interaction process between society and the environment by combining the economic, social, and environmental interests of society.

The ecological factor becomes system-forming in the concept of sustainable economic development.

However, the problem of the environmental factor of sustainable development is still insufficiently developed by economics in both theoretical and applied aspects.

The effective attraction of natural resources on an interactive basis, application of heat-saving constructions, technologies, formation, and realization on this basis of the strategy of long-term sustainable development is one of the priorities of construction.

Thermal protection of buildings requires a fundamental revision of the materials used and technical solutions of building envelopes. Now it is almost impossible to provide the necessary indicators of thermal protection in single-layer structures of brick walls or structurally insulating lightweight concrete with high density and thermal conductivity. Compliance with current regulations requires the use of multilayer structures with effective types of insulation materials.

The production base of effective thermal insulation materials needs to conduct research on the development of such materials and technical solutions for fencing structures based on them from local raw materials and industrial waste. This will contribute to the sustainable development of the construction industry.

References

1. *Рейтинг енергоефективності України*. Режим доступа: http://www.energyindex.com.ua

2. Карп И.Н., Никитин Е.Е. *Пути решения проблем коммунальной энергетики*. Режим доступа: http://esco-ecosys.narod.ru/2011_12/art104.pdf

3. Патон Б.Є., Долінський А.А., Геєць В.М., Кухар В.П., Басок Б.І., Базєєв Є.Т., Подолець Р.З. (2014). Пріоритети Національної стратегії теплозабезпечення населених пунктів України. *Вісник Національної академії наук України*, 9, 29-47

4. ДБН В.2.6-31:2016 (2017). *Теплова ізоляція будівель*. Київ: Мінрегіонбуд України

5. Мировые тенденции повышения энергоэффективности зданий (2012). *Энергосбережение*, 5, 38-42

6. Богінська Л.О. (2020). Визначення стратегії розвитку будівельного підприємства. *Інфраструктура ринку*, 30, 123-127

7. Balmer R.T. (2011). *Modern Engineering Thermodynamics*. Elsevier

8. Hepbasli A. (2012). Low exergy (LowEx) heating and cooling systems for sustainable buildings and societies. *Renewable and Sustainable Energy Reviews*, 16(1), 73-104

9. Husarski K., Srokowski S. (1978). Problem dostosowania rozwiazan budowlanych do zmiennoscitechnologieznuch. *Inwest. Budow.*, 24, 48-49

10. Korjakins A., Upeniece L., Bajare D. (2013). Heat insulation materials of porous ceramics, using plant filler. *4th International Conference Civil Engineering`13 Proceedings. Part I Construction and materials*, 169-175

11. Beregovoi V.A., Proshin A.P., Beregovoi A.M, Soldato S.N (2000). Heat-Conducting Properties of Small-Power- Hungry Cellular Concrete. *Asian Journal of Civil Engineering (Building and Housing)*, 1(4), 56-64

12. Proshin A.P., Beregovoi V.A., Beregovoi A.M, Volcova E.A. and oth. (2001). New thermal insulation materials. *Problems and prospects in ecological engineering*. Tenerife, Spain, 108-110

13. Voller V.R., Felix P., Swaminathan C.R. (1996). Cyclic phase change with fluid flow. *Int. J. Numer. Meth. Heat Transfer Fluid Flow*, 6, 57-64

14. Pelke R. (1976). *Energieeinsparung in der Klimatechnik*, 6, 156-158

1. *Energy efficiency rating of Ukraine*. Access mode: http://www.energyindex.com.ua

2. Karp I., Nikitin E. *Ways to solve problems of communal energy*. Access mode: http://esco-ecosys.narod.ru/2011_12/art104.pdf

3. Paton B., Dolinsky A., Geets V., Kuhar V., Basok B., Bazeev E., Podolets R. (2014). Priorities of the National strategy of heat supply of settlements of Ukraine. *Bulletin of the National Academy of Sciences of Ukraine*, 9, 29-47

4. DBN B.2.6-31:2016 (2017). Thermal insulation of buildings. Kyiv: Ministry of Regional Development, Construction and Housing of Ukraine

5. World trends in improving the energy efficiency of buildings (2012). *Energy saving*, 5, 38-42

6. Boginska L. (2020). Definition of strategy of development of the construction enterprise. *Market Infrastructure*, 30, 123-127

7. Balmer R.T. (2011). *Modern Engineering Thermodynamics*. Elsevier

8. Hepbasli A. (2012). Low exergy (LowEx) heating and cooling systems for sustainable buildings and societies. *Renewable and Sustainable Energy Reviews*, 16(1), 73-104

9. Husarski K., Srokowski S. (1978). Problem dostosowania rozwiazan budowlanych do zmiennoscitechnologieznuch. *Inwest. Budow.*, 24, 48-49

10. Korjakins A., Upeniece L., Bajare D. (2013). Heat insulation materials of porous ceramics, using plant filler. *4th International Conference Civil Engineering`13 Proceedings. Part I Construction and materials*, 169-175

11. Beregovoi V.A., Proshin A.P., Beregovoi A.M, Soldato S.N (2000). Heat-Conducting Properties of Small-Power- Hungry Cellular Concrete. *Asian Journal of Civil Engineering (Building and Housing)*, 1(4), 56-64

12. Proshin A.P., Beregovoi V.A., Beregovoi A.M, Volcova E.A. and oth. (2001). New thermal insulation materials. *Problems and prospects in ecological engineering*. Tenerife, Spain, 108-110

13. Voller V.R., Felix P., Swaminathan C.R. (1996). Cyclic phase change with fluid flow. *Int. J. Numer. Meth. Heat Transfer Fluid Flow*, 6, 57-64

14. Pelke R. (1976). *Energieeinsparung in der Klimatechnik*, 6, 156-158

Збірник наукових праць. Галузеве машинобудування, будівництво
Academic journal. Industrial Machine Building, Civil Engineering

http://journals.nupp.edu.ua/znp
https://doi.org/10.26906/znp.2021.56.2509

UDC 624.131: 624.154

Efficient foundation pits solutions for restrained urban conditions

Vynnykov Yuriy[1], Kharchenko Maksym[2], Akopian Mkrtich[3*], Aniskin Aleksej[4]

[1] National University «Yuri Kondratyuk Poltava Polytechnic» https://orcid.org/0000-0003-2164-9936
[2] National University «Yuri Kondratyuk Poltava Polytechnic» https://orcid.org/0000-0002-1621-2601
[3] National University «Yuri Kondratyuk Poltava Polytechnic» https://orcid.org/0000-0002-5271-6639
[4] University North, Varaždin, Croatia https://orcid.org/0000-0002-9941-1947
*Corresponding author E-mail: armenia3579@gmail.com

There are presented analysis results of the new multi-story residential building construction's impact on the existing development, constructive and technological measures for the arrangement of an excavation, deeper than the existing foundations' footing level, with minimal costs and minimal negative impact on the surrounding buildings. In particular, its excavation stages, results of the excavation shoring strength calculation, as well as proposals for the technical condition monitoring of existing buildings in the process of new construction were introduced. The calculation of the new construction's impact, including the arrangement of the pit, was performed in a plane, nonlinear formulation by the finite element method (FEM). Numerical modeling of the system "base - foundations of the existing building - shoring construction" was performed using an elastic-plastic soil model with the Mohr-Coulomb strength criterion.

Keywords: soaked loess base, excavation shoring, spread foundation, pile foundation, settlement, stress-strained state, finite element method

Ефективні рішення влаштування котлованів у тісній забудові

Винников Ю.Л.[1], Харченко М.О. [2], Акопян М.К.[3*], Аніскін А.[4]

[1, 2, 3] Національний університет «Полтавська політехніка імені Юрія Кондратюка»,
[4] Північний університет, Вараждин, Хорватія
*Адреса для листування E-mail: armenia3579@gmail.com

Викладено результати аналізу впливу на існуючу забудову нового будівництва багатоповерхового житлового будинку, конструктивні й технологічні заходи з улаштування більш глибокого, ніж рівень підошви існуючих фундаментів котловану, за мінімальних затрат та мінімального негативного впливу на оточуючу забудову, зокрема, стадійність його відкопування, дані розрахунку міцності елементів огородження котловану, а також пропозиції щодо моніторингу технічного стану існуючих будівель у процесі будівництва. Грунти майданчику – переважно замоклі лесовані суглинки. Фундаменти існуючих будинків – стрічкові, а нового – із задавлених паль, об'єднаних залізобетонними ростверками: стрічковими під стінами та окремими під колонами. Розрахунок впливу нового будівництва, зокрема й влаштування котловану, виконано у плоскій нелінійній постановці методом скінченних елементів (МСЕ). Моделювання системи «основа – фундаменти існуючої будівлі – конструкція огородження» виконано із застосуванням пружно-пластичної моделі ґрунту з критерієм міцності Кулона – Мора. Наведено приклади результатів моделювання МСЕ деформацій грунтового масиву на різних стадіях улаштування огородження котловану. Розрахунками елементів огородження котловану з урахуванням стадійності виймання грунту та врахуванням мінімальних затрат, встановлено, що огородження котловану можливо влаштувати з шпунтових паль (двутаври №30Ш) з кроком 1 м та між ними дерев'яної забірки. Обгрунтовано, що для збільшення стійкості й зменшення деформацій вертикальних елементів огородження котлован на початкових стадіях слід розробляти котлован під захистом грунтової берми, а надалі – з встановленням обвязувальної балки, розкосів, підкосів і поступовим підведенням підлоги й зовнішньої стіни паркінгу. За результатами моделювання визначено, що максимальні горизонтальні переміщення огородження котловану на різних стадіях його влаштування коливаються від 0.8 до 2.3 см у зоні існуючих будівель. Максимальні вертикальні переміщення основ фундаментів існуючих будівель склали 0.8 см, що не перевищує допустимих за нормами величин.

Ключові слова: замокла лесована основа, огородження котловану, фундамент на природній основі, пальовий фундамент, осідання, напружено-деформований стан, метод скінчених елементів

Introduction

One of the current problems of modern construction in dense urban development is the danger of additional absolute and relative uneven deformation of the existing buildings' foundations, structures, and underground utilities due to new construction. Geotechnical experience shows that due to the impact of construction and operation of new facilities, the bases of the surrounding buildings' foundations are sometimes significantly deformed, and occasionally further operation of these buildings becomes dangerous [1-8].

Thus, a classic case of such influence in a weak soils environment was a five-story residential building built on piles, on the corner of Povitroflotsky and Peremohy avenues in Kyiv. Additional loading of its pile base from the side of the new five-storey building-insert on a slab foundation led to the emergency condition of the load-bearing structures of the adjacent part of the existing building.

Another problematic geoengineering task was not only to improve the design, installation, and execution of works in a deeper (compared to the level of the existing foundations' footing) excavation in the area of existing development [5, 7, 9, 10], but also to minimize the cost of protective measures.

Review of the research sources and publications

Limit additional absolute and relative bases' deformations of the surrounding structures' foundations, located in the influence area of deep pits or communications, depending on the type of these objects and their technical condition category [2, 5-7].

In the case of designing bases and foundations, as well as underground components of new buildings and structures or objects to be reconstructed, under conditions of dense urban development, geoengineering monitoring is performed to assess the impact of new buildings on the stress-strain state (SSS) of the surrounding soil, in particular, and foundations of the surrounding buildings. Under these conditions, graphical, analytical, graph-analytical, numerical, and other methods proved efficient in practice [1, 2, 4-7, 9-16].

If the excavation of the foundation pit with free slopes for the new construction is not justified by calculations, usually the excavation shoring of different types and technologies is used, for example [5, 7, 9-11, 13, 14, 16]:

– sheet piling (thin wooden, metal, reinforced concrete, plastic flat or profile retaining walls, the stability of which provided by the deep immuration in the ground or in combination with ground anchors, stiffeners, struts, etc.); retaining berms and unloading trenches have gained some popularity as a supplement to sheet piling, especially in conditions of weak soils; this option has a limit on the pits depth up to 5 - 6 m;

– excavation shoring such as "wall in the ground"; makes it possible to dig excavation of a considerable depth;

– shoring from tangent and secant drilled piles makes it possible to dig excavation of considerable depth;

– soil-cement excavation shoring made by deep soil mixing or jet cementation technology; has a limit on the excavation depth up to 5… 6 m;

– application of the Top-Down technology (vertical elements of shoring are arranged by the "wall in soil" technology, from drilled secant or drilled tangent piles), etc.; enables excavation of the deepest pits, including ones in the dense urban development.

As a rule, the choice of each design and the technological solution is influenced by several factors: geoengineering and hydrogeological conditions; technical state of existing buildings; economic; constructive, organizational-technological, many others [5, 7, 9-11, 13-16].

Definition of unsolved aspects of the problem

Each time the geoengineer must estimate the SSS of a rather complex and variable system in the development process, which includes the soil mass with the actual and projected groundwater level, existing foundations and superstructure of buildings in a certain technical condition, underground engineering networks, excavation at different stages and elements of its shoring, foundations of the new building and its load-bearing structures, take into account the cost of the proposed design solutions.

In particular, the efficiency and reliability of the above system are influenced by certain actual parameters of the excavation shoring, which are statistically variable: the increment and penetration depth of the shoring elements; geometric location of the capping beam; eccentricity of the excavation wall axis to the axis of the shoring's vertical element; geometric parameters of the existing surrounding buildings' foundations; physical and mechanical properties of the soils massif; technological issues during jacking the vertical elements; dynamic effects on the excavation edge; flooding of the excavation, etc.

Correct consideration of the possible variability of these factors, as well as the development of the excavation staging, can minimize the possible impact of new construction on surrounding buildings and existing networks with the required level of reliability and at the same time have minimal costs compared to alternative methods of excavation in certain conditions.

The existing regulative system of scientific and technical monitoring of buildings and structures [17] has not taken into account the features of the above-mentioned geoengineering problem yet.

Problem statement

Therefore, the purpose of the study is to minimize the impact of new construction to regulatory standards utilizing the actual construction site in dense development (number of surrounding residential buildings is more than one) with soaked loess loans and the excavation's bottom level deeper than the level of the existing foundations' footing at the cheapest possible excavation shoring solution.

In particular, the following tasks are highlighted:

– determining the area of the possible impact of new construction on the surrounding buildings;

– analysis of the new construction impact on the surrounding buildings with the definition of the allowable additional impact during performing the excavation;

– development of constructive and technological

measures to minimize the possible impact of new construction on the surrounding buildings and existing underground networks;

– substantiation of the excavation workflow with minimization of the impact on existing buildings;

– calculation of strength and deformability of the elements of the excavation shoring taking into account the variability of the actual geometric parameters;

– development of recommendations for monitoring the technical condition of existing buildings in the process of new construction.

Basic material and results

The site of the full-scale object is located at the corner of Pushkin and Vatutina streets in Poltava (Fig. 1). The roadway of Vatutina street is 5.5 m away from the excavation, and Pushkina st. - 5.3 m.

The new building is one-section, eight-story, with public facilities on the ground floor and underground parking. The multi-story part is adjoined by a one-story underground car park through a contraction joint. The height of the underground floor is 3.9 m, and the depth of the excavation is over 4.0 m.

In construction terms, the new building is a framed monolithic structure from the foundation to the slab above the ground floor. Above that, it's a frameless structure with longitudinal and transverse load-bearing walls and interflooring of precast slabs. Its foundation is piles C140.35-8 (section 0.35x0.35 m, length 14 m), connected by a reinforced concrete spread grille under the walls and separate reinforced concrete grilles under the columns. The consequence class of the building is CC2.

From the analysis of the general plan and constructive parameters of the new building, it is possible to generalize that for the underground parking construction, it is necessary to dig an excavation 4.8 m deep (to a datum of 152.3 m) with vertical slopes.

Excavation and the new building foundations' performance will have an impact on existing buildings. Thus, the zone of negative influence (Fig. 1), in particular, includes the existing six-story residential building on Vatutina St. 9/68, five-story residential building on Pushkina St. 66A (at a distance of 7.2 m from the excavation), the roadway of Pushkina St. with a network of underground communications (taking into account the pillar crane area) and the roadway of Vatutina St., etc.

The building on Vatutina St. 9/68 has 6 floors, including the attic, and under the whole building, there is a basement (depth of the underground part - 2.2 m). Its shape in plain view is rectangular with overall axial dimensions 23.25x13.36 m and 18.5 m height. The structural scheme is frameless.

The load-bearing walls are longitudinal external and internal.

The foundations of load-bearing and self-supporting walls are spread monolithic reinforced concrete, shallow laying, on a natural base, the foundations footing depth from the ground level is 2.2 - 2.5 m. The bearing stratum of the base (Fig. 2) is an engineering geological element (EGE) heavy silty loam, stiff (EGE-2) loam with a thickness of up to 1.8 m. The spread foundation edge is 0.5 - 0.8 m away from the excavation. The general technical condition of the building is defined as "2" - satisfactory, and therefore the allowable additional settlement of its base from the influence of the new building should not exceed 20 mm, and their relative unevenness - 0.0015 [2].

a)

b)

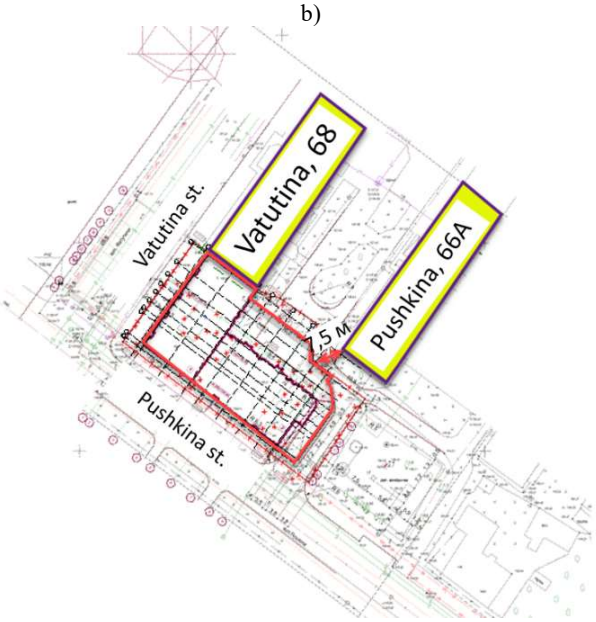

c)

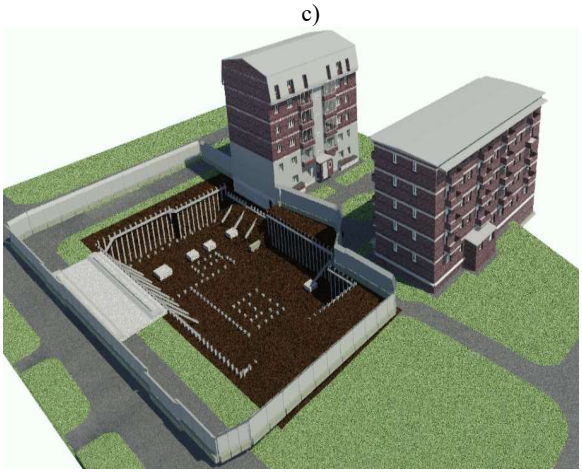

Figure 1 – Layout schematic of the site in:
a – full-scale conditions before the excavation;
b – in plain view;
c – in spatial dimension (design proposal)

A five-storey building on Pushkina St66A was built according to the 1-511 series, with a technical underground under the entire building. It has a rectangular shape in plan view with overall dimensions in the axes of 12.0x33.6 m. The load-bearing elements are external and internal longitudinal walls. Structural scheme - frameless with longitudinal load-bearing walls and stairwells in the form of stiffening cores. Foundations of walls - spread, precast reinforced concrete, a shallow foundation on a natural base. The bearing layer of their footing is EGE-2 (Fig. 2). The building is 7.2 m away from the edge of the future excavation. The general technical condition of the object - "2" - is satisfactory (as one that contains structures with the technical condition of category "2", but there are no structures of responsibility category A1, A or B with the technical condition of category "3" or "4"). Permissible additional settlement of its base from the influence of the new building should not exceed 10 mm, and their relative unevenness - 0.0015 [2].

Geomorphologically, the site is confined to the Poltava loess plateau. The thickness of the loess strata does not exceed 8 m on site. However, in the case of the soil massif soaking, settlement from the net weight is absent. Lithologically, the section up to a depth of 20 m is represented by silty heavy loams (EGE-2 and EGE-4 - stiff) and light (EGE-3 - fluxional, IGE-5a - soft-firm, IGE-5b - fluid-firm), as well as light silty, semi-hard clay (EGE-6). The layers are covered with bulk soil (EGE-1) with a thickness of 0.8 - 1.8 m. The soil strata are sufficiently sustained for the depth and area of the massif.

At the time of surveys and investigations, the groundwater level was recorded at 4.2 - 4.5 m below the ground surface (approximately at the level of the future excavation's bottom), it is expected to rise to 2.0 m.

According to the results of the existing buildings' investigation, the sections of the greatest influence of the new construction on these buildings and communications are highlighted (Figs. 3 and 4).

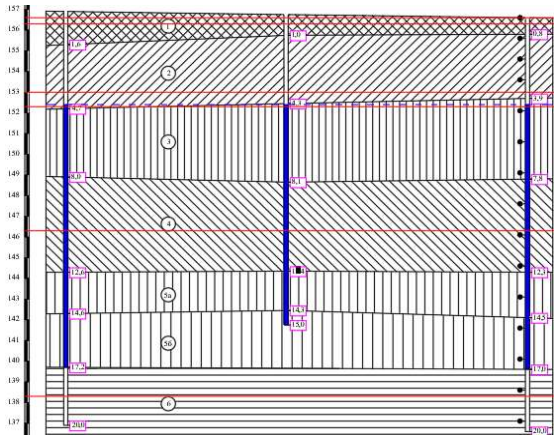

Figure 2 – Geotechnical cross-section of the site

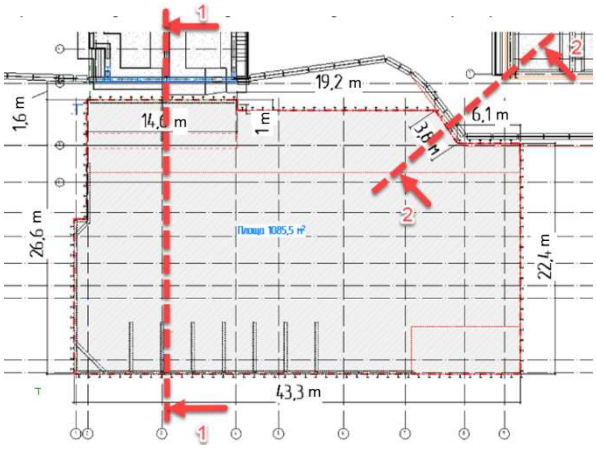

Figure 3 – Scheme of the design sections

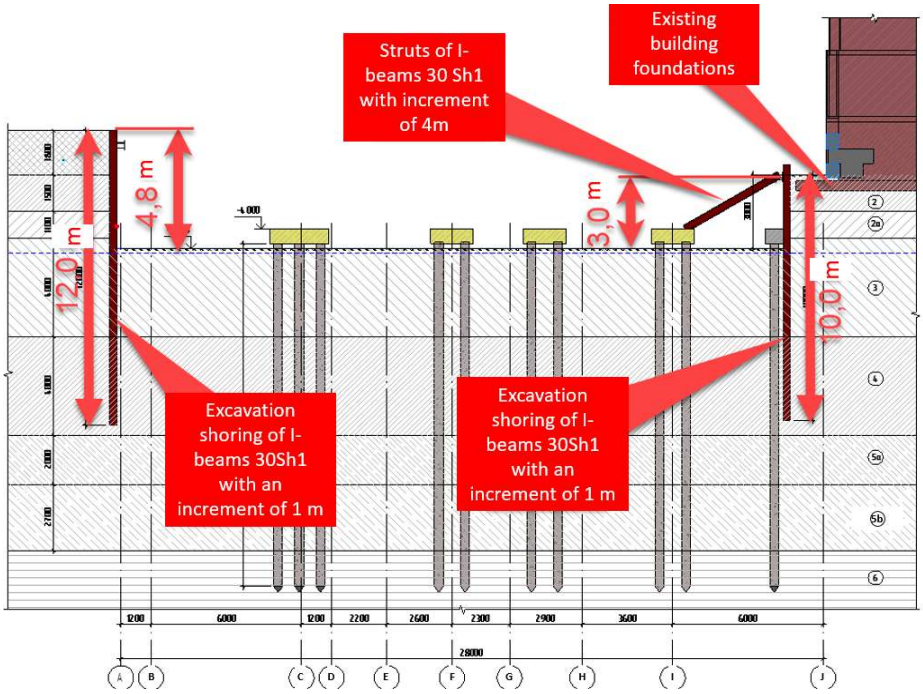

Figure 4 – Section 1-1 (6-storey building and tower crane for new construction along the axis «A»)

As an example we will consider results of only the basic calculations of the excavation shoring, influence of new construction on the existing building, checks of deformations during excavation, and an underground part of a new building on section 1-1 (passes through the six-storeyed building). Its foundations are 0.5 - 0.8 m from the edge of the excavation and the depth of the excavation in this section is 4.8 m (Fig. 4).

To reduce the load on the shoring, its depth was reduced by performing a preliminary ("pioneer") excavation with a depth of 1.8 m near the building. At the same time along with the existing building on Vatutina St., 9/68 there will be removed almost the entire bulk layer. Then from the bottom of the "pioneer" excavation vertical elements of the shoring will be pressed down (metal piles of I-beams 30Sh1 10 m long, with an increment of 1.0 - 1.5 m), between which a wooden fence and a capping beam will be installed. The proposed technology has the lowest cost compared to Larssen sheet piling and is arranged in the shortest time compared to drilling piles or "wall in the ground" (no need to wait for concrete to cure and it is possible to excavate the soil immediately after immersion of metal piles). It is expedient to create the offered protection on the following stages:

1 – immersion from the ground surface of pressed piles for a new building (before the arrangement of the excavation); erection of the vertical shoring elements along the contour of the excavation except for the area near the building (Fig. 5);

2 – digging the "pioneer" excavation to a depth of 1.8 m from the surface; pressing the piles of a shoring from I-beams 30Sh1 between excavation and the base of the existing building (fig. 6);

3 – excavation to the design depth under the protection of a soil berm 3.2 m wide with a slope of 45 - 50 ° (Fig. 7);

4 – an arrangement in the upper part of the shoring (0.5 m from the surface) of the capping distribution beam of I-beams 30Sh1, installation of I-beams 30Sh1 struts with an increment of 4 m on pre-arranged grilles of the future building (Fig. 8);

5 – works performance on arrangement of spread grilles under the parking wall, the parking floor arrangement, which will act as a spacer system and will accept the load from the shoring, it is also advisable to perform vertical reinforced concrete structures (pylons, walls) to the struts level and only after gaining strength with concrete to remove the struts and continue to perform monolithic work (Fig. 9).

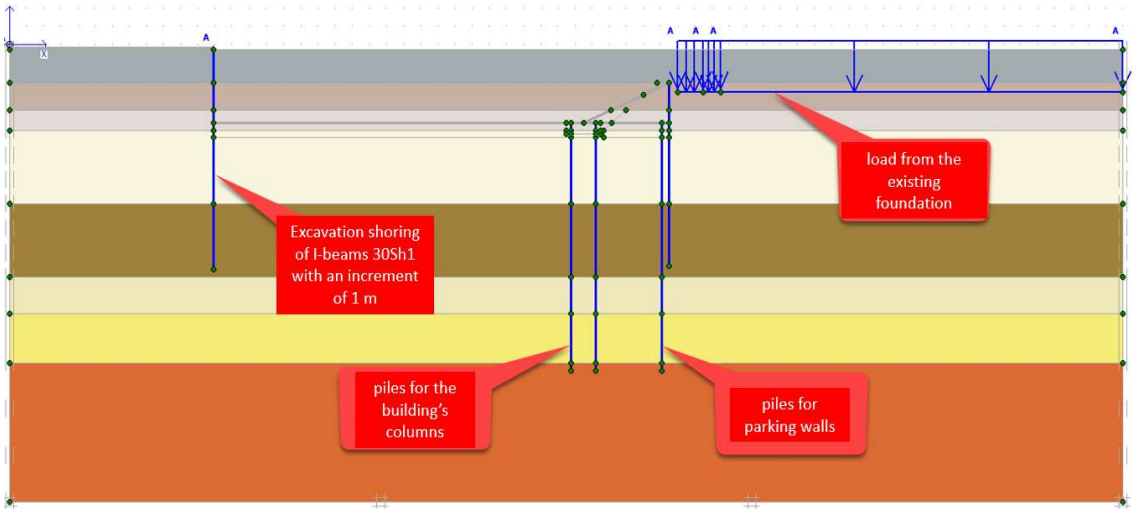

Figure 5 – Stage 1 of the excavation shoring erection in section 1-1

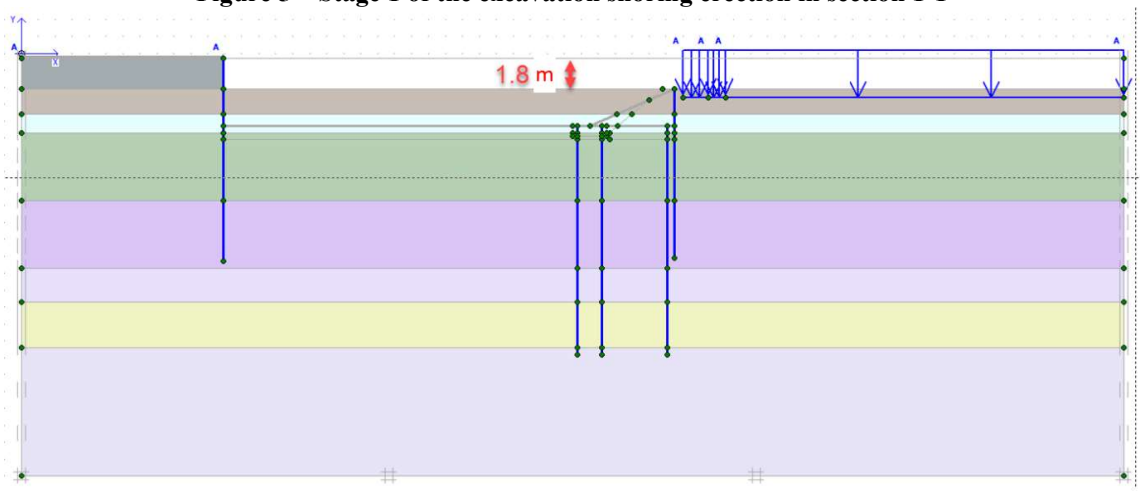

Figure 6 – Stage 2 of the excavation shoring erection in section 1-1

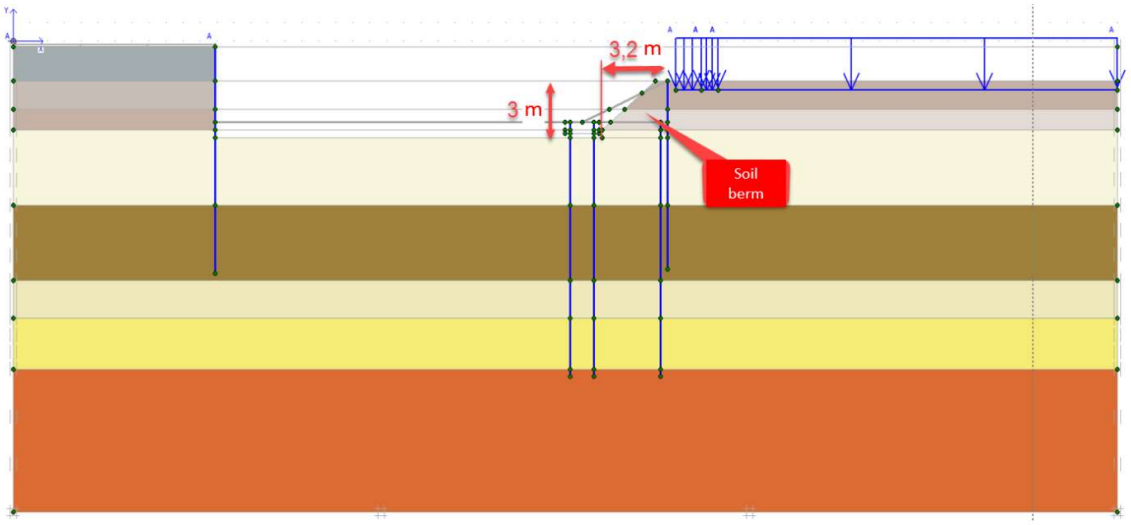

Figure 7 – Stage 3 of the excavation shoring erection in section 1-1

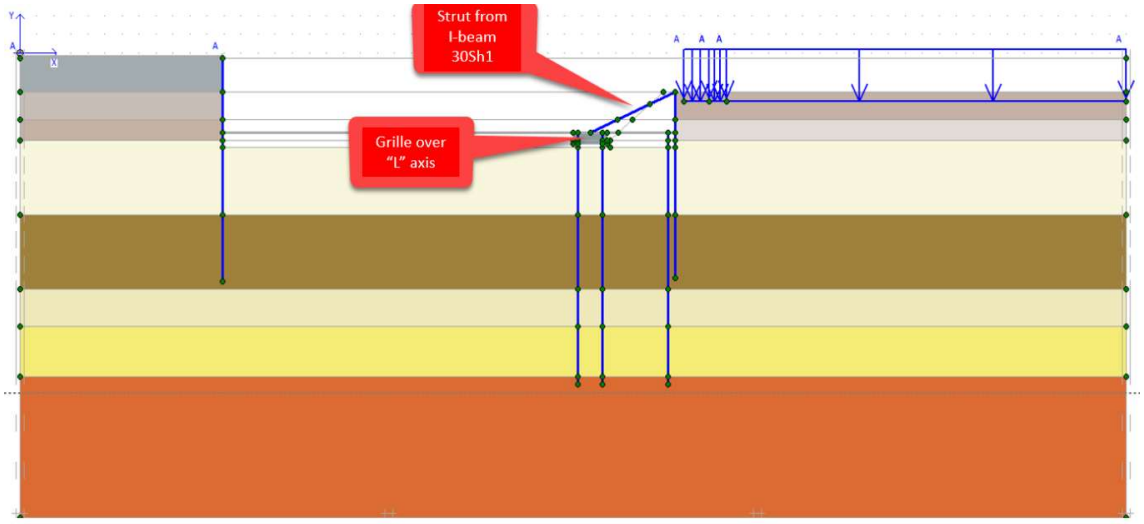

Figure 8 – Stage 4 of the excavation shoring erection in section 1-1

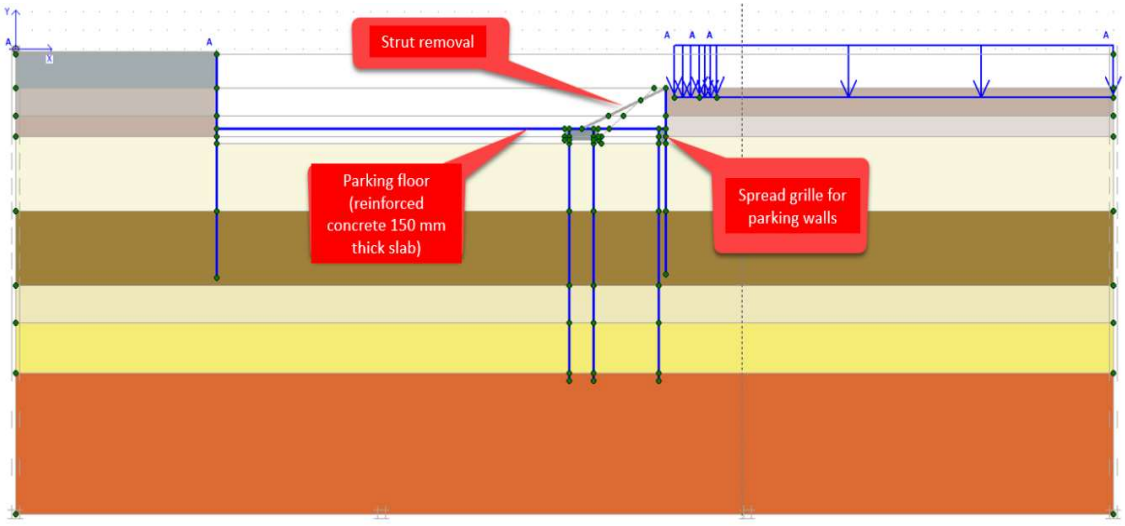

Figure 9 – Stage 5 of the excavation shoring erection in section 1-1

Similar studies were performed in cross-sections 2-2.

In the area where there are no communications and existing buildings, the criterion of calculation was taken as the strength and stability of the excavation shoring system. Horizontal displacements in this area should not exceed 10 cm. In the area of communications and buildings, horizontal displacements are limited so that the vertical deformations of the existing building foundations do not exceed the normative depending on the technical building's condition.

The spatial view of the excavation shoring is shown in Fig. 10.

The calculation of the new construction influence (namely the excavation in sections 1-1 and 2-2) was performed in a plane nonlinear formulation by the finite element method (FEM).

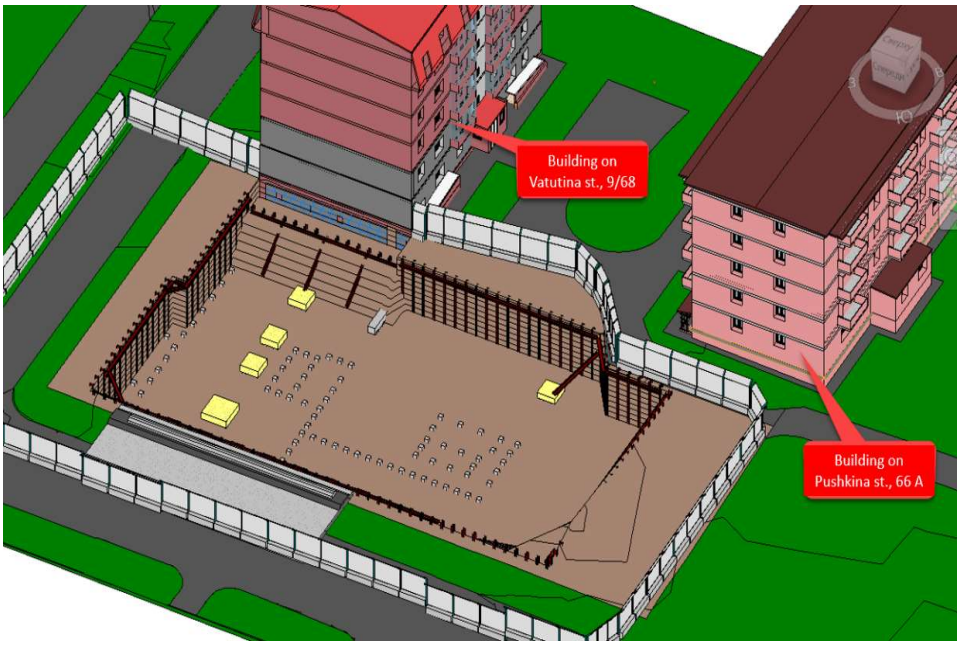

Figure 10 – Spatial view of the excavation and its shoring

To solve the problem, a software package for finite element analysis of geoengineering problems was used. Numerical modeling of the system "base - foundations of the existing building - construction of the shoring" was performed using a well-tested elastic-plastic model of the soil with the Coulomb - Mohr criterion of strength to solve similar problems.

Under these conditions, when using an elastic-plastic model of the soil with the strength criterion of Coulomb - Mohr, the known hypotheses of soil mechanics are accepted, such as:

1) the soil within each finite element is taken as a homogeneous isotropic medium;

2) at deformations, the integrity of a massif remains;

3) shapeshifting deformations are nonlinear;

4) vectors of the principal plastic deformations (and their velocities) and the principal stresses at a complex stress state are assumed to be coaxial;

5) load - simple (components of the stresses deviator increase in proportion to one parameter);

6) the coaxiality of stress and strain tensors are preserved.

The design schemes of the FEM for sections 1-1 modeling the influence of new construction at each stage are given in Fig. 5 - 9. In addition, at the initial stage, the initial stress state was modeled from the net weight of the foundation soils and existing buildings, but the deformations that occurred were zeroed because this SSS is the initial for further calculations.

Calculations of the excavation shoring elements, taking into account the stages of excavation, in particular, it is established that the shoring should be made of sheet piles (I-beams 30Sh), which should be pressed in increments of 1 m, with a wooden fence between them.

To increase the stability and reduce the deformation of the vertical elements, the development of the excavation is provided in the initial stages under the protection of the soil berm, and further - with the installation of capping beams, braces, struts, and gradual supply of the floor and outer wall of the parking lot.

Similar results of the massif's deformations at different stages of excavation shoring by FEM modeling were obtained for section 2-2 and in the area of the pillar crane.

For example, for section 2-2, excavation with minimization of the influence on the existing building is justified in the following stages:

1 – before the excavation from the surface of the site jacking the piles for the new building; immersion of vertical elements of shoring (I-beams 30Sh1) on an excavation contour; its excavation to the design mark under the protection of the berm from the ground (at an angle of about 55° with a width of 2.4 m at the base and 1.0 m at a depth of 2.4 m from the planning level); beyond the contour of the excavation arrangement of I-beams 30Sh1 capping beam at a depth of 2.4 m from the surface.

2 – installation of struts (I-beam 30Sh1), which on one side rest in the embedded part in the grilles (set in the process of concreting the grilles), and on the other one – in the capping beam; removal of the soil berm, due to which the load from the shoring is partially transferred to the foundations of the new building.

3 – works on the arrangement of spread grilles under a parking wall, the installation of its floor which will carry out a role of a spacer system and will accept loading from the shoring, it is also recommended to execute vertical reinforced concrete designs (pylons, walls) to the level of struts and only after concrete cures to remove struts and to continue performance of monolithic works.

For unloaded zones along axes 1, 9, and A it is advisable to arrange the excavation in stages:

1 – arrangement of excavation shoring from a platform surface from I-beams 30Sh1 12 m long pressed piles with an increment of 1.0 m;

2 – the pit excavation to a design depth of 4.8 m under the protection of a soil berm 2.0 m wide and 2.0 m high with a horizontal platform 1 m wide at the top;

3 – arrangement of a capping beam at a depth of 2.4 m from the surface, after which it is possible to cut the ground berm with grips up to 6 m and erect underground monolithic structures, including vertical (walls and pylons), etc.

There is also a shoring in the area of the pillar crane in the A axis – for the period of construction and installation works (the crane is located on the edge of the excavation between the axes 2 and 6) under the protection of a soil berm and struts with an increment of 4 m from double I-beams 30Sh1.

In fig. 11 some photos of the excavation shoring process are shown, and in Fig. 13 there are presented technological solutions for the erection of the underground part of the building in the area of the elements of the shoring.

Figure 11 – Photo of the excavation shoring installation near the existing 5-story building

In order to minimize additional settlement of the existing building, it is planned to remove the strut of the excavation shoring only after installing not only the grille, but also after erecting a certain part of the vertical outer and transverse inner monolithic walls.

To confirm the calculated data on additional settlements of the foundations' base of the existing buildings, it is necessary to perform field observations in the excavation process.

The purpose of monitoring is to preserve the operational reliability and suitability of residential buildings bordering the new development zone. Its main task is periodic geodetic, including automated, surveys to quickly detect the deterioration of the technical buildings' condition or the approximation of actual (measured) sediments and slopes to their limits, control over the technology of excavation, and so on. Therefore, the following composition of geotechnical and geodetic monitoring in the process of construction of a new building was adopted:

– installation of settlement (wall) points and automated measuring and information system;

– system of instrumental (deformations measurement of foundations' bases by wall points) and visual (photo fixation) observations of existing structures;

– evaluating the results of observations and comparing them with the predicted data;

– development, if necessary, of measures to eliminate unacceptable deviations and negative consequences;

– control over the implementation of decisions.

The frequency of monitoring can be adjusted at different stages of new building construction with the deterioration of the technical condition of buildings or the approach of the measured settlements and slopes to the limit values.

a)

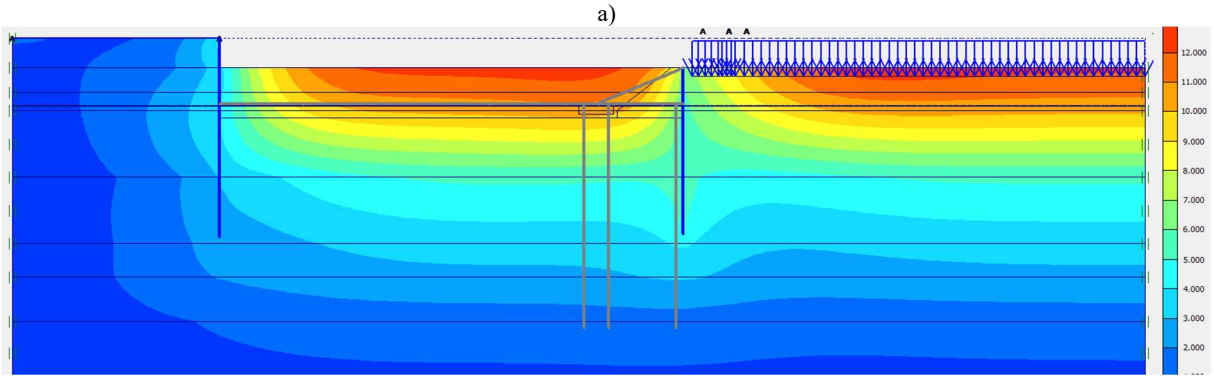

b)

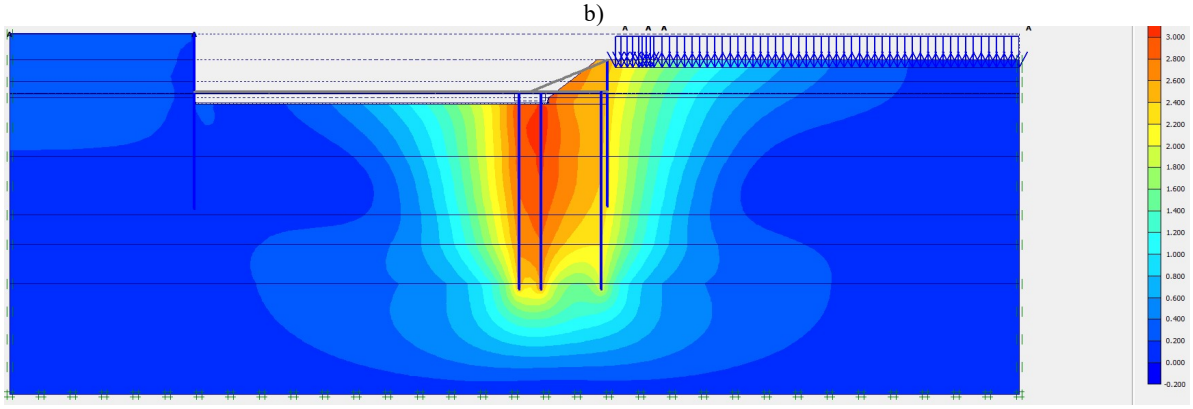

c)

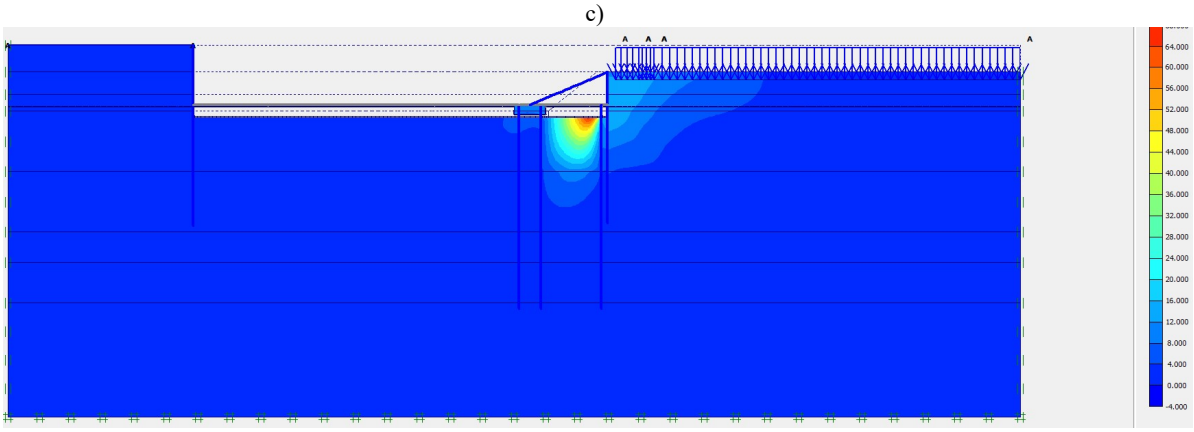

d)

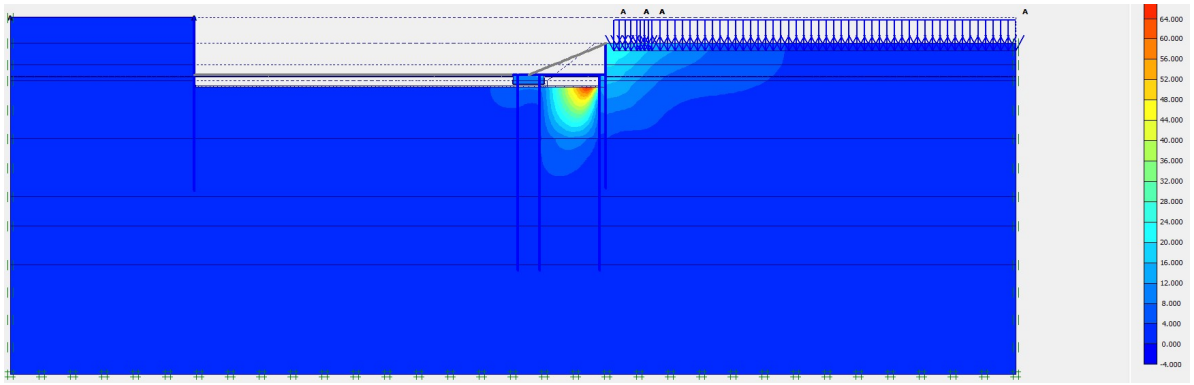

Figure 12 – Deformations of the soil mass according to the FEM modeling at the stages of excavation shoring performance:

a – execution of the "pioneer" excavation (maximum elevation of the bottom of the pit - up to 13 mm); b – arrangement of the excavation under the protection of the soil berm (maximum deformation - up to 3.2 mm at the bottom of the excavation); c – arrangement of a strut and removal of a soil berm (the maximum deformations - to 68 mm at the bottom of excavation from soil heaving); d – arrangement of the parking floor and spread grille and removal of the strut (maximum deformation - up to 68 mm at the bottom from the soil heaving, ie did not increase compared to the previous stage)

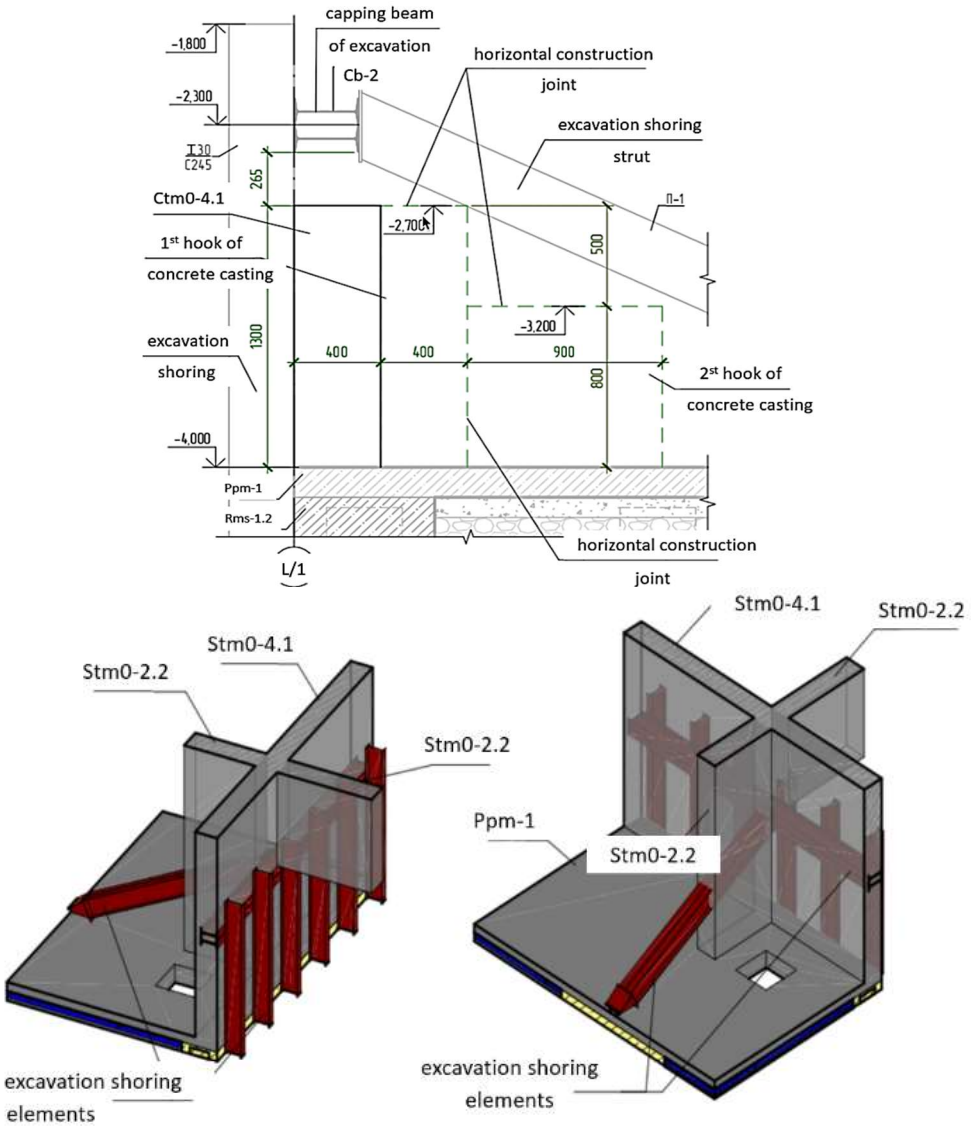

Figure 13 – Technological scheme of performance of the underground part of the building in the area of the shoring

Conclusions

Thus, on a typical full-scale object (multi-apartment residential building on piles) in the conditions of dense development (six- and five-story residential buildings on the shallow foundations and urban infrastructure) and soaked loess soil, it was minimized to regulatory requirements, the possible impact of new construction in a deeper excavation compared to the existing foundations level.

1. According to the results of the calculation of the excavation shoring stability in section 1-1 (depth 3 m taking into account the "pioneer" excavation with a depth of 1.8 m), it is established that its shoring can be made of vertical elements (I-beams 30Sh1) 10 m long with an increment of 1.0 m and struts with an increment of 4 m (from I-beams 30Sh1), between the elements, it should be created a wooden fence of boards with a thickness of 50 mm and connect with a capping beam (I-beam 30Sh1). The maximum additional settlement of the existing residential building foundations will not exceed 8 mm. This excavation technology is the cheapest.

2. According to the results of the calculation of the excavation shoring stability in section 2-2, it is determined that the shoring should be made of vertical elements (I-beams 30Sh1) 12 m long with an increment of 1.0 m and struts with an increment of 6 m, between the elements, a wooden fence of boards 50 mm thick should be made and connected by a capping beam (I-beam 30Sh1). The depth of the excavation is 4.7 m. The maximum additional settlement of the foundations of the existing building reaches 8.5 mm. In addition, it was found that after the arrangement of the parking floor and spread grille under its walls in the case of removal of the strut the foundations' settlement may increase to 12.5 mm, which is more than the maximum allowable value of 10 mm. Therefore, when carrying out work, the struts should not be removed until the vertical basement wall is erected to the bottom of the strut.

References

1. EN 1990:2002/A1:2005/AC (2010). *Eurocode: Basis of Structural Design*. The European Union Per Regulation 305/2011, Directive 98/34/EC, Directive 2004/18/EC

2. ДБН В.2.1-10: 2018. (2018). *Основи і фундаменти будівель та споруд. Основні положення*. Київ: Міністерство регіонального розвитку, будівництва та житлово-комунального господарства України

3. Briaud J.-L. (2013). *Geotechnical Engineering: Unsaturated and Saturated Soils*. Wiley

4. Бойко І.П., Носенко В.С. (2012). Вплив послідовності зведення суміжних секцій висотного будинку на перерозподіл зусиль у пальових фундаментах *Збірник наук праць. Галузеве машинобудування, будівництво*, 4(34)-1, 54-60

5. Мангушев Р.А., Никифорова Н.С. (2017) *Технологические осадки зданий и сооружений в зоне влияния подземного строительства*. Москва: Изд-во АСВ.

6. Кушнер С.Г. (2008). *Расчет деформаций оснований зданий и сооружений*. Запорожье: «ИПО Запорожье»

7. Улицкий В.М., Шашкин А.Г., Шашкин К.Г. (2010). *Геотехническое сопровождение развития городов*. Санкт-Петербург: «Георекострукция»

8. Тугаєнко Ю.Ф., Марченко М.В. Ткаліч А.П., Логінова Л.О. (2018). *Природа деформування ґрунтів: монографія*. Одеса: Астропринт

9. Katzenbach R., Leppla S., Seip M. & Kurze S. (2015) Value Engineering as a basis for safe, optimized and sustainable design of geotechnical structures. *Proc. of the XVI ECSMGE Geotechnical Engineering for Infrastructure and Development*. Edinburg, 601-606
https://doi.org/10.1680/ecsmge.60678.vol2.073

10. Chang Yu Ou. (2006). *Deep Excavation. Theory and Practice*. London: CRC Press.
https://doi.org/10.1201/9781482288469

11. Pinto A., Fartaria C., Pita X. & Tomásio R. (2017). FPM41 high rise building in central Lisbon: innovative solutions for a deep and complex excavation. *Proc. of the 19th Intern. Conf. on Soil Mechanics and Geotechnical Engineering*. Seoul: COEX, 2029-2032

12. Шапиро Д.М. (2013). Метод конечных элементов в строительном проектировании. Воронеж: «Научная книга»

13. Zotsenko M., Vynnykov Yu. (2020) Base deformation's features during deep foundation pit excavation. *Academic Journal. Industrial Machine Building, Civil Engineering*, 2(55), 76-81
https://doi.org/10.26906/znp.2020.55.2346

14. Josifovski J., Susinov B. & Markov I. (2015) Analysis of soldier pile wall with jet-grouting as retaining system for deep excavation *Proc. of the XVI ECSMGE Geotechnical Engineering for Infrastructure and Development*. Edinburg, 3953-3958
https://doi.org/10.1680/ecsmge.60678

15. Chau K. (2013) Numerical Methods. *Proc. of the 18th Intern. Conf. on Soil Mechanics and Geotechnical Engineering*, 647-654

16. Nguyen Van-Hoa & Nikiforova N. (2018). The choice of soil models in designof deep excavation in soft soils of Viet Nam. *MATEC Web of Conferences*, 251, 04033
https://doi.org/10/1051/matecconf/201825104033

17. ДСТУ-Н Б В.1.2-17:2016. (2017). *Настанова щодо науково-технічного моніторингу будівель та споруд*. Київ: ДП «УкрНДНЦ»

1. EN 1990:2002/A1:2005/AC (2010). *Eurocode: Basis of Structural Design*. The European Union Per Regulation 305/2011, Directive 98/34/EC, Directive 2004/18/EC

2. DBN V.2.1-10: 2018. (2018). *Bases and foundations of buildings and structures. Main principles.* Kyiv: Ministry of Regional Development, Construction, and Housing of Ukraine

3. Briaud J.-L. (2013). *Geotechnical Engineering: Unsaturated and Saturated Soils*. Wiley

4. Boyko I.P. & Nosenko V.S. (2012). Influence of the erection sequence of adjacent sections of a high-rise building on the redistribution of forces in pile foundations *Academic Journal. Industrial Machine Building, Civil Engineering*, 4(34)-1, 54-60

5. Mangushev R.A. & Nykyforova N.S. (2017) Technological settlements of buildings and structures in the underground construction influence zone. Moscow: Publishing house ASV.

6. Kushner S.G. (2008). *Settlements calculation of bases of buildings and structures*. Zaporizhzhia: «IPO Zaporozhye»

7. Ulitskii V.M., Shashkin A.H. & Shashkin K.H. (2010). *Geotechnical provision of urban development*. Saint-Petersburg: «Georeconstruction»

8. Tugaienko Yu.F., Marchenko M.V. Tkalich A.P. & Loginova L.O. (2018). *The nature of soil deformation: monograph*. Odessa: Astroprint

9. Katzenbach R., Leppla S., Seip M. & Kurze S. (2015) Value Engineering as a basis for safe, optimized and sustainable design of geotechnical structures. *Proc. of the XVI ECSMGE Geotechnical Engineering for Infrastructure and Development*. Edinburg, 601-606
https://doi.org/10.1680/ecsmge.60678.vol2.073

10. Chang Yu Ou. (2006). *Deep Excavation. Theory and Practice*. London: CRC Press.
https://doi.org/10.1201/9781482288469

11. Pinto A., Fartaria C., Pita X. & Tomásio R. (2017). FPM41 high rise building in central Lisbon: innovative solutions for a deep and complex excavation. *Proc. of the 19th Intern. Conf. on Soil Mechanics and Geotechnical Engineering*. Seoul: COEX, 2029-2032

12. Shapiro D.M. (2013). Finite element method in construction design. Voronezh: "Scientific book"

13. Zotsenko M., Vynnykov Yu. (2020) Base deformation's features during deep foundation pit excavation. *Academic Journal. Industrial Machine Building, Civil Engineering*, 2(55), 76-81
https://doi.org/10.26906/znp.2020.55.2346

14. Josifovski J., Susinov B. & Markov I. (2015) Analysis of soldier pile wall with jet-grouting as retaining system for deep excavation *Proc. of the XVI ECSMGE Geotechnical Engineering for Infrastructure and Development*. Edinburg, 3953-3958
https://doi.org/10.1680/ecsmge.60678

15. Chau K. (2013) Numerical Methods. *Proc. of the 18th Intern. Conf. on Soil Mechanics and Geotechnical Engineering*, 647-654

16. Nguyen Van-Hoa & Nikiforova N. (2018). The choice of soil models in designof deep excavation in soft soils of Viet Nam. *MATEC Web of Conferences*, 251, 04033
https://doi.org/10/1051/matecconf/201825104033

17. DSTU-N B V.1.2-17:2016. (2017). *Guidelines for scientific and technical monitoring of buildings and structures*. Kyiv: DP «UkrNDNC»

Збірник наукових праць. Галузеве машинобудування, будівництво
Academic journal. Industrial Machine Building, Civil Engineering
http://journals.nupp.edu.ua/znp
https://doi.org/10.26906/znp.2021.56.2510

UDC 622.276.72

Utilizing low-frequency ultrasound as a countermeasure to asphalt-resin-paraffin deposition in oil pipelines

Nazarenko Ivan[1]*, Nesterenko Tetiana[2], Nesterenko Mykola [3], Bernyk Iryna[4]

[1] Kyiv National University of Construction and Architecture https://orcid.org/0000-0002-1888-3687
[2] National University «Yuri Kondratyuk Poltava Polytechnic» https://orcid.org/0000-0002-2387-8575
[3] National University «Yuri Kondratyuk Poltava Polytechnic» https://orcid.org/0000-0002-4073-1233
[4] Vinnytsia National Agrarian University https://orcid.org/0000-0002-1367-3058
*Corresponding author E-mail: i_nazar@i.ua

The experimental data on the low-frequency ultrasound effect on asphalt-resin-paraffin deposits (ARPD) occurring in oil transportation through pipelines are presented. As a result of the empirical data statistical processing, a correlation was obtained, which enables the prediction of the ultrasonic exposure time required to remove ARPD from the surface of the pipes. The temperature regime changed from the time of ARPD formations exposure to the ultrasonic influence was analyzed. The proposed algorithm for finding the ultrasonic treatment optimal operational parameters can be used not only in the selection of ultrasonic equipment parameters, which control ARPD in pipelines but also in the run-in hole ultrasonic equipment's operating parameters selection in certain fields conditions

Keywords: asphalt-resin-paraffin deposits, oil pipeline, temperature conditions, ultrasound, ultrasonic equipment

Використання ультразвуку низької частоти як методу боротьби з асфальто-смоло-парафіновими відкладеннями у нафтопроводах

Назаренко І.І.[1]*, Нестеренко Т.М.[2], Нестеренко М.М.[2], Берник І.М.[4]

[1] Київський національний університет будівництва та архітектури
[2] Національний університет «Полтавська політехніка імені Юрія Кондратюка»
[3] Національний університет «Полтавська політехніка імені Юрія Кондратюка»
[4] Вінницький національний аграрний університет
*Адреса для листування E-mail: i_nazar@i.ua

Проаналізовано існуючі методи механічного, теплового та хімічного впливу на асфальто-смоло-парафінові відкладення (АСПВ). Виявлено, що незважаючи на велику кількість робіт про парафінізацію трубопроводів, які транспортують нафту і нафтопродукти (магістральні трубопроводи, місцеві трубопроводи, шлейфи свердловин, внутрішньопромислові трубопроводи), та про методи боротьби з АСПВ, метод ультразвукової обробки вивчений недостатньо повно. Проведено лабораторні дослідження впливу ультразвукових хвиль низької частоти на АСПВ зі шлейфа нафтової свердловини. Наведено дані експериментальних досліджень впливу ультразвукових хвиль низької частоти (20 – 40 кГц) на АСПВ, що виникають при транспортуванні нафти та нафтопродуктів по трубопроводах. Отримано залежність у результаті статистичної обробки експериментальних даних, яка дає можливість прогнозувати час ультразвукового впливу, необхідний для видалення АСПВ від поверхні трубопроводів, що транспортують нафту та нафтопродукти. Визначено, що найбільший вплив на масу видалених АСПВ має час ультразвукової взаємодії. Проаналізовано зміну температурного режиму під часу ультразвукового впливу на асфальто-смоло-парафінисті відкладення. Застосовано метод комплексного впливу кавітуючого поля та теплового ефекту від ультразвукових хвиль (сферична модель розповсюдження теплових та ультразвукових хвиль) для отримання залежності, що дозволяє визначити прогнозований перепад температури, за якого відбудеться видалення АСПВ. Запропоновано алгоритм пошуку оптимальних параметрів режиму ультразвукової обробки, який може бути використаний не тільки при підборі параметрів роботи ультразвукового обладнання, яке застосовується для боротьби з АСПВ у трубопроводах , а і для обладнання, яке спускається безпосередньо у свердловину

Ключові слова: асфальто-смоло-парафінові відкладення, нафтопровід, температурний режим, ультразвук, ультразвукове обладнання

Introduction

Asphalt-resin-paraffin depositions (ARPD) are one of the problems that cause complications in the operation of technological equipment, tanks, and pipelines in the production, collection, transportation, and storage of oil.

The accumulation of ARPD in the pipelines leads to a sharp drop in system performance – increased pressure drops and reduced capacity. Nowadays, there are many methods of combating ARPD oil, most of which are based on thermochemical methods, the use of which is associated with high costs and reduced safety of work performed [1–3].

Existing methods of purely mechanical impact do not give high positive results in pipelines, because the usual flow rates do not provide the necessary effort to affect the scrapers on the dense layers of ARPD. Experience in vibration treatment of highly paraffinic oils has shown a negative effect on the durability of pipeline systems' structural elements.

Thus, at present, there are no effective, safe, and environmentally friendly methods of ARPD removal at oil pipelines.

Review of the research sources and publications

Thermal, chemical, and mechanical methods of ARPD removal are used in oil production. Thermal methods are based on the paraffin tendency to melt at temperatures exceeding 50 °C and drain from the heated surface. Creating the necessary temperature requires a special heat source that can be placed directly in the area of depositions [4 – 6].

Currently, technologies are utilizing: hot oil or water as the heat carrier; steam; ground & downhole electric furnaces; induction flow heaters; reagents in the interaction of which exothermic reactions occur.

The disadvantages of these methods are their high energy consumption, electrical and fire hazard, unreliability, and low efficiency of the applied technologies. The use of solvents to remove deposits that have already formed is one of the most well-known and widespread methods in the technological processes of production, transportation, storage, and refining of oil.

However, the problem of solvent selection for specific conditions is far from being solved. As a rule, the selection of ARPD solvents is carried out empirically. This is due to the lack of information about their structure and properties, as well as the insufficient mechanism knowledge of the petroleum dispersed system interaction with solvents.

Mechanical methods involve the removal of already formed ARPD deposits. A number of various design scrapers have been developed for this purpose.

The use of ARPD control methods is greatly complicated by the fact that its use often requires the pipeline's shutdown.

The method of using coatings gave a generally positive effect, but the high cost of pipe production with enamel and epoxy coating did not allow the coated pipes to be used. Today the application of this method is very limited.

A large number of scientific papers are devoted to the mechanism of magnetic oil treatment, water-oil, and water systems. The theory of magnetic influence on liquid media containing impurities of ferromagnetic particles is proposed.

Definition of unsolved aspects of the problem

Problems of the ultrasonic technologies research for application in the oil and gas industry were addressed in the following papers [7 – 9]. Most of the research has been done in the last two decades and lacks requirements and recommendations for the use of ultrasound equipment for ARPD removal. Also, the authors of [8, 9] approached the use of ultrasound mainly to intensify the impact on the bottom-hole zone of the well; the use of it to clean the pipelines was not given due attention.

Despite a large number of papers on the paraffinization of main oil pipelines and counter measuring ARPD methods, the method of ultrasonic treatment is not fully understood. However, in the transportation and storage of oil in the systems of collection and pipeline transport, the paraffinization problem has always remained a priority.

Problem statement

Therefore, the research aims to study the efficiency and feasibility of ARPD treatment with ultrasonic waves.

To achieve this, the following tasks are set: experimental studies of ultrasound influence on ARPD samples; obtaining a relationship between the mass of ARPD, the time of ultrasonic treatment, and the frequency of ultrasonic waves; based on experimental studies, obtaining the dependence to determine the optimal time for ultrasonic treatment.

Basic material and results

The mechanism of the ultrasound impact is still insufficiently studied [10, 11], so, at this time, it is impossible to assess how the melting of ARPD occurs due to ultrasonic waves.

To study the effect of ultrasonic waves on ARPD, a multifactorial experiment was performed on metal samples (fig. 1).

Figure 1 – Sample before experimental research

Metal plates were used as samples, which were weighed on electronic scales before applying ARPD on them. Then ARPD was applied to the plates in the same amount.

A sampling of ARPD and their analysis was performed directly during the technical diagnostics of

wells. The component composition of the plug was determined in the laboratory by the standard method.

Table 1 presents the component composition of the samples taken from the well of PJSC "Ukrnafta". Type ARPD P/S+A – paraffinic.

In table 1 take the following notation: p-n – paraffin-naphthenic hydrocarbons; l-a – light aromatic hydrocarbons; m-a – medium aromatic hydrocarbons; h-a – heavy aromatic hydrocarbons; resins I – benzene resins; resins II – alcohol-benzene resins.

The samples were placed in an ultrasonic cleaner, the study was performed according to the parameters of the planning matrix of the experiment (Table 2). At the same time, variation of 2 factors was carried out: ultrasonic influence with an interval of 10, 15, 20 minutes and frequencies of 20, 30, and 40 kHz. Let us denote the factors: time – t (factor №1) and frequency of sound – f (factor №2).

After each experiment, the sample was dried and weighed again (Fig. 2). The difference in ARPD mass before and after the experiment gives the mass of ARPD detached from the surface. As a result of the experiment, there was the percentage of destroyed ARPD from the total mass of the applied ARPD entered in the table.

Samples after examination were photographed and magnified on an electron microscope (fig. 3-5).

Figure 2 – Sample after short-term exposure to ultrasound

Figure 3 – Sample after prolonged exposure to ultrasound

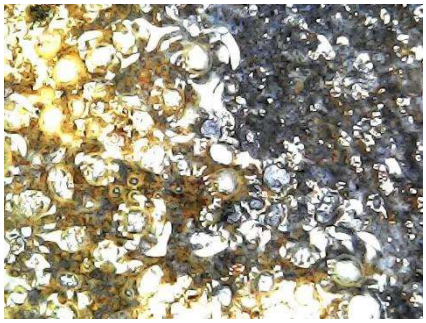

Figure 4 – Magnification of the sample under the microscope immediately after the examination (with cavitation bubbles)

Figure 5 – Magnification of the sample under the microscope

Table 1 − The results of the hydrocarbon type content studies ARPD

Composition, %							
Hydrocarbons				Resins I	Resins II	Asphaltenes	Paraffin
p-n	l-a	m-a	h-a				
39,2	17,1	11,2	14,7	5,6	10,8	1,4	14,6

Table 2 − Experiment planning matrix 3^2

Experiment #	Factor №1			Factor №2		
	-1	0	+1	-1	0	+1
1	10			20		
2	10				30	
3	10					40
4		15		20		
5		15			30	
6		15				40
7			20	20		
8			20		30	
9			20			40

As a result of experimental data statistical analysis, the correlation (1) and graphs of functions were obtained (fig. 6, 7). The results' probability of exceedance is R=0.975.

The equation for determining the mass of destroyed ARPD taking into account the paired linear and quadratic interactions has the following form

$$m = 0.347 + 0.204t + 0.126f - 0.048t_1^2 + 0.07tf \ . \quad (1)$$

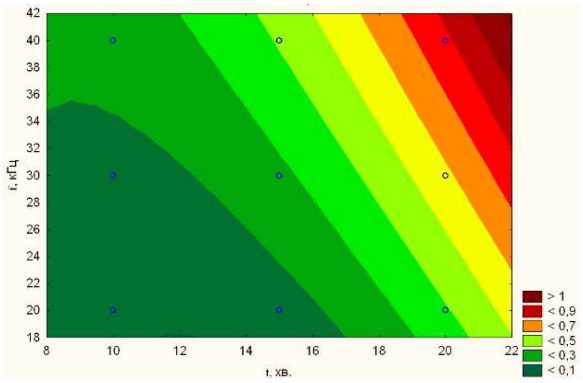

Figure 6 – Cross-section of the ARPD response surface (in fractions)

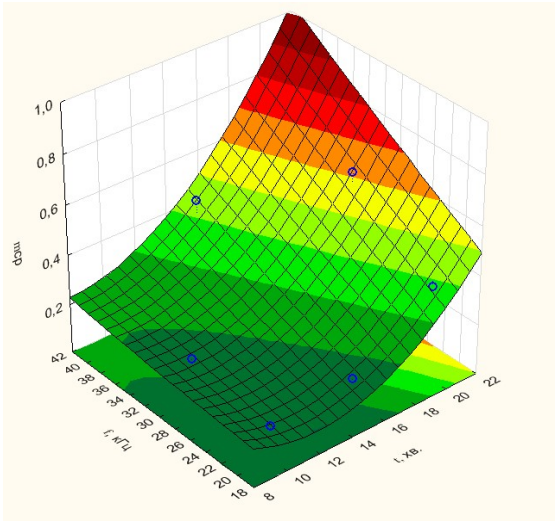

Figure 7 – Correlation of the amount of ARPD versus the frequency and time of ultrasonic interaction

To assess the effect of ultrasound on the purification process from ARPD, it's needed to use a well-known method that accounts for the complex effect of the cavitation field and the thermal effect of ultrasonic waves [12].

A mathematical description of one of the effect hypotheses will be offered next, taking into account the experimental studies' results.

It has been experimentally established that ARPD deposits are simultaneously affected by 2 effects: thermal effect and ultrasonic waves effect.

Heat distribution simulation is well studied and known equations are used for this process. We assume that we will further analyze the spherical model of thermal and ultrasonic wave propagation.

Heat distribution in spherical coordinates is

$$\frac{\partial T}{\partial t} = -\frac{\lambda}{\rho \cdot c_v}\left[\frac{1}{r^2}\cdot\frac{\partial}{\partial r}\left(r^2 \cdot \frac{\partial T}{\partial r}\right)\right], \quad (2)$$

where T – ARPD temperature in the studied volume;
r – coordinate in spherical coordinates;
ρ –ARPD density;
λ – thermal conductivity index.

Assuming that the increase in temperature is due to the power of thermal radiation in the ultrasonic emitter, it is possible to add a boundary condition

$$\frac{\partial T}{\partial r_{r=r_0}} = \frac{Q}{\lambda F}, \quad (3)$$

where Q – heat source capacity;
F – the surface area of the heat source;
r_0 – conditional dimension of the heat source.

However, the mechanism of ultrasound's influence on the ARPD temperature characteristics is still unclear. It was suggested that this effect depends on the intensity of ultrasonic waves.

A harmonic symmetric spherical wave in a medium without absorption is given by the equation

$$u(r,t) = \frac{A}{r}\cdot e^{-i\omega t \pm kr}, \quad (4)$$

where A – the amplitude of ultrasonic oscillations.

The attenuation of ultrasonic oscillations leads to the appearance in the equation of an additional constant multiplier reduced to a unit path length. As a result, for a plane wave propagating along the x-axis, it is possible to write the following

$$I = A_0 \cdot e^{-ax} e^{-ix(t - x/c\, x)}, \quad (5)$$

where a – the attenuation coefficient of ultrasonic waves ARPD.

Thus, the intensity of ultrasonic waves, taking into account the attenuation can be estimated as

$$I = \frac{A_1}{r}\cdot e^{-ar}, \quad (6)$$

where A_1 – reflection coefficient of the medium properties and the parameters of the ultrasonic wave.

Therefore, based on the assumption that the effect of ultrasound depends on the intensity of oscillations at a given point and this dependence is directly proportional, we can write the following equation:

$$\frac{\partial T}{\partial t} = \chi \frac{1}{r}\cdot e^{-ar}, \quad (7)$$

where χ – reflection coefficient of the medium properties and the parameters of ultrasonic waves on thermal exposure.

Note that in general, the coefficient χ may be different for different amplitude-frequency characteristics of the emitter.

Thus, the change in temperature to a certain extent with ARPD is generally described as a functional correlation:

$$\frac{\partial T}{\partial t} = f\left(\frac{\lambda}{\rho c_v}\left[\frac{1}{r^2}\cdot\frac{\partial}{\partial r}\left(r^2\frac{\partial T}{\partial r}\right)\right], \chi\frac{1}{r}\cdot e^{-ar}\right). \quad (8)$$

Let's represent this dependence using the regression analysis. Perform decomposition in a polynomial:

$$\frac{\partial T}{\partial t} = f\left(\frac{\lambda}{\rho c_v}\left[\frac{1}{r^2}\cdot\frac{\partial}{\partial r}\left(r^2\frac{\partial T}{\partial r}\right)\right], \chi\frac{1}{r}\cdot e^{-ar}\right)\approx$$

$$\approx C_1\frac{\lambda}{\rho c_v}\left[\frac{1}{r^2}\cdot\frac{\partial}{\partial r}\left(r^2\frac{\partial T}{\partial r}\right)\right] + C_2\cdot\chi\frac{1}{r}\cdot e^{-ar} + . \quad (9)$$

$$+ C_3\cdot\chi\frac{1}{r}\cdot e^{-ar}\cdot\frac{\lambda}{\rho c_v}\left[\frac{1}{r^2}\cdot\frac{\partial}{\partial r}\left(r^2\frac{\partial T}{\partial r}\right)\right]$$

Applying the condition that in the absence of ultrasound (ie when $\chi = 0$) the equation must be converted into the thermal conductivity equation:

$$\left.\frac{\partial T}{\partial t}\right|_{\chi=0} = C_1\frac{\lambda}{\rho c_v}\left[\frac{1}{r^2}\cdot\frac{\partial}{\partial r}\left(r^2\frac{\partial T}{\partial r}\right)\right] = \quad (10)$$

$$= \frac{\lambda}{\rho c_v}\left[\frac{1}{r^2}\cdot\frac{\partial}{\partial r}\left(r^2\frac{\partial T}{\partial r}\right)\right]$$

thereby, $C_1 = 1$.

Next, we will define the number C_2. Suppose there is an ultrasonic effect, but no thermal effect. It is known that the waves themselves are not sources of heat, so the temperature change should not occur:

$$\left.\frac{\partial T}{\partial t}\right|_{Q=0} = C_2\cdot\chi\frac{1}{r}\cdot e^{-ar} = 0. . \quad (11)$$

Hence, $C_2 = 0$. Therefore

$$\frac{\partial T}{\partial t} = \frac{\lambda}{\rho c_v}\left[\frac{1}{r^2}\cdot\frac{\partial}{\partial r}\left(r^2\frac{\partial T}{\partial r}\right)\right] +$$

$$+ C_3\cdot\chi\frac{1}{r}\cdot e^{-ar}\cdot\frac{\lambda}{\rho c_v}\left[\frac{1}{r^2}\cdot\frac{\partial}{\partial r}\left(r^2\frac{\partial T}{\partial r}\right)\right] = . \quad (12)$$

$$= \left(1 + C_3\cdot\chi\frac{1}{r}\cdot e^{-ar}\right)\frac{\lambda}{\rho c_v}\left[\frac{1}{r^2}\cdot\frac{\partial}{\partial r}\left(r^2\frac{\partial T}{\partial r}\right)\right]$$

Substituting $C_3\cdot\lambda = \cdot\chi_0$

$$\frac{\partial T}{\partial t} = \left(1 + \chi_0\frac{1}{r}e^{-ar}\right)\frac{\lambda}{\rho c_v}\left[\frac{1}{r^2}\cdot\frac{\partial}{\partial r}\left(r^2\frac{\partial T}{\partial r}\right)\right]$$

$$\frac{\partial T}{\partial t} = \left(1 + \chi_0\frac{1}{r}e^{-ar}\right)\frac{\lambda}{\rho c_v}\left[\frac{2}{r}\cdot\frac{\partial T}{\partial r}\cdot\frac{\partial^2 T}{\partial r^2}\right]. \quad (13)$$

Therefore, the equation for modeling the ultrasonic effect on ARPD is obtained.

Neglecting the effect of convection and diffusion, the time to raise the temperature from T_1 to T_2, we obtain the required time for appropriate heating

$$t = \frac{\rho V\left[c\left(T_2 - T_1\right) + \lambda_n\right]}{\eta Q}, \quad (14)$$

V – approximate volume of ARPD;
T_1 – initial temperature ° C;
T_2 – final temperature °C;
ρ – density of ARPD, kg/m^3;
c – heat capacity ARPD, W/K·m^3;
Q – power consumption of the ultrasonic installation, kW;
η – efficiency of the ultrasonic emitter;
λ_n – melting heat of ARPD, kJ/kg.

On the other hand, the time of ultrasonic exposure can be expressed from equation (1) (ignoring the quadratic interaction of time)

$$t = \frac{m_1 - 0.347 - 0.126f}{0.204} = 4.9m_1 - 1.7 - 0.62f ,, \quad (15)$$

$$4.9m_1 - 1.7 - 0.62f = \frac{m(c(T_2 - T_1) + \lambda_n)}{\eta Q} , \quad (16)$$

$$m(c\Delta T + \lambda_n) = \eta Q(4.9m_1 - 1.7 - 0.62f) , \quad (17)$$

$$mc\Delta T = \eta Q(4.9m_1 - 1.7 - 0.62f) - m\lambda_n , \quad (18)$$

$$\Delta T = \frac{\eta Q(4.9m_1 - 1.7 - 0.62f)}{mc} - \frac{m\lambda_n}{mc} =$$

$$= \frac{4.9\eta Q m_1}{mc} - \frac{1.7\eta Q}{mc} - \frac{0.62\eta Q f}{mc} - \frac{m\lambda_n}{mc} =$$

$$= \frac{4.9\eta Q}{c} - \frac{1.7\eta Q}{V\cdot\rho\cdot c} - \frac{0.62\eta Q f}{V\cdot\rho\cdot c} - \frac{\lambda_n}{c} = \quad (19)$$

$$= \frac{4.9\eta Q - \lambda_n}{c} - \frac{1.7\eta Q + 0.62\eta Q f}{V\cdot\rho\cdot c}$$

Therefore, the predicted temperature difference at which the ARPD will be removed can be determined by the formula

$$\Delta T = \frac{4.9\eta Q - \lambda_n}{c} - \frac{1.7\eta Q + 0.62\eta Q f}{V\cdot\rho\cdot c} . \quad (20)$$

Conclusions

Experimental studies of the ultrasonic influence mechanism on the solid's surface suggest the possibility of using the ultrasonic method to countermeasure ARPD.

Experimental studies were planned according to the method of experiment planning, which reduced the volume of studies to nine experiments (with three iterations at each point of the experiment), while not reducing the reliability of the results and the correlation adequacy. The obtained equations for determining the quantity of removed ARPD depending on the time and frequency of ultrasonic interaction enable predicting the time required to get rid of ARPD on the pipe surface. The results' probability of exceedance is R=0.975.

After analyzing the obtained graphs and correlations, it was determined that the time of ultrasonic interaction has the greatest influence on the mass of removed ARPDs because in the response surface equation the coefficient is the largest and positive.

The proposed algorithm for finding the ultrasonic treatment optimal operational parameters can also be used in the run-in hole ultrasonic equipment's operating parameters selection in certain field conditions.

References

1. Дмитриева А. Ю., Залитова М.В., Старшов М.Х. (2014). Исследование основных причин образования вязких (аномальных) нефтей. *Вестник Казанского технологического университета,* 1, 254-256

2. Towler B., Chejara K. & Mokhatab S. (2007). Experimental Investigations of Ultrasonic Waves Effects on Wax Deposition During Crude-Oil Production. *SPE Annual Technical Conference and Exhibition*. Anaheim, 253-269 http://dx.doi.org/10.1016/j.ultsonch.2018.03.023

3. Matvієnko A., V. Savik & P. Molchanov. (2018). Multilevel system of magnet and thermal deparafinization with external insulating coatings. *Naukovij visnik nacional'nogo girnichogo universitetu*, 3 (165), 36-44 http://dx.doi.org/10.29202/nvngu/2018-3/2

4. Онищенко В.О., Винников Ю.Л., Зоценко М.Л., Пічугін С.Ф., Харченко М.О., Степова О.В., Савик В.М., Молчанов П.О., Винников П.Ю., Ганошенко О.М. (2018). *Ефективні конструктивно-технологічні рішення об'єктів транспортування нафти і нафтопродуктів у складних інженерно-геологічних умовах.* Полтава: ПолтНТУ

5. Онищенко В.О., Винников Ю.Л., Зоценко М.Л., Харченко М.О., Ларцева І.І., Бредун В.І., Нестеренко Т.М. (2019). *Ефективні конструктивно-технологічні рішення об'єктів зберігання нафти і нафтопродуктів у складних інженерно-геологічних умовах.* Полтава: ПолтНТУ

6. Копей Б.В., Кузьмін О.О., Онищук С.Ю. (2014). *Обладнання для попередження відкладень асфальтосмолистих речовин, парафіну та піску*. Івано-Франківськ: ІФНТУНГ

7. Wong S., Van der Bas F. & Zuiderwijk P. (2004). High-power/high-frequency acoustic stimulation: A novel and effective wellbore stimulation technology. *SPE Production & Facilities,* 19(4), 183-188 http://dx.doi.org/10.2118/84118-MS

8. Abramov V., Mullakaev M., Abramova A., Esipov I. & Mason T. (2013). Ultrasonic technology for enhanced oil recovery from failing oil wells and the equipment for its implemention. *Ultrasonic Sonochemistry.* 20 (5), 1289-1295 http://dx.doi.org/10.1016/j.ultsonch.2013.03.004

9. Van der Bas F., Rouffignac E., Zuiderwijk P. & Batenburg D. (2004). Near Wellbore Stimulation by Acoustic Waves. *11th ADIPEC: Abu Dhabi International Petroleum Exhibition and Conference.* Abu Dhabi, United Arab Emirates http://dx.doi.org/10.2118/88767-MS

10. Bernyk I., Nazarenko I. & Luhovskyi O. (2018) Effect of rheological properties of materials on their treatment with ultrasonic cavitation. *Materials and technology*, 4, 465-468 http://dx.doi.org/10.17222/mit.2017.021

11. Nazarenko I., Dedov O., Bernyk I., Rogovskii I., Bondarenko A., Zapryvoda A. & Titova L. (2020). Determination of stability of models and parameters of motion of vibrating machines for technological purpose. *Eastern-European Journal of Enterprise Technologies*, 7 (108), 71-79 http://dx.doi.org/10.15587/1729-4061.2020.217747

12 Щурова Е.В., Крысь А.О., Хурамшина Р.А., Валеев А.Р. (2020). Удаление асфальтосмоло-парафиновых отложений из резервуаров для хранения нефти с применением ультразвукового воздействия. *Транспорт и хранение нефтепродуктов и углеводородного сырья*, 5-6, 29-33

1. Dmitrieva A., Zalitova M. & Starshov M.Kh. (2014). Investigation of the main reasons for the formation of viscous (abnormal) oils. *Bulletin of Kazan Technological University*, 1, 254-256

2. Towler B., Chejara K. & Mokhatab S. (2007). Experimental Investigations of Ultrasonic Waves Effects on Wax Deposition During Crude-Oil Production. *SPE Annual Technical Conference and Exhibition*. Anaheim, 253-269 http://dx.doi.org/10.1016/j.ultsonch.2018.03.023

3. Matvієnko A., V. Savik & P. Molchanov. (2018). Multilevel system of magnet and thermal deparafinization with external insulating coatings. *Naukovij visnik nacional'nogo girnichogo universitetu*, 3 (165), 36-44 http://dx.doi.org/10.29202/nvngu/2018-3/2

4. Onishchenko V., Vinnikov Y., Zotsenko M., Pichugin S., Kharchenko M., Stepova O., Savik M., Molchanov P., Vinnikov P. & Ganoshenko O. (2018). *Effective constructive-technological solutions of oil and oil products transportation facilities in complicated geotechnical conditions*. Poltava: PoltNTU

5. Onishchenko V., Vinnikov Y., Zotsenko M., Kharchenko M., Lartseva I., Bredun V. & Nesterenko T. (2019). *Effective Constructive-Technological Solutions for Oil and Petroleum Products Storage in Complex Engineering and Geological Conditions*. Poltava: PoltNTU

6. Kopey B., Kuzmin O. & Onishchuk S. (2014). *Equipment for the prevention of deposits of asphalt, paraffin and sand*. Ivano-Frankivsk: IFNTUNG

7. Wong S., Van der Bas F. & Zuiderwijk P. (2004). High-power/high-frequency acoustic stimulation: A novel and effective wellbore stimulation technology. *SPE Production & Facilities,* 19(4), 183-188 http://dx.doi.org/10.2118/84118-MS

8. Abramov V., Mullakaev M., Abramova A., Esipov I. & Mason T. (2013). Ultrasonic technology for enhanced oil recovery from failing oil wells and the equipment for its implemention. *Ultrasonic Sonochemistry,* 20 (5), 1289-1295 http://dx.doi.org/10.1016/j.ultsonch.2013.03.004

9. Van der Bas F., Rouffignac E., Zuiderwijk P. & Batenburg D. (2004). Near Wellbore Stimulation by Acoustic Waves. *11th ADIPEC: Abu Dhabi International Petroleum Exhibition and Conference.* Abu Dhabi, United Arab Emirates http://dx.doi.org/10.2118/88767-MS

10. Bernyk I., Nazarenko I. & Luhovskyi O. (2018) Effect of rheological properties of materials on their treatment with ultrasonic cavitation. *Materials and technology*, 4, 465-468 http://dx.doi.org/10.17222/mit.2017.021

11. Nazarenko I., Dedov O., Bernyk I., Rogovskii I., Bondarenko A., Zapryvoda A. & Titova L. (2020). Determination of stability of models and parameters of motion of vibrating machines for technological purpose. *Eastern-European Journal of Enterprise Technologies*, 7 (108), 71-79 http://dx.doi.org/10.15587/1729-4061.2020.217747

12. Shchurova E., Krys A., Khuramshina R. & Valeev A. (2020). Removal of asphalt-resin-paraffin deposits from oil storage tanks using ultrasonic treatment. *Transport and storage of petroleum products and hydrocarbons*, 5-6, 29-33

Збірник наукових праць. Галузеве машинобудування, будівництво
Academic journal. Industrial Machine Building, Civil Engineering
http://journals.nupp.edu.ua/znp
https://doi.org/10.26906/znp.2021.56.2511

UDC 624.15.001

The determining cross-section width of discrete restraining structures

Shapoval Volodymyr[1*], Ponomarenko Ivan[2], Shashenko Dmytro[3], Grigoryev Alexey[4]

[1] Technical University Dnipro Polytechnic https://orcid.org/0000-0003-2993-1311
[2] Cherkasy State Technological University https://orcid.org/0000-0003-4296-3975
[3] Technical University Dnipro Polytechnic https://orcid.org/0000-0002-0762-8306
[4] Technical University Dnipro Polytechnic https://orcid.org/0000-0000-0000-000X
*Corresponding author E-mail: ivan1990ponomarenko@gmail.com

Currently, there is no single method for determining the width of the cross-section for the elements of anti-landslide retaining structures with a rectangular cross-section (or the diameter of the elements with a round cross-section) at a known distance between them. An algorithm for determining the diameter (in the case of a transitional view of a round shape) or the smaller side (in the case of a transverse transition of a rectangular shape) of anti-vessels supporting structures at a known distance between them is presented. In the course of the above work, obtained analytical dependencies that allow us to determine: the width of the cross-section for the elements of anti-slip retaining structures with a rectangular cross-section (or the diameter of the elements with a round cross-section) at a known distance between them, the step of arranging the elements of anticonvulsant supporting structures with a rectangular cross-sectional shape (or the diameter of the elements of a circular cross-sectional shape) at a known distance between them.

Keywords: landslide, retaining structure, diameter element, width element, step elements.

Визначення ширини поперечного перерізу дискретних утримуючих споруд

Шаповал В.Г.[1*], Пономаренко І.О.[2], Шашенко Д.О.[3], Григор'єв О.Є.[4]

[1] Національний технічний університет «Дніпровська політехніка»
[2] Черкаський державний технологічний університет
[3] Національний технічний університет «Дніпровська політехніка»
[4] Національний технічний університет «Дніпровська політехніка»
*Адреса для листування E-mail: ivan1990ponomarenko@gmail.com

В даний час не існує єдиної методики визначення ширини поперечного перерізу для елементів протизсувних утримуючих конструкцій з прямокутною формою поперечного перерізу (або діаметру елементів з круглою формою поперечного перерізу) при відомій відстані між ними. Було проведено теоретичні дослідження геомеханічних процесів з використанням аналітичних і чисельних математичних методів. Виконано аналіз і узагальнення результатів теоретичних досліджень. Представлено алгоритм визначення діаметру (в разі поперечного перерізу круглої форми) або меншої сторони (в разі поперечного перерізу прямокутної форми) протизсувних утримуючих конструкцій при відомій відстані між ними. В результаті отримано аналітичні залежності, що дозволяють визначити: ширину поперечного перерізу для елементів протизсувних утримуючих конструкцій з прямокутною формою поперечного перерізу (або діаметру елементів з круглою формою поперечного перерізу) при відомій відстані між ними, крок розстановки елементів протизсувних утримуючих конструкцій з прямокутною формою поперечного перерізу (або діаметру елементів з круглою формою поперечного перерізу) при відомій відстані між ними. Отримані аналітичні дані також можуть бути використані в якості попередніх даних при виконанні розрахунків з використанням сучасних програмних комплексів як по ґрунту, так і по матеріалу.

Ключові слова: зсув, утримуюча конструкція, діаметр елементу, ширина елементу крок елементів.

Introduction

Currently, in the anti-landslide restraining structures design, the following problems occur [1-3]:

1) The use of solid restraining structures (restraining walls) is a very costly and laborious process.

2) During such consumption, there appear problems with cutting the slope and, as a consequence, the stability loss, as well as the drainage of groundwater.

3) According to the spatial layout, the following restraining structures are distinguished:

– linear or extended objects, which include retaining walls, trench fences, anti-landslide structures, etc.

– point or discontinuous objects, which include fences of pits, chambers, wells, anti-landslide structures, etc.

In turn, point objects are subdivided into single-row and multi-row (from several rows of separately standing connected or unconnected retaining structures).

An alternative to solid anti-landslide structures is discrete containing structures [2, 3, 4], however, the following problems use occurs:

– the strength loss and soil stability risks, which are located between the elements of the discrete restraining structure and, as a result - soil destruction located in the zone of the restraining structure influence - and further - landslide descent.

– discrete (especially multi-row) restraining structures create a barrage effect for underground waters; the result is groundwater level rising and, as a consequence, a deterioration in the soil condition in the restraining structure influence zone - and further - its destruction.

Review of the research sources and publications

The retaining structures' design should include:

– retaining structure type selection;

– selection of a method for constructing a retaining structure;

– choice of dimensions, depth of the retaining structure, and its main geometric parameters;

– structures attach type selection;

– selection of materials for the retaining structure;

– the choice of the method of protection against groundwater;

– checking the bearing capacity of the base containing the structure according to the first and second groups of limiting states.

Nowadays, L. K. Ginzburg (1), N. N. Maslov (2) and (3), R. Hill (4), S. I. Make (5), G. E. Hennessy (6) [3-7] formulas are most often used to determine the spacing size for the anti-landslide discrete restraining structures placement.

$$b = \frac{6 \cdot \xi^2 \cdot H \cdot c \cdot \cos(\alpha) - E_{op} \cdot [2 \cdot -tg(\varphi)]}{0.2 \cdot E_{op} \cdot \xi^2 \cdot \cos(\alpha)}; \qquad \xi = \frac{E_{op} \cdot \sqrt{E_{op}^2 - 2 \cdot E_{op} \cdot H \cdot c \cdot tg(\varphi)}}{4 \cdot H \cdot c} \qquad (1)$$

$$b = \frac{\pi \cdot \gamma \cdot H \cdot D \cdot \left(D \cdot tg(\varphi) + \frac{H}{2} + \frac{c}{\gamma \cdot tg(\varphi)} \right)}{E_{op} \cdot \left(ctg(\varphi) + \varphi - \frac{\pi}{2} \right)} \qquad (2)$$

$$b = \frac{c \cdot \pi \cdot \gamma \cdot H \cdot D}{E_{op}} \qquad (3)$$

$$b = \frac{2 \cdot H_c \cdot c_c \cdot \pi \cdot D \cdot \left(1 + \frac{\pi}{2} \right)}{E_{op}} \qquad (4)$$

$$b = 1.52 \cdot D \cdot \ln\left(\frac{7 \cdot H \cdot c - E_{op}}{9 \cdot H \cdot c} \right) \qquad (5)$$

$$b = 2 \cdot \frac{c}{E} \cdot D \cdot h \ . \qquad (6)$$

where b is the distance between the containing elements in the axes;

D is the diameter of the circular shape containing element section or the smaller side of the rectangular element;

E_{op} is shearing pressure;

H is the soil thickness at the location of the restraining structure;

c and φ are soil strength characteristics [8];

γ is soil specific gravity;

α is the inclination angle to the horizon of the sliding soil massif.

Each of the above formulas only partially takes into account the strength characteristics of the soil and restraining structures.

Definition of unsolved aspects of the problem

Nowadays, there is no single method for determining the width of the cross-section for elements of anti-landslide retaining structures with a rectangular cross-sectional shape (or the diameter of elements with a circular cross-sectional shape) with a known distance between them.

Problem statement

The main goal of the presented article was to find analytical dependencies that allow determining the following design parameters of discrete anti-landslide structures:

– the width of the cross-section for the elements of anti-landslide restraining structures with a rectangular cross-sectional shape (or the diameter of elements with a circular cross-sectional shape) at a known distance between them.

– the spacing of the anti-landslide restraining structures elements with a rectangular cross-sectional shape (or the diameter of elements with a circular cross-sectional shape) at a known distance between them.

Basic material and results

Equalities (1) - (6) analyzing.

From equality (1) it follows that the distance between the restraining elements is measured in unit fractions, which is not correct. In addition, there is not presented the intersection parameters of the restraining structure in this formula. Therefore, this dependence will not be considered in the future.

From equality (2) it follows that when the specific cohesion is equal to zero (i.e. for absolutely loose soil), the distance between the elements of the containing structure can be nonzero. This contradicts experimental data and modern concepts of the behavior under a load of ideally loose soils. Therefore, this dependence will not be considered in further research.

Determining the diameter of the circular cross-section or the width of the rectangular element cross-section of the restraining structure, the equalities (3) - (6) concerning the parameter "D" were solved. In this case, the following is presented:

– for the N.N. Maslov solution (original formula (3)):

$$D = \frac{b \cdot E_{op}}{c \cdot \pi \cdot H} \; ; \qquad (7)$$

– for the R. Hill solution (original formula (4)):

$$D = \frac{b \cdot E_{op}}{c \cdot (2 + \pi) \cdot H} \; ; \qquad (8)$$

– for the S.I. Matsiy solution (original formula (5)):

$$D = \frac{0.658 \cdot b}{\ln\left(\frac{7 \cdot c \cdot H - E_{op}}{9 \cdot c \cdot H}\right)} \; ; \qquad (9)$$

- for the R. E. Hennes solution (original formula (6)):

$$D = \frac{b \cdot E_{op}}{2 \cdot c \cdot \pi \cdot H} \; ; \qquad (10)$$

Analysis of formulas (3) - (10), which have a physical meaning, allowed us to conclude that they do not include such an important characteristic as the angle of internal friction.

The following research materials are aimed at solving this contradiction.

The research task was the basis for its solution, the assumptions were formulated as follows:

– upon the destruction of the soil massif interacting with the discrete retaining structure, an arch of a fall of unit thickness is formed, directed by its convex part towards the shear displacement vector. For the sake of simplicity, take it as a pointed arch (see. design scheme in Fig. 1);

– a uniformly distributed load q is applied to the arch, which is numerically equal to the ratio of the landslide pressure E_{op} to the thickness of the soil layer H (ie $q = \frac{E_{op}}{H}$; see Fig. 1);

It was assumed that the destruction of the soil between the elements of the discrete restraining structure (in the diagram, this soil is indicated in yellow) occurs in the center of the arch span.

– the arches support rest on adjacent elements of the discrete restraining structure. In this case, horizontal R_h and vertical R_v reactions occur;

– the rock destruction mechanism is displacement. Therefore, its fracture behavior obeys the Coulomb-Mohr strength condition [8, 9]:

$$\left.\begin{array}{l} \dfrac{\sigma_1 - \sigma_3}{\sigma_1 + \sigma_3 + 2 \cdot c \cdot ctg(\varphi)} = \sin(\varphi) \\ \\ \sigma_1 > \sigma_2 > \sigma_3 \end{array}\right\} \qquad (11)$$

where σ_1, σ_2, σ_3 are principal normal stresses;
φ is an angle of internal friction;
c is a specific cohesion.

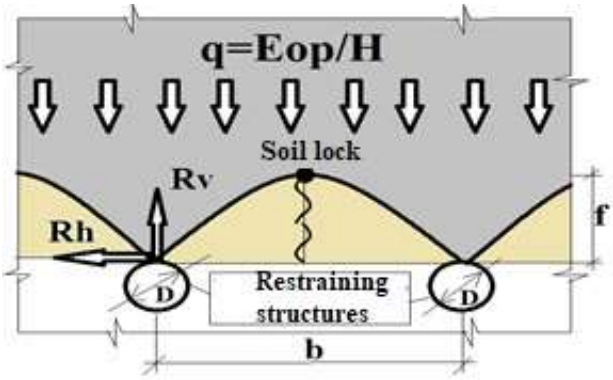

Figure 1 – Scheme for calculating the diameters of discrete restraining structures elements and the distances between them

– strength characteristics of the soil are known (its specific cohesion c and the angle of internal friction φ).

– known as either the element spacing of the anti-landslide restraining structure or the cross-section diameter of the element restraining structure of a circle shape or the smaller side of the rectangular cross-section shape.

– when the soil is destroyed between the restraining structure elements, a fallen arch with a lifting arrow f is formed.

Within the framework of the Coulomb-Mohr strength criterion, it is necessary to determine:

– the section diameter D, to a known element spacing of the anti-landslide restraining structure b.

– the element spacing of the anti-landslide restraining structure b, to a known cross-section diameter of the restraining structure element D.

The algorithm for determining the diameter (in the case of a circular cross-section) or the smaller side (in the case of a rectangular cross-section) of anti-landslide restraining structures with a known distance between them is shown below:

Vertical R_v and horizontal R_h reactions in the arch abutment are equal:

$$R_v = \frac{q \cdot b}{2} \ ;$$
$$R_h = \frac{q \cdot b^2}{8 \cdot f} \ ; \qquad (12)$$
$$q = \frac{E_{op}}{H} \ .$$

The following stresses effect the contact between the displacement and the restraining structure surface:

– directed against the shear, is numerically equal to:

$$\sigma_{R_v} = \frac{R_v}{D} = \frac{q \cdot b}{2 \cdot D} \ ; \qquad (13)$$

– directed parallel to the line along which the restraining structures are placed, is numerically equal to:

$$\sigma_{R_h} = \frac{R_h}{D} = \frac{q \cdot b^2}{8 \cdot f \cdot D} \ ; \qquad (14)$$

– vertical, numerically equal to:

$$\sigma_v = \gamma \cdot z \ ; \qquad (15)$$

Of the stresses considered, the largest is the stress due to the vertical reaction R_v at the arch abutment, and the smallest stress is zero. This is due to the fact that horizontal reactions in adjacent arch abutments cancel each other out. In connection with the above, we have:

$$\sigma_1 = \sigma_{R_v} = \frac{R_v}{D} = \frac{q \cdot b}{2 \cdot D} \ ; \qquad (16)$$
$$\sigma_2 = 0$$

After, substituting the principal stresses (16) into the Coulomb-Mohr strength criterion (11) and solving the equality obtained in this way concerning the diameter of the restraining structure element D:

$$D = \frac{q \cdot b}{4 \cdot c} \cdot \frac{1 - \sin(\varphi)}{\cos(\varphi)} \ . \qquad (17)$$

The equality (17) allows you to determine the safe distance between the restraining elements. It is equal to:

$$b = \frac{4 \cdot c \cdot D}{q} \cdot \frac{\cos(\varphi)}{1 - \sin(\varphi)} \ . \qquad (18)$$

Equalities (17) and (18) make it possible to determine the diameters of the anti-landslide discrete restraining structure elements for a soil layer of unit thickness. Taking into account the entire thickness of the sliding soil massif, use in (17) and (18) is $q = \frac{E_{op}}{H}$:

$$D = \frac{E_{op} \cdot b}{4 \cdot c \cdot H} \cdot \frac{1 - \sin(\varphi)}{\cos(\varphi)} \ ;$$
$$b = \frac{4 \cdot c \cdot D \cdot H}{E_{op}} \cdot \frac{\cos(\varphi)}{1 - \sin(\varphi)} \qquad (19)$$

The formulas' (19) disadvantage is that they can only be applied to homogeneous bases. To eliminate this drawback, replace their strength characteristics with the weighted average values $\overline{c}$ and $\overline{\varphi}$. In this case, equalities (19) take the form:

$$\left.\begin{aligned} D &= \frac{E_{op} \cdot b}{4 \cdot c \cdot H} \cdot \frac{1 - \sin(\varphi)}{\cos(\varphi)} \\ b &= \frac{4 \cdot c \cdot D \cdot H}{E_{op}} \cdot \frac{\cos(\varphi)}{1 - \sin(\varphi)} \\ \overline{c} &= \frac{\sum_{i=1}^{m} c_i \cdot h_i}{h}; \overline{\varphi} = \frac{\sum_{i=1}^{m} \varphi_i \cdot h_i}{h} \end{aligned}\right\} \qquad (20)$$

where c_i , φ_i – strength characteristics i-th soil layer with a thickness h_i and soil layers number m.

In general, it was concluded that the obtained formulas allow to determine the diameter and elements' spacing of anti-landslide restraining discrete structures.

In this case, the obtained dependences are free from internal contradictions given in formulas (1) - (10).

These data are very important in the calculation and design of discrete restraining structures.

Conclusions

In the course of this article, analytical dependencies were obtained that allow calculating the step of placing discrete anti-landslide restraining structures with a known diameter and contrariwise, the diameter (or the cross-section width) of discrete anti-landslide restraining structures with a known step of their placement.

The obtained simple analytical data can also be used as preliminary data for performing calculations using modern software systems for soil and material equally.

References

1. Билеуш А.И. (2009). *Оползни и противооползневые мероприятия*. Київ: Наукова думка

2. Гинзбург Л.К. (2007). *Противооползневые сооружения*. Днепр: Лира ЛТД

3. Гинзбург Л.К. (1979). *Противооползневые удерживающие конструкции*. Москва: Стройиздат

4. Лапидус Л.С., Шадунц К.Ш. (1962). Укрепление откосов слабых насыпей сваями. *Вопросы геотехники*, 5, 48-55

5. Маций С.И. (1991). *Взаимодействие свайных рядов с грунтом оползней* (Автореферат дис. канд. техн. наук). С-Петербург: Ленинградский государственный технический университет

6. Маций С.И. (2007). Взаимодействие оползневого грунта со сваями с учетом конфигурации удерживающего сооружения. *Основания, фундаменты и механика грунтов*, 2, 8-12

7. Хилл Р. (1956). *Математическая теория пластичности*. Москва: ГИТТЛ

8. Шаповал В.Г, Шаповал А.В., Моркляник Б.В., Андреев В.С. (2010). *Механика грунтов*. Днепропетровск: Пороги

9. Шашенко А.Н., Пустовойтенко В.П., Сдвижкова Е.А. (2015). *Геомеханика*. Киев: Национальный горный университет

10. Сіренко А.П. (2013). Критична відстань між утримуючими елементами для зсувних та зсувонебезпечних схилів Чернівецької області. *Екологічна безпека*, 13, 73-76 https://itgip.org/wpcontent/uploads/2021/03/2019-29-1.pdf

11. Sirenko A.P. To the analysis of methods of calculation of stability of use and their classification. *Екологічна безпека та природокористування*, 1(29), 79 - 86 https://itgip.org/wp-content/uploads/2021/03/2019-29-1.pdf

12. Угненко Є.Б., Тимченко О.М., Ужвієва О.М., Орел Є.Ф., Сорочук Н.І. (2019). *Геодезичні дослідження при визначенні зсувних процесів на ділянках шляхів сполучення у гірській місцевості* Київ: «Кондор» http://lib.kart.edu.ua/bitstream/123456789/2230/1/НП.pdf

1. Bileush A.I. (2009). *Landslides and anti-landslide measures*. Kyiv: Naukova Dumka

2. Ginzburg L.K. (2007). *Landslide structures.* Dnipro: Lira LTD

3. Ginzburg L.K. (1979). *Anti-landslide retaining structures.* Moscow: Stroyizdat

4. Lapidus L.S., Shadunts K.Sh. (1962). *Strengthening the slopes of weak embankments with piles. Geotechnical issues*, 5, 48-55

5. Matsiy S.I. (1991). *Interaction of pile rows with landslide soil (Abstract of the thesis. Candidate of technical sciences)*. St. Petersburg: Leningrad State Technical University

6. Matsiy S.I. (2007). *Interaction of landslide soil with piles, taking into account the configuration of the retaining structure. Foundations, foundations and soil mechanics*, 2, 8-12

7. Hill R. (1956). *Mathematical theory of plasticity*. Moscow: GITTL

8. Shapoval V.G., Shapoval A.V., Morklyanik B.V., Andreev V.S. (2010). *Soil mechanics*. *Dnepropetrovsk: Rapids.*

9. Shashenko A.N., Pustovoitenko V.P., Sdvizhkova E.A. (2015). *Geomechanics*. Kiev: National Mining University

10. Sirenko A.P. (2013). Critical distance between restraining elements for landslide and landslide-prone slopes of the Chernivtsi region. *Environmental safety*, 13, 73-76 https://itgip.org/wpcontent/uploads/2021/03/2019-29-1.pdf

11. Sirenko A.P. To the analysis of methods of calculation of stability of use and their classification. *Екологічна безпека та природокористування*, 1(29), 79 - 86 https://itgip.org/wp-content/uploads/2021/03/2019-29-1.pdf

12. Ugnenko E.B., Timchenko A.N., Uzhvieva A.N., Orel E.F., Sorochuk N.I. (2019). *Geodetic research in the determination of landslide processes on sections of communication lines in mountainous areas* Kiev: "Kondor" http://lib.kart.edu.ua/bitstream/123456789/2230/1/НП.pdf

Збірник наукових праць. Галузеве машинобудування, будівництво
Academic journal. Industrial Machine Building, Civil Engineering

http://journals.nupp.edu.ua/znp
https://doi.org/10.26906/znp.2021.56.2512

UDC 628.92:[711.62:728

Determination of insolation conditions and selection of the optimal orientation of residential buildings

Yurin Oleg[1], Zyhun Alina[2]*, Galinska Tatiana [3], Avramenko Yurii [4]

[1] National University «Yuri Kondratyuk Poltava Polytechnic» https://orcid.org/0000-0002-9290-9048
[2] National University «Yuri Kondratyuk Poltava Polytechnic» https://orcid.org/0000-0002-1743-2294
[3] National University «Yuri Kondratyuk Poltava Polytechnic» https://orcid.org/0000-0002-6138-2757
[4] National University «Yuri Kondratyuk Poltava Polytechnic» https://orcid.org/0000-0003-2132-5755
*Corresponding author E-mail: alinazygun@gmail.com

The project is devoted to the determination of insolation conditions and the choice of optimal orientation of residential buildings, considering the latitude of the terrain of Poltava. Presently, there is a change from construction according to standard designs to individual design and the process of consolidation of residential construction in cities continues by new construction in the historic built-up areas. Compacting and increasing the number of floors inevitably worsens insolation in the living rooms of existing houses due to the additional shading of their windows, which leads to a decrease in the duration of insolation. The factor of rational planning of the territory and the optimal orientation of the house on the cardinal points, the correct choice of floors and configuration in the plan get special significance.

Keywords: duration of insolation, optimal orientation of the residential building, insolation ruler.

Визначення умов інсоляції та вибір оптимальної орієнтації житлових будинків

Юрін О.І.[1], Зигун А.Ю. [2]*, Галінська Т.А.[3], Авраменко Ю.О.[4]

[1,2,3,4] Національний університет «Полтавська політехніка імені Юрія Кондратюка»
*Адреса для листування E-mail: alinazygun@gmail.com

Виконання санітарно-гігієнічних вимог при проектуванні житла здійснюється відповідно до умов фізико-географічного районування території України і включає у себе вимоги до інсоляції, природного освітлення, провітрювання, іонізації та мікроклімату приміщень житлових будинків. Робота присвячена визначенню умов інсоляції та вибору оптимальної орієнтації житлових будинків з урахуванням широти місцевості м. Полтава. На сьогоднішній час відбувається перехід від будівництва за типовими проектами до індивідуального проектування та триває процес ущільнення житлової забудови у містах шляхом нового будівництва в історично сформованій забудові. При розміщенні нового будівництва в існуючій забудові слід забезпечити дотримання вимог чинних нормативних документів щодо інсоляції. Наявність природного світла в оселі є важливим параметром, добре інсольовані будинки та квартири користуються попитом. Ущільнення й збільшення поверховості забудови неминуче погіршує інсоляцію в житлових приміщеннях існуючих будинків через додаткове затінення їх вікон, що призводить до зменшення тривалості інсоляції. Тривалість інсоляції приміщення залежить від орієнтації вікон по сторонам світу, розмірів, товщини огороджувальних конструкцій і відстані від будівель, розташованих поблизу. Слід зазначити, що на тривалість (наявність) інсоляції впливають також інші архітектурно-планувальні елементи будівель: балкони, карнизи, лоджії, що затіняють вікна. Будівельні норми й правила для житлових приміщень регламентують тривалість інсоляції та кількість кімнат у квартирі, у яких має бути забезпечена нормативна тривалість інсоляції. Умови й час інсоляції приміщень в Україні встановлюються Санітарними нормами і правилами інсоляції, а також відповідними типологічними будівельними нормами й правилами. Особливого значення набуває фактор раціонального планування території й оптимальної орієнтації будинку за сторонами світу, правильний вибір поверховості та конфігурації у плані.

Ключові слова: тривалість інсоляції, оптимальна орієнтація житлового будинку, інсоляційна лінійка.

Introduction

Insolation of rooms along with their illumination, temperature-humidity, and noise conditions play a significant role in ensuring a comfortable mode of living.

Insolation regulation and calculation is the most acute lighting, economic and socio-legal problem, because these calculations restrain the desire of investors, landholders and tenants to overdensify urban development.

Review of the research sources and publications

Insolation in residential buildings should primarily take into account the requirements of national sanitary legislation, which is based on the study of natural and climatic conditions of different regions of Ukraine, to create the necessary living conditions and public health [1-3].

The determination process begins with the development of space-planning solutions for the new building. Then an insolation calculation is made using a solar map or an insolation ruler [4, 5, 6].

Issues of insolation rationing were dealt with by Dunaev B. A., Vernesku D., Zemtsov V. A., Skryl I.N., Haharin V. H., Pidhornyi O.L., Yehorchenkov V.O., Elahin B.T., Sergeychuk O., Martynov V. The results of their research are presented in the works [7-40].

Definition of unsolved aspects of the problem

Design of residential building standards do not allow apartments where all rooms orientation to the north side of building. Rooms with windows on the north facade of houses in cold weather are not insolated at all, and in summer they receive some morning and evening "sliding" sunlight, which almost does not enter to the room.

However, there is often a breach of insolation standards due to the orientation of the facades of houses to the north-west and north-east in urban planning practice (such situations are found when it is necessary to consider the existing road network), and when the insufficient distance is between the houses.

Therefore, the choice of optimal orientation of the house on the cardinal points is quite relevant task.

Problem statement

The purpose of the work is to research the insolation of the rooms of a residential house.

Tasks of research are:

- analysis of insolation conditions in the rooms of a residential building with different orientation to the cardinal points;
- choosing the optimal orientation for the house.

Basic material and results

Insolation is an important health factor, so the standards of insolation must be satisfied in the rooms of residential and public buildings and in the area of residential development. The optimal effectiveness of insolation is achieved by providing a daily continuous 2.5-3-hour exposure to direct sunlight to premises and territories. Insolation provides a health-improving, psychophysiological, bactericidal, thermal effect. The normalization is conducted in the spring and autumn period of the year, taking into account the light and climate characteristics of different areas of the country and the characteristics of the building. The requirements of the standards are achieved by the appropriate placement, orientation and layout of the buildings.

The standardized duration of insolation should be provided not less than in one living room of 1-, 2-, 3-room apartments and not less than in two living rooms of 4- to 5-room apartments. In multistory buildings (9 or more floors) allowed a single interruption of insolation of residential and public buildings (except as listed above) on condition of increasing the total duration of insolation during the day by 0.5 hours respectively for each zone.

Limitation of the excessive thermal effect of insolation in rooms and areas during the hot season should be ensured by appropriate planning and orientation of buildings, landscaping, using sun protection devices, and, if necessary, air conditioning and indoor cooling systems. Limiting the thermal effects of insolation areas should be provided by shading from buildings, special shading devices, and rational landscaping.

The year-round shading of the facades of buildings and residential areas is not allowed. Mid-year shadows (from September 22 to March 22) shall not exceed 40% of the total area of the housing areas free from housing development.

The duration of insolation of the room is calculated on the ground floor of the building through the central point of the lighting penetration, the dimensions of which meet the requirements of the norms of natural lighting of the premises. It is necessary to keep in mind the location and size of the building elements shading the lighting penetrations (shading houses, canopies, balconies, loggias, porticos, shutters, etc.).

Calculation of the duration of insolation is made for the premises in which it is normalized in accordance with the requirements of the norms [2,3].

During the analysis of insolation norms in multistory residential buildings, if apartments located under each other have the same layout on all floors, the calculated apartments are taken on the lowest residential floor. The duration of insolation on all other floors of the corresponding rooms will not be less.

If the ground floor has apartments with the same layout and orientation, the calculation of the duration of insolation of these apartments is advisable to start with the apartment that is most shaded by the opposite buildings and the relief of the area (in the absence of a shading building). If this apartment meets the standards, all other similar apartments will have a satisfactory insolation regime.

It is advisable to start calculating the duration of insolation with the living room that has the best insolation conditions in multi-room apartments according to the following attributes:

– favorable orientation;
– absence of summer facilities;
– the largest geometric dimensions of a window;
– the longest distance from neighboring houses.

If the insolation standards are met in this room, and the apartment consists of at most three living rooms, the insolation standards are also met for the apartment as a whole. It is necessary to check insolation of the next room according to the probability of meeting the standards for 4-, 5-room apartments, and checking of two rooms for apartments consisting of six or more rooms.

The degree of suitability of window orientation for insolation conditions is determined (Fig. 1), depending on the requirements for insolation mode of the premises.

It is advisable to calculate using an insolation ruler for calculating the duration of insolation of the territory of residential buildings.

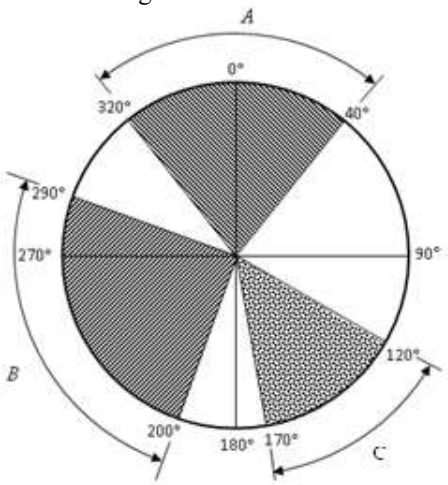

Figure 1 – Insolation characteristics of the horizon sectors on the territory of Ukraine.
A – insolation deficiency sector;
B – overheating sector
(for III and IV building-climatic regions);
C – sector of highest effect of ultraviolet radiation

Ukraine uses insolation rulers constructed for each whole degree from 45° to 52° north latitude. The nearest insolation ruler, depending on the geographic latitude, is taken for a particular calculation site. The scale of the insolation ruler should coincide with the scale of the general plan.

Calculation of the duration of insolation with the insolation ruler is performed in this sequence:

- the horizontal angle of insolation is determined α: in calculating the duration of insolation of the room – is on the plan of the room, considering the vertical screening elements of the lighting aperture (Fig. 2), in calculating the duration of insolation of the territory α = 180°;
- insolation ruler is oriented on the sides of the horizon according to the orientation of the general plan and aligned in such a way that the pole of the graph (the point where the sun's rays coincide), coincides with calculation point;
- the sectors of shading by the opposite buildings and the surface of the terrain are defined within the horizontal angle of insolation;
- the calculated duration of insolation is determined from 7^{00} to 17^{00} as the difference between the duration of insolation within the horizontal angle of insolation and the duration of shading by opposite houses and relief.

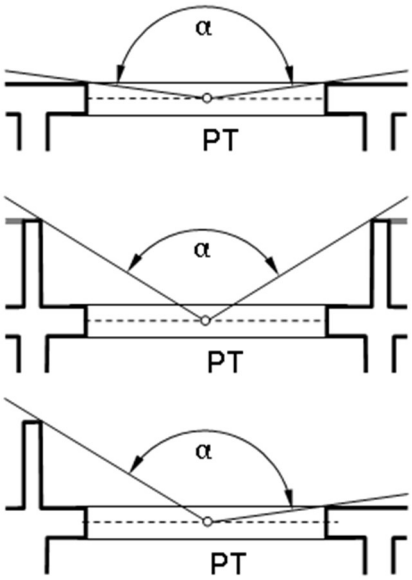

Figure 2 – Determination of the horizontal angle of insolation in rectangular windows

The method using the insolation ruler is used in the following calculations to calculate the duration of insolation of the premises for two days of the year, which is March 22 and September 22. Complying with regulatory requirements on these days usually guarantees their fulfillment throughout the entire calculation period.

A group of radial lines is conducted, an insolation graph is constructed using an additional graph, taking into account the latitude of Poltava (Fig. 3).

We used the plan of the apartment house with dimensions in the axes 16,2*32,1 m to perform the calculations.

The structural plan of the building is designed rigid, with longitudinal load-bearing and transverse non-bearing walls throughout the height of the building.

There are three two-bedroom apartments and one three-bedroom apartment on each floor (Fig. 4). The apartments include loggias.

The first calculation of the insolation of the rooms was performed with the longitudinal axis of the house in the direction of North-South (Fig 5.).

As the location of the rooms relative to the longitudinal axis of the house in the direction of the world and the size of the window openings in the rooms of different apartments are the same, so it is possible to determine the duration of insolation for only one case.

Apartment №2.

If the house is located with its longitudinal axis in the North-South direction, the insolation duration will be: - in room №3 of apartment №2 is the same as in room №2 of apartment №1;

- in room №4 of apartment №2 is the same as in room №1 of apartment №1.

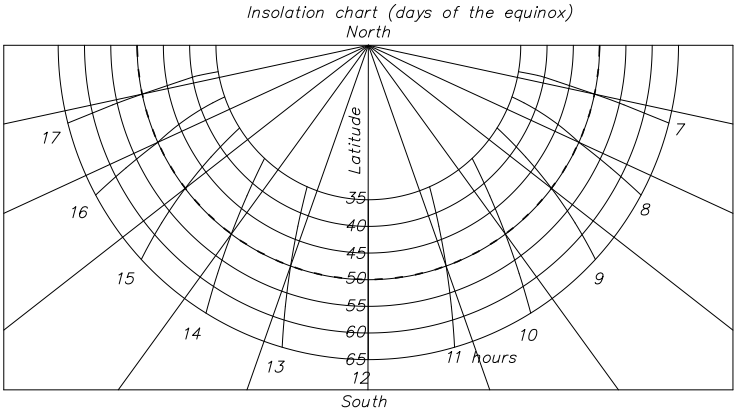

Figure 3 – Construction of the insolation diagram, taking into account the latitude of Poltava

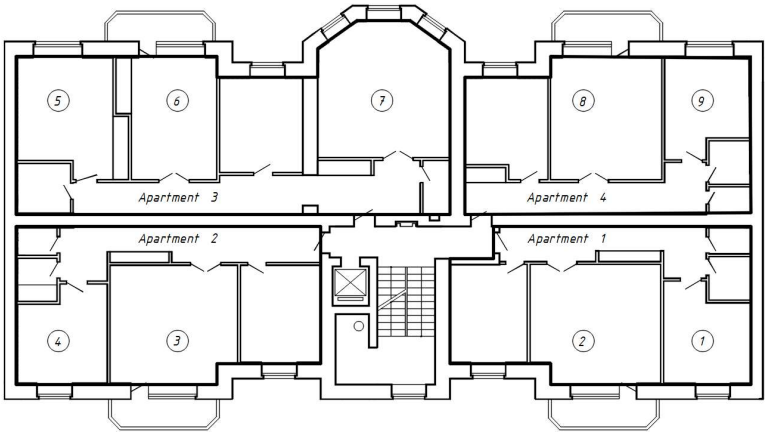

Figure 4 – Calculation scheme of the house. 1-9 – numbers of rooms, which can be calculated

Apartment №4.

If the house is located with its longitudinal axis in the North-South direction, the insolation duration will be: - in room №8 of apartment №4 is the same as in room №6 of apartment №3;

- in room №9 of apartment №4 is the same as in room №5 of apartment №3.

The results of the calculations are summarized in Table 1.

Table 1 – Duration of insolation of the rooms of the house from North-South direction

№ of the apartment	№ room	Beginning of insolation		End of insolation		Duration of insolation, hour.	Fulfillment of standards for insolation of the room	Fulfillment of the standards for insolation of the apartment
1	1	13 h 15 m		17 h 00 m		3 h 45 m	+	+
	2	12 h 38 m		17 h 00 m		4 h 22 m	+	
2	3	12 h 38 m		17 h 00 m		4 h 22 m	+	+
	4	13 h 15 m		17 h 00 m		3 h 45 m	+	
3	5	7 h 00 m		10 h 28 m		3 h 28 m	+	+
	6	7 h 00 m		11 h 21 m		4 h 21 m	+	
	7	7 h 00 m	7 h 00 m	8 h 2 m	12 h 20 m	5 h 20 m.	+	
		7 h 00 m		10 h 45 m				
		7 h 00 m		12 h 20 m				
4	8	7 h 00 m		11 h 21 m.		4 h 21 m	+	+
	9	7 h 00 m		10 h 28 m		3 h 28 m	+	
Duration of insolation in the rooms of the house (per floor)								37 h 12 m

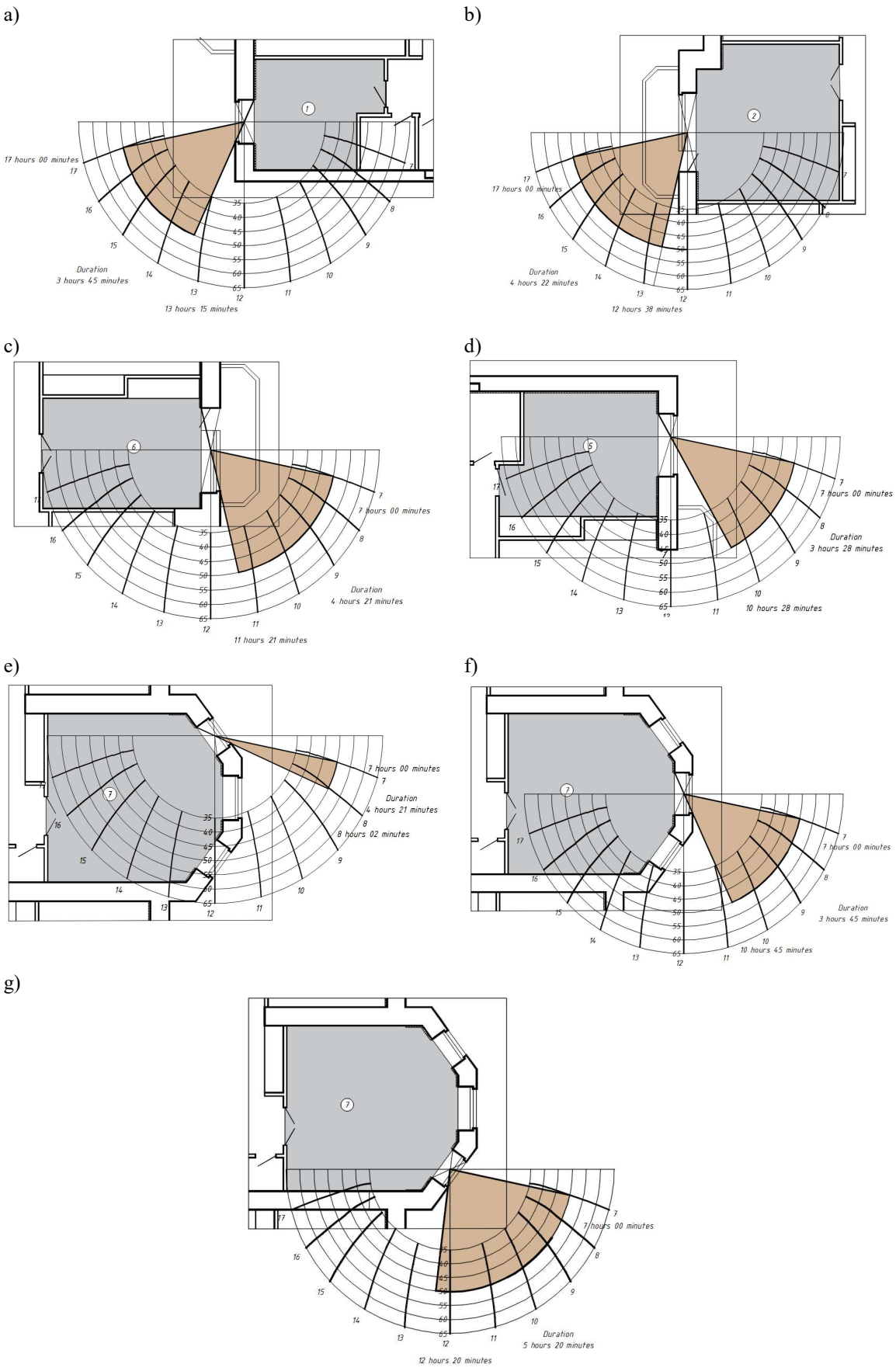

Figure 5 – Determining the duration of insolation in:
a) room №1 of apartment №1; b) room №2 of apartment №1; c) room №6 of apartment №3;
d) room №5 of apartment №3; e) room №7(window №1) of apartment №3;
f) room №7(window №2) of apartment №3; g) room №7(window №3) of apartment №3

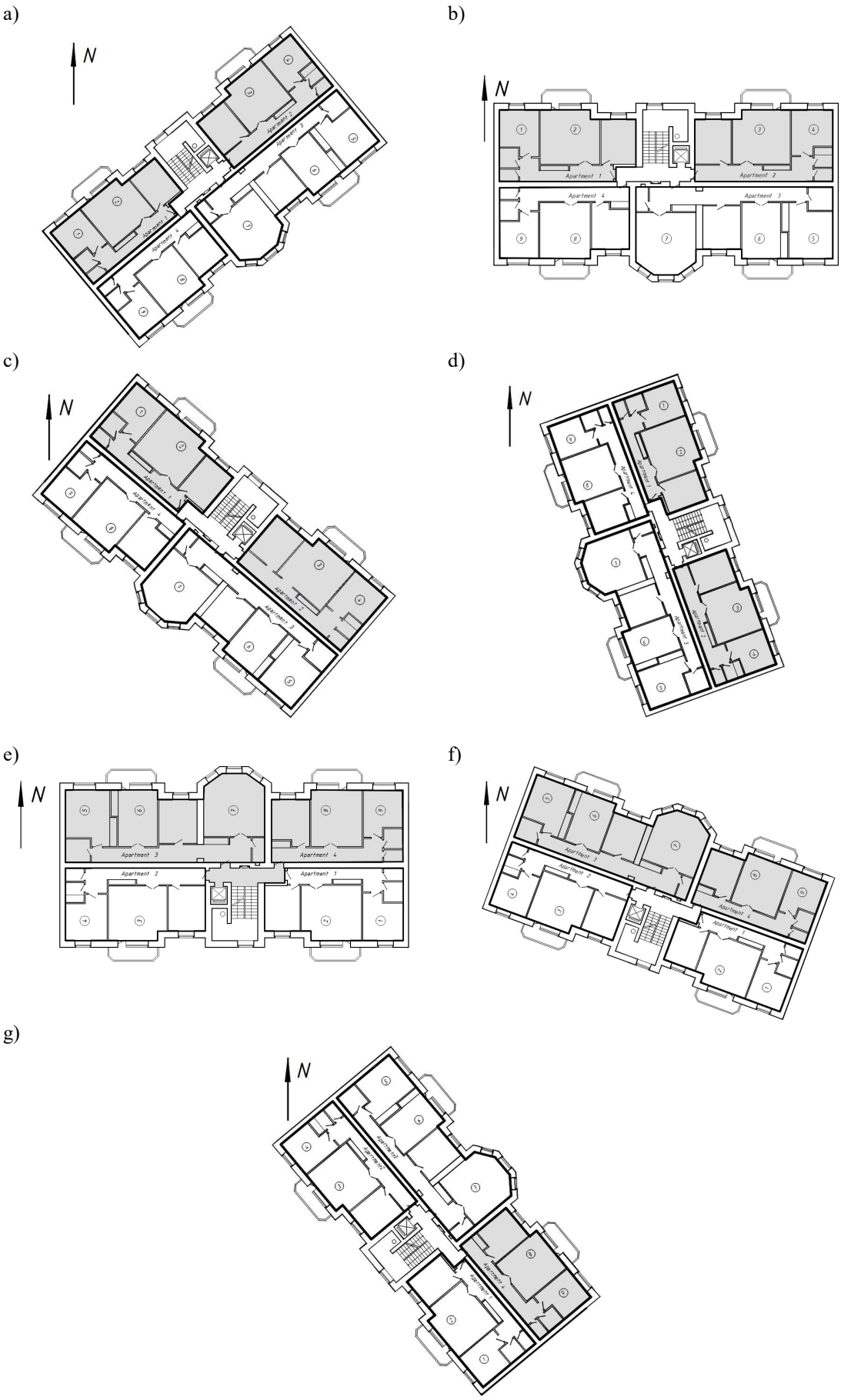

Figure 6 – Rooms where insolation standards are not met depending on the rotation of the longitudinal axis of the house from North-South direction:
a) by 60°; b) by 90°; c) by 120°; d) by 150° e) by 240°; f) by 270°; g) by 300°

The insulation standards for all apartments are complied when the longitudinal axis of buildings is oriented in the North-South direction.

Similarly, we calculate the insolation of the rooms when the longitudinal axis of the house is turned by 30º, 60º, 90º, 120º, 150º, 180º, 210º, 240º, 270º , 300º and 330º from North-South direction.

The norms of insolation are not met in apartments when the longitudinal axis of the house is turned by 60º, 90º, 120º, 150º,240º, 270º and 300º (Fig. 6).

The choice of the optimal orientation of the residential building was made according to the following indicators:

- the value of total insolation of apartments in a residential building (per typical floor) (Fig. 7);
- the number of rooms where the insolation requirements are met (Fig. 8);
- the number of rooms where the insolation requirements are met (Fig. 9);
- the number of rooms where the insolation requirements are met (Fig.10).

Table 2 summarizes the indicators shown in the graphs of Figures 7 - 10.

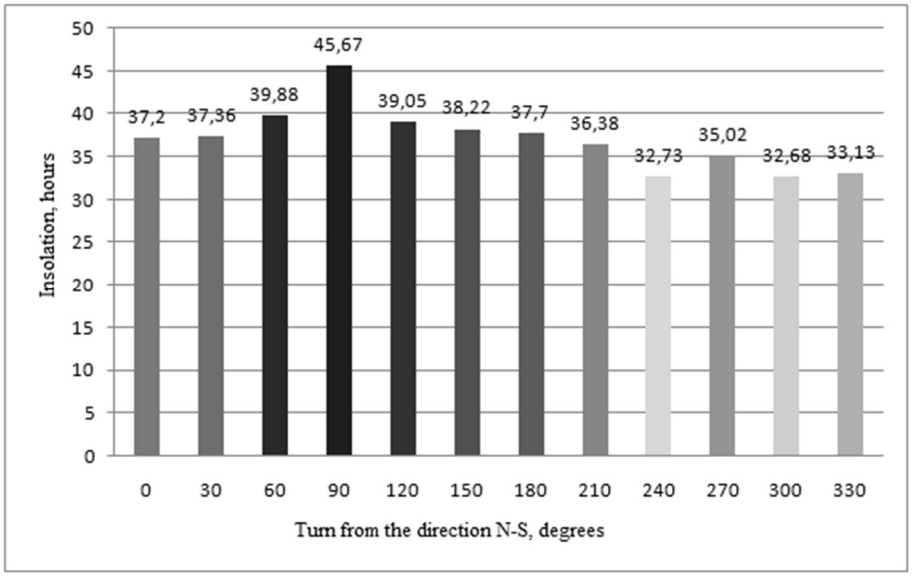

Figure 7 – Cumulative insolation of apartments depending on the rotation of the longitudinal axis of the house from North-South direction

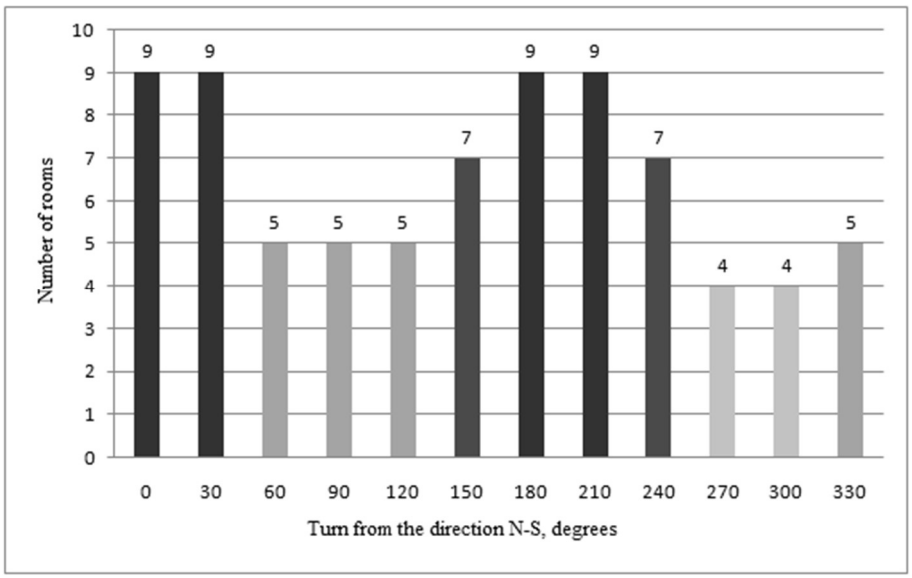

Figure 8 – Number of rooms where insolation requirements are met depending on the rotation of the longitudinal axis of the house from North-South direction

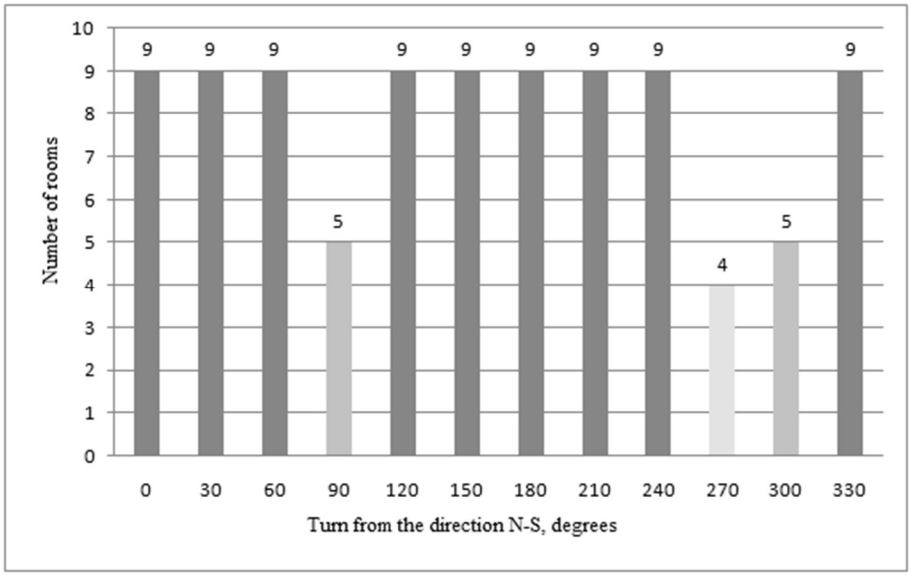

Figure 9 – Number of rooms where insolation occurs depending on the rotation of the longitudinal axis of the house from North-South direction

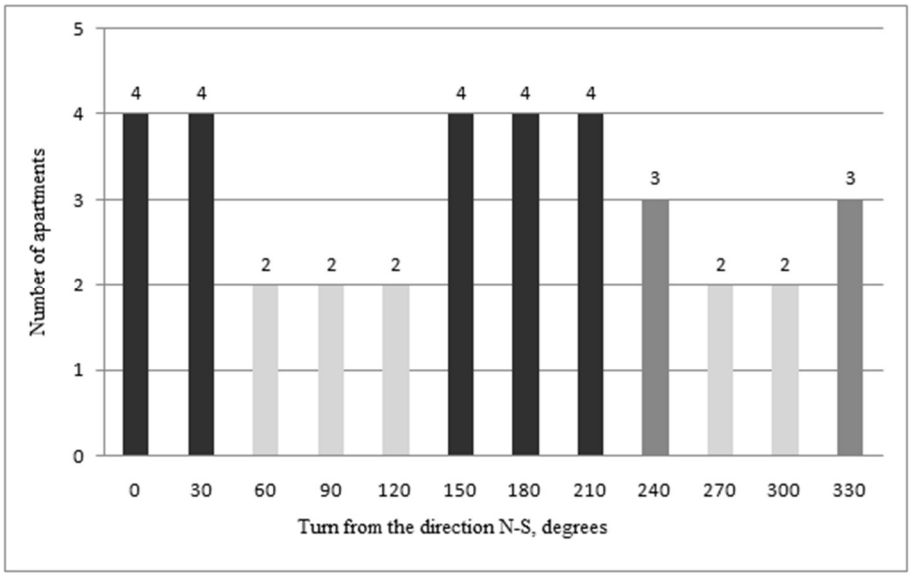

Figure 10 – Number of apartments where insolation requirements are met depending on the rotation of the longitudinal axis of the house from North-South direction

Table 2 – Duration of insolation of the rooms of the house from North-South direction

Name of parameter	The value of the indicator when the longitudinal axis of the house is turned from North-South direction by											
	0°	30°	60°	90°	120°	150°	180°	210°	240	270°	300°	330°
Cumulative insolation of apartments in a residential building	7	6	2	1	3	4	5	8	12	9	11	10
Number of rooms where insolation requirements are met	1	1	3	3	3	2	1	1	2	4	4	3
Number of rooms where insolation occurs	1	1	1	2	1	1	1	1	1	3	2	1
Number of apartments where insolation requirements are met	1	1	3	3	3	1	1	1	2	3	3	2
Sum of the indicators	**10**	**9**	**9**	**9**	**10**	**8**	8	**11**	**17**	**17**	**20**	**16**

Conclusions

The total insolation in all rooms of the house (per typical floor) is greatest when the longitudinal axis of the house is turned from North-South direction by 90° and 60°.

The biggest number of rooms that meet the requirements of insolation when the longitudinal axis of the house is turned from North-South direction by 0°, 30°, 180° and 210°.

The biggest number of rooms where insolation occurs when the longitudinal axis of the house is turned from North-South direction by 0°, 30°, 60°, 120°, 150°, 180°, 210°, 240°,150°, 210° and 330°.

Insolation requirements in one of the apartments are not satisfied when the longitudinal axis of the house is turned from North-South direction by 60º,90º, 120º, 270º,300º,330º.

According to the sum of all indicators, the worst orientation is when the longitudinal axis of the house is returned from North-South direction by 300º.

The smallest sum of indicators when the longitudinal axis of the house is turned by 180° from the direction of North-South, as seen in Table 2, is the optimal orientation of the residential building.

References

1. ДБН В.2.2-15-2019. (2019). *Житлові будинки. Основні положення*. Київ: Мінрегіонбуд України

2. ДБН Б.2.2-12:2019. (2019). *Планування і забудова територій*. Київ: Мінрегіонбуд України

3. ДБН В.2.5-28:2018. (2018). *Природне і штучне освітлення*. Київ: Мінрегонбуд України

4. ДСТУ-Н Б В.2.2-27:2010 (2010). *Настанова з розрахунку інсоляції об'єктів цивільного призначення*. Київ: Укрбудінформ

5. ДСП 173-96. (1996). *Державні санітарні правила планування і забудови населених пунктів*. Київ: Міністерство охорони здоров'я України

6. Lychko V.V., Skryl I.N. (1986). Effect of insolation on microflora. *Svetotehnika*, 9, 17

7. Скрыль И.Н. (1991). *Влияние инсоляции на воздухообмен в высокоплотной застройке (с учетом наружных ограждений)* (дис. д-ра техн. наук). Полтавский инженерно-строительный институт, Полтава

8. Скриль І.Н. (1992). *Інсоляція житла*. Київ: Будівельник

9. Скрыль И.Н., Киселев О.П. (1989). *Авторское свидетельство № 1525647. Инсоляционный прибор*. Открытия и изобретения

10. Sergeychuk O., Martynov V., Usenko D. (2018). The definition of the optimal energy-efficient form of the building. *International Journal of Engineering and Technology*, 7(3), 667-671
https://doi:10.14419/ijet.v7i3.2.14611

11. Сергейчук О.В. (2000). Геометричні питання врахування інфрачервоного опромінення і розрахунку інсоляції приміщень. Прикладна геометрія та інженерна графіка, 67, 128-131

12. Мартинов В.Л. (2013). Визначення оптимальної орієнтації енергоефективних будівель з дотриманням норм освітленості та інсоляції. *Вісник Кременчуцького національного університету імені Михайла Остроградського*, 5, 173-176

13. Мартинов В.Л. (2016). Оптимізація параметрів форми, утеплювача, орієнтації енергоефективних будівель з урахуванням вимог освітлення та інсоляції. *Енергоефективність в будівництві та архітектурі*, 8, 207-213

14. Collares-Pereira M., Rabl A. (1979). The average distribution of solar radiation-correlations between diffuse and hemispherical and between daily and hourly insolation values. *Solar Energy*, 22(2), 155-164
https://doi:10.1016/0038-092X(79)90100-2

1. DBN V.2.2-15-2019. (2019). *Residential buildings. Substantive provisions.* Kyiv: Ministry of Regional Development of Ukraine

2. DBN B.2.2-12:2019. (2019). *Planning and development of territories.* Kyiv: Ministry of Regional Development of Ukraine

3. DBN V.2.5-28:2018. (2018). *Natural and artificial lighting.* Kyiv: Ministry of Regional Development of Ukraine

4. DSTU-N B V.2.2-27:2010 (2010). *Guidelines for calculating the insolation of civil facilities.* Kyiv: Ukrarkhbudinform

5. DSP 173-96. (1996). *State sanitary rules of planning and construction of settlements.* Kyiv: Ministry of Health of Ukraine

6. Lychko V.V., Skryl I.N. (1986). Effect of insolation on microflora. *Svetotehnika*, 9, 17

7. Skryl I.N. (1991). *Influence of insolation on air exchange in high-density building (taking into account external protections) (dissertation of the doctor of technical sciences).* Poltava Civil Engineering Institute, Poltava

8. Skryl I.N. (1992). *Housing insolation.* Kyiv: Budivelnyk

9. Skryl I.N., Kiselev O.P. (1989). *Author's certificate № 1525647. Insolation device.* Discoveries and inventions

10. Sergeychuk O., Martynov V., Usenko D. (2018). The definition of the optimal energy-efficient form of the building. *International Journal of Engineering and Technology*, 7(3), 667-671
https://doi:10.14419/ijet.v7i3.2.14611

11. Serheichuk O.V. (2000). Geometric issues of taking into account infrared radiation and calculating the insolation of the premises. Applied geometry and engineering graphics, 67, 128-131

12. Martynov V.L. (2013). Determining the optimal orientation of energy efficient buildings in compliance with lighting and insolation. *Bulletin of Kremenchug National University named after Mykhailo Ostrogradsky,* 5, 173-176

13. Martynov V.L. (2016). Optimization of parameters of form, insulation, orientation of energy efficient buildings taking into account the requirements of lighting and insolation. *Energy efficiency in construction and architecture*, 8, 207-213

14. Collares-Pereira M., Rabl A. (1979). The average distribution of solar radiation-correlations between diffuse and hemispherical and between daily and hourly insolation values. *Solar Energy*, 22(2), 155-164
https://doi:10.1016/0038-092X(79)90100-2

15. Саньков П.М., Ткач Н.О., Возіян К.О., Єрмолаєва Ю.П. (2016). Забезпечення повноцінного освітлення та інсоляції житлових приміщеннях в умовах реконструкції. *Міжнародний науковий журнал*, 5(2), 18-21

16. Елагин Б.Т., Прядко Н.В. (2003). Инсоляционные расчеты в архитектуре. Макеевка: ДонГАСА

17. Андропова О.В. (2017). Класифікація будинків і споруд за вимогами до норм інсоляції. *Energy-efficiency in civil engineering and architecture*, 9, 11-16

18. Yurin O., Avramenko Y., Leshchenko M., Rozdabara O. (2020) Research of Possible Methods of Increasing the Duration of the Insolation of Rooms in Residential Buildings. *Lecture Notes in Civil Engineering*, 73, 312-323 https://doi.org/10.1007/978-3-030-42939-3_32

19. Darula S., Christoffersen J., Malikova M. (2015). Sunlight and Insolation of Building Interiors. *Energy Procedia*, 7, 1245-1250 https://doi:10.1016/j.egypro.2015.11.266

20. Подгорный А. (1981). К вопросу автоматизации инсоляционных расчетов. Прикладная геометрия и инженерная графика. *Будівельник*, 31, 12-15

21. Sergeychuk O., Radomtsev D. (2016). Implementation of CIE general sky model approach in ukraine and effects on room illuminance mode. *International Journal of Smart Home*, 10(1), 57-70 https://doi:10.14257/ijsh.2016.10.1.07

22. Вернеску Д., Эне А. (1981). *Инсоляция и естественное освещение в архитектуре и градостроительстве*. Київ: Будівельник

23. Єгорченков В.О. (2000). Світловий клімат України і його облік при проектуванні систем природного освітлення будинків. *Збірник наукових праць. Галузеве машинобудування, будівництво*, 6, 32-37

24. *Инсоляция и плотность застройки в градостроительстве. Аналитическая справка. АС-8-86*. (1986). Харьков: УКРНИИНТИ Госплана УССР

25. Шмаров И.А., Земцов В.А., Коркина Е.В. (2016). Инсоляция: практика нормирования и расчета. *Жилищное строительство*, 7, 48-53

26. Земцов В.А., Гагарин В Г. (2009). Инсоляция жилых и общественных зданий. *Перспективы развития. Academia. Архитектура и строительство*, 5

27. Нагаева О.С., Пешкичева Н.С., Германова Т.В. (2012). Инсоляция как один из критериев, определяющий минимальное расстояние между зданиями. *Успехи современного естествознания*, 6, 189-190

28. Шмаров И А., Земцов В.А., Гуськов А.С., Бражникова Л.В. (2020). Инсоляция помещений как средство ограничения распространения COVID-19, гриппа и ОРВИ в городской среде. *Academia. Архитектура и строительство*, (4)

29. Ожималова В.О. (2021). Инсоляция жилых зданий. *Инновации. Наука. Образование*, 33, 1489-1493

30. Рыжих В.Д. (2015). Инсоляция как неотъемлемая часть архитектурного проектирования и жизни человека. *Образование, наука, производство*, 2317-2321

31. Дунаев Б А. (1979). *Инсоляция жилища*. Москва, Стройиздат

32. Олейнюк О.Р. (2013). Інсоляція та мікрокліматичні особливості формування флори у внутрішніх двориках історичної частини Львова. *Науковий вісник НЛТУ*, 23(5).

33. Бохонюк А. И. (2004). *Инсоляция жилища. Пособие по проектированию инсоляции жилых зданий и территорий застройки (для широт Украины)*. К.: Киев ЗНИИЭП

34. Тимошенко Е. В., Сиордия Д. Т. (2017). Улучшение инсоляции искусственными способами. *Академическая публицистика*, (12), 444-449

15. Sankov P.M., Tkach N.O., Voziyan K.O., Yermolaeva Yu.P. (2016). Ensuring full lighting and insolation of residential premises in the conditions of reconstruction. *International scientific journal*, 5(2), 18-21

16. Elagin B.T., Pryadko N.V. (2003). *Insolation calculations in architecture.* Makeevka: DonGASA

17. Andropova O.V. (2017). Classification of buildings and structures according to the requirements for insolation standards. *Energy-efficiency in civil engineering and architecture*, 9, 11-16

18. Yurin O., Avramenko Y., Leshchenko M., Rozdabara O. (2020) Research of Possible Methods of Increasing the Duration of the Insolation of Rooms in Residential Buildings. *Lecture Notes in Civil Engineering*, 73, 312-323 https://doi.org/10.1007/978-3-030-42939-3_32

19. Darula S., Christoffersen J., Malikova M. (2015). Sunlight and Insolation of Building Interiors. *Energy Procedia*, 7, 1245-1250 https://doi:10.1016/j.egypro.2015.11.266

20. Podgornyiy A. (1981). On the issue of automation of insolation calculations. Applied Geometry and Engineering Graphics. *Budivelnyk*, 31, 12-15

21. Sergeychuk O., Radomtsev D. (2016). Implementation of CIE general sky model approach in ukraine and effects on room illuminance mode. *International Journal of Smart Home*, 10(1), 57-70 https://doi:10.14257/ijsh.2016.10.1.07

22. Vernesku D., Ene A. (1981). *Insolation and natural lighting in architecture and urban planning*. Kyiv: Budivelnyk

23. Yehorchenkov V.O. (2000). Light climate of Ukraine and its consideration in the design of natural lighting systems of buildings. *Academic journal. Industrial Machine Building, Civil Engineering*, 6, 32-37

24. *Insolation and building density in urban planning. Analytical reference. AC-8-86. (1986).* Kharkov: UKRNINTI Gosplan of the Ukrainian SSR

25. Shmarov I.A., Zemtsov V.A., Korkina E.V. (2016). Insolation: the practice of rationing and calculation. *Housing construction*, 7, 48-53

26. Zemtsov V.A., Gagarin V.G. (2009Insolation of residential and public buildings. *Development prospects. Academy. Architecture and construction*, 5

27. Nagaeva O.S., Peshkicheva N.S., Germanova T.V. (2012). Insolation as one of the criteria that determines the minimum distance between buildings. *Successes of modern natural science*, 6, 189-190

28. Shmarov I.A., Zemtsov V.A., Guskov A.S., Brazhnikova L.V. (2020). Insolation of premises as a means of limiting the spread of COVID-19, influenza and SARS in the urban environment. *Academy. Architecture and construction*, (4).

29. Ozhimalova V.O. (2021). Insolation of residential buildings. *Innovation. The science. Education*, 33, 1489-1493

30. Ryizhih V.D. (2015). Insolation as an integral part of architectural design and human life. *Education, science, production*, 2317-2321

31. Dunaev B.A. (1979). *Home insolation.* Moscow, Stroyizdat

32. Oleiniuk O.R. (2013). Insolation and microclimatic features of flora formation in the courtyards of the historical part of Lviv. Scientific Bulletin of NLTU, 23(5)

33. Bohonyuk A. I. (2004). *Home insolation. Manual for the design of insolation of residential buildings and development areas (for the latitudes of Ukraine). Kiev ZNIIEP*

34. Timoshenko E.V., Siordiya D.T. (2017). *Improving insolation by artificial means. Academic journalism*, (12), 444-449

35. Darula S., Christoffersen J., Malikova M. (2015). Sunlight and insolation of building interiors. *Energy Procedia*, 78, 1245-1250

36. Ling C.S., Ahmad M.H., Ossen D.R. (2007). The effect of geometric shape and building orientation on minimising solar insolation on high-rise buildings in hot humid climate. *Journal of Construction in Developing Countries*, 12(1), 27-38.

37. An J., Yan, D., Guo S., Gao Y., Peng J., Hong T. (2020). An improved method for direct incident solar radiation calculation from hourly solar insolation data in building energy simulation. *Energy and Buildings*, 227 https://doi:10.1016/j.enbuild.2020.110425

38. Valladares-Rendón L.G., Lo S.L. (2014). Passive shading strategies to reduce outdoor insolation and indoor cooling loads by using overhang devices on a building. *Building Simulation*, 7(6), 671-681

39. Causone F., Corgnati S.P., Filippi M., Olesen B.W. (2010). Solar radiation and cooling load calculation for radiant systems: Definition and evaluation of the direct solar load. *Energy and Buildings*, 42(3), 305-314 https://doi:10.1016/j.enbuild.2009.09.008

40. Maestre I.R., Blázquez J.L.F., Gallero F.J.G., Cubillas P.R. (2015). Influence of selected solar positions for shading device calculations in building energy performance simulations. *Energy and Buildings*, 101, 144-152 https://doi:10.1016/j.enbuild.2015.05.004

35. Darula S., Christoffersen J., Malikova M. (2015). Sunlight and insolation of building interiors. *Energy Procedia*, 78, 1245-1250

36. Ling C.S., Ahmad M.H., Ossen D.R. (2007). The effect of geometric shape and building orientation on minimising solar insolation on high-rise buildings in hot humid climate. *Journal of Construction in Developing Countries*, 12(1), 27-38.

37. An J., Yan, D., Guo S., Gao Y., Peng J., Hong T. (2020). An improved method for direct incident solar radiation calculation from hourly solar insolation data in building energy simulation. *Energy and Buildings*, 227 https://doi:10.1016/j.enbuild.2020.110425

38. Valladares-Rendón L.G., Lo S.L. (2014). Passive shading strategies to reduce outdoor insolation and indoor cooling loads by using overhang devices on a building. *Building Simulation*, 7(6), 671-681

39. Causone F., Corgnati S.P., Filippi M., Olesen B.W. (2010). Solar radiation and cooling load calculation for radiant systems: Definition and evaluation of the direct solar load. *Energy and Buildings*, 42(3), 305-314 https://doi:10.1016/j.enbuild.2009.09.008

40. Maestre I.R., Blázquez J.L.F., Gallero F.J.G., Cubillas P.R. (2015). Influence of selected solar positions for shading device calculations in building energy performance simulations. *Energy and Buildings*, 101, 144-152 https://doi:10.1016/j.enbuild.2015.05.004

Збірник наукових праць. Галузеве машинобудування, будівництво
Academic journal. Industrial Machine Building, Civil Engineering
http://journals.nupp.edu.ua/znp
https://doi.org/10.26906/znp.2021.56.2513

UDK 342.211

Intellectual property in construction

Rohovyi Stanislav[1], Yurchenko Oksana[2]*

[1] Sumy National Agrarian University https://orcid.org/0000-0002-9431-5884
[2] Sumy National Agrarian University https://orcid.org/0000-0001-6498-2339
*Corresponding author E-mail: oksana.yurchenko@snau.edu.ua

The article considers the economic approach to the assessment of intellectual property rights. The place and role of intellectual property in the activities of construction entities are described. The purpose of the article is a comprehensive analysis of the place and role of intellectual property in the concept of economic sustainability of construction companies, as well as identifying the most important areas and practical measures to intensify the use of intellectual property in their activities. Achieving the goal was solved by methods of theoretical research on intellectual property issues of the construction industry; research of innovations in the field of theory and practice of construction production.

Key words: construction, intellectual property, intangible assets

Інтелектуальна власність в будівництві

Роговий С.І.[1], Юрченко О.В.[2]*

[1] Сумський національний аграрний університет
[2] Сумський національний аграрний університет
*
Адреса для листування E-mail: oksana.yurchenko@snau.edu.ua

У статті розглянуто економічний підхід оцінки прав на інтелектуальну власність, який визначається конкретними комерційними інтересами суб'єктів ринкової економіки. Доведено, що покупець, купуючи права власності на результати інтелектуальної діяльності, повинен, перш за все, виходити з власних конкретних можливостей використання цих результатів з прибутком. Підтверджено, що в даний час ключовим фактором розвитку економіки є інтелектуальні ресурси - знання та інформація. Проведено аналіз існуючих класифікацій складових інтелектуальної власності будівництва. Розкрито основні підходи до визначення поняття «інтелектуальна власність». Описано місце та роль інтелектуальної власності у діяльності суб'єктів будівництва. Мета статті полягала в комплексному аналізі місця і ролі інтелектуальної власності в концепції економічної стійкості будівельних підприємств, а також виявлення найважливіших напрямків і практичних заходів щодо активізації процесів використання інтелектуальної власності в їх діяльності. Досягнення мети вирішувалося методами теоретичних досліджень щодо питань інтелектуальної власності будівельної сфери; дослідженням інновацій в області теорії і практики будівельного виробництва. Процес затвердження інтелектуальної власності в українському правовому полі і на ринку - дуже складний і суперечливий процес, особливо якщо мова йде про будівництво, де основним джерелом прибутку є матеріальне виробництво, а не інші дії з якими б то не було об'єктами інтелектуальної власності. Для підвищення ефективності будівельного виробництва в перспективі, для поліпшення економічних показників діяльності будівельних підприємств і для досягнення максимального прибутку, необхідно вишукувати нові джерела, якими можуть і повинні стати об'єкти інтелектуальної власності та права користування ними.

Ключові слова: будівництво, інтелектуальна власність, нематеріальні активи

Introduction

In the context of the economic development of the country or its individual industries, the scale and quality level of intellectual property become the most important indicators of the durability of market positions both at the state level and at the regional level and at the level of individual enterprises and organizations.

Intellectual property as a new phenomenon requires qualitatively different views and approaches than developed in the previous historical and economic period. It is possible that in today's conditions, unfamiliar innovative thinking has not fitted into the usual, traditional concepts and schemes yet.

The solution to this problem requires multilateral research, first of all, a theoretical understanding of economic and legal concepts and categories of intellectual property, as well as practical developments in the field of commercial and economic use of intellectual property in order to increase the profitability of construction enterprises.

Review of research sources and publications

Economics has made a significant contribution to the study of intellectual problems in the days of command-and-control principles of management, but from the point of view of political economy. A significant place in the development of these problems belongs to such scientists as Anchishkin A., Elmeev V., Shcherbakov A., Shishkov G., Voychinsky A., Yudelevich M., Zavlin P. and others.

Research in this direction was carried out in the works of Kekukh B., Kolyada N., Korchagin A., Kozyrev A., Nikonov A., Novoseltsev O., Oleynikov S., Orekhov A., Polyakova S., Yakutin Y., Yurieva T. and others.

Definition of unsolved aspects of the problem

In our opinion, in the modern economic literature there are not enough publications devoted to the definition of the place of intellectual property in enterprises in the implementation of the concept of its commercial and domestic use. There is almost no work on the issues of alternative use of intellectual property in the activities of construction companies in order to increase profitability and profitability indicators.

Objective of the work and research methods

The purpose of the article is a comprehensive analysis of the place and role of intellectual property in the concept of economic sustainability of construction enterprises, as well as identifying the most important directions and practical measures to enhance the use of intellectual property in their activities.

The goal was achieved by the following methods:

– theoretical research on intellectual property in the construction sector;

– research of innovations in the field of theory and practice of construction production.

Basic material and results

Intellectual property is the result of the intellectual, creative activity of one person (author, performer, inventor, etc.) or several people [1].

Intellectual property in the system of economic activity acquires the status of intangible assets. It accompanies investment and innovation activities. Objects of intellectual property rights in economic activity are assets that have the appropriate characteristics, and, above all, the price (value). Their use should be considered from the standpoint of economics, investment, pricing, and accounting.

All over the world, the processes of incorporation of intellectual property into economic circulation have been going very rapidly lately. In fact, we are talking about unaccounted funds of enterprises. On the one hand, they are not taxed, and it becomes possible to dispose of property without the consent of the owner, and on the other hand, an enterprise that does not amortize its intellectual property overpays income taxes. Therefore, the corresponding development funds are not formed. Moreover, it thereby unwittingly refuses the additional income received as a result of the transfer of rights to use intellectual property objects on the basis of licensing agreements and other transactions. Therefore, the belief in the uselessness of including intellectual property objects in the property complex of an enterprise is today a serious mistake. In addition, if an enterprise uses an intellectual property object in its activities, then, according to the legislation, it must be reflected in the enterprise's reporting documents. Otherwise, the use of this intellectual property object is considered illegal [11, 15].

Today, one of the decisive conditions for the development of the construction market and the growth of construction production is the ever-expanding range of technological processes, which is based on a great variety of modern building materials and means of mechanization.

The steady trend of improving existing and creating new technologies is characterized by a focus on achieving the requirements of creating competitive products. The release of such products can be customized only on the basis of the latest technological solutions and with the use of intellectual property objects.

In the scientific literature, there are significant differences in approaches to the composition of intellectual property objects. Nowadays, there is no unified system in the formation of intellectual property objects, which negatively affects not only the practice of their use in the activities of individuals and legal entities, including in not only the assessment of business, but also in understanding the possibilities of protection, including from unfair competition [13].

We have identified the most acceptable and most frequently used objects of intellectual property in construction (Fig. 1):

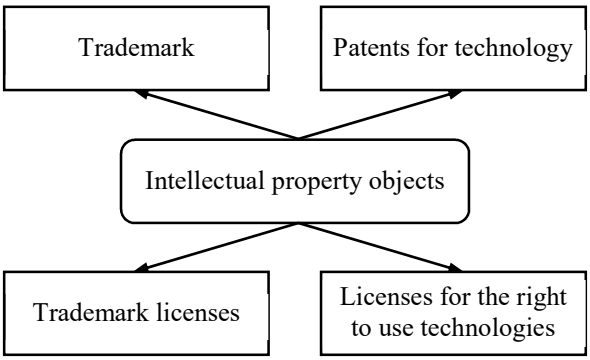

Figure 1 – Objects of intellectual property in construction

The acquisition of intangible assets is carried out under a license agreement on the transfer of rights to use the subject of the license and the relevant conditions specified in the license agreement. Trading in licenses is the implementation of trade agreements under which the seller (licensor) grants the buyer (licensee) the right (license) to use an intangible asset (subject of the license) on the terms of the license agreement, as well as to carry out operations in the secondary market for intangible assets.

It should be borne in mind when assessing the value of objects of intellectual property rights, only valid titles of protection (patents, certificates, etc.) and license agreements (contracts) are taken into account, considering the annexes to them, which determine the value of such objects [3].

We came to the conclusion that the decision on the advisability of creating and introducing intellectual property objects into the production and economic activities of construction enterprises should be made on the basis of the economic effect, determined in accordance with the annual production of construction products.

We believe that it is necessary and sufficient for construction companies to calculate the effect of the use of new technology on the following three options:

– calculation of the annual economic effect from the use of new technology;

– calculation of the annual economic effect from the introduction of new technology based on the rationalization proposal;

– determination of the profit received from the use of new technology in the production process.

If we are talking about the trademark of the enterprise, in this case a simple analysis of the cash flows of revenue and profits obtained using this trademark is sufficient.

The inclusion of intellectual capital in the economic circulation depends on the goals pursued by each enterprise:

– if the enterprise needs to generate a significant amount of authorized capital without diversion of funds, it is necessary to use the first case (contribution to the authorized capital);

– if the company plans to obtain a loan, loan, loan and it needs to increase profitability, profitability and efficiency, you should use the second case (voluntary conveyance);

– if the main task of the enterprise is to put on the balance of intellectual property with the subsequent receipt of income from the sale of licenses for the right to use these objects to other individuals or legal entities, then the enterprise puts the intellectual property on the balance sheet at cost (as an object created within the enterprise itself) [12].

Legal regulation of intellectual property is an important area of development of the Ukraine legal system in modern conditions. Intellectual property is a new phenomenon of public life. And the future of the country largely depends on how it will develop, including what its legal support and legal status of a creative person will be.

The construction process begins with design. Often, during the implementation of development projects between customers and developers of the construction project, there are disputes concerning the observance and protection of copyright. Sometimes customers violate the rights of the developer of an architectural project, illegally using or otherwise violating the rights of the author, and sometimes, on the contrary, the authors abuse their position, demanding that customers pay additional fees. Such issues can be avoided with a proper elaboration of the terms of the project development contract [14,16].

Architectural activity is a complex conglomeration of numerous processes, including the creation of an architectural project, the development of design, and working documentation, the ultimate goal of which is to create an architectural object in the form of buildings, structures, etc. However, only some of these processes are subject to legal protection of copyright. Judicial and arbitration practice clarified that the object of legal protection is not all project documentation on the creation of a real estate object, but only its architectural part, as the embodiment of the author's creative idea [2].

There is a state system for the legal protection of intellectual property.

A system is a set of elements that have characteristic features, parameters, and spatial structure that ensure the achievement of a single revenge or function. The structure of the system can be represented as a graph. The subsystem in turn can be a system that consists of a set of its elements (Fig. 2).

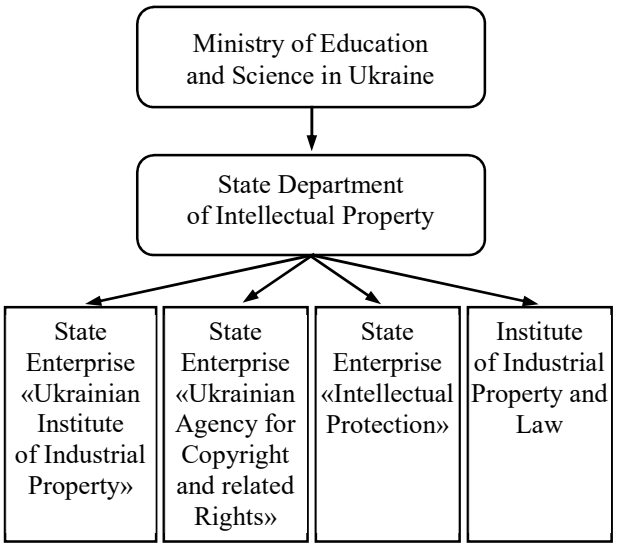

Figure 2. The state system structure of intellectual property legal protection [4]

The analysis of Western experience in the valuation of intangible assets showed that a promising direction for assessing the business of companies is a concept based on the use of the theory of the optimal portfolio of exclusive rights. It is the assessment of the entire set of intellectual property of companies, and not of individual objects linked into a single optimal portfolio, that will make it possible to effectively use intangible assets to manage business in a company, as well as to control more significant shares of world technology markets.

Modern business actually has three types of capital: financial, physical and intellectual. Each of the three capitals is often divided into equity and debt. It is interesting to note that not only money, but also tangible and intangible assets and even temporary personnel can be used as a loan.

First of all, in the management system of the enterprise, where the dominant role is given to intellectual capital, the priorities change in favor of working with staff to find new valuable ideas and increase intellectual advantages over competitors. In this case, the legal protection of creative results is mandatory to avoid large losses in the future.

In the creative potential of enterprise employees it is necessary to take into account the following characteristics that determine the level of intellectual capital:

1) the degree of business reputation of the organization;

2) qualification and experience of the company's employees;

3) regular development and introduction of new achievements of science and technology into production;

4) release of original products that are in demand on the commodity market;

5) the presence in the organization of a structural unit, the main functions of which should be innovation [8].

Intellectual capital should be understood as accumulated by saving and effectively organizing a fund of economic benefits in the form of intellectual advantages that can be converted into money and capital goods. Intellectual capital is attracted to the economic and commercial turnover by its owners as the most important investment resource and factor of production in order to obtain super-profits.

Its use is based on the principles of market relations and is associated with factors of time, risk, liquidity and payback.

It is intellectual capital that sets the pace and nature of the renewal of production technologies and their products, which then become the main competitive advantage in the market. Intellectual capital is not just good brains and, as a result, good technical and organizational solutions.

This is, first of all, a system of capital sustainable intellectual advantages of a given company or firm in the market. It is one thing to have these advantages, and another thing to know how to use them.

Intellectual capital is an intangible asset (IA) of an enterprise that:

– has no physical substance;

– manifests itself by its economic properties;

– gives rights and privileges to their owner;

– generates income for their owner [7].

In the construction industry, the following main types of work and activities can be classified as intellectual capital in general:

– formation of plans for investment programs and local decisions;

– all stages of investment activity;

– organization of research and design work;

– analysis of the results of topography and geological exploration;

– all types of design and engineering work;

– optimization of design solutions;

– development of organizational and technological solutions for construction;

– organization of material and technical support;

– logistics of transport and supply operations;

– creation of new materials;

– development of new designs and calculation methods [9].

To substantiate plans for capital investments in construction, it is necessary to perform a large amount of various intellectual and creative works, the material return of which can manifest itself only after a significant period of time and only after the practical implementation of the plan.

It should be noted that at all stages of construction activities there is intellectual capital, the value of which, depending on the cost of a particular stage, can be roughly presented as shown in table 1.

Since the costs of the stages are usually known (estimates, bank documents, etc.), it is not difficult to determine the price of intellectual capital as part of a work stage. A more difficult task is to determine dividends for creators of intellectual capital, which may arise during the implementation of the project and after the start of operation of the construction facility. Usually the

revenue part from the sale of construction projects, in contrast to industrial goods, arises after many years.

Complex construction projects can be put into operation for many years (gas and oil pipelines, residential areas, seaports, highways, railways, etc.). Therefore, the economic and construction sciences need to develop methods for calculating the cost of intellectual capital for the main stages and varieties of ways to implement investments in construction.

To use the results of intellectual activity in its activities, the enterprise must have special rights that differ significantly from property rights to tangible objects.

Table 1 – The importance of intellectual capital in the main stages of construction [6]

Names of stages of works	Share of intellectual costs,%	Share of associated costs (business trips, equipment)
1. Development of investment programs and validity of construction plans	70	30
2. Organization of research and design work, data processing of topology and geological exploration, construction optimization	60	40
3. Design work and optimization of design solutions	90	10
4. Development of organizational and technological solutions for construction	95	5
5. Organization of material and technical support, logistics of transport and supply operations	50	50
6. Development of new materials, structures and calculation methods	60	40

The monopoly on the use of the obtained results of intellectual activity in legal terminology is called the exclusive right and means that no one has the right to use an intangible object without the permission of the owner.

For the successful implementation of the innovation process, an adequate organization of intellectual property management is required, including a mechanism for the creation and further commercialization of intellectual property.

For the effective development of international exchange of technologies in the construction sector, appropriate conditions are needed:

– legal (protection of intellectual property in a foreign state);

– financial (lending, insurance, improving the efficiency of financial settlement schemes);

– institutional (the presence of international organizations regulating the international exchange of production technologies);

– innovative (improvement of existing technologies and their subsequent transfer) [10].

The trends in the development of intellectual resources in leading Western firms are associated with the following key points:

– continuous development and implementation of new strategies for personnel training in order to deepen the intellectualization of labor;

– development of the creative abilities of the individual on the basis of a continuous increase in investment in human capital;

– expansion of the practice of software cooperation of companies in the form of joint laboratories or inter-firm scientific and technical centers, illustrated by the positive dynamics of indicators such as the number of joint patents; growth in the scale of corporate patenting and licensing, including and general on the basis of cooperative interaction: in the field of innovation;

– development of effective strategies [4].

The main problem in the field of intellectual property is ensuring that the rights of the copyright holder are respected.

Many countries of the world have managed to achieve this, and as for Ukraine, we still need to learn a lot from other developed countries. We have not created such conditions. This, of course, damages the country's business reputation and undermines its credibility, not only economically, but also politically. Therefore, the state should pay special attention to this problem and take effective measures to combat infringers of intellectual property rights, in particular in the construction sector.

Conclusions

The modern model of the system integrated innovation process, the diversity of intellectual products necessitate the development of intellectual property relations and the improvement of their legal regulation.

Today, the problems of economic development and increasing the profits of construction companies through the involvement, expert evaluation, legal consolidation and use in the turnover of intellectual property are relevant.

The perception of intellectual property as one of the most important categories for Ukraine has not yet taken place, that is, it has not become the norm. The process of approval of intellectual property in the Ukrainian legal field and in the market is a very complex and controversial process, especially when it comes to construction, where the main source of income is material production and no other actions with any intellectual property.

To increase the efficiency of construction production in the future, to improve the economic performance of construction enterprises and to achieve maximum profit, it is necessary to seek new sources, which can and should become objects of intellectual property and the right to use them.

References

1. Вікіпедія [Електронний ресурс]. Режим доступу: https://uk.wikipedia.org/wiki/

2. Еннан Р. (2011). Права на результати інтелектуальної діяльності: зміст та сутність. *Теорія і практика інтелектуальної власності*, 6, 10-15

3. *Інтелектуальна власність в Україні: Проблеми теорії і практики* (2002). Київ: Інститут держави і права ім. В. М. Корецького

4. Підопригора О.А., Бутнін-Сіверський О.Б., Дроб'язко В.С. (2004). *Право інтелектуальної власності*. Київ: Видавничий Дім "Ін Юре"

5. Arbor A. (1996). *Technological competitiveness of Japanese multinationals*. Michigan University Press

6. Chandler A., Solvele J. (1998). *The Dynamic firm. The role of technology strategy organization and regions*. Oxford

7. May C. (2000). *The Global Political Economy of Intellectual Property Rights: The New Enclosures?* Routledge

8. Мэггс П.Б. (2000). *Интеллектуальная собственность*. Москва: Юрист

9. Рейли Р., Швайс Р. (2005). *Оценка нематериальных активов*. Москва: Квинто Консалтинг

10. Rodov I., Leliart Ph. (2002). FIMIAM: financial method of intangible assets measurement. *Journal of Intellectual Capital*, 3, 323-336

11. *Medium Term Strategic Plan for WIPO* (2010). A/48/3. [Електронний ресурс]. Режим доступу: http://www.wipo.int

12. *Unified Patent Court.* [Електронний ресурс]. Режим доступу: https://www.unified-patent-court.org

13. *GNU Lesser General Public License* / Free Software Foundation. URL: http://www.gnu.org/licenses/lgpl.html

14. Qian Y. (2007). Do National Patent Laws Stimulate Domestic Innovation in a Global Patenting Environment? A Cross-Country Analysis of Pharmaceutical Patent Protection, 1978-2002. *The Review of Economics and Statistics*, 89(3), 436-453
http://dx.doi.org/10.1162/rest.89.3.436

15. *Global Leadership Forecast 2018. 25 Research Insights to Fuel Your People Strategy. Development Dimensions International* (2018). [Електронний ресурс]. Режим доступу: https://www.ddiworld.com

16. *World Intellectual Property Indicators 2018* (2018). [Електрон. ресурс]. Режим доступу: http://www.wipo.int

17. Granstrand O. (2010). *Industrial Innovation Economics and Intellectual Property*. Gothenburg: Svenska Kulturkompaniet

1. Wikipedia [Electronic resource]. Acess mode: https://uk.wikipedia.org/wiki/

2. Ennan R. (2011). Rights to the results of intellectual activity: content and essence. *Theory and practice of intellectual property*, 6, 10-15

3. *Intellectual property in Ukraine: Problems of theory and practice*. (2002). Kyiv : Institute of State and Law V.M. Koretsky

4. Pidoprygora O., Butnin-Siversky O., Drobiazko V. (2004). *Intellectual Property Law*. Kyiv: Publishing House "In Jure"

5. Arbor A. (1996). *Technological competitiveness of Japanese multinationals*. Michigan University Press

Chandler A. Solvele J. The Dynamic firm. The role of technology strategy organization and regions. Oxford, 1998. – 469 pp.

7. May C. (2000). *The Global Political Economy of Intellectual Property Rights: The New Enclosures?* Routledge

8. Meggs P.B. (2000). *Intellectual property*. Moscow: Jurist

9. Reilly R., Schweiss R. (2005). *Valuation of intangible assets*. Moscow: Quinto Consulting

10. Rodov I., Leliart Ph. (2002). FIMIAM: financial method of intangible assets measurement. *Journal of Intellectual Capital*, 3, 323-336

11. *Medium Term Strategic Plan for WIPO* (2010). A/48/3 [Electronic resource]. Acess mode: http://www.wipo.int

12. *Unified Patent Court*. [Electronic resource]. Acess mode: https://www.unified-patent-court.org

13. *GNU Lesser General Public License* / Free Software Foundation. URL: http://www.gnu.org/licenses/lgpl.html

14. Qian Y. (2007). Do National Patent Laws Stimulate Domestic Innovation in a Global Patenting Environment? A Cross-Country Analysis of Pharmaceutical Patent Protection, 1978-2002. *The Review of Economics and Statistics*, 89(3), 436-453
http://dx.doi.org/10.1162/rest.89.3.436

15. *Global Leadership Forecast 2018. 25 Research Insights to Fuel Your People Strategy. Development Dimensions International* (2018). [Electronic resource]. Acess mode: https://www.ddiworld.com

16. *World Intellectual Property Indicators 2018* (2018). [Electronic resource]. Acess mode: http://www.wipo.int

17. Granstrand O. (2010). *Industrial Innovation Economics and Intellectual Property*. Gothenburg: Svenska Kulturkompaniet

Збірник наукових праць. Галузеве машинобудування, будівництво
Academic journal. Industrial Machine Building, Civil Engineering
http://journals.nupp.edu.ua/znp
https://doi.org/10.26906/znp.2021.56.2514

UDC 658.382

Risk-oriented approach to identifying hazards in the construction industry of Ukraine

Zyma Oleksandr[1*], Pahomov Roman[2], Redkin Oleksandr[3]

[1] National University «Yuri Kondratyuk Poltava Polytechnic» https://orcid.org/0000-0001-7484-7755
[2] National University «Yuri Kondratyuk Poltava Polytechnic» https://orcid.org/0000-0001-9169-8296
[3] National University «Yuri Kondratyuk Poltava Polytechnic» https://orcid.org/0000-0002-6449-050X
*Corresponding author E-mail: zymaae@gmail.com

An attempt to improve the analytical method for determining the criteria for the risk degree in the construction industry was presented in this paper. The risk management process as a set of actions that is part of the overall business management was analyzed. Features of systemic occupational safety risk management were identified. The stages of an occupational safety management system design based on hazard identification were presented. The main objectives of the risk-oriented approach to ensuring the systems' reliability based on the acceptable risk concept were formulated. A method for determining the criteria by which the risk degree of an accident or an injury is assessed, for the possibility of planning supervisory activities at the enterprise was proposed

Keywords: construction, injuries, risk degree, risk criteria, risk-oriented approach

Ризик-орієнтований підхід визначення небезпек у будівельній галузі України

Зима О.Є.[1]*, Пахомов Р.І.[2], Редкін О.В.[3]

[1] Національний університет «Полтавська політехніка імені Юрія Кондратюка»
[2] Національний університет «Полтавська політехніка імені Юрія Кондратюка»
[3] Національний університет «Полтавська політехніка імені Юрія Кондратюка»
*Адреса для листування E-mail: zymaae@gmail.com

У даній роботі наведена спроба удосконалення аналітичного методу визначення критеріїв ступеня ризику на об'єктах будівельної галузі. Проведено аналіз обставини та причини нещасних випадків на підприємствах будівельної галузі та виробництва будівельних матеріалів. Визначено параметри на яких повинна ґрунтуватися оцінка ризиків аварій, нещасних випадків і надзвичайних ситуацій на потенційно небезпечних об'єктів, а моделювання відповідних небезпечних подій та ситуацій, їх вплив на здоров'я населення. Проаналізовано процес управління ризиком, як комплекс дій, що є частиною загального управління бізнесом. Визначено особливості системного управління ризиками безпеки праці. Розроблено і наведено стадії проектування, впровадження контролю і корегування системи управління безпекою праці на основі ідентифікації небезпек, яка базується на ризик-орієнтованому підході і відповідає сучасним тенденціям і вимогам нормативної бази України. Сформульовано основні завдання ризик-орієнтованого підходу забезпечення надійності складних технічних систем для безпеки людей і довкілля, розглянуто методи оцінювання ступеня небезпеки промислових об'єктів та наукових засад концепції прийнятного ризику. Визначено оціночний показник, за яким вид економічної діяльності суб'єкта господарювання з питань безпеки праці відноситься до одного з трьох ступенів ризику (високий, середній, незначний), а також розглянуто питання встановлення прийнятного ризику на об'єктах будівельної галузі. Запропоновано методику визначення критеріїв на основі ризик-орієнтованої моделі, за якими оцінюється ступінь ризику виникнення аварії або нещасного випадку для можливості планування наглядової діяльності на промисловому підприємстві. На основі аналізу статистичних даних про травматизм на підприємствах будівельної галузі були визначені види економічної діяльності з високим ступенем ризику

Ключові слова: будівництво, травматизм, ступінь і критерії ризику, ризик-орієнтований підхід

Introduction

Analyzing the circumstances and causes of accidents at the construction site, it was found that the vast majority of them occur due to falls from a height during the construction of buildings with a monolithic-frame method. Mistakes of various kinds can cost lives, deteriorating health, and cause significant material loss. In practice, it is not possible to achieve absolute safety, there is always a certain excess risk.

Risk, according to the Law of Ukraine High-risk objects", is the probability degree of a certain negative event that may occur at a certain time under certain circumstances [1]. This is the possibility of any event that contributes to the emergence of negative results in human activities. In the life safety theory, the risk is understood as the negative action results of any factor or their complexity.

Risk is a term that has universal meaning, it refers to an action that can or should occur with uncertainty.

Risk is a chance at which something unforeseen and undesirable can happen. Risk is the probability of negative action in the area of human presence.

Risk is a quantitative characteristic of the impact of hazards created by human activities, i.e. the number of deaths, morbidity, disability caused by exposure to a particular hazard. Risk is directly related to the concept of damage, i.e. with the probability of death or damage to the object, the less studied the risks, the more damage. In this regard, there is a need for information accumulation and analysis on various adverse events in order to clarify the general trends and patterns of events manifestation.

Construction, in comparison with the coal, chemical, socio-cultural sphere and trade, transport, etc., belongs to one of those industries which are characterized by the probability of a significant number of risks. In addition, an important role is given to financial risks in the construction industry, which arises due to unpredictable changes in legislation or the economy, given the construction process investment and capital intensity duration. These risks may adversely affect the results.

The main measures to reduce construction risk levels include the development of plans. Such plans should include the following tasks: risk management and motivational regulation.

In the construction industry, the level of risk can increase from insignificant to unacceptable. Reducing the risk level depends on the personal qualities of the employee involved in the work process, as well as on measures to reduce it.

Determination of accident risk assessments should be based on the results of monitoring the technical condition of potentially dangerous objects, statistical data on accidents and emergencies of man-made nature, comprehensive monitoring of dangerous geological and hydrometeorological processes, the state of natural complexes, and modeling of relevant dangerous events and situations. their impact on public health.

The application of risk assessment methodology allows the development of mechanisms and strategies of various regulatory measures to improve the safety of industrial facilities; establish limits on the variability of risk values and uncertainties associated with limited initial data or unresolved scientific problems.

Review of the research sources and publications.

The essence of risk management and its place in the activities of enterprises are revealed in the works of N. Vnukova, M. Golovanenko, T. Golovach, L. Donets, O. Dubrova, I. Ivchenko, O. Kuzmin, V. Kravchenko, V. Lukyanova, E. Stanislavchyk, A. Starostina, D. Stefanych, and others.

The analysis of well-known publications [5…9] showed that although today there are some studies in the field of theory and practice of risk assessment, but there are still methodological implementing problems of risk-oriented approach to risk assessment.

Definition of unsolved aspects of the problem

The methodology of analysis and assessment of accident risk at industrial facilities has been actively developing, so the development of new and improvement of existing approaches, models, and methods of accident risk assessment and their computer implementation remain an urgent task for our country.

Problem statement

The main purpose of this article is to improve the analytical methods for determining the criteria for the risk degree in the construction industry.

Basic material and results

An effective risk management process cannot be a set of fragmented actions, as it must be formed into a set of actions that is part of the overall business management. Features of systemic occupational safety risk management are:

– a continuous process that covers the entire organization;

– carried out by employees of all levels of the organization;

– used during the strategy development and formation;

– is used by the whole organization, at each level, and by each unit and includes risk portfolio analysis at the organization level;

– aimed at identifying events that may affect the company and managing risks so that they do not exceed the risk appetite;

– provides management with reasonable guarantees of goals achievement.

In the absence or lack of statistical data on risks in the industrial enterprise, in particular, in the workplace, when solving the problem of occupational safety risk management, the risk manager should:

I. At the planning stage:

1. Identify hazards.
2. Identify possible danger and choose the damage rate.
3. Identify the possible consequences of the danger.
4. Determine the damage probability (frequency).
5. Quantitatively or qualitatively assess (calculate) the risk.

II. At the implementation stage:

1. Have the skills and abilities to meet the requirements of functional responsibilities and authorities, resources, and roles.

2. Conduct training, to determine competencies.

3. Inform about the order of communication, participation, and information.

4. Have the skills and abilities to manage documentation, operations, and determine compliance.

5. Develop the measures to prevent emergencies and respond to them in case of occurrence.

III. At the stage of verification:

1. The presence of internal audit.

2. Records management.

3. Determine the effectiveness.

4. Assess compliance with the law.

5. Investigate incidents, inconsistencies, corrective and preventive actions.

IV. At the stage of adjustment:

1. Analysis by management.

2. Sources of information for hazard identification are:

– normative-legal and technical acts, scientific-technical literature, local normative acts, etc.;

– results of state sanitary and epidemiological supervision;

– the results of production control over compliance with sanitary rules and the implementation of sanitary and anti-epidemic (preventive) measures;

– results of workplaces certification;

– results of sanitary-epidemiological assessment;

– the results of monitoring the technological process, production environment, workplace, the work of contractors, external factors (roads, catering, climatic conditions, etc.);

– results of analysis of questionnaires, forms, etc.;

– results of audit (survey) of colleagues and employees;

– practical experience.

September 15, 2015, a new version of the international standard ISO 14001:2015 "Environmental Management Systems" was officially released.

March 12, 2018, a new version of the international standard ISO 45001:2018 "Occupational Health and Safety Management Systems" was released. The transition period to the new versions is 36 months (3 years) [4, 5]. According to these normative documents, in the specified terms, at each enterprise, the labor safety management system on the basis of danger identification which is based on the risk-oriented approach should be created (corrected).

The risk-oriented approach (ROA) in the field of security is based on the position that any hazards (in the industrial sphere, in everyday life), despite their diversity, have the same nature of origin and the same logic of events. The ROA's main tasks are to create a scientific basis for ensuring the reliability of complex technical systems for human safety and the environment, to develop methods for assessing the danger degree of industrial facilities, and the scientific basis of the acceptable risk concept. Reducing the risk of danger requires certain costs and involves investing in natural, manmade, and social spheres. The dependence of the total (technical plus socio-economic) risk on the society's total costs for security is described by a curve that has a minimum in the case of achieving the optimal ratio between investments in the natural, technical and social spheres. The acceptable risk area is within the total risk minimum dependence of exposure to the society general costs aimed at security. Risk management is the search for a trade-off between the cost of reducing the likelihood of a dangerous event or loss from it and the benefits of using hazardous technologies, materials, products, and so on.

There are three risk determining methods:

– apriori – the use of which allows determining the numerical value of the risk in advance, regardless of experience, for example, in the case when a dangerous event did not occur;

– a posteriori – the use of which allows determining the numerical value of risk according to previous experience, for example, according to statistics;

– aesthetic – the use of which involves expert assessment of processes and phenomena by experts, as well as by conducting opinion polls of certain groups or the general population.

In the a priori risk definition, the dangerous event possibility is calculated as a classical interpretation of probability. The dangerous event probability is defined in this case as the ratio of the number of situations in which this event occurs to the total number of situations in which it can occur (provided that all situations are equally possible and incompatible). The use of the apriori calculation type is limited because situations that can be described mathematically with the necessary accuracy are rare in practice.

In a posteriori risk determination, the probability frequency concept is used. Due to this concept, it is used the real data on the dangerous event occurrence over a fairly long time period and under the same observation conditions. The probability calculation, in this case, is reduced to the relative frequency occurrence calculation of a dangerous random event in the aggregate of all possible random events. These calculations are based on the law of large numbers and, due to the availability and sufficient objectivity of statistical data, have wide practical application.

The application of the risk determination aesthetic method is mostly forced due to the lack of necessary mathematical and statistical information about the events, the probability of which must be assessed. However, it should be borne in mind that expert evaluation involves not only the use of objective materials but also based on the experts' understanding of the real situations patterns. Therefore, despite some limitations of the esthetic method's effective capabilities, it is widely used in practice.

The best results in predicting the risk magnitude give a comprehensive, simultaneous application of all three methods: apriori, a posteriori and aesthetic.

The theoretical and methodological basis of risk research is created by risk theory. Its development takes place in two main directions:

1) the practical application of a special part of applied mathematics - mathematics of stochastic processes;

2) the economy of probabilistic losses and identifying ways to reduce or prevent them.

Quantitative hazard analysis always begins with a preliminary study, the main purpose of which is to identify the hazard source. Danger sources identification, danger development research, and its analysis are obligatory components of a technique called preliminary analysis of dangers (PAD). PAD conducting in practical conditions is simplified and formalized through the use of pre-prepared questionnaires, special questionnaires, tables, pre-analysis matrices, etc.

In order to quantify the accidents probability using methods based on modeling random processes of accidents occurrence and development, and to assess the losses due to the implementation of adverse events often use deterministic methods. This comprehensive application of deterministic and probabilistic methods makes it possible to calculate the accidents risk at industrial facilities.

Among the most common quantitative methods in assessing the risk of software accidents are logical and probabilistic methods, including "event tree", "failure tree", "minimum paths" and "minimum intersections", as well as statistical methods of data processing on the failure of technological systems. Statistical methods are used with minimal assumptions, but require a large amount of statistical information.

The combination of available statistical information and additional information, including the knowledge and experience of experts, allows reducing the requirements for the required volume of statistical data. Thus, in the absence of statistics on accidents over a period of time, such expert methods as the Delphi method, the method of hierarchy analysis, morphological analysis, fuzzy logic methods, etc. are used to assess the negative event probability. In addition, the calculation of accident risk is also performed using the probabilistic method, which is used to estimate the frequency or probability of rare adverse events with severe consequences, statistics on which are virtually absent.

Acceptable risk is the estimated indicator by which the economic activity type of the business entity on occupational safety is one of the three risk levels (high, medium, insignificant) is [2].

Criteria for the risk degree, based on the risk concept, in our opinion, should be determined by assessing the risk degree from economic activity and the value of the maximum allowable level and depending on it to establish a gradation for high, medium, and low risks.

In the countries of Europe (Germany, France, Austria, Ukraine) to assess production use:

1. Injury frequency rate (k_{fr}) (quantitative indicator), ie the ratio of the accidents total number for the relevant period N_0 to the total number of employees p in this period, which is per 1000 employees:

$$K_{fr}=(N_0/p)\times 1000.$$

2. Integrated indicator of production occupational risk (I_{pr}). It is determined by the ratio of the costs for the relevant period for compensation to the persons injured at work ($\sum E_{cc}$) to the actual labor costs ($\sum E_{lc}$) for this period:

$$I_{pr}=\sum E_{cc}/(\sum E_{lc}\times 100)$$

3. Severity traumatism rate (k_t) (qualitative indicator), ie the ratio of the total number of disability days D to the number of accidents N_0:

$$K_t=D/N_0.$$

4. Disability rate (k_d) determines the number of lost working days per 1000 workers:

$$K_d=(D/p)\times 1000.$$

5. The risk of an accident (R) is defined as a quantitative measure of danger, which takes into account the probability of negative consequences (accidents) of economic activity and the possible amount of losses from them. The risk of danger realization is calculated within the probability frequency concept according to the formula of relative frequency occurrence of a dangerous accidental event in the aggregate of all possible accidental events:

$$R = n / N$$

where n is the number of events with undesirable consequences over a period of time; N is the maximum possible number of similar events for the same time interval.

But none of the above indicators take into account the permanent loss of ability to work and death and therefore can not fully characterize the level of injuries. This requires the use of at least one other indicator. This indicator is the ratio of death and injuries (k_{fi}):

$$k_{di} = \frac{N_{di}}{N_0}100\%,$$

where N_{di} – the number of accidents that resulted in death and injury.

It is proposed to calculate the risk assessment in the construction industry for harm to the health of workers during economic activity by multiplying the one accident probability during the year by the probability of losing one worker during the year the corresponding number of working days due to the accident. To do this, use the following indicators:

– the average annual number of accidents (accidents with temporary disability and fatal accidents) for the last three years;

– the average number of employees in the construction and construction materials industry for the last three years;

– the average annual number of lost working days due to disability for work due to accidents at work for the last three years.

This study proposes the following procedure for assessing the level of safety in the construction industry and the building materials industry:

– the frequency of accidents in the relevant case of economic activity is calculated by the formula:

$$L_A = N_{av}/(E_{av}\times 240),$$

where L_A – frequency of accidents per year; N_{av} – the average annual number of accidents in the last three years; E_{av} – the average number of employees for the last three years; 240 – the average number of working days per year, including vacation.

$$N_{av} = (N_{av1}+N_{av2})\times 1000,$$

where N_{av1} – the average annual number of accidents in the last three years, excluding fatal accidents; N_{av2} – the average annual number of fatal accidents in the last three years; 1000 – the coefficient that transforms the number of fatal accidents into the number of accidents with temporary disability. According to the International Labor Organization (ILO), the average ratio of fatal and total accidents at work in Western Europe is 1:1000.

The probability that an accident may occur during a year is calculated by the formula:

$$P_A = 1 - e^{-LAt}$$

where P_A – the probability of an accident during a year; t – interval equal to one year.

The disability rate in the relevant type of economic activity is calculated by the formula:

$$L_D = D_{av}/(E_{av}\times 240),$$

where L_D – disability rate; D_{av} – the average number of working days lost due to accidents at work.

The loss probability by one employee during the year of the working days' corresponding number due to an accident (R_D) is calculated by the following dependence

$$P_S = 1-e^{-LDt}$$

Thus, the occurrence of an accident during the year can be calculated by the formula:

$$R = P_A \times P_D.$$

Acceptable risk, in relation to which the degree of risk will be divided into three indicators – high, medium, insignificant – can be considered the risk of an accident in Ukraine, calculated on the arithmetic mean, taken over the past three years (R_{av}).

According to the International Regulated Scale of Mortality Risks, several benchmarks are distinguished according to the degree of acceptability: the risk is neglected, the risk is acceptable, the risk is extremely acceptable, the risk is excessive.

With neglected risk, the probability of a dangerous event is so small that it does not exceed the natural (background) level.

With an acceptable risk, the probability of a dangerous event is considered acceptable by society (acceptable), based on the achieved levels of life, economic and socio-political development, as well as the state of science and technology.

The numerical value of the minimum risk of fatal hazards corresponds to the average risk on the International orderly scale of mortal hazards ($R_I = a\times 10^{-6}$).

Thus, the following criteria can be used to assess the risk: high risk is a risk that exceeds R_{av}, the medium risk is equal to or less than R_{av}, but more than R_I, insignificant is equal to or less than R_I.

The application of these indicators will make it possible to determine the criteria by which the risk degree of an accident is assessed for the possibility of planning supervisory activities.

If the conditionally acceptable risk is 2×10^{-5}, then the assessment of the risk degree is carried out on the basis of the data shown in table 1.

Table 1 - Risk assessment criteria

Risk level	Risk degree
$>2\times 10^{-5}$	High
$2\times 10^{-5} – 1{,}01\times 10^{-6}$	Average
$\leq 10^{-6}$	Insignificant

Based on the analysis of statistical data on injuries at industrial enterprises, high-risk economic activities were identified. For enterprises in the construction industry, the data are shown in table 2.

Table 2 - Types of economic activity in Ukraine with a high-risk degree (construction industry)

№	Types of economic activity	P_A	P_D	$R\times 10^{-3}$	Risk degree
1.	Erection of metal structures	0,223	0,000934	21	
2.	Other special construction works	0,205	0,00097	19,9	
3.	Construction of main pipelines, communication lines, and power supply	0,251	0,000537	13,5	
4.	Production of precast concrete and reinforced concrete products	0,178	0,000722	12,8	Високий
5.	General construction	0,181	0,000424	7,68	
6.	Installation of heating, ventilation, and air conditioning systems	0,1508	0,00033	4,98	

Conclusions

The authors of the article are convinced that the introduction of an international system of occupational safety risk-oriented management in industrial enterprise activities allows to identify hazards and assess occupational risks. The proposed method of preventing hazards or dangerous situations allows to ensure the stability of development, increase the level of security, through the implementation of all activities in controlled conditions.

The considered indicators provide an opportunity to determine the criteria by which the risk degree of an is assessed in order to be able to plan measures to improve working conditions.

References

1. *Закон України «Про об'єкти підвищеної небезпеки»* [Електронний ресурс]. – Режим доступу: http://zakon3.rada.gov.ua

2. *Закон України «Про основні засади державного нагляду (контролю) у сфері господарської діяльності»* [Електронний ресурс]. – Режим доступу: https://zakon.rada.gov.ua/laws/show/877-16#Text

3. ISO 45001:2018 *«Системи менеджмента охорони здоров'я і безпеки праці – Вимоги і рекомендації до виконання»* [Електронний ресурс]. – Режим доступу: https://pqm-online.com

4. ISO 14001:2015 *«Системи екологічного менеджмента – Вимоги і настанови до виконання»* [Електронний ресурс]. – Режим доступу: https://www.certification.ua

5. Богданова О.В. (2016). Комбінований метод оцінки ризику травматизму для промислового підприємства. *Проблеми охорони праці в Україні*, 31, 52-63

6. Борис О.П. (2018). Ризик-орієнтований підхід у системі орцінювання пожежної безпеки. *Інвестиції: практика та досвід*, 22, 137-140 https://doi:10.32702/2306-6814.2018.22.137

7. Герасименко О.М. (2019). *Ризик-орієнтований підхід до забезпечення економічної безпеки підприємства: концептуальні засади*. Черкаси: Видав. О. Третяков

8. Schwab K. (2016). The Fourth Industrial Revolution: what it means, how to respond. [Electronic resource]. - Access mode: https://www.weforum.org

9. Марущак С.М. (2008). Комплексна оцінка ризику в процесі забезпечення економічної безпеки підприємства. *Науково-методичний журнал Чорноморського нац. університету ім. Петра Могили*, 86(99), 108-114

10. Zhdakaeva M. V. (2021). *Analysis of risk assessment models used to implement the labor safety management system algorithm* https://doi:10.1007/978-3-030-69421-0_108

11. Baiburin D. A. (2018). Evaluation of building collapse risk with damage localization. *IOP Conference Series: Materials Science and Engineering,* 451(1) https://doi:10.1088/1757-899X/451/1/012066

12. Bamforth P. (2003)/ Probabilistic approach for predicting life cycle costs and performance of buildings and civil infrastructure. *Proc. 2nd Int. Symposium on Integrated Lifetime Engineering of Buildings and Infrastructures*, 553-558

13. Raizer V.D. (2010). *Theory Reliability of Structures.* Mjscow: Publishing house ASV

14. Bobryashov V.M., Bushuev N. (2020). On the features of production, design and reliability assessment of enclosing composite structures with effective thermal insulation. *IOP Conference Series: Materials Science and Engineering*, 919(2) https://doi:10.1088/1757-899X/919/2/022007

15. Pshenichkina V.A., Babalich V.S., Sukhina K.N., Dubovsky M.E. (2020). Reliability assessment of reinforced concrete structures during commissioning. *IOP Conference Series: Materials Science and Engineering*, 913(2) https://doi:10.1088/1757-899X/913/2/022013

16. Bobryashov V.M., Bushuev N. (2020). On the features of production, design and reliability assessment of enclosing composite structures with effective thermal insulation. *IOP Conference Series: Materials Science and Engineering*, 919(2) https://doi:10.1088/1757-899X/919/2/022007

1. *Law of Ukraine "On high-risk facilities"* [Electronic resource]. - Access mode: http://zakon3.rada.gov.ua

2. *Law of Ukraine "On the basic principles of state supervision (control) in the sphere of economic activity"* [Electronic resource]. - Access mode: https://zakon.rada.gov.ua/laws/show/877-16#Text

3. ISO 45001: 2018 *"Occupational Health and Safety Management Systems - Requirements and Recommendations for Implementation"* [Electronic resource]. - Access mode: https://pqm-online.com

4. ISO 14001: 2015 *"Environmental management systems - Requirements and guidelines for implementation"* [Electronic resource]. - Access mode:https://www.certification.ua

5. Bogdanova O.V. (2016). Combined method of risk assessment of injuries for industrial enterprises. *Problems of labor protection in Ukraine*, 31, 52-63

6. Boris O.P. (2018). Risk-oriented approach in the system of fire safety assessment. *Investments: practice and experience*, 22, 137-140 https://doi:10.32702/2306-6814.2018.22.137

7. Gerasimenko O.M. (2019). *Risk-oriented approach to ensuring the economic security of the enterprise: conceptual principles*. Cherkasy: Published O. Tretyakov

8. Schwab K. (2016). The Fourth Industrial Revolution: what it means, how to respond. [Electronic resource]. - Access mode: https://www.weforum.org

9. Marushchak S.M. Complex risk assessment in the process of ensuring the economic security of the enterprise. *Scientific method magazine Petro Mohyla Black Sea National University*, 86(99), 108-114

10. Zhdakaeva M. V. (2021). *Analysis of risk assessment models used to implement the labor safety management system algorithm* https://doi:10.1007/978-3-030-69421-0_108

11. Baiburin D. A. (2018). Evaluation of building collapse risk with damage localization. *IOP Conference Series: Materials Science and Engineering,* 451(1) https://doi:10.1088/1757-899X/451/1/012066

12. Bamforth P. (2003)/ Probabilistic approach for predicting life cycle costs and performance of buildings and civil infrastructure. *Proc. 2nd Int. Symposium on Integrated Lifetime Engineering of Buildings and Infrastructures*, 553-558

13. Raizer V.D. (2010). *Theory Reliability of Structures.* Mjscow: Publishing house ASV

14. Bobryashov V.M., Bushuev N. (2020). On the features of production, design and reliability assessment of enclosing composite structures with effective thermal insulation. *IOP Conference Series: Materials Science and Engineering*, 919(2) https://doi:10.1088/1757-899X/919/2/022007

15. Pshenichkina V.A., Babalich V.S., Sukhina K.N., Dubovsky M.E. (2020). Reliability assessment of reinforced concrete structures during commissioning. *IOP Conference Series: Materials Science and Engineering*, 913(2) https://doi:10.1088/1757-899X/913/2/022013

16. Bobryashov V.M., Bushuev N. (2020). On the features of production, design and reliability assessment of enclosing composite structures with effective thermal insulation. *IOP Conference Series: Materials Science and Engineering*, 919(2) https://doi:10.1088/1757-899X/919/2/022007

Збірник наукових праць. Галузеве машинобудування, будівництво
Academic journal. Industrial Machine Building, Civil Engineering
http://journals.nupp.edu.ua/znp
https://doi.org/10.26906/znp.2021.56.2515

UDC 514.18

Topological importance of the segments of the technical system structure

Usenko Valerii[1]*, Vorontsov Oleg[2], Usenko Irina[3], Kodak Olga[4]

[1] National University «Yuri Kondratyuk Poltava Polytechnic» https://orcid.org/0000-0002-4937-6442
[2] National University «Yuri Kondratyuk Poltava Polytechnic» https://orcid.org/0000-0001-7339-9196
[3] National University «Yuri Kondratyuk Poltava Polytechnic» https://orcid.org/0000-0002-6217-4423
[4] National University «Yuri Kondratyuk Poltava Polytechnic» https://orcid.org/0000-0001-6138-6101
*Corresponding author E-mail: valery_usenko@ukr.net

The article discusses the structure of a redundant technical system in the form of a graph. It is indicated that the structure of a technical system is modeled by an undirected graph. The most important and least important elements of this structure from the point of view of topology have been identified and substantiated. The distribution of the number of spanning trees and cyclic subgraphs passing through each element of the structure of the technical system is shown. The relative distribution of linked subgraphs by structure sections is given. This representation, together with the representation of the total number of related subgraphs, conveys the participation of elements in the connectivity of the technical system. The topological significance of the structure sections of the technical system is shown, taking into account the restrictions that this structure is multipolar

Keywords: graph theory, system structure, structural reliability

Топологічна важливість ділянок структури технічної системи

Усенко В.Г.[1]*, Воронцов О.В.[2], Усенко І.С.[3], Кодак О.А.[4]

[1] Національний університет «Полтавська політехніка імені Юрія Кондратюка»
[2] Національний університет «Полтавська політехніка імені Юрія Кондратюка»
[3] Національний університет «Полтавська політехніка імені Юрія Кондратюка»
[4] Національний університет «Полтавська політехніка імені Юрія Кондратюка»
*Адреса для листування E-mail: valery_usenko@ukr.net

Розглянуто структуру резервованої технічної системи як граф, ребрами якого прийнято ділянки структури, а вершинами – вузли структури. Основні завдання дослідження надійності полягають у встановленні і обґрунтуванні вимог по надійності до системи і її складових частин, у виборі принципових напрямів проектного забезпечення надійності на етапах створення системи. Зазначено, що структура технічної системи моделюється неорієнтованим графом. Надійність структури мережі залежить від числа її резервованих та нерезервованих працездатних станів. Зі збільшенням останніх надійність структури збільшується і, відповідно, навпаки. Виявлено, що врахування ймовірності існування всіх працездатних станів дасть більш точну порівняльну оцінку надійності структури технічної системи. Для визначення числа циклічних зв'язних підграфів, що проходять через кожний елемент системи використовується алгоритм пошуку в глибину. Показано обчислення числа циклічних підграфів що проходять через дану ділянку. Визначено та проілюстровано циклічні підграфи структури технічної системи, що моделюють працездатні стани з резервом. Виявлено найважливіші ділянки для заданої системи за топологією, бо вони найбільш вразливі для структури. При виході останніх з ладу рівень працездатності структури буде значно меншим. І навпаки, з вилученням найменш важливих ділянок надійність структури знизиться в меншій мірі завдяки структурній надлишковості, що реалізована іншими ділянками. Приведено відносний розподіл зв'язних підграфів по ділянкам структури. Це представлення разом з поданням загального числа зв'язних підграфів передає участь ділянок у зв'язності структури технічної системи. Зазначено, що чим більшим є відносне число підграфів ділянки, тим важливішою є ділянка для зв'язності структури і навпаки. Показано топологічну важливість ділянок структури технічної системи за обмежень, що дана структура є багатополюсником, тобто кожний вузол має бути зв'язаним з кожним іншим вузлом структури.

Ключові слова: теорія графів, структура системи, структурна надійність

Introduction

To design and maintain complex systems, it is necessary to study the impact of their components on reliability [7-10]. Determination of the system structure components influence helps to solve the problems of optimal redundancy and reliability distribution among the elements [8]. This is necessary for monitoring, analyzing failures, restoring systems, and obtaining a generalized picture of the effect on the structural reliability of the failures process system of elements or their groups (components).

Review of the research sources and publications

In the studies carried out on the reliability of various technical systems [1-5], attention is focused on identifying the basic requirements for their reliability, reliability indicators were given, and methods for determining the number of spanning trees that can be associated with the limiting operational states of the topological structure were given. The number of spanning trees passing through each section of the structure is taken as an indirect indicator for comparing different structures in terms of reliability [2]. The literature provides a calculation of the number of spanning trees in graphs [1] and shows how to determine the number of spanning trees passing through individual sections of the structure [2]. However, for a more accurate assessment of each element's importance in the system structure, one should take into account all possible working conditions structure, including cyclic connected subgraphs of the structure [3].

Definition of unsolved aspects of the problem

To date, an assessment of the topological importance of the elements of the structure of a technical system as a characteristic of the elements' reliability distribution in the system structural reliability has not been derived.

Problem statement

The main tasks of the reliability study are to establish and substantiate the reliability requirements for the system and its components, in the choice of the principal directions and rational strategies for the design reliability assurance, in the elaboration of the reliability assurance issues at the subsequent system creation stages [4, 16, 17].

Basic material and results

The publication [8] reflects the ways of establishing the structural system elements' significance. There are limitations: there is no initial possibility of the parts reliability. A matrix of paths is used to find the significance of a system element as a value of its rank (R_i). Rank is the number of a particular element ties with others

$$R_i = \frac{A_i + A_i^2}{\sum_{i=1}^{m}\left(A_i + A_i^2\right)} \qquad (1)$$

where A_i, A^2_i are the sums of the direct matrix paths rows with ones in the main diagonal and of the same matrix squared, respectively.

After studying the principle of system operation, a graph is drawn up that simulates the dominance of elements and a matrix of dominance. The value of the functional and structural rank of the element is

$$R_i = \frac{B_i + B_i^2}{\sum_{i=1}^{m}\left(B_i + B_i^2\right)} \qquad (2)$$

where B_i, B_i^2 are the sums of the adjacency matrix rows and the same matrix squared.

The disadvantage of this method is that it does not set items with zero ranks. There is also no definition of the degree of mutual elements' influence.

In [13], the concept of the elements' weight in the system reliability was formulated. It does not depend on probability based on the concept of Boolean difference and the use of a logical-probabilistic method for studying the reliability of systems [10]. In [7], the reliability impact magnitude constituent components of the structure on the reliability of the system are described. This value is determined statistically.

Accordingly [11], the transition from the reliability parameters of individual elements to the reliability of their groups is insufficient without studying the importance of the component formed by the two elements. The influence of two elements on the system reliability is shown: temporary (conjunctive), total disjunctive, or separately (strictly disjunctive). The study describes finding the importance of two elements in the system reliability analysis. There is a prospect of generalization for a huge number of the system parts by the induction method.

Scientific sources [11, 14] highlight the property of weight for two elements. The weight of any logical function is determined by a probabilistic function with the condition of equal probability of truth and falsity of all arguments of the algebraic function of logic.

Most of the known methods for determining the magnitude of the impact of individual elements on the reliability of a system use the probability of initiating events. In [12], the structural significance of the element in a system with a monotonic structure in the form of a partial derivative is presented

$$B\left(i \setminus R\right) = \frac{\partial R_c}{\partial R_i} \qquad (3)$$

where $R_c=f(R_1,...,R_m)$ is the system reliability depends on R_i.

If the value of R_i is unknown, the significance of the element x_i is expressed with a value of 0.5 for the reliability of all elements:

$$B\left(i\right) = \left.\frac{\partial R_c}{\partial R_i}\right|_{R_1=...R_m=0,5} \qquad (4)$$

In publications [9, 13], the partial derivative is the significance of the element:

$$\zeta_i = \frac{\partial R_c}{\partial R_i} = P\left\{\Delta_{x_i} y\left(x_m^{'}\right) = 1\right\} \qquad (5)$$

where R_i is element reliability, R_c is system reliability.

Replacement in expression (4) of the variables x_i and x'_m by the value 0.5 for all i=1,...,m gives the dependence of the element's action:

$$g_{x_i} = P\left\{\Delta_{x_i} y\left(x'_m\right)=1\right\}\Big|_{R_1=\ldots R_m=0,5} \quad (6)$$

In expressions (5) and (6), the influence of an element quantitatively coincides with the concept of significance.

But there is a difference: the weight g_{xi} is included in the logical model and the structural significance to the probabilistic one [10]. The reliability is

$$R_1 R_{c1}^{(i)} + Q_i R_{c0}^{(i)} = R_1 R_{c1}^{(i)} + (1-R_i) R_{c0}^{(i)} \quad (7)$$

$$R_{c1}^{(i)} - R_{c0}^{(i)} = \zeta_i \quad (8)$$

where

$$R_{c1}^{(i)} = P(y_{c1}^{(i)}(x_m) = 1)$$

$$R_{c0}^{(i)} = P(y_{c0}^{(i)}(x_m) = 1)$$

Formula (8) is the basis of methods for calculating the significance of systems. Element significance is interpreted as the speed of the system's reliability changing. It detects elements, an increase in the reliability of which by an amount ΔR_i increases the reliability of the system by an amount

$$\Delta R_{\tilde{n}} = \zeta_i \Delta R_i \quad (9)$$

The significance ζ_i of an element depends not only on its place in the structure of the system but also on the reliability R_i of all other elements, except for itself. The probabilistic representation of significance helps to interpret the significance of an item as the system reliability if the item is in working order. The concept of an element's contribution was described in the study [10]. The contribution of an element to the system reliability is equal to:

$$B_{x_i} = R_i \frac{\partial R_c}{\partial R_i} = R_i \zeta_i \quad (10)$$

Formula (6) can be represented as

$$R_c - R_{c0}^{(i)} = R_i (R_{c1}^{(i)} - R_{c0}^{(i)}) = R_i \zeta_i \quad (11)$$

The contribution of the element B_{xi} is the probabilistic part of the reliability of the system R_c, which it receives with the restoration of the operability of the element R_i. Taking into account (9), the value of the contribution is presented as an increase in the reliability of the system by attracting an element to its structure, or by restoring its operability. Damage to an element of the structure of the system is the product of the probability of failure Q_i of the element by its significance

$$C_{x_i} = Q_i \frac{\partial R_c}{\partial R_i} = Q_i \zeta_i \quad (12)$$

The relationship between the contribution and loss of an element coincides with the ratio of its probabilities to reliability and failure [10]:

$$\frac{B_i}{C_i} = \frac{R_i}{Q_i} \quad (13)$$

Consider the structure of the redundant technical system (TS) as a graph A, edges of which we take parts of the structure x_i, i=1,...,n, and the vertices are the nodes of the structure v_j,j=1,...,m. The structure of TS is modeled by an undirected graph, the connections between nodes exist in two directions. The subgraph T_i of this graph, which has no cycles but has edges that connect all vertices of graph A, is a trunk tree. For the structure of the TS, such a tree simulates the operating state, which is the limit because it has no structural redundancy.

When the structure is inoperable, at least one node of the structure has no connection with other nodes and this corresponds to the removal of one or more edges of graph A that connect this vertex with others.

The reliability of the network structure depends on the number of its unreserved operational states. The number of remaining trees in graph A determines the number of these states [3]. As the number of trunks increases, the reliability of the structure increases, and, accordingly, as the number of trunks decreases, the reliability of the structure decreases, $P_i > P_j$, if $T_i > T_j$.

The number of carcass trees of a given graph is calculated from a symmetric binary matrix of adjacency of vertices, in which the elements of the main diagonal are numerical values of the degrees of the corresponding vertices [1]. Ever, in the structure of the TS, not only non-reserved but also redundant operational states are possible, which are modeled by connected cyclic subgraphs B_i of graph A of the structure of the TS. The sum probability of any related events number is reflected by the known formula [3]:

$$P\left(\sum_{i=1}^{n}(B_i)\right) = \sum_{i=1}^{n} P(B_i) - \sum_{i,j} P(B_i B_j) + \sum_{i,j,k} P(B_i B \ldots + (-1)^{n-1} P(B_1 B_2 .. \quad (14)$$

where B_i is a random event of the existence of a structure working state, which is modeled by the subgraph Q_i of graph A, n is the possible number of states, i = 1,…,n. The number of all possible subgraphs of graph A is 2^x, where x is the number of edges of graph A. If we take into account that always one of them is trivial, then the number of all possible subgraphs having edges

$$H_x = \sum_{j=1}^{x} \binom{x}{j} = 2^x - 1 \quad (15)$$

For the structure shown in Fig. 1 such subgraphs are $H_8 = 2^8 - 1 = 255$.

It is obvious that taking into account the probability of the existence of all working conditions will give a more accurate comparative assessment of the TS structure reliability. If the number of cyclic subgraphs in the TS structure increases with the change of its internal connections, the TS reliability will increase, ie $P_i > P_j$, if $B_i > B_j$ and $Q_i > Q_j$.

Thus, the working states of the TS structure correspond to the cover trees and cyclic subgraphs of the structure graph. All vertices of graph A are connected by edges, and when one edge that is part of a loop is removed, the subgraph remains connected. When one edge is removed outside the cycle, the connection with one or more vertices of the graph is lost (the graph splits into two parts, which are components of connectivity) and this corresponds to the inoperable state of the TS structure.

It is possible to determine the number of cyclic connected subgraphs Q_i passing through each element of the system using the depth search algorithm [6]. The algorithm is based on a systematic search of the graph vertices in such an order that each edge x_i and each vertex of the graph v_i is considered only once.

The transition from the vertex v_j to v_{j+1} is the edge x_i that connects them. Using the depth search algorithm, you can view all possible subgraphs of the structure graph. The connected cyclic subgraph Q_i of graph A should contain a tree [1]. Therefore, the selection of a connected subgraph is performed by checking for the presence of a T_i tree.

The number of cyclic subgraphs Q_i passing through this section x_i is calculated by the formula

$$Q_i = S_n - S'_{n-1} \qquad (16)$$

where S_n is the total number of connected subgraphs in the graph of structure A with a given section x_i; S'_{n-1} is the number of connected subgraphs without plot x_i.

Take the structure of the technical system (Fig. 1). T_8=32 different carcass trees pass through the whole structure; it has 32 different limit working states (Fig. 2) and Q_8=34 cyclic subgraphs (Fig. 3). If you remove segment x_1 from the structure (denote the segment x_1 through its ends, which are nodes 1-4). Graph A becomes subgraph A'. The number of remaining trees will be $T'_8 = det\ A'$= 24. Using the depth search algorithm, determine the number of cyclic subgraphs Q'_8=26. The number T and the number Q decreased by the number of subgraphs passing through section x_1, respectively.

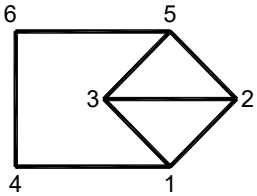

Figure 1 −The structure of the technical system

$T_{1\text{-}4}=T_i-T_j$=24 different carcass trees and $Q_{1\text{-}4}=Q_i-Q_j$=28 different cyclic subgraphs of the structure pass through sections $x_{1\text{-}4}$, $x_{4\text{-}6}$, $x_{5\text{-}6}$. These segments are the most important for this structure in terms of topology because they are the most vulnerable to the structure. The least important for this structure is the area $x_{2\text{-}3}$ because the smallest number of trees $T_{2\text{-}3}$ = 16 and $Q_{2\text{-}3}$ = 26 cyclic subgraphs pass through it. In the event of its failure (removal), the network structure will be more workable than in the removal of the above areas because it has a structural surplus, which is implemented in other segments.

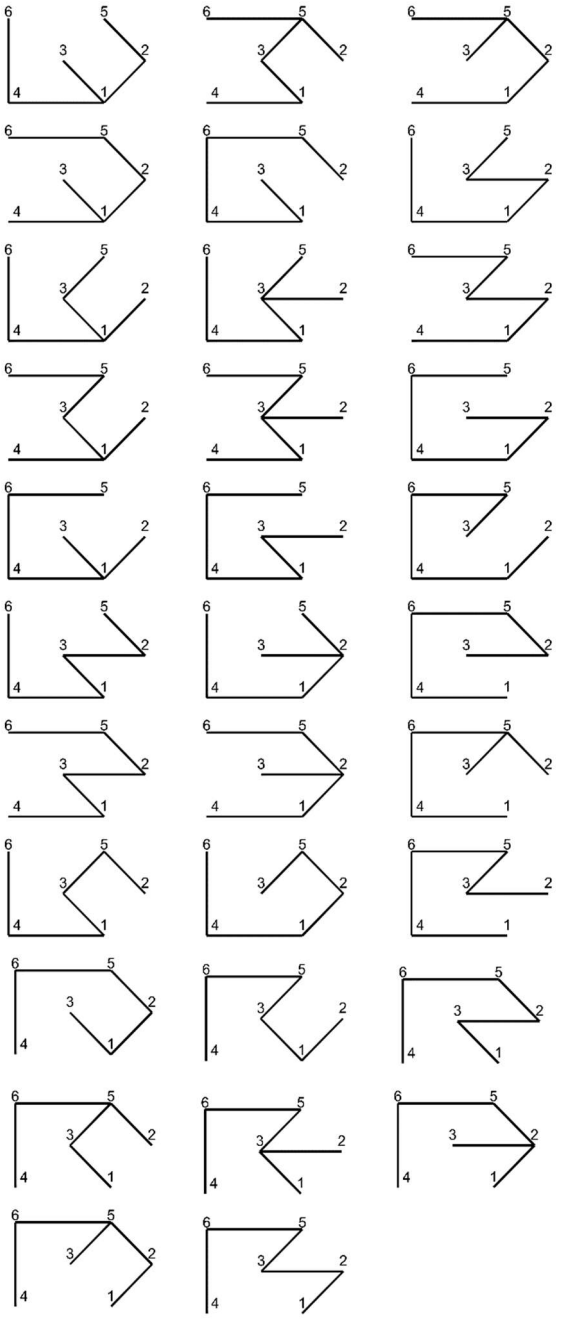

Figure 2 − All 32 carcass trees illustrate the ultimate operating state of a structure without reserve

In Fig. 4 shows the distribution of the trunk tree number passing through each section x_i of the TS structure. In fig. 5 – distribution of the number of cyclic subgraphs Q_i by structure sections. If the number of spanning trees for sections $x_{4\text{-}6}$ and $x_{2\text{-}3}$ is equal to $T_{4\text{-}6}$=24 and $T_{2\text{-}3}$=16, then taking into account the distribution of the numbers of cyclic subgraphs (Fig. 5), these values will change slightly: respectively, for section $x_{4\text{-}6}$ we have $Q_{4\text{-}6}$ = 52, and for section $x_{2\text{-}3}$ we obtain $Q_{3\text{-}5}$ = 42 (Fig. 6).

To study the distribution of reliability between elements of the system structure, we use the number of all connected subgraphs (carcass trees and cyclic subgraphs):

$$F_i = T_i + Q_i \quad (17)$$

where F_i is the number of all connected subgraphs, T_i is the number of truncated trees, Q_i is the number of connected cyclic subgraphs.

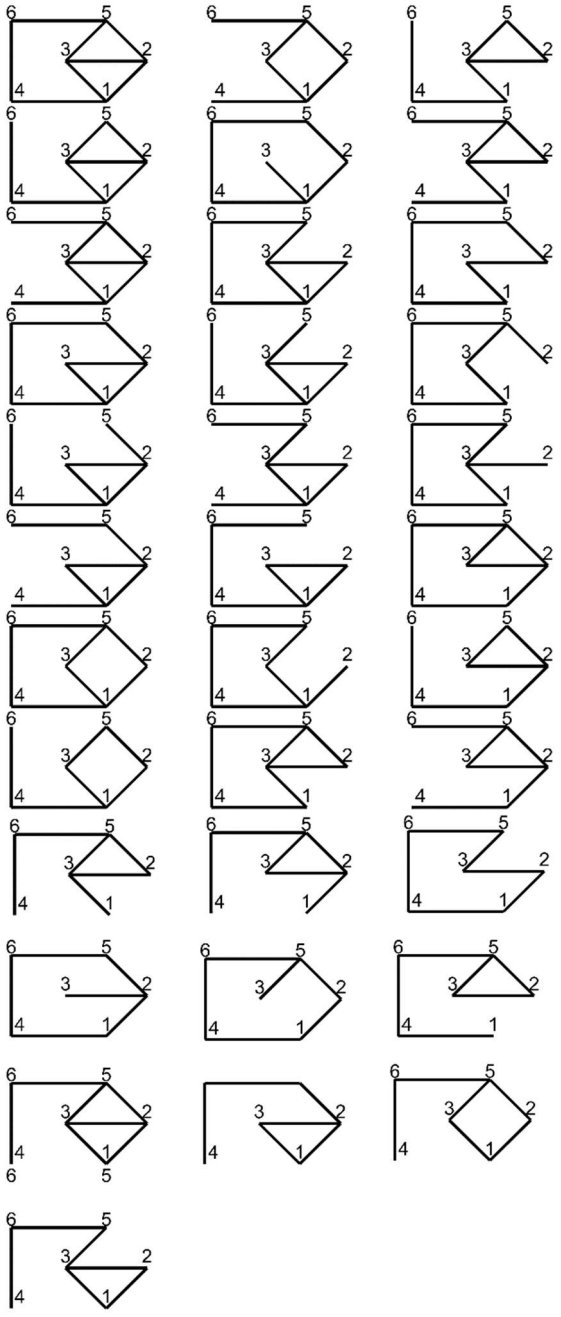

Figure 3 − All 34 cyclic subgraphs of the structure of the TS, simulating working conditions with a reserve

We will accept the distribution of connected subgraphs numbers on the TS structure sites is

$$C_i = \frac{F_i}{F} \quad (18)$$

where F_i – the number of connected subgraphs passing through the section x_i; F - the number of connected subgraphs passing through the whole structure modeled by graph A.

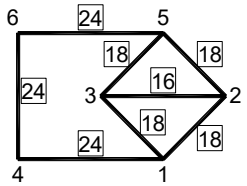

Figure 4 − Distribution of the number of carcass trees passing through sections of the structure

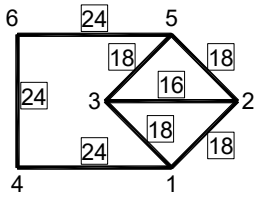

Figure 5 − Distribution of the number of cyclic subgraphs passing through sections of the structure

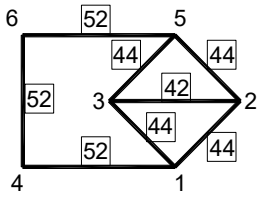

Figure 6 − Distribution of the numbers of all connected subgraphs by sections of the structure

In fig. 7 shows the relative distribution of connected subgraphs by sections of the structure.

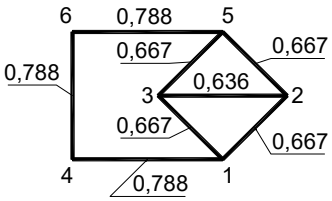

Figure 7 − Topological importance of TS structure

This representation, together with the representation of the total number of connected subgraphs, for example, for a given structure $F = 32 + 34 = 66$, indirectly conveys the sites' participation in the connectedness of the TS structure. It should be noted that the relative number of subgraphs C_i in segment x_i is a greater subgraph for the coherence of the structure and vice versa. $C_i > C_{i+1}$, where C_i is the topological importance of the site, C_{i+1} is the topological importance of the site x_{i+1}. In fig. 7 shows the topological importance of parts of the TS structure for the limited fact that this structure is multipolar, each university must be connected to each other node structure.

Conclusion

The participation of the structure segments in the distribution of the technical system reliability by elements can be estimated by the number of subgraphs: carcass trees and connected cyclic subgraphs of the technical system structure graph.

Assessment of the topological significance of a technical system structural element is a characteristic of the distribution of the elements' reliability in structural reliability of the system. Coverage trees and cyclic subgraphs of the structure graph correspond to the operating state of a technical system.

When less important segments fail, the network structure will be more efficient than removing critical segments, since it has structural redundancy implemented in other segments and vice versa.

More subgraphs of a segment than other segments indicate a higher level of structure importance and vice versa. The topological importance of the system structure elements is limited by the fact that this structure has many poles: input and output nodes. In this case, each node of the structure must be connected to each other.

References

1. Свами М., Тхуласираман К. (1984). *Графы, сети и алгоритмы*. Москва: Мир
2. Новохатний В.Г., Яворский Э.Б., Запорожец С.С. (1981). О топологических характеристиках анализа надежности трубопроводных сетей. *Деп. ВНИИИС,* 2302. Москва: ВНИИИС
3. Reinschke K., Ushakov I. (1987). *Application of Graph Theory for Reliability Analysis*. Berlin: Verlag Technik
4. Бобров В.И. (2004). *Надежность технических систем*. Москва: МГУП
5. Надежность и эффективность в технике: Справочник (1990). Под ред. В.И. Патрушева, А.И. Рембезы. Москва: Машиностроение
6. Кристофидес Н. (1978). *Теория графов. Алгоритмический подход*. Москва: Мир
7. Кузнецов Н. Ю. (1989). Об оценке влияния надежности различных элементов на надежность системы в целом. *Кибернетика*, 5, 110-119
8. Нечипоренко В.И. (1968). *Структурный анализ и методы построения надежных систем*. Москва: Сов. радио
9. Рябинин И.А. (2000). *Надежность и безопасность структурно-сложных систем*. С.-Петербург: Политехника
10. Рябинин И.А., Черкесов Г.Н. (1981). *Логико-вероятностные методы исследования надежности структурно-сложных систем.* Москва: Радио и связь
11. Рябинин И.А., Парфенов Ю.М. (1991). Определение характеристик важности совокупности элементов энергетической системы при исследовании ее безопасности. *Энергетика и транспорт,* 1, 44-57
12. Birnbraum Z.W. (1969). On the importance of different components in a multi-component system. Multivariate Analyses. *Academic Press*, 2, 581-592
13. Ryabinin I. A. (1976). *Reliability of Engineering Systems. Principles and Analysis*. Moscow: Mir
14. Ryabinin I. A. (1994). A Suggestion of a New Measure of System Components Importance by Means of a Boolean Difference. *Microelectronics and Reability*, 34(4), 603-613
15. Usenko V., Kodak O., Usenko I. (2020). Geometric reliability model of the five site redundant structure. *Engineering Review*, 40, 2, 10-15
http://doi.org/10.30765/er.40.2.02
16. Jin-Zhang Jia, Zhuang Li, Peng Jia, Zhi-guo Yang (2020). Reliability Analysis of Common Cause Failure Multistate System Based on CUGF. *Mathematical Problems in Engineering*, 2020, 1-14
https://doi.org/10.1155/2020/4608124
17. Cheng-Fu Huang, Ding-Hsiang Huang, Yi-Kuei Lin (2020). Network Reliability Evaluation for a Distributed Network with Edge Computing. *Computers & Industrial Engineering,* 147, 10649
https://doi.org/10.1016/j.cie.2020.106492

1. Swami M., Thulasiraman K. (1984). *Graphs, networks and algorithms.* Moscow: Mir
2. Novokhatny V.G., Yavorsky E.B., Zaporozhets S.S. (1981). On the topological characteristics of the analysis of the reliability of pipeline networks. *Dep. VNIIIS,* 2302. Moscow: VNIIIS
3. Reinschke K.,Ushakov I. (1987).*Application of Graph Theory for Reliability Analysis*. Berlin: Verlag Technik
4. Bobrov V.I. (2004). *Reliability of technical systems*. Moscow: MGUP
5. *Reliability and efficiency in technology: Handbook* (1990). Ed. V.I. Patrushev, A.I. Rembeza. (1990). Moscow: Mechanical Engineering
6. Christofides N. (1978). *Graph Theory*. *Algorithmic approach*. Moscow: Mir
7 Kuznetsov N. Yu. (1989). On the assessment of the reliability influence of various elements on the reliability system as a whole. *Cybernetics*, 5, 110-119
8. Nechiporenko V.I. (1968). *Structural analysis and methods for constructing reliable systems*. Moscow: Sov. radio
9. Ryabinin I.A. (2000). *Reliability and safety of structurally complex systems*. St. Petersburg: Polytechnic
10. Ryabinin I.A., Cherkesov G.N. (1981). *Logical-probabilistic methods for studying the structurally reliability of complex systems*. Moscow: Radio and communication
11. Ryabinin I.A., Parfenov Yu.M. (1991). Determination of the characteristics of the importance of a set of elements of the energy system in the study of its safety. *Energy and transport*, 1, 44-57
12. Birnbraum Z.W. (1969). On the importance of different components in a multi-component system. Multivariate Analyses. *Academic Press*, 2, 581-592
13. Ryabinin I. A. (1976). *Reliability of Engineering Systems. Principles and Analysis*. Moscow: Mir
14. Ryabinin I. A. (1994). A Suggestion of a New Measure of System Components Importance by Means of a Boolean Difference. *Microelectronics and Reability*, 34(4), 603-613
15. Usenko V., Kodak O., Usenko I. (2020). Geometric reliability model of the five site redundant structure. *Engineering Review*, 40, 2, 10-15
http://doi.org/10.30765/er.40.2.02
16. Jin-Zhang Jia, Zhuang Li, Peng Jia, Zhi-guo Yang (2020). Reliability Analysis of Common Cause Failure Multistate System Based on CUGF. *Mathematical Problems in Engineering*, 2020, 1-14
https://doi.org/10.1155/2020/4608124
17. Cheng-Fu Huang, Ding-Hsiang Huang, Yi-Kuei Lin (2020). Network Reliability Evaluation for a Distributed Network with Edge Computing. *Computers & Industrial Engineering,* 147, 10649
https://doi.org/10.1016/j.cie.2020.106492

Збірник наукових праць. Галузеве машинобудування, будівництво
Academic journal. Industrial Machine Building, Civil Engineering
http://journals.nupp.edu.ua/znp
https://doi.org/10.26906/znp.2021.56.2516

UDC 621.923.01

Substantiation of the temperature regime of the differential pump of electromagnetic action

Korobko Bogdan[1], Pavlikov Andriy[2], Kivshyk Anton[3]*

[1] National University «Yuri Kondratyuk Poltava Polytechnic» https://orcid.org/0000-0002-9086-3904
[2] National University «Yuri Kondratyuk Poltava Polytechnic» https://orcid.org/0000-0002-5654-5849
[3] National University «Yuri Kondratyuk Poltava Polytechnic» https://orcid.org/0000-0003-3135-6811
*Corresponding author E-mail: anton.kivshik3@ukr.net

The article discusses the temperature of the working body caused by Foucault currents circulating inside of the working body of a differential pump of electromagnetic action. The article begins with a theory describing the nature of the Foucault current and the causes of the plunger heating. Then there is a characteristic of the differential pump of electromagnetic action. The following is a description of the structures of the working bodies of the differential pump of electromagnetic action. The estimated data of the working body are entered in the table. These tables are taken into account when plotting. The theory substantiates the conditions of heating of the working body, the existence of eddy currents, and also the influence of the temperature of the actuator on the operation of the differential pump. The description shows what role the plunger plays in the operation of the differential pump. The article described in detail the interaction of the working body and the solenoid of the differential pump.

Keywords: differential pump, finishing mixture, plunger, Foucault current

Обґрунтування температурного режиму роботи диференціального насоса електромагнітної дії

Коробко Б.О.[1], Павліков А.М.[2], Ківшик А.В.[3]*

[1] Національний університет «Полтавська політехніка імені Юрія Кондратюка»
[2] Національний університет «Полтавська політехніка імені Юрія Кондратюка»
[3] Національний університет «Полтавська політехніка імені Юрія Кондратюка»
*Адреса для листування E-mail: anton.kivshik3@ukr.net

У статті досліджується зміна температури робочого органа диференційного насоса електромагнітної дії, що спичинюється струмами Фуко в середині цього робочого органа. Розглянуто теоретичні основи виникнення вихрового струму та причини нагріву плунжера. Наведено опис конструктивних особливостей та розрахункові характеристики різних типів робочих органів диференційного насоса електромагнітної дії. Теоретично обґрунтовано умови нагріву робочого органа диференційного насоса та існування шкідливих струмів, а також вплив температури плунжера на роботу диференційного насоса. Досліджено вплив плунжера на технічні характеристики диференційного насоса. Описано взаємодію робочого органу та котушки диференційного насоса електромагнітної дії, а також вплив геометричних особливостей на величину температури нагріву плунжера та пагубних струмів. Від вибору матеріалу з якого можна виготовить робочий орган залежить температури нагріву плунжера і величина несприятливого струму. Проведено детальний опис всіх процесів котрі відбуваються в робочому органі. Представлені та детально описані характеристики робочих органів які виготовлені з різного матеріалу та методом порошкової металургії. Це загалом дає можливість аналізувати конструкцію плунжера диференційного насоса електромагнітної дії. За рахунок ретельного вибору матеріалу а також конструкційної особливості робочого органа диференційного насоса вдалося отримати суттєву економію електроенергії, що було детально розкрито в таблиці та показано на графіках температурно опірної характеристики (ТОХ).

Ключові слова: диференціальний насос, оздоблювальна суміш, плунжер, струм Фуко.

Introduction

Today in Ukraine there are about 800 models of pumps, which differ in their principle of operation, performance, power, discharge pressure, and the structure of the working bodies. However, the problem of increasing their economic efficiency while ensuring high reliability remains particularly acute. One of the ways to solve this problem is to reduce the material consumption of the product and reduce electricity consumption during operation [1, 7]. In turn, this requires the introduction of new science-based pump designs or design changes to existing models.

Review of the research sources and publications

Initial data on the differential pump are obtained as a result of standard acceptance tests of the design in the laboratory. The main purpose of this data is to improve the performance of the differential pump. In addition, the results of statistical tests of the pump affect the design standards. This process was especially intensified with the invention of other pump designs [7]. Numerous publications since the 1950s [1 – 12] are devoted to the statistical description of the mechanical characteristics of the design of a differential pump, in particular its performance. This is especially true of the reliable statistical parameters of the pump performance required to increase the transport of the finishing material. This is emphasised, in particular, in the publications prepared by the scientific school "Creation of theoretical foundations for calculation, design, and implementation of effective means of complex mechanisation of finishing works in construction" of the National University “Yuri Kondratyuk Poltava Polytechnic” [1].

Definition of unsolved aspects of the problem

Currently, the problem of creating pumps for which a minimum amount of construction materials are used is quite acute. Manufactured pumps consume a minimum amount of electricity while having maximum performance. The operation of such pumps is short. Now the urgent task is to create a differential pump of electromagnetic action, which is able to work rationally. The differential pump of electromagnetic action is able to provide an increased level of efficiency during operation to 52% with long service life.

With a large number of differential pumps of electromagnetic action, their design diversity is very large. The manufacture of a differential pump of electromagnetic action, which consumes a small amount of electricity, is an urgent problem for the development of the pumping industry.

Problem statement

The aim of the article is to highlight the results of research of the plunger differential pump of electromagnetic action intended for pumping construction finishing mixtures. Analysis of literature sources on this topic and experimental studies show that in the working body of such a pump there is a loss of energy to heat the plunger and solenoid winding, which leads to reduced efficiency. The cause of heating is the Foucault current, which begins to circulate in the working body when moving the plunger. It is proposed to minimize the negative impact of Foucault current by breaking the closed-loop of the magnetic circuit, namely by using a separate plunger or a plunger made by powder metallurgy.

In order to create a cost-effective model of the differential pump of electromagnetic action and its further implementation in production, the following tasks are solved:

- the factors leading to energy losses in the working body of the differential pump of electromagnetic action are revealed;
- by selecting the material of the plunger and due to its separate structure, the formation of Foucault currents in the working body is minimised and, accordingly, energy losses for heating are reduced, which increases the efficiency of the pump;
- in order to reduce the heating temperature of the plunger, a large working body was created to reduce the temperature caused by Foucault currents;
- in order to determine the mode of operation of the differential pump at which the pump will consume a minimum of electricity at maximum capacity, a graph of the temperature-resistance characteristic is created.

Basic material and results

The research is carried out on a plunger differential pump of electromagnetic action, the structure of which is shown in Figure 1.

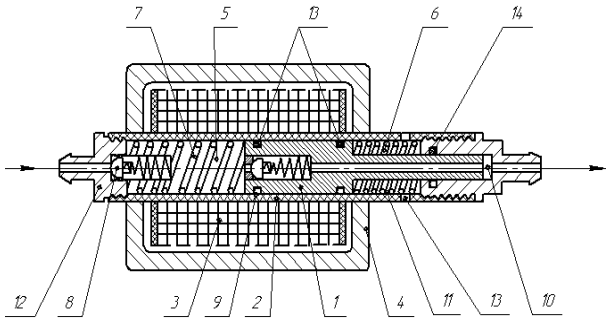

Figure 1 – Differential pump of electromagnetic action:
1 – plunger; 2 – housing; 3 – electromagnet winding;
4 – a magnetic circuit of the winding;
5 – suction cavity; 6 – compensating spring;
7 – working spring; 8 – suction valve;
9 – discharge valve; 10 – compensation chamber;
11,12 – injection and suction fittings;
13, 14 – cuff seals

The pump of the proposed structure works as follows. When a current is applied to the solenoid winding 3, an electromagnetic field is generated, which causes the plunger 1 to move towards the suction valve 8 by compressing the working spring 7. The finishing mixture, which is present in the suction cavity 5, is also compressed. It causes the discharge valve 9 to open and is fed through the hole in the plunger to the discharge fitting 12. After stopping the supply of current under the

action of the working spring 7, the plunger 1 returns to the opposite position creating a vacuum in the suction cavity 5. Under the influence of the vacuum suction valve 8 opens and the finishing mixture fills the cavity 5. Next, the winding 3 is again supplied with current and the cycle is repeated.

The electromagnetic differential pump has no auxiliary mechanical gears, so its efficiency is higher than other pump models. However, there is a disadvantage associated with the loss of energy in the drive.

The operating cycle of the pump consists of two stages, each of which is accompanied by the movement of the plunger. Because the plunger has a certain resistance, when it moves in a magnetic field there are Foucault currents, which are harmful because they lead to loss of energy to heat the plunger. In this case, the operation of the pump becomes economically unprofitable.

Given that the maximum value of Foucault current reaches in a closed circuit, it is advisable to use a separate plunger or plunger made by powder metallurgy, which allows breaking the circuit and reducing the negative impact of Foucault currents [1, 8].

Thus, the process of pumping the mixture by the pump consists of two cycles; each cycle depends on the process of Foucault's current initiation in the plunger and is associated with the magnetic flux flowing in the magnetic circuit.

Under the action of alternating current in the coil, there is the generation of magnetic flux in the magnetic circuit. The magnetic field density is 57.4 T. The density of the magnetic field generates voltage. As the magnetic flux density increases, the voltage increases. Foucault's current is formed as a result of the interaction of voltage and resistance. Increasing the frequency of the network produces an increase in Foucault's current. The plunger is heated as follows. The magnetic flux interacts with the plunger to form an EMF. EMF and resistivity create Foucault's current. The plunger heats up.

The differential pump [1, 8] has a coil that passes current and a working body that pumps the finishing mixture. The plunger and the coil are connected by a metal magnetic core. When current is applied through the magnetic circuit, the magnetic flux in the plunger will be voltage. The maximum Foucault current is generated in the working bodies of the closed circuit. The coil heats up. The eddy current will reduce the magnetic flux density. The decrease in magnetic field density is directly proportional to the electromotive force. This disturbs the balance between the voltage of the coil supplied from the socket and the EMF of the self-induction of the coil. The coil current will increase. As the current in the coil increases, the magnetic field density increases when the plungers of the open circuit equilibrium are restored. Heating the plunger reduces the coil current. Therefore, the occurrence of Foucault current in closed-loop plungers causes an increase in current in the working coil of the pump, heating the plunger. This makes the use of a differential pump economically impractical.

Thus, the process of Foucault currents in the plunger is associated with the magnetic flux flowing in the magnetic circuit and depends on the heating temperature of the plunger.

A voltage is applied to the coil of a differential pump from the mains, which together with the coil resistance depends on the following parameters: resistivity of the wire from which the coil is wound, length of the coil wire, and cross-sectional area of the wire. The electric current generates a magnetic inductance that depends on the dielectric constant of the vacuum, the current circulating in the coil, the number of turns of the coil, and the length of the solenoid core. Magnetic inductance produces a magnetic flux in the magnetic circuit that depends on the magnetic induction, the cross-sectional area of the coil, and the angle between the magnetic induction vector and the perpendicular to the cross-sectional area of the coil core. The magnetic flux produces an electromotive force in the working body of the differential pump, which in turn depends on the speed of the plunger, the magnetic induction of the coil, the circular length of the working body, and the position of the differential pump. The electromotive force together with the resistance of the working body consisting of the resistivity of the material, the circular length of the working body, the area of the longitudinal section of the plunger forms a Foucault current.

The Foucault current depends on the frequency (control value) and the frequency is inversely proportional to the length of the plunger, its mass, and the resistance of the working body. Due to the Foucault current, the working body is heated and the magnetic inductance is formed in the direction opposite to the magnetic inductance of the coil, which depends on the magnetic permeability of the material, Foucault current circulating in the working body, and radius of the working body. The temperature of the plunger is related to the Foucault current and the reactance of the differential pump coil. The reactance of the coil depends on the frequency of the current and magnetic induction. Magnetic induction depends on the following parameters: the number of turns of the coil, the cross-sectional area of the coil core, the length of the wire from which the coil is wound, the magnetic permeability of the vacuum, the magnetic permeability of the plunger, and the time required for maximum plunger heating. The magnetic inductance of the working body creates a magnetic flux also inversely proportional to the magnetic flux generated by the solenoid. Therefore, the coil of the differential pump takes more electricity than working with a cut plunger. The retraction force of the plunger depends on the number of turns of the coil, the length of the wire from which the coil is wound, and the Foucault current circulating in the plunger of the differential pump. The performance of the differential pump is the product of the suction force on the cross-sectional area of the plunger.

The differential pump has an air gap between the working body and the coil and does not have various auxiliary mechanical parts and therefore the efficiency of the differential pump of electromagnetic action is higher than in other models of pumps.

Since the translational movement of the plunger of the differential pump does not depend on the direction of the current transmitted to it, each differential pump can be driven by alternating current. However, in this case, its power is significantly reduced. The reason for this is that alternating current, passing through the coil, creates in the magnetic circuit so-called Foucault currents, the formation of which is a significant part of the electrical energy transmitted to the pump. In addition, in DC pumps, the excitation energy of the coil is consumed only once at the beginning of the action, after which the magnetization of the magnetic conductors remains unchanged. In a differential AC pump, the magnetic conductors are re-magnetized with each change in the direction of the current, which consumes some energy.

Heating of the working body causes power losses during operation. These include losses due to current heating of the coil of the differential pump, heating of the magnetic circuit from hysteresis and eddy currents, and to some extent due to heating from friction with air.

Seven working bodies of the differential pump are considered in the work. Each plunger, depending on the magnitude of the Foucault currents, has its own heating temperature. Each plunger was made of different materials or has a different structure (Figs. 2 – 15).

In Fig. 16 is shown a working body with dimensions. For further calculations, the plunger is imaginarily divided into two cylinders. The volumes and areas of the longitudinal sections are added.

Figure 2 – Plunger with a diameter of 23 mm

Figure 3 – Working body with a diameter of 30 mm

Figure 4 – Working body with a diameter of 23 mm

Figure 5 – Plunger with an important diameter of 30 mm

Figure 6 – Plunger with a diameter of 30 mm

Figure 7 – Plunger with a thickness of 23 mm

Figure 8 – Plunger with a thickness of 30 mm

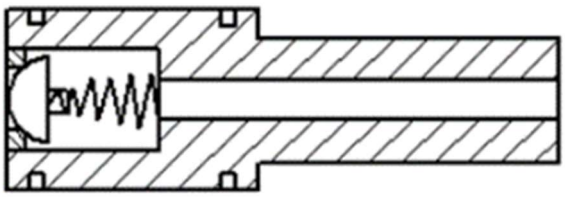

Figure 9 – Working body made of steel

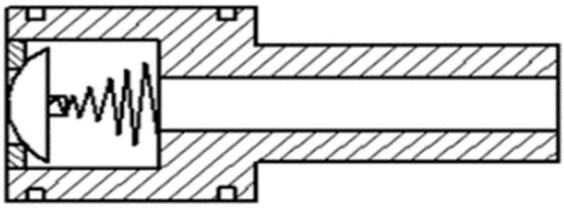

Figure 10 – Working body made of cast iron

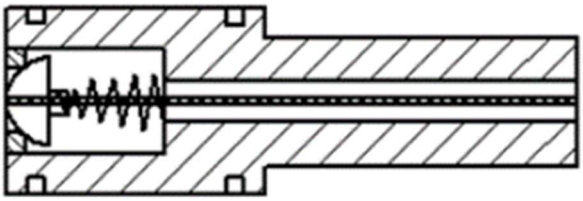

Figure 11 – Working body made of steel (separate)

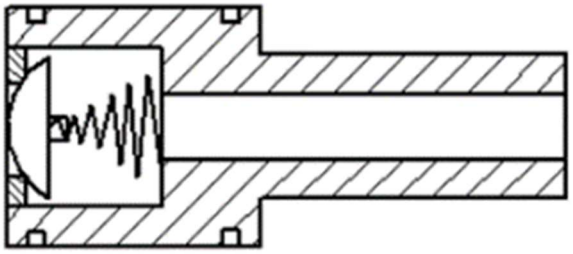

Figure 12 – Plunger made of steel

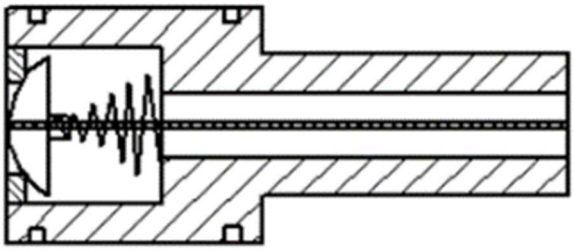

Figure 13 – Plunger made of steel (split)

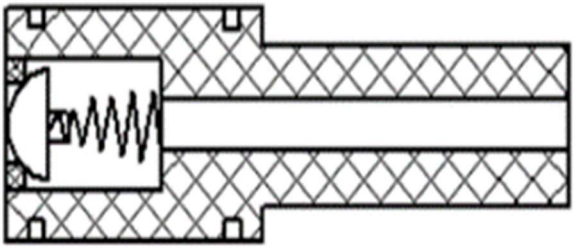

Figure 14 – Plunger made of ground iron

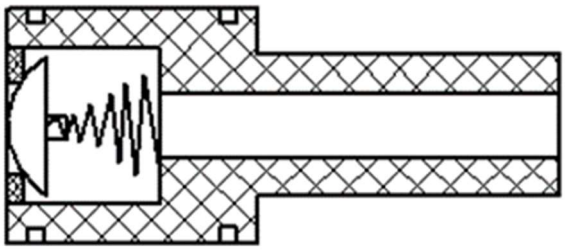

Figure 15 – Plunger made by powder metallurgy method

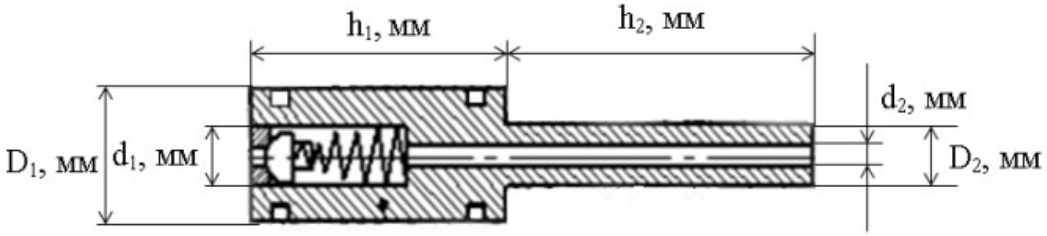

Figure 16 – Sketch of the working body of the differential pump

In the mathematical description of the process of heating the plunger, it is considered as two hollow cylinders with a resistivity of a certain value. Consider the case where the plunger is in a uniform magnetic field. The resistance of the plunger at known dimensions of the working body is determined [6] as

$$R_{work} = \rho \cdot \frac{l}{S_1} \ , \qquad (1)$$

where ρ is the resistivity;
l is the length of the solenoid, m;
S_1 is the area of the longitudinal section of the plunger, mm^2.

Since the frequency of the alternating current in the network from which the pump is fed has known (50 Hz), the amount of current circulating in the working body has found [9] by Foucault's law

$$I = \frac{W}{R} \ , \qquad (2)$$

where W is a current frequency, Hz;
R is the resistance of the working body, Ohm.

If the plunger has a solid structure, then Foucault's currents circulate in it. The heating temperature of the plunger is found [6] according to the Joule-Lenz law using the reactance of the solenoid winding

$$T = I^2 \cdot X_L \cdot t \ , \qquad (3)$$

where I is Foucault current, A;
X_L is the reactance of the winding, Ohm;
t is the time required for maximum heating of the plunger, s.

Taking into account that part of the thermal energy is transferred from the working body to the pumped medium, according to the Joule-Thompson formula [4] the degree of cooling of the plunger is determined

$$t = m \cdot c \ (t_i - t_f) \ , \qquad (4)$$

where m is the weight of the plunger, kg;
c is the specific heat of the working body, kJ/(kg·K);
t_i is an initial temperature of the working body, ^{0}C;
t_f is the final temperature of the working body, ^{0}C.

Thus, the values of voltage U, current I, and operating time t form the work of the electric current, and Q_0, Q_m form the efficiency of mechanical action which on the basis of experimental studies forms the efficiency of the differential pump of electromagnetic action [5]

$$\eta = \frac{A_u}{A_i} + \frac{N_T}{N} \cdot 100\% \ , \qquad (5)$$

where: A_u – useful work, J;
A_t – total work, J.

The electromotive force that moves the plunger may be determined from experimental data on the heating temperature of the working body, the time of its operation, and the reactance of the solenoid winding

$$u = \sqrt{\frac{T \cdot X_L}{t}} \ , \qquad (6)$$

where T – heating temperature of the working body, ^{0}C;
X_L – reactance of the winding, Ohm;
t is the operating time of the pumps.

The value of the Foucault current is obtained on the basis of data on the heating temperature of the working body, the operating time of the pump, and the reactance of the winding

$$I = \sqrt{\frac{T}{X_L \cdot t}} \ , \qquad (7)$$

The research is conducted for plungers of solid and separate structures made of different materials. Steel, cast iron, and iron powder are chosen as the plunger material (Figs. 2 – 8).

The conducted calculations and studies show the following. Foucault currents are present in solid steel with a diameter of 23 mm (Fig. 2), cast iron, and steel with a diameter of 30 mm (Fig. 3, 4) plungers. The resistance of the plungers, determined by dependence (1) is minimal. In this case, according to Ohm's law, Foucault's currents reach maximum values.

Separate steel plungers with a diameter of 23 mm (Fig. 5) and a diameter of 30 mm (Fig. 6), as well as made by powder metallurgy with diameters of 23 mm (Fig. 7) and a diameter of 30 mm (Fig. 8) have maximum resistance and therefore, they have infinitesimal Foucault currents.

Studies of Foucault currents values depending on the geometric dimensions (diameter) of the plunger show the following: eddy current value in a steel plunger with a diameter of 23 mm is less than a steel plunger with a diameter of 30 mm, and it is more than in a plunger made of cast iron with a diameter of 30 mm.

The plunger is made of steel with a diameter of 30 mm due to the minimum frequency and has lower Foucault current values. The steel plunger with a diameter of 23 mm has the maximum frequency and therefore has the highest value of Foucault current. The plunger made of cast iron has a medium frequency and therefore the value of the Foucault current is intermediate.

Depending on the material and geometric dimensions, the heating temperature in steel plunger with a diameter of 23 mm is 374 ^{0}C, in cast iron plunger with a diameter of 30 mm is 264 ^{0}C, in steel plunger with a diameter of 30 mm is 286 ^{0}C. As can be seen, the steel plunger with a diameter of 23 mm has a higher heating temperature than the plunger with a diameter of 30 mm. This is due to the more intense heat dissipation from the plunger of larger diameter.

The 30 mm steel plunger has a higher heating temperature than the 30 mm cast iron working body due to the different electromotive forces given in the working body.

Although separate plungers have no energy loss due to heating, their use is not advisable, as they cannot withstand high pumping pressures. Thus, for a working body with a diameter of 23 mm, the maximum pressure is 0.8 MPa, for a working body with a diameter of 30 mm it is 0.5 MPa.

It should also be noted that the plunger made by powder metallurgy might contain different amounts of the

metal component due to which you can adjust the magnetic susceptibility of the plungers.

Tables 1 – 2 show the main physical quantities that were obtained as a result of the study. Some of the results, such as Foucault's current values, plunger heating temperature, and pumping heating temperature, were obtained by calculation, and the other part was obtained as a result of the experiment. The operating time of the solenoid winding is taken in random order. The initial temperature of the plunger and its heating temperature, the resistance of the solenoid winding were determined experimentally.

Table 1 – Physical effect of the plunger temperature on the pumping of the finishing material

No	Plunger type	Magnetic flux Φ, Wb	The maximum heating temperature of the plunger t, ^{0}C	Retraction force $\vec{F}$ F, N	Pumping pressure P, MPa
1	Steel with diameter 23 mm	310	374	39,2	0,18
2	Cast iron with diameter 30 mm	190	264	54	0,15
3	Steel with diameter 30 mm	149	286	49	0,1

Table 2 – Physical parameters of the differential pump of electromagnetic action

No	Plunger type	Theoretical data					Practical data						
		Reactive winding resistance X_L, Ohm	EMF plunger U, V	Foucault current I, A	Plunger heating temperature	Plunger temperature during pumping t, °C	Winding time t, min	Reactive winding resistance X_L, Ohm	EMF plunger U, V	Foucault current I, A	Initial temperature of the plunger t, °C	Plunger heating temperature	Plunger temperature during pumping t, °C
1	Steel d = 23 mm	27130	32	2,4	60	– 19,4	5	13502	51,4	23,3	18	70	– 5,4
2	Steel d = 30 mm		65,1	2	304	– 29			50,2	15		75	– 7
3	Cast iron d = 30 mm		58	2,1	46	– 3			31	3		35	– 3

Note: The sign "–" means endothermic process.

The graph presented in Figure 17 shows the dependence of the heating temperature of the plunger on the winding resistance. Lines 1, 2, 3 are obtained by calculation and show the change in the physical parameters of steel plungers with diameters of 23 and 30 mm, and cast iron plunger with a diameter of 30 mm. Analysing the graphical dependencies, it can be seen a rapid increase in the heating temperature of the steel plunger at a constant resistance. Maximum temperatures of plungers have the following values: 320 ^{0}C, 46 ^{0}C, 304 ^{0}C. Lines 4, 5, 6 show the dependence of the temperature of the plungers at constant resistance, which is obtained experimentally. The temperatures of the plungers have the following values 70 ^{0}C, 35 ^{0}C, 75 ^{0}C.

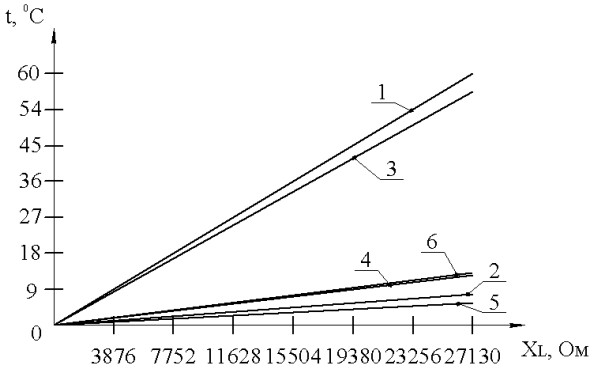

Figure 17 – Graph of the dependence of the heating temperature of the plunger on the winding resistance:
1, 2, 3 – respectively, a steel plunger with a diameter of 23 mm and a diameter of 30 mm, a cast iron plunger with a diameter of 30 mm (theoretical values);
4, 5, 6 – respectively steel plunger with a diameter of 23 mm and a diameter of 30 mm, a cast iron plunger with a diameter of 30 mm (experimental values)

Figure 18 illustrates a three-dimensional graph of the dependence of the heating temperature of the plunger on independent factors, built in the Excel software environment. The reactive resistance of the differential pump winding with a step of 714 Ohms is plotted on the abscissa axis. The heating temperature of the plunger with a step of 17.5 ^{0}C is plotted on the ordinate axis. The operating frequency with a step of 13 Hz is plotted on the axis of the application. The operating frequency of the plunger was found experimentally. Their analysis allows concluding that most of the heating temperature of the pump plunger is influenced by the frequency of translational movements. To ensure proper performance at balanced energy costs, it can be recommended the following ranges of parameters: density of finishing mixture ρ = 1045 kg / m^3; the frequency of translational movements of the plunger of the differential pump n = 50 Hz

If the frequency of translational movements of the working body of the differential pump will be increased, on the one hand, it will lead to a sharp increase in the heating temperature of the plunger, and on the other hand, in the general case, to increase the pumping intensity of the finishing material. But, given the peculiarities of the studied differential pump, in which the working body is inextricably linked with the mortar, the increase in the frequency of its translational motion is limited. Therefore, based on the previous considerations, taking into account the graphical dependencies (Figs. 17 – 18) and analytical expression (2), we can recommend the operating value of the translational frequency of the plunger of the differential pump equal to 50 Hz.

Comparing the experimental data (Fig. 17, lines 4, 5, 6) with the values of the heating temperature of the plunger of the differential pump calculated by the theoretical dependence (4), it can be concluded that the discrepancy in the results does not exceed 10%. Moreover, within the basic operating frequencies of translational motion (about 50 Hz) the coincidence is quite accurate, which confirms the necessary accuracy of the proposed theoretical method.

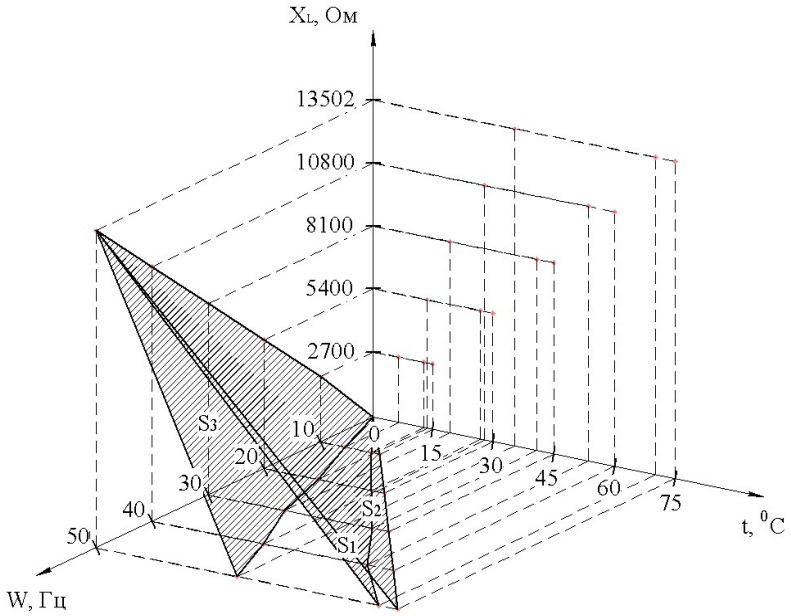

Figure 18 – Three-dimensional graph of temperature-resistance characteristics

S_1 t, ^{0}C = 2, 4617E-11+1.4*X+3,0717E-11*Y

S_2 t, ^{0}C = 6,1456E-11+1,5*X+7,6764E-11*Y

S_3 t, ^{0}C = 1,2308E-11+0,7*X+1,5359E-11*Y

Conclusions

In the examination of the working bodies of the differential pump, it should be noted that each plunger is made of different material and therefore has a different resistivity. A three-dimensional graph has three different planes intersecting at a common point. Therefore, the differential pump works productively under the following conditions, frequency 50 Hz, reactance 13502 Ohm, and temperature 35^{0}C.

References

1. Коробко Б.О., Жигілій С.М., Ківшик А.В. (2019). Математичне моделювання закону руху поршня диференційного насоса для будівельної суміші. *Збірник наукових праць. Галузеве машинобудування, будівництво*, 1(52), 13-20 https://doi.org/10.26906/znp.2019.52.1665

2. Korobko B., Vasyliev Ye. (2017). Test Method for Rheological Behavior of Mortar for Building Work. *Acta Mechanica et Automatica*, 11(3), 173-177 https://doi.org/10.1515/ama-2017-0025

3. Онушко В.В., Шефер О.В. (2007). *Трансформатори*. Полтава, ПолтНТУ

4. Шефер О.В., Галай В.М., Крицький В.В. (2015). Діагностування електродвигунів складних електромеханічних систем. *Системи управління, навігації та зв'язку*, 2, 56-60

5. Онушко В.В., Шефер О.В. (2015). *Електричні машини*. Полтава, ПолтНТУ

6. Шефер О.В., Дзівіцький В.Д. (2015). Діагностування та неруйнівний контроль параметрів асинхронних електродвигунів на основі аналізу спектрів споживаного струму. *Збірник наукових праць за матеріалами Всеукраїнської науково-практичної конференції «Електронні та мехатронні системи: теорія, інновації, практика»*. Полтава, ПолтНТУ, 81-83

7. Срібнюк С. (2017). *Насоси і насосні установки.* Центр навчальної літератури

8. Коробко Б.О., Ківшик А.В. (2020). Теоретичне обґрунтування робочих процесів і режимів роботи диференційного насоса електромагнітної дії. *Збірник наукових праць за матеріалами міжнародної конференції «Building innovations 2020»*. Полтава, ПолтНТУ, 110-112

9. Шефер О.В., Мякушко Р.В. (2015) .Діагностика параметрів та неруйнівний контроль асинхронних електродвигунів. *Збірник наукових праць за матеріалами Всеукраїнської науково-практичної конференції «Електронні та мехатронні системи: теорія, інновації, практика»*. Полтава, ПолтНТУ, 84-85

10. Korobko B., Kivshyk A., Kulagin D. (2022). Experimental Study of the Efficiency of the Differential Pump of Electromagnetic Action on the Basis of Mathematical Modeling of the Parameters of Its Operation. *Lecture Notes in Civil Engineeringthis*, 181, 203-213

11. Васильєв Є.А., Васильєв О.С. (2016). Фактори впливу на об'ємний ККД поршневого розчинонасоса та шляхи його підвищення. *Науковий вісник будівництва*, 2(84), 349-352 http://77.121.11.9/handle/PoltNTU/1141

12. Veleschuk V., Vlasenko A., Vlasenko Z., Petrenko I., Malyi Y., Borshch V., Borshch O., Shefer A. (2019). Current-voltage characteristic and electroluminescence of UV LEDs 365 nm at liquid nitrogen temperature. *Optica Applicata*, 49, 125-133 https://doi.org/10.5277/j.renene.2019.03.041

13. Васильєв Є.А., Васильєв А.В., Попов С.В. (2017). Зменшення енерговитрат при транспортуванні будівельних розчинів розчинонасосами з механічним приводом. *Матеріали VI Міжнародної науково-технічної конференції «Актуальні задачі сучасних технологій».* Тернопіль: ТНТУ

14. Васильєв Є.А., Васильєв О.С. (2019). Вибір матеріалу для багатошарової діафрагми розчинонасоса з метою підвищення її зносостійкості. *Матеріали IX міжнародної науково-практичної конференції «Комплексне забезпечення якості технологічних процесів та систем».* Чернігів: ЧНТУ

1. Korobko B., Zhyhylii S., Kivshyk A. (2019). Mathematical simulation of the motion law of differential mortar pump piston intended for construction mix. *Academic journal. Series: Industrial Machine Building, Civil Engineering*, 1(52), 13-20 https://doi.org/10.26906/znp.2019.52.1665

2. Korobko B., Vasyliev Ye. (2017). Test Method for Rheological Behavior of Mortar for Building Work. *Acta Mechanica et Automatica*, 11(3), 173-177 https://doi.org/10.1515/ama-2017-0025

3. Onushko V.V., Shefer O.V. (2007). Transformers. Poltava, PoltNTU

4. Schaefer O.V., Galay V.M., Kritsky V.V. (2015). Diagnosis of electric motors of complex electromechanical systems. *Control, Navigation and Communication Systems,* 2, 56-60

5. Onushko V.V., Schaefer O.V. (2015). Electric cars. Poltava, PoltNTU

6. Schaefer O.V., Divitsky V.D. (2015). Diagnosis and non-destructive control of parameters of asynchronous electric motors based on the analysis of current consumption spectra. *Collection of scientific works on the materials of the All-Ukrainian scientific-practical conference "Electronic and mechatronic systems: theory, innovation, practice".* Poltava, PoltNTU, 81-83

7. Sribnyuk S. (2017). Pumps and pumping units. Center for Educational Literature

8. Korobko B.O., Kivshik A.V. (2020). Theoretical substantiation of working processes and operating modes of differential pump of electromagnetic action. *Collection of scientific papers based on the materials of the international conference "Building innovations 2020".* Poltava, PoltNTU, 110-112

9. Schaefer O.V., Myakushko R.V. (2015). Diagnosis of parameters and non-destructive testing of asynchronous electric motors. *Collection of scientific works on the materials of the All-Ukrainian scientific-practical conference "Electronic and mechatronic systems: theory, innovation, practice".* Poltava, PoltNTU, 84-85

10. Korobko B., Kivshyk A., Kulagin D. (2022). Experimental Study of the Efficiency of the Differential Pump of Electromagnetic Action on the Basis of Mathematical Modeling of the Parameters of Its Operation. *Lecture Notes in Civil Engineeringthis*, 181, 203-213

11. Vasiliev E.A., Vasiliev O.S. (2016). Factors influencing the volumetric efficiency of the piston mortar pump and ways to increase it. *Scientific Bulletin of Construction,* 2 (84), 349-352 http://77.121.11.9/handle/PoltNTU/1141

12. Veleschuk V., Vlasenko A., Vlasenko Z., Petrenko I., Malyi Y., Borshch V., Borshch O., Shefer A. (2019). Current-voltage characteristic and electroluminescence of UV LEDs 365 nm at liquid nitrogen temperature. *Optica Applicata*, 49, 125-133 https://doi.org/10.5277/j.renene.2019.03.041

13. Vasiliev E.A., Vasiliev A.V., Popov S.V. (2017). Reduction of energy consumption during transportation of mortars by pumps with a mechanical drive. *Proceedings of the VI International Scientific and Technical Conference "Actual Problems of Modern Technologies".* Ternopil: TNTU

14. Vasiliev E.A., Vasiliev O.S. (2019). The choice of material for the multilayer diaphragm of the mortar pump in order to increase its wear resistance. *Proceedings of the IX International Scientific and Practical Conference "Comprehensive Quality Assurance of Technological Processes and Systems".* Chernihiv: ChNTU

15. Korobko B., Vasyliev O., Rohozin I., Vasyliev Ye. (2018). Signature Analysis of the Hydraulic Accumulators when Using in Energy Recovery Systems in Automobiles. *International Journal of Engineering & Technology*, 7(4.8), 713-719
https://doi.org/10.14419/ijet.v7i4.8.27446
16. Kaczynski R., Vasyliev O., Vasyliev Ye. (2018). The Fracture Process of the Mortar Pump's Work Surfaces with Abrasive Particles. *International Journal of Engineering & Technology*, 7(3.2), 154-159
https://doi.org/10.14419/ijet.v7i3.2.14394
17. Rohozin I., Vasyliev O., Pavelieva A. (2018). Determination of Building Mortar Mixers Effectiveness. *International Journal of Engineering & Technology*, 7(3.2), 360-366
https://doi.org/10.14419/ijet.v7i3.2.14553
18. Korobko B., Zadvorkin D., Vasyliev Ye. (2018). Energy Efficiency of a Hydraulically Actuated Plastering Machine *International Journal of Engineering & Technology*, 7(3.2), 203-208
https://doi.org/10.14419/ijet.v7i3.2.14403
19. Korobko B. (2016). Investigation of energy consumption in the course of plastering machine's work. *Eastern-European Journal of Enterprise Technologies*, 4/8 (82), 4-11
https://doi.org/10.15587/1729- 4061.2016.73336

15. Korobko B., Vasyliev O., Rohozin I., Vasyliev Ye. (2018). Signature Analysis of the Hydraulic Accumulators when Using in Energy Recovery Systems in Automobiles. *International Journal of Engineering & Technology*, 7(4.8), 713–719
https://doi.org/10.14419/ijet.v7i4.8.27446
16. Kaczynski R., Vasyliev O., Vasyliev Ye. (2018). The Fracture Process of the Mortar Pump's Work Surfaces with Abrasive Particles. *International Journal of Engineering & Technology*, 7(3.2), 154-159
https://doi.org/10.14419/ijet.v7i3.2.14394
17. Rohozin I., Vasyliev O., Pavelieva A. (2018). Determination of Building Mortar Mixers Effectiveness. *International Journal of Engineering & Technology*, 7(3.2), 360-366
https://doi.org/10.14419/ijet.v7i3.2.14553
18. Korobko B., Zadvorkin D., Vasyliev Ye. (2018). Energy Efficiency of a Hydraulically Actuated Plastering Machine *International Journal of Engineering & Technology*, 7(3.2), 203-208
https://doi.org/10.14419/ijet.v7i3.2.14403
19. Korobko B. (2016). Investigation of energy consumption in the course of plastering machine's work. *Eastern-European Journal of Enterprise Technologies*, 4/8 (82), 4-11
https://doi.org/10.15587/1729- 4061.2016.73336

Збірник наукових праць. Галузеве машинобудування, будівництво
Academic journal. Industrial Machine Building, Civil Engineering
http://journals.nupp.edu.ua/znp
https://doi.org/10.26906/znp.2021.56.2517

UDC 629.463.32

Load Calculation of the Load-carrying Structure of a Tank Car in Operating Modes

Fomin Oleksij1*, Lovska Alyona[2]

[1] State University of Infrastructure and Technologies https://orcid.org/0000-0003-2387-9946
[2] Ukrainian State University of Railway Transport https://orcid.org/0000-0002-8604-1764
*Corresponding author E-mail: alyonalovskaya.vagons@gmail.com

The article determines dynamic load and strength of the load-carrying structure of a tank car with elastic-friction connections in the boiler bearings and between boiler bearings and the boiler bearer. It was established that the use of elastic-friction connections allows to reduce the dynamic load on the tank car by almost 36% in comparison with the prototype. The results of stress calculation showed that the maximum equivalent stresses in the load-carrying structure of a tank car occur in the interaction area of the center sill with the draw-bar and do not exceed the allowable values. The conducted research will allow to increase the operational efficiency of tank cars by reduction of operating costs, and will also promote the creation of their innovative designs.

Keywords: transport mechanics, tank car, load-carrying structure, dynamic load, strength, fatigue strength coefficient.

Визначення навантаженості несучої конструкції вагона-цистерни при експлуатаційних режимах

Фомін О.В.[1]*, Ловська А.О.[2]

[1] Державний університет інфраструктури та технологій
[2] Український державний університет залізничного транспорту
*Адреса для листування E-mail: alyonalovskaya.vagons@gmail.com

Підвищення ефективності експлуатації залізничної галузі вимагає впровадження інноваційних конструкцій рухомого складу, зокрема вагонів. Найбільш розповсюдженим типом вагону для перевезення наливних вантажів є вагони-цистерни. Несуча конструкція вагонів-цистерн випробовує дії значних циклічних навантажень в експлуатації. Це викликає їх пошкодження. В матеріалах статті наведені результати щодо удосконалення несучої конструкції вагона-цистерни шляхом зменшення динамічної навантаженості посередництвом впровадження пружно-фрикційних зв'язків між котлом та його опорами, а також між опорами та рамою. Для обґрунтування запропонованого рішення використано класичні методи теорії коливань та динаміки вагонів, методи розв'язання диференціальних рівнянь руху, зокрема, метод Рунге-Кутта, реалізований в програмному комплексі MathCad, а також метод скінчених елементів, здійснений в SolidWorks Simulation. Проведено визначення динамічної навантаженості та міцності несучої конструкції вагона-цистерни з пружно-фрикційними зв'язками в опорах котла та між опорами та рамою. Встановлено, що використання пружно-фрикційних зв'язків дозволяє зменшити динамічну навантаженість вагона-цистерни у порівнянні з прототипом майже на 36%. Результати розрахунку на міцність показали, що максимальні еквівалентні напруження в несучій конструкції вагона-цистерни виникають в зоні взаємодії хребтової балки зі шворневою та не перевищують допустимих значень. При цьому проектний строк служби несучої конструкції більше ніж на 20% вищий за строк служби вагона-прототипу. Коефіцієнт опору втомі з урахуванням запропонованих конструкційних рішень склав 4,2, що вдвічі перевищує допустимий. Проведені дослідження дозволять підвищити ефективність експлуатації вагонів-цистерн шляхом зменшення витрат на утримання, а також сприятимуть створенню їх інноваційних конструкцій.

Ключові слова: транспортна механіка, вагон-цистерна, несуча конструкція, динамічна навантаженість, міцність, коефіцієнт опору втомі

Introduction

Ensuring the efficient operation of railroads' rolling stock as a leading branch of the transport network requires putting modern car designs in operation. At the same time, promotion of competitiveness of the railway industry leads to increased requirements not only for technical-and-economic indicators of railroads rolling stock, but also for the possibility of adapting structures to the appropriate operating conditions.

One of the busiest load-carrying types of cars in operation are tank cars, due to the mobility of the goods transported in them. Most of them are tank liquid cargos that have their own degree of freeness due to the tank ullage.

Review of the research sources and publications

Areas for improvement of the design of railway tank cars are discussed in [1]. The paper presents an improved design of a tank car, the outstanding feature of which is that the boiler has conical open-end inserts and a gapless coupler drawbar hook.

Paper [2] considers the options for design and technical solutions which may improve the efficiency of liquid cargo transportation in tank cars. The authors of the article have chosen the most rational schematic construction, which will help increase the productivity of tank cars usage.

It is important to say that the mentioned paper does not propose measures to reduce the dynamic load on the load-carrying structures of tank cars in operation.

The results of a computer-based simulation of the hydrodynamic load of the manhole area of the tank car are covered in the article [3]. The paper presents the study of the load on the joint when changing the height of the part of the manhole shell, located inside the boiler. However, no design solutions have been proposed to reduce the load on the tank car boiler.

Theoretical aspects of determining the residual life of a tank car for dangerous cargo are considered in [4]. The paper presents the structural scrutiny of load-carrying structures of the tank cars, which have depleted their guideline lives. The peculiarities of tank cars' testing technique are highlighted in this research. However, the paper does not specify any solutions for the possibility of reducing the load on the load-carrying structures of tank cars to extend their service life.

Paper [5] considers the load on the load-carrying structure of a tank car under operation conditions, taking into account the shunting collision of the tank car. The authors of this scientific work have determined the influence of liquid cargo on the dynamic load of the boiler.

Also, the study of the impact of liquid cargo on the load of the tank car boiler is carried out in [6]. It was established in this scientific work that the liquid cargo has an impact on the distribution of loads between the front and rear wheel groups of the car. At the same time, the authors of the above-mentioned works did not offer any measures to reduce the load on the tank car in operation.

Papers [7, 8] offer the substantiation of measures on reduction of dynamic loading on load-carrying structures of cars at operational modes. The studies, conducted regarding open railroad freight cars and platform cars, confirmed the feasibility of the proposed solutions. However, no measures to reduce the dynamic load on the load-carrying structures of tank cars were discussed in these papers.

Definition of unsolved aspects of the problem

The load-carrying structure of tank cars is subject to the loads that occur during operating conditions. The most common of these are vertical loads, caused by railway line unevennesses. Due to the cyclical nature of such loads, load-carrying structures of tank cars may suffer damages, and hence it will lead to the necessity of appropriation of additional costs for their maintenance. This necessitates the development and implementation of measures to improve load-carrying structures of tank cars to reduce their dynamic load in operation. In order to reduce the dynamic load on the load-carrying structures of tank cars, the authors propose the use of elastic-friction connections between the boiler and boiler bearings and between boiler bearings and the boiler bearer. However, the implementation of such innovations at the first level requires scientific justification and comprehensive calculations.

Problem statement

The aim of the article is to determine the dynamic load on the load-carrying structure of a tank car with elastic-friction connections in boiler bearings and between boiler bearings and the boiler bearer. To achieve this goal, the following tasks should be completed:

– to determine the dynamic load on the load-carrying structure of a tank car with elastic-friction connections in boiler bearings and between boiler bearings and the boiler bearer;

– to carry out stress calculation of the load-carrying structure of a tank car;

– to calculate the design lifetime, as well as the fatigue strength coefficient of the load-carrying structure of a tank car.

Basic material and results

In order to reduce the dynamic load on the load-carrying structure of a tank car, it is proposed to use elastic-friction connections between the boiler and boiler bearings, as well as between boiler bearings and the boiler bearer (Fig. 1).

To determine vertical accelerations acting on the tank car's boiler, mathematical modelling was performed. The design model of the tank car is shown in Fig. 2.

When composing the differential equations of motion of the tank car, it is stated that it moves empty, as under such conditions the greatest load on the load-carrying structure is observed. It is taken into account that the railway line has viscoelastic characteristics, and the reactions of the railway line are proportional to both its deformation and the speed of this deformation [9].

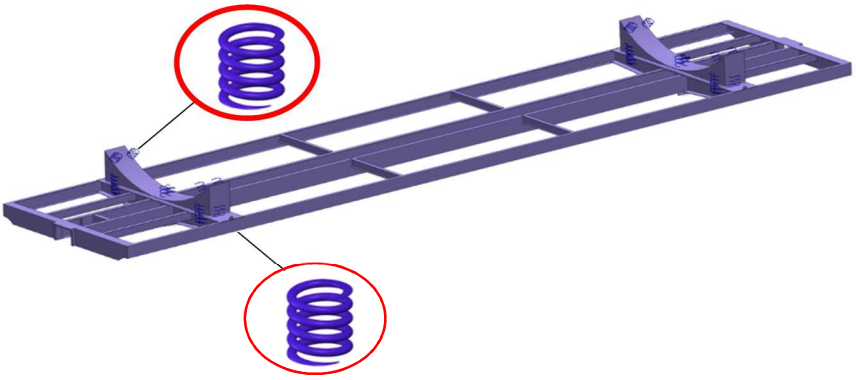

Figure 1 – Arrangement of elastic-friction elements on the boiler bearings and between boiler bearings and the boiler bearer

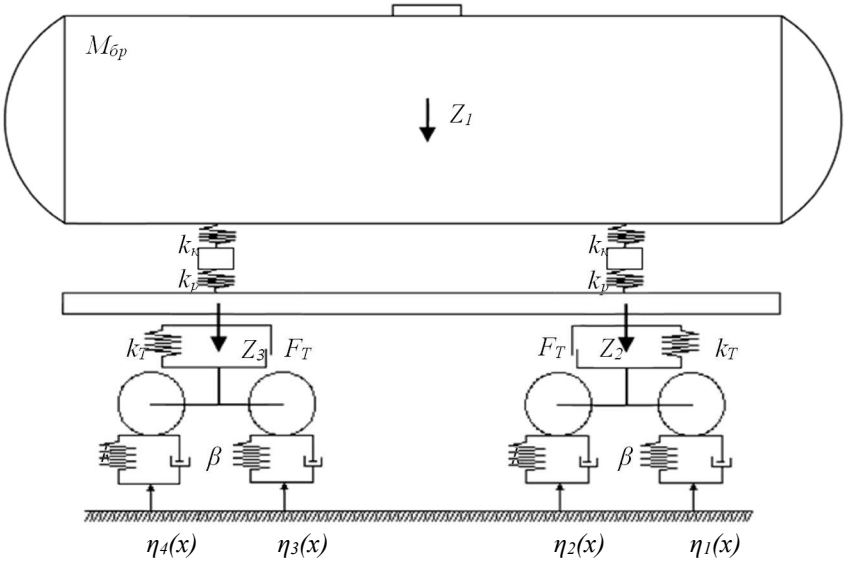

Figure 2 – Calculation scheme of a tank car

Differential equations of motion of the tank car have the following form:

$$M_1 \cdot \ddot{q}_1 + C_{1,1} \cdot q_1 + C_{1,2} \cdot q_2 + C_{1,3} \cdot q_3 = \\ = -F_{TP} \cdot \left(sign\left(\frac{d}{dt}\delta_1 \right) + sign\left(\frac{d}{dt}\delta_2 \right) \right) \quad (1)$$

$$M_2 \cdot \ddot{q}_2 + C_{2,1} \cdot q_1 + C_{2,2} \cdot q_2 + B_{2,2} \cdot \dot{q}_2 = \\ = F_{TP} \cdot sign\left(\frac{d}{dt}\delta_1 \right) + k(\eta_1 + \eta_2) + \\ + \beta\left(\frac{d}{dt}\eta_1 + \frac{d}{dt}\eta_2 \right) \quad (2)$$

$$M_3 \cdot \ddot{q}_3 = -C(y_1 - y_2) - M_3 \cdot g \quad (3)$$

where M_i – inertial coefficients of the oscillating system elements (the load-carrying structure of a tank car, two bogies and the boiler);
C_{ij} – elasticity characteristics of the oscillating system elements, which are determined by the values of the stiffness coefficient of the springs;
B_{ij} – scattering function;
q_i – generalised coordinates corresponding to the translational displacement relative to the vertical axis, the car's boiler, the first and second set of wheels;
k – railway line stiffness;
β is the damping coefficient;
F_F – frictional force in the spring grouping;
δi – deformations of springing elements of the spring hanger; $\eta(t)$ is the unevenness of the railway line.

In the equations of motion (1) – (3) we accept:

$Z_1 \sim q_1$ – the coordinate that characterises the translational movements of the load-carrying structure of a tank car relative to the vertical axis;

$Z_2 \sim q_2$ – the coordinate that characterises the translational movements of the first car facing the engine and relative to the vertical axis;

$Z_3 \sim q_3$ – the coordinate that characterises the translational movements of the second car facing the engine and relative to the vertical axis.

The connection of the boiler with boiler bearings, of boiler bearings with the boiler bearer and of the boiler bearer with the travel carriage was described as a serial elastic coupling (Fig. 3):

$$C = \frac{2k_k \cdot 2k_p \cdot 2k_T}{2k_k + 2k_p + 2k_T}\ , \qquad (4)$$

where k_k is the stiffness of the springs between the boiler and boiler bearings;
k_p – stiffness of springs between boiler bearings and the boiler bearer;
k_T – stiffness of the springs of the spring hanger.

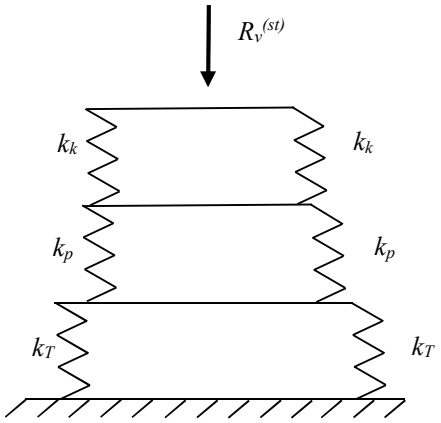

Figure 3 – The scheme of load transfer from the tank car boiler to the bogies ($R_v^{(st)}$ - vertical static load)

It is taken into account that the rigidity of the connection between the boiler and its bearings, boiler bearings and the boiler bearer, between the boiler bearer and the travel carriage is described as parallel coupling. That is, the total stiffness between the boiler and its bearings is $2k_k$, between boiler bearings and boiler bearer – $2k_r$, between the boiler bearer with the travel carriage – $2k_T$.

Railway line unevenness was described by a periodic function [9]

$$\eta(t) = \frac{d}{2}(1 - \cos \omega t)\,, \qquad (5)$$

where d is the unevenness depth, which is given;
ω is the oscillation frequency.

The input parameters to the mathematical model are given in table 1. The calculations were carried out based on the parameters of the car model 18-100.

Table 1 – Input parameters to the mathematical model

Parameter name	Value
LOAD CARRYING STRUCTURE mass, t	 14,9
CARS mass, t spring hanger stiffness, kN/m relative friction coefficient	 4,3 8000 0,1
RAILWAY LINE damping factor, kN s/m stiffness, kN/m unevenness amplitude, m unevenness length, m	 200 100000 0,01 25

The calculation was made for a tank car model 15-1443-06.

The solution of the differential equations of motion (1) – (3) was carried out in the MathCad software package [10 – 12].

The initial motions and velocities are set to zero.

The solution of the model in the MathCad software package was complied in the following form:

$$F(t,y) = \begin{bmatrix} y_2 \\ y_4 \\ y_6 \\ \dfrac{-F_{TP}\cdot\left(sign\left(\frac{d}{dt}\delta_1\right)+sign\left(\frac{d}{dt}\delta_2\right)\right) - C_{1,1}\cdot y_1 - C_{1,2}\cdot y_3 - C_{1,3}\cdot y_5}{M_1} \\ \dfrac{F_{TP}\cdot sign\left(\frac{d}{dt}\delta_1\right)+k\left(\eta_1+\eta_2\right)+\beta\left(\frac{d}{dt}\eta_1+\frac{d}{dt}\eta_2\right) - C_{2,1}\cdot y_1 - C_{2,2}\cdot y_2 - B_{2,2}\cdot y_4}{M_2} \\ \dfrac{F_{TP}\cdot sign\left(\frac{d}{dt}\delta_2\right)+k\left(\eta_3+\eta_4\right)+\beta\left(\frac{d}{dt}\eta_3+\frac{d}{dt}\eta_4\right) - C_{3,1}\cdot y_1 - C_{3,3}\cdot y_3 - B_{3,3}\cdot y_6}{M_3} \end{bmatrix}, \qquad (6)$$

$$Z = rkfixed\ (Y_0,\ t_n,\ t_k,\ n,\ F).$$

With $y_1 = q_1$, $y_3 = q_3$, $y_5 = q_5$, $y_2 = \dot{y}_1$, $y_4 = \dot{y}_3$, $y_6 = \dot{y}_5$,

The results of the calculation are shown in Fig. 4, 5.

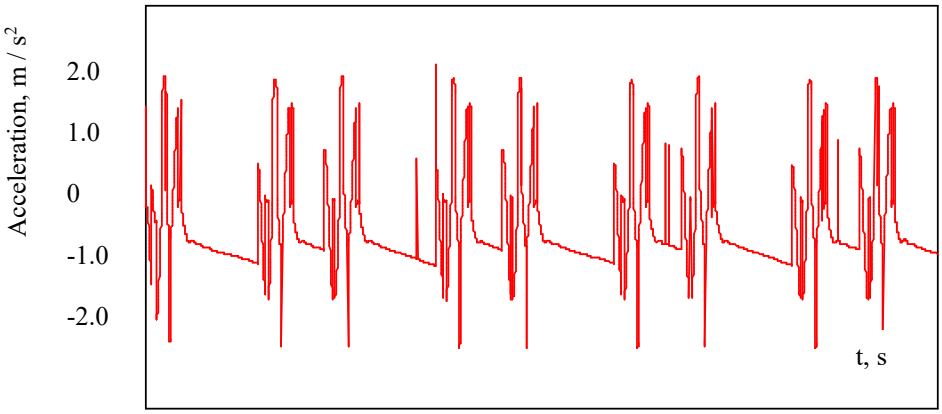

Figure 4 – Acceleration of the load-carrying structure in the centre of inertia

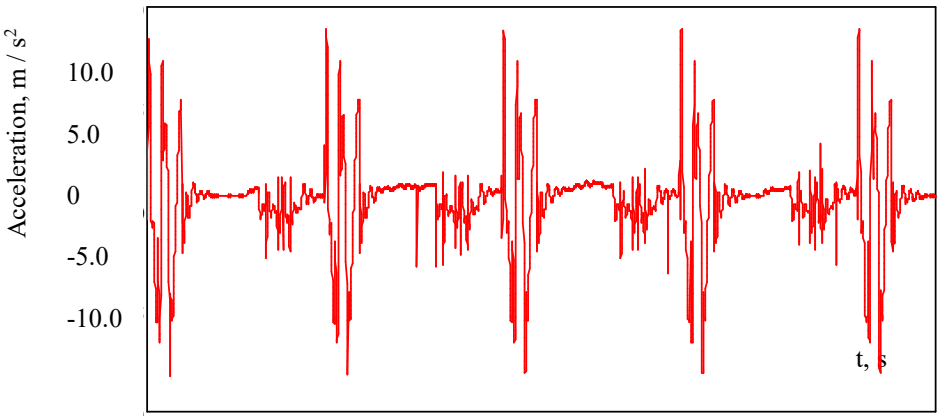

Figure 5 – Acceleration of carts

The maximum vertical acceleration of the load-carrying structure of the empty tank car is 1.35 m/s^2 (0.14 g), and the carts – 8.91 m/s^2 (0.91 g). Based on the calculations, it can be concluded that the run of the car is assessed as "excellent" [13, 14]. At the same time, the use of elastic-friction connections allows to reduce the dynamic load of the tank car by almost 36% in comparison with the prototype. The total stiffness of the elastic connection between the boiler with boiler bearings, of boiler bearings with the boiler bearer and of the boiler bearer with the travel carriage must not exceed 4360 kN/m.

At the next stage of the study, the strength of the load-carrying structure of a tank car was calculated. Graphic work was carried out in the software package "SolidWorks".

The calculation was performed by the finite element method in the "SolidWorks Simulation" software package.

The finite element model of the load-carrying structure of a tank car is shown in Fig. 6. The optimal number of grid elements was determined by the grapho-analytical method [15, 16]. Spatial isoparametric tetrahedra were used as finite elements [17-19]. The number of grid elements was 721195, the number of joints – 232420. The maximum size of the grid element is 40 mm, the minimum – 8 mm, the maximum ratio of the sides of the elements – 93.724, the percentage of elements with the ratio of the sides less than three – 21.8, more than ten – 0.414.

The design model of the load-carrying structure of a tank car is shown in Fig. 7. Determination of the strength of the load-carrying structure of a tank car was carried out for the first design mode – "jerk – tension". It is taken into account that the load-bearing structure is subjected to a longitudinal load P_L, which is applied to the front draft lugs of automatic couplers and is equal to 2.5 MN, liquid cargo pressure is P_P, and vertical load is P_V, which takes into account dynamic load, determined by mathematical modelling. The rate of acceleration, acting on the load-carrying structure of a tank car when moving in the loaded state was about 3.0 m / s^2 (0.3 g).

The fastening of the model was carried out in the areas of resting on the carts. The construction material is grade steel 09G2S. The results of the stress calculation are shown in Fig. 8 and 9.

The maximum equivalent stresses occur in the area of interaction of the center sill with the draw-bar and are about 250 MPa and do not exceed the allowable equivalent stresses [13, 14]. The maximum displacements were 8.3 mm and were concentrated in the manhole area.

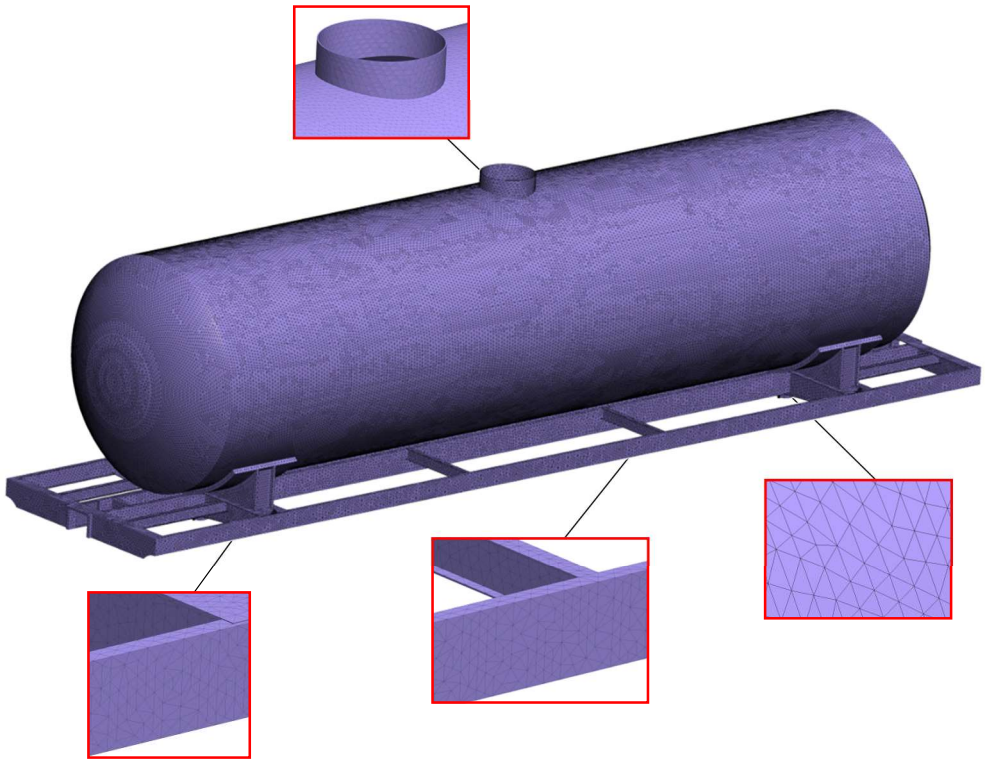

Figure 6 – Finite element model of the load-carrying structure of a tank car

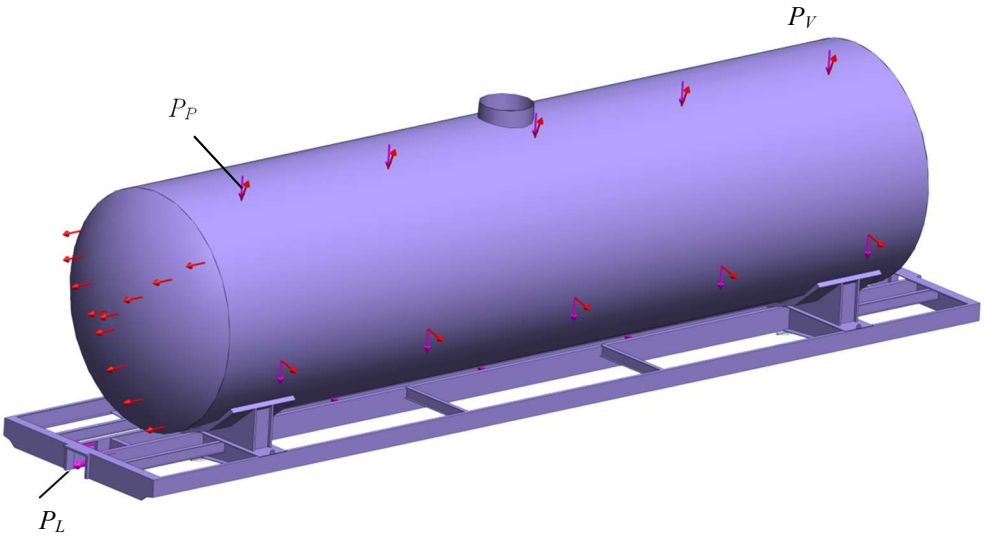

Figure 7 – The design model of the load-carrying structure of a tank car

Figure 8 – Stress state of the load-carrying structure of a tank car in the first design mode ("jerk")

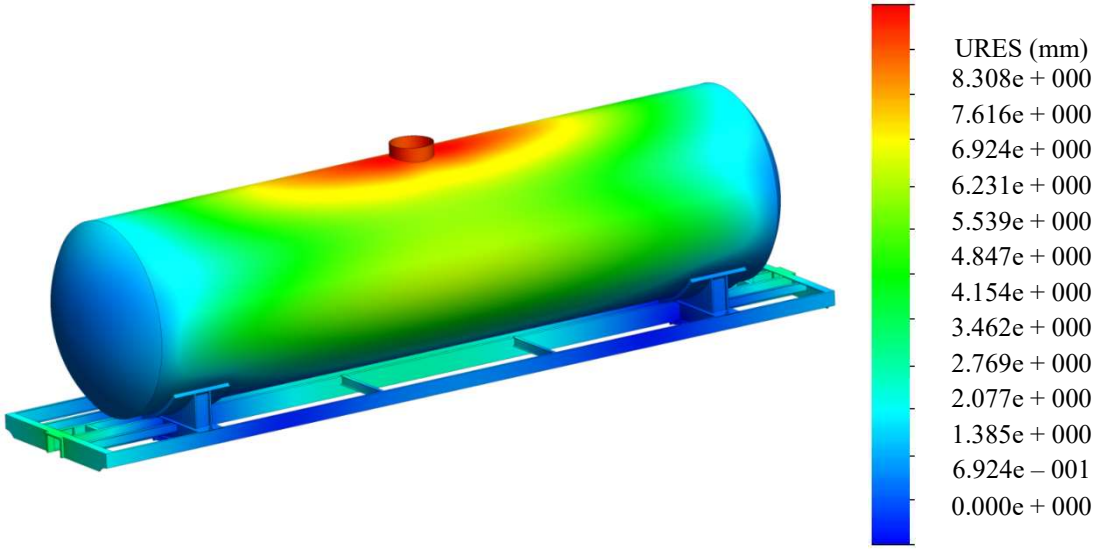

Figure 9 – Displacements in the joints of the load-carrying structure of a tank car in the first design mode ("jerk")

To determine the operational life of the tank car we used the method, described in [20]:

$$T_n = \frac{\left(\frac{\sigma_{-1D}}{[n]}\right)^m \cdot N_0}{B \cdot f_e \cdot \sigma_{sw}\left(k_{dv} + \frac{\psi_\sigma}{K_\sigma}\right)^m} \qquad (7)$$

where σ_{-1D} is the average value of the endurance limit;
n is the allowable assurance coefficient;
m is the degree of fatigue curve;
N_0 – test base;
B – coefficient that characterises the time of the object's continuity of service in seconds;
$f_в$ – effective frequency of dynamic stresses;
σ_{sw} – stress from static weight load;
k_{dv} – coefficient of vertical dynamics;
ψ_σ – sensitivity factor;
K_σ is the total coefficient of reduction of fatigue strength.

When determining the amplitude of equivalent dynamic stresses, we took into account the coefficient of influence of lateral forces equal to 1.1.

The following input parameters are taken into account in the calculations: σ_{-1D} = 245 MPa; n = 2; m = 8; $N_0 = 10^7$; $B = 3.0 \cdot 10^6$ s; $f_в$ = 2,7 Hz; ψ_σ / K_σ = 0,2.

The strength calculation was performed to determine the stresses from the static weight load of the load-carrying structure of a tank car. It was established that the maximum equivalent stresses in the load-carrying structure of a tank car are 87.5 MPa.

In this case, the design lifetime of the load-carrying structure of a tank car is more than 20% higher than the design lifetime of the prototype car. It is important to say that the obtained value of the design lifetime should be specified taking into account additional studies of the longitudinal load of the load-carrying structure of a tank car and experimental (field or benchmark tests) studies.

Also in the framework of the study, the fatigue resistance of the load-carrying structure of a tank car was calculated.

The calculation of fatigue resistance was carried out taking into account the assurance coefficient n by the formula [21]:

$$n = \frac{\sigma_{-1D}}{\sigma_{a,e}} \geq [n] , \qquad (8)$$

where $\sigma_{a,e}$ is the calculated value of the amplitude of dynamic stress of the conditional symmetric cycle, reduced to the base N_0, equivalent in damaging action to the value of the amplitudes in the real mode of random operating tensions during the design lifetime, MPa;

$[n]$ – allowable factor of safety against fatigue failure.

The calculation results showed that there is a probability of occurrence of stresses with a level of σ_1, that is 0.95 values of $\sigma_{a,e}$ = 58.3 MPa. Hence the coefficient of fatigue resistance is 4.2. However, due to the lack of experimental data, the allowable value of the coefficient of fatigue resistance is assumed to be 2.2. Therefore, condition (8) is met and the fatigue strength of the load-carrying structure of a tank car is provided.

Conclusions

1. Determination of the dynamic load of the load-carrying structure of a tank car with elastic-friction connections in the boiler bearings and between the bearings and the boiler bearer was carried out. It was established that the maximum vertical acceleration of the load-carrying structure of an empty tank car is 1.35 m/s^2 (0.14 g), and carts – 8.91 m/s^2 (0.91 g). At the same time, the use of elastic-friction connections allows to reduce the dynamic load of the tank car by almost 36% in comparison with the prototype.

2. The stress calculation of the load-carrying structure of a tank car was carried out. The maximum equivalent stresses occur in the area of interaction of the center sill with the draw-bar and are about 250 MPa and do not exceed the allowable stress values. The maximum displacements were 8.3 mm and were concentrated in the manhole area.

3. The calculation of the design lifetime was made, as well as of the coefficient of fatigue resistance of the load-carrying structure of a tank car. It was established that the design lifetime of the load-carrying structure of a tank car is more than 20% higher than the design lifetime of the prototype car. The coefficient of fatigue resistance was 4.2, which is twice as allowable.

The conducted research will allow to increase the operational efficiency of tank cars, and will also promote the creation of their innovative designs.

References

1. Атаманчук Н.А., Цыганская Л.В. (2013). Направления совершенствования конструкций вагонов-цистерн для перевозки нефтепродуктов. *Транспорт Российской Федерации*, 3(46), 14-17

2. Собержанский А.Н., Цыганская Л.В. (2010). Совершенствование конструкций вагонов-цистерн. *Вісник Дніпро-вського національного університету залізничного транспорту ім. академіка В. Лазаряна,* 35, 25-28

3. Путято А.В. (2009). Компьютерное моделирование гидродинамической нагруженности области люка-лаза вагона-цистерны. *Вестник Гомельского государственного технического университета им. Сухого*, 1, 79-86

4. Кельріх М.Б., Фомін О.В., Прокопенко П.М., Сова С.С. (2020). Теоретичні аспекти визначення залишкового ресурсу вагона-цистерни для небезпечних вантажів. *Вісник Східноукраїнського національного університету ім. Володимира Даля*, 5(261), 5-9 https://doi.org/10.33216/1998-7927-2020-261-5-5-9

5. Ashtiani I.H., Rakheja S., Ahmed W. (2019). Investigation of coupled dynamics of a railway tank car and liquid cargo subject to a switch-passing maneuver. *Proceedings of the Institution of Mechanical Engineers, Part F: Journal of Rail and Rapid Transit*, 233(10), 1023-1037 https://doi.org/10.1177/0954409718823650

6. Shi H., Wang L., Nicolsen B., Shabana A.A. (2017). Integration of geometry and analysis for the study of liquid sloshing in railroad vehicle dynamics. *Proceedings of the Institution of Mechanical Engineers, Part K: Journal of Multi-Body Dynamics, 231*(4), 608-629 https://doi.org/10.1177/1464419317696418

1. Atamanchuk N.A., Tsyganskaya L.V. (2013). Directions for improving the design of tank cars for the transportation of petroleum products. *Transport of the Russian Federation*, 3(46), 14-17

2. Soberzhansky A.N., Tsyganskaya L.V. (2010). Improving the design of tank cars. *Bulletin of Dnipro National University of Railway Transport named after Academician V. Lazaryan*, 35, 25-28

3. Putyato A.V. (2009). Computer simulation of the hydrodynamic loading of the manhole area of a tank car. *Bulletin of the Sukhoi State Technical University of Gomel*, 1, 79-86

4. Kelrich M.B., Fomin O.V., Prokopenko P.M., Sova S.S. (2020). Theoretical aspects of determining the residual resource of a tank car for dangerous goods. *Bulletin of the Volodymyr Dahl East Ukrainian National University*, 5(261), 5-9 https://doi.org/10.33216/1998-7927-2020-261-5-5-9

5. Ashtiani I.H., Rakheja S., Ahmed W. (2019). Investigation of coupled dynamics of a railway tank car and liquid cargo subject to a switch-passing maneuver. *Proceedings of the Institution of Mechanical Engineers, Part F: Journal of Rail and Rapid Transit*, 233(10), 1023-1037 https://doi.org/10.1177/0954409718823650

6. Shi H., Wang L., Nicolsen B., Shabana A.A. (2017). Integration of geometry and analysis for the study of liquid sloshing in railroad vehicle dynamics. *Proceedings of the Institution of Mechanical Engineers, Part K: Journal of Multi-Body Dynamics, 231*(4), 608-629 https://doi.org/10.1177/1464419317696418

7. Fomin O., Lovska A., Kulbovskyi I, Holub H., Kozarchuk I., Kharuta V. (2019). Determining the dynamic loading on a semi-wagon when fixing it with a viscous coupling to a ferry deck. *Eastern-European Journal of Enterprise Technologies*, 2/7(98), 6-12
https://doi.org/10.15587/1729-4061.2019.160456
8. Фомін О.В., Ловська А.О. (2021). Визначення вертикальних прискорень несучої конструкції вагона-платформи з в'язкими зв'язками у повздовжніх балках. *Вчені записки Таврійського національного унів-ту ім. В.І. Вернадського. Технічні науки*, 32(71)1, 135-140
9. Дьомін Ю.В., Черняк Г.Ю. (2003). *Основи динаміки вагонів*. Київ: КУЕТТ
10. Fomin O., Lovska A., Píštěk V., Kučera P. (2019). Dynamic load effect on the transportation safety of tank containers as part of combined trains on railway ferries. *Vibroengineering Procedia*, 29, 124-129
https://doi.org/10.21595/vp.2019.21138
11. Fomin O., Kulbovskiy I., Sorochinska E., Sapronova S., Bambura O. (2017). Experimental confirmation of the theory of implementation of the coupled design of center girder of the hopper wagons for iron ore pellets. *Eastern-European Journal of Enterprise Technologies*, 5, 11-19
https://doi:10.15587/1729-4061.2017.109588
12. Kondratiev A., Gaidachuk V., Nabokina T., Tsaritsynskyi A. (2020). New possibilities in creating of effective composite size-stable honeycomb structures designed for space purposes. *Advances in Intelligent Systems and Computing*, 1113, 45-59
https://doi.org/10.1007/978-3-030-37618-5_5
13. ДСТУ 7598:2014. (2015). *Вагони вантажні. Загальні вимоги до розрахунків та проектування нових і модернізованих вагонів колії 1520 мм*. Київ
14. ГОСТ 33211-2014. (2016). *Вагоны грузовые. Требования к прочности и динамическим качествам*. Москва
15. Lovska A.A. (2015). Peculiarities of computer modeling of strength of body bearing construction of gondola car during transportation by ferry-bridge. *Metallurgical and Mining Industry*, 1, 49-54
16. Lovska A., Fomin O. (2020). A new fastener to ensure the reliability of a passenger coach car body on a railway ferry. *Acta Polytechnica*, 60(6), 478-485
17. Kelrykh M., Fomin O. (2014). Perspective directions of planning carrying systems of gondolas. *Metallurgical and Mining Industry*, 6, 64-67
18. Lovska A. (2018). Simulation of loads on the carrying structure of an articulated flat car in combined transportation. *International Journal of Engineering & Technology*, 7(4.3), 140-146
https://doi.org/10.14419/ijet.v7i4.3.19724
19. Vatulia G.L., Lobiak O.V., Deryzemlia S.V., Verevicheva M.A., Orel Ye.F. (2019). Rationalization of cross-sections of the composite reinforced concrete span structure of bridges with a monolithic reinforced concrete roadway slab. *IOP Conference Series: Materials Science and Engineering*, 664, 012014
https://doi:10.1088/1757-899X/664/1/012014
20. Устич П.А., Карпыч В.А., Овечников М.Н. (1999). *Надежность рельсового нетягового подвижного состава*. Москва
21. Сенько В.И., Макеев С.В., Комиссаров В.В., Скороходов С.А. (2018). Особенности определения коэффициента запаса сопротивления усталости конструкций подвижного состава. *Вестник Белорусского государственного университета транспорта. Наука и транспорт*, 1(36), 5-9

7. Fomin O., Lovska A., Kulbovskyi I, Holub H., Kozarchuk I., Kharuta V. (2019). Determining the dynamic loading on a semi-wagon when fixing it with a viscous coupling to a ferry deck. *Eastern-European Journal of Enterprise Technologies*, 2/7(98), 6-12
https://doi.org/10.15587/1729-4061.2019.160456
8. Fomin O.V., Lovska A.A. (2021). Determination of vertical accelerations of the load-bearing structure of a platform car with viscous connections in longitudinal beams. *Scientific notes of the V.I. Vernadsky Tauriia National University. Technical Sciences*, 32(71)1, 135-140
9. Dyomin Yu.V., Chernyak G.Yu. (2003). *Fundamentals of car dynamics*. Kyiv: QUETT
10. Fomin O., Lovska A., Píštěk V., Kučera P. (2019). Dynamic load effect on the transportation safety of tank containers as part of combined trains on railway ferries. *Vibroengineering Procedia*, 29, 124-129
https://doi.org/10.21595/vp.2019.21138
11. Fomin O., Kulbovskiy I., Sorochinska E., Sapronova S., Bambura O. (2017). Experimental confirmation of the theory of implementation of the coupled design of center girder of the hopper wagons for iron ore pellets. *Eastern-European Journal of Enterprise Technologies*, 5, 11-19
https://doi:10.15587/1729-4061.2017.109588
12. Kondratiev A., Gaidachuk V., Nabokina T., Tsaritsynskyi A. (2020). New possibilities in creating of effective composite size-stable honeycomb structures designed for space purposes. *Advances in Intelligent Systems and Computing*, 1113, 45-59
https://doi.org/10.1007/978-3-030-37618-5_5
13. DSTU 7598:2014. (2015). *Freight Wagons. General reguirements to calculation and designing of the new and modernized 1520 mm gauge wagons*. Kyiv
14. GOST 33211-2014. (2016). *Freight wagons. Requirements to structural strength and dynamic qualities*. Moskov
15. Lovska A.A. (2015). Peculiarities of computer modeling of strength of body bearing construction of gondola car during transportation by ferry-bridge. *Metallurgical and Mining Industry*, 1, 49-54
16. Lovska A., Fomin O. (2020). A new fastener to ensure the reliability of a passenger coach car body on a railway ferry. *Acta Polytechnica*, 60(6), 478-485
17. Kelrykh M., Fomin O. (2014). Perspective directions of planning carrying systems of gondolas. *Metallurgical and Mining Industry*, 6, 64-67
18. Lovska A. (2018). Simulation of loads on the carrying structure of an articulated flat car in combined transportation. *International Journal of Engineering & Technology*, 7(4.3), 140-146
https://doi.org/10.14419/ijet.v7i4.3.19724
19. Vatulia G.L., Lobiak O.V., Deryzemlia S.V., Verevicheva M.A., Orel Ye.F. (2019). Rationalization of cross-sections of the composite reinforced concrete span structure of bridges with a monolithic reinforced concrete roadway slab. *IOP Conference Series: Materials Science and Engineering*, 664, 012014
https://doi:10.1088/1757-899X/664/1/012014
20. Ustich P.A., Karpych V.A., Ovechnikov M.N. (1999). *Reliability of rail non-traction rolling stock*. Moscow
21. Senko V.I., Makeev S.V., Komissarov V.V., Skorokhodov S.A. (2018). Features of determining the fatigue resistance factor of rolling stock structures. *Bulletin of the Belarusian State University of Transport: Science and Transport*, 1(36), 5-9

Збірник наукових праць. Галузеве машинобудування, будівництво
Academic journal. Industrial Machine Building, Civil Engineering
http://journals.nupp.edu.ua/znp
https://doi.org/10.26906/znp.2021.56.2518

UDC 624.016:624.046.2

Deformability of bends continuous three-span preliminary self-stressed steel concrete slabs

Hasenko Anton[1]*

[1] National University «Yuri Kondratyuk Poltava Polytechnic» https://orcid.org/0000-0003-1045-8077
*Corresponding author E-mail: gasentk@gmail.com

Continuous steel reinforced concrete structures with the use of monolithic reinforced concrete slab as a compressed part of the section and steel profile part as stretched are widely used in civil building. However, the continuous monolithic reinforced concrete slab is uneven due strength to the different values of the support and span moments of the extreme and middle spans. The conducted experimental researches confirm expediency of the development of a two-stage method of manufacturing (concreting) of continuous multi-span monolithic reinforced concrete slab on fixed formwork (the first stage - concreting of the middle span; the second stage - concreting of the extreme spans) in order to balance the level of deflections in all spans slab. The proposed method allows to effectively use the load-bearing capacity of the continuous slab's reinforcement with the same support installation step of the steel reinforced concrete floor.

Keywords: civil building, experimental research, steel concrete continuous slab, two-stage method of concreting.

Деформативність згинаних нерозрізних трипролітних самонапружених сталезалізобетонних плит

Гасенко А.В.[1]*

[1] Національний університет «Полтавська політехніка імені Юрія Кондратюка»
*Адреса для листування E-mail: gasentk@gmail.com

Багатопрогінні згинані сталезалізобетонні конструкції із застосуванням монолітної залізобетонної плити у якості стиснутої частини перерізу та сталевої профільної частини у якості розтягнутої добре зарекомендували себе за рахунок високої технологічності влаштування та значної експлуатаційної несучої здатності як в цивільному, так і в промисловому будівництві. Проте нерозрізна монолітна залізобетонна плита, що влаштована по сталевих балках розміщених з однаковим кроком, під дією експлуатаційного навантаження при однаковому армуванні крайніх і середніх прольотів має не однаковий рівень напружень за рахунок різних значень опорних та прольотних моментів крайніх і середніх прольотів. Зменшення крайніх прольотів шляхом змінного кроку встановлення сталевих балок є незручним із технологічної точки зору, так як вимагає додаткових індивідуальних конструктивних рішень влаштування нерегулярних опор під ці балки. Для врівноваження рівня використання несучої здатності монолітної плити нерозрізних багатопрогінних сталебетонних плит запропонована двоетапна методика їх виготовлення (бетонування). Суть цієї методики бетонування полягає у створенні попередніх самонапружень (напружень, протилежних тим, що виникатимуть у процесі експлуатації) структурних частин конструкції виключно від їх власної ваги та технології виготовлення без застосування інших заходів попереднього напруження (механічного, електротермічного чи електротермомеханічного). Під час першої черги виготовлення плити виконується бетонування середнього прольоту в ході якого від власної ваги бетону створюються попередні самонапруження сталевої частини перерізу крайніх прольотів (вигин вверх сталевої частини протилежно експлуатаційному). Після набору бетоном першої черги бетонування міцності, виконується друга черга бетонуванні крайніх прольотів в ході чого створюються попередні самонапруження бетонної частини перерізу виготовленого за першим етапом середнього прольоту (вигин вверх бетонної частини). Проведені експериментальні дослідження двох зразків нерозрізних трипрогінних сталебетонних плит, виготовлених за запропонованою двоетапною методикою, підтвердили, що за рахунок змінної в процесі виготовлення жорсткості перерізів середнього та крайніх прольотів плити можливо врівноважувати рівень одночасного вичерпування несучої здатності плити у всіх прольотах

Ключові слова: двоетапний метод бетонування, експериментальні дослідження, сталебетонна нерозрізна плита, цивільне будівництво

Introduction

Bent steel reinforced concrete structures consist of steel load-bearing beams, which work mainly in tension, and a concrete shelf, which works in compression and at the same time performs the functions of a rigid disk and a solid plate. These constructions are widely used in civil and industrial buildings [1]. To increase the size of the spans and reduce the cross section of the floor slabs, the latter performs a continuous static-indeterminate multi-run scheme. Also to reduce the cross-sectional height of the steel beam, it is combined for joint work with the concrete shelf with the help of special design solutions. Combining steel and concrete cross-sectional parts of the structure into joint work increases the overall load-bearing capacity and reliability of the structure [2-3].

Thanks to a specially structure or technology for the manufacture of bent steel reinforced concrete structures, scientists achieve in them the redistribution of stresses between their structural parts and the self-stress of individual elements from their own weight or mounting technology [4]. Thus, preliminary self-stresses are created, opposite to those that arise during the operation of structural parts of steel reinforced concrete structures.

Review of the research sources and publications

Preliminary stresses in steel concrete structures can be created by the following measures: use of stress cement for preparation of concrete mortar [5], provision of design measures for additional compaction of fresh concrete mortar (centrifugation in individual tubular concrete elements of spatial steel concrete structures) [6], or for preliminary reinforcement (sprungs) [7-8], changes the free-body diagrams of the transverse frame [9-10], changes in the geometric characteristics of the section or the design scheme of the elements in the manufacturing process, specially developed step-by-step technology for the manufacture of structures [11], etc.

High-tech and high load-bearing capacity are distinguished by reinforced concrete planar structures with the use of profiled decking as a fixed formwork and additional reinforcement of the slab [12-13].

Definition of unsolved aspects of the problem

Continuous monolithic reinforced concrete slab, arranged on steel beams placed with the same pitch, under the action of operating load with the same reinforcement of the extreme and middle spans has not the same stress level due to different values of reference and span moments of the extreme and middle spans. Reduction of extreme spans by a variable step of installation of steel beams is inconvenient from the technological point of view as it demands additional individual constructive decisions of the device of irregular support under these beams.

Problem statement

The purpose of this work is to develop and experimental study of a special method of concreting two stages of continuous three-span monolithic slab of reinforced concrete structure, which will create a prestress opposite to that which will occur during operation, structural parts of the structure solely from their own weight and manufacturing technology without other mechanical, electrothermal or electro thermomechanical pre-stressing measures.

Research methods

A set of complementary methods of theoretical and experimental research was used to solve the defined tasks and achieve the set goal:

– methods of system and comparative analysis in the development of the prototypes design of reinforced concrete slabs;

– experimental methods for studying the stress-strain state and load-bearing capacity in tests of preliminary self-stressed reinforced concrete slabs;

– methods of mathematical statistics in the analysis of the experimental studies results of preliminary self-stressed reinforced concrete slabs.

Basic material and results

To optimize and balance the level of the load-bearing capacity of the monolithic slab in steel reinforced concrete bent structures, it is proposed to use a two-stage method of installing a monolithic slab in the reinforced concrete floor.

During the first stage of concreting (see fig. 1, a), a monolithic concrete slab is arranged through the span. Usually, first of all, it is necessary to concrete medium spans as during operational loading they have a greater margin of bearing capacity (see fig. 1, c). The grips' width in the monolithic plate arrangement is adjusted according to the location of zero bending moments' points on the diagram of internal forces along the beam's length. It should be noted that the options for concreting grippers allow making these supports at the time of the second stage of concreting more rigid or hinged (so-called "imaginary hinges" are created). At this stage, the steel part of the section (steel beams or profiled sheet) in the concreting areas from the weight of freshly laid mortar bends down and thus causes other parts of the section steel part in the "free" spans to bend up.

After the concrete gains the design strength of the first stage, perform concreting of the floor and other parts. At this stage (see fig. 1, b), the concreting areas are bent downwards due to the weight of freshly laid concrete, thus forcing the sections of the concreting first stage (already reinforced concrete section) to bend upwards. At this stage, the deflections values in adjacent spans can be adjusted by steel and reinforced concrete sections' stiffness, as well as the supports sections' stiffness.

The expected resource-saving result of the developed monolithic slab installation method: it is possible to create preliminary stresses opposite to the operating stresses in the steel part of the floor section, located in the spans of the concreting second stage, and the monolithic reinforced concrete slab of the concreting first stage.

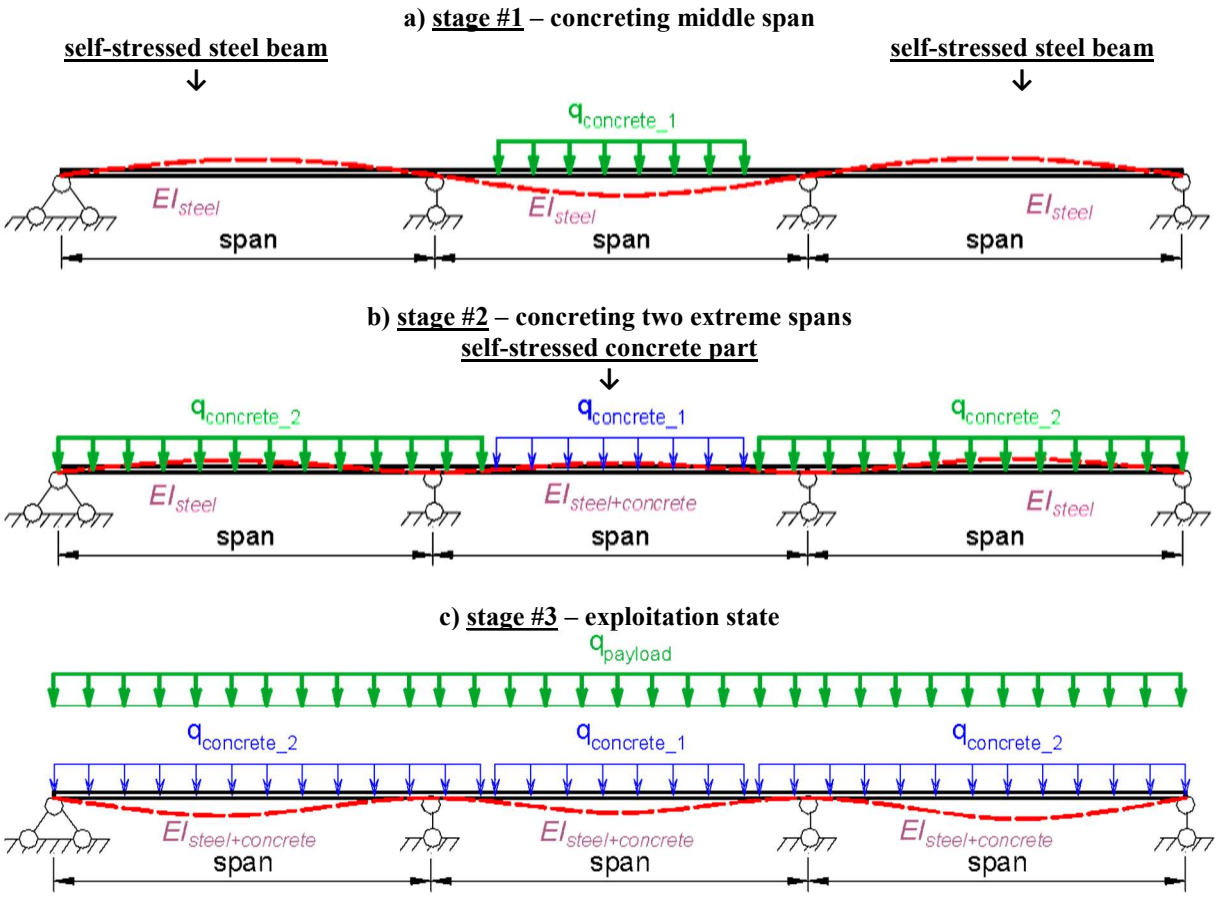

Figure 1 – The stages of the manufacturing preliminary self-stressed steel concrete slab

For experimental research of the offered technique of the monolithic plate installation, two samples of reinforced concrete continuous slabs were made on non-removable formwork from profiled steel sheeting, arranged according to a three-span scheme. Three spans lengths are equal: 1900-1900-1900 mm. Two test samples were made and tested in two stages. First, the middle span was concreted, and after the concrete strength of this design set, the extreme spans were concreted. The two samples differed in the grippers' width at the two concreting stages, as shown in Fig. 2-3.

The first experimental sample steel reinforced concrete slab is marked 1,7-2,3-1,7 CRCS 0,53×6,0 (see fig 2). For the first sample, the length of the section of the concreting first stage was equal to 2300 mm (see fig 2, b). This length comes out on 1/10 of the span outside the middle supports to the extreme spans. Accordingly, the length of the concreting second stage was 1700 mm (see fig 2, c). For this sample at the time of the concreting second stage, the middle supports were more rigid compared to the stiffness of the span parts of the outer spans' slab. That is the middle supports were relatively rigid.

The second experimental sample steel reinforced concrete slab is marked 2,1-1,5-2,1 CRCS 0,53×6,0 (see fig 3). For the second sample, the length of the section of the concreting first stage was equal to 1500 mm (see fig 3, b). This length comes in on 1/10 of the span to the middle span. Accordingly, the length of the concreting second stage was 2100 mm (see fig 3, c). For this sample at the time of the concreting second stage, the middle supports had the same stiffness as the stiffness of the span parts of the outer spans' plate. That is a "nominal hinge" was artificially created on the middle supports.

The overall size of the samples in the plan was 6,0×0,53 m. The external fixed formwork was profiled steel sheeting type К35-0,5 (here 35 is the height of the profiled steel sheeting in mm; 0.5 is the thickness of this profiled steel sheeting in mm). The height of the concrete shelf above the upper corrugation of the profiled flooring was 35 mm. Thus, the total height of plates was equal to 70 mm.

Reinforcement of the monolithic slab is made of rods with a diameter of 4 mm in the stretched zone of concrete in each wave of the profiled flooring (see Fig. 4, a). The yield strength of this rods steel equals 1300 MPa. For joint work of the profiled steel sheeting and a concrete slab used vertical anchors with a diameter of 4 mm and a length of 60 mm (see Fig. 3, a-b), installed in each wave of the profiled steel sheeting with a step of 100… 200 mm (see Fig. 4, b). The top of the adjacent waves' anchors was connected in the transverse direction by rods with a diameter of 4 mm and length of 500 mm.

First experimental sample <u>1,7-2,3-1,7 CRCS 0,53×6,0</u>

a)

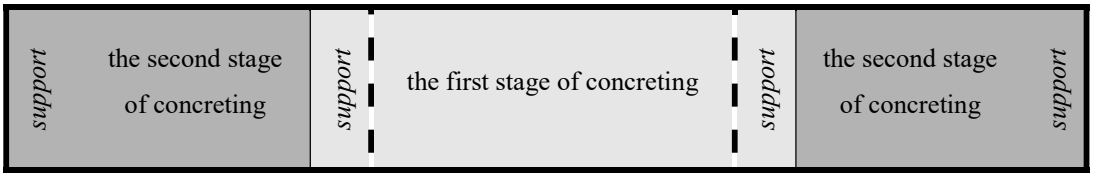

b)

c)

Figure 2 – First experimental sample of steel reinforced concrete three-span continuous slab on a non-removable formwork from a profiled steel sheeting:
a) scheme of grippers concreting samples; b) view of the sample after the first stage of concreting; c) view of the sample after the second stage of concreting

Second experimental sample <u>2,1-1,5-2,1 CRCS 0,53×6,0</u>

a)

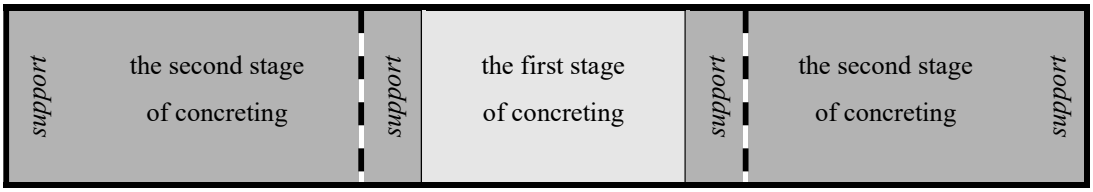

b)

c)

Figure 3 – First experimental sample of steel reinforced concrete three-span continuous slab on a non-removable formwork from a profiled steel sheeting:
a) scheme of grippers concreting samples; b) view of the sample after the first stage of concreting; c) view of the sample after the second stage of concreting

a)

b)

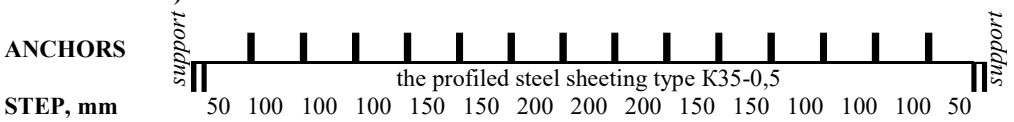

Figure 4 – Reinforcement of one monolithic slab span:
a) general view; b) the step of installing anchors in the lower wave of the profiled steel sheeting

Measuring instruments during the research were installed symmetrically, taking into account the possibility of duplication of different instruments readings at characteristic points, in areas with the most expected values of deformation, or areas of possible destruction. When the load reached 80% of the limit, devices that could be damaged were removed from the sample.

To measure the vertical deflections of the profiled steel sheeting during concreting from the own weight of freshly laid concrete mortar and during the experimental load, clock-type indicators IC-10 were used. Division price of indicators IC-10 equal 0.01 mm. Limit of displacement measurements of indicators IC-10 equal 10 mm. Figure 5 shows the layout of the indicators along the length of the samples.

Experimental samples loading of reinforced concrete slabs was carried out at the age of concrete for more than 28 days. Prior to the tests, the readiness of the test rig was tested: the correct position of the test structure, test loads of the structure check the correctness of the installation of devices and their ability to measure deformations, ease of loading structures, and ease of reading on measuring instruments, consistency of test crew members.

The loading was performed by artificial small-sized loads – ceramic hollow bricks (see Fig. 6). To determine the weight of the brick, a selective weighing was performed: 5 bricks out of each 50 bricks used (i.e. approximately 1/10 of the total number of bricks used for loading were weighed).

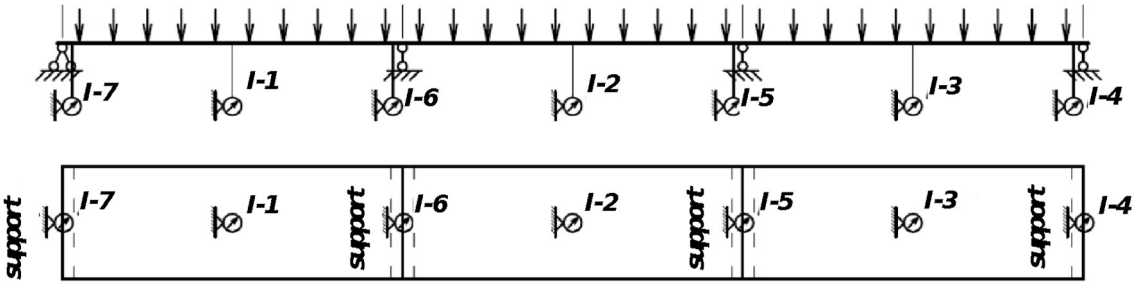

Figure 5 – Scheme of installation of clock-type indicators IC-10

Figure 6 – General view of steel reinforced concrete slab during loading with bricks

As a result of experimental studies of two samples of steel reinforced concrete slabs, a significant amount of information on their deformability and strength under different schemes of their loading is presented. The following are only the most characteristic results for each sample with a uniform length of loading.

According to the results of previously conducted separate studies of physical and mechanical characteristics of the materials used, it is established that the materials (steel and concrete) adopted for the manufacture of test samples have physical and mechanical properties characteristic of materials used in building design. The variability of concrete strength according to the results of tests of standard cubes, depending on the design class and group of samples was 8.05-21.4%; variability of steel strength was 2.7-4.7%.

Experimental studies of samples of steel reinforced concrete slabs were delayed in time, which is associated with the time of a concrete set of monolithic reinforced concrete slabs of design strength. Manufacturing, namely concreting of samples of reinforced concrete slabs, was performed in two stages (see fig. 2-3). Therefore, the total production time of samples of steel reinforced concrete slabs was about two months. In the manufacturing process at each stage of concreting were measured deflections in the characteristic cross sections of the sample by weight of freshly laid concrete mixture (see Fig. 5). Below is an analysis of the change in deflections along the length of the sample during the two stages of manufacture and the actual payload.

When loading only the profiled steel sheeting type K35-0,5 brick, deflections of the extreme spans of the plate were 3.8 times less than the deflections in the middle span.

For sample №1 with concreted middle supports in the first stage of production, the weight of the concrete mortar of the second stage (concreting of the extreme spans) did not affect the deflections of the middle span (see Fig 7). However, during the payload of this sample, the deflections were leveled in all three spans.

For sample №2 with non-concreted middle supports at the first stage of production, the weight of the concrete solution of the second stage (concreting of the extreme spans) equalized the deflections in all three spans (see Fig. 8). However, during the payload of this sample, the deflections of the extreme spans were 1.75 times greater than the deflections of the middle span.

Figures 7 and 8 show graphs of maximum deflections along the length of samples of steel reinforced concrete slabs at the end of the two stages of concreting and at maximum load with a small load – hollow ceramic brick.

As can be seen from these graphs of deflection changes, the arrangement of concreting of the first stage outside the middle supports allows to regulate the development of deflections in the extreme and middle spans and as a result, balances their values in order to simultaneously exhaust their load-bearing capacity. Due to the two-stage method of manufacturing steel reinforced concrete slabs, it is possible to change the stiffness of the sections in the manufacturing process and thus achieve optimal deflections along the length of the continuous structure.

The destruction of steel reinforced concrete slabs occurred suddenly as a result of cracks in the upper zone of concrete on the middle supports, in the area of maximum bending moment in the stretched area in the upper section fibers.

Thus, the used test method and the adopted measuring instruments and schemes of their placement allowed to obtain the necessary objective experimental data on the development of deformations and the nature of the destruction of the studied samples.

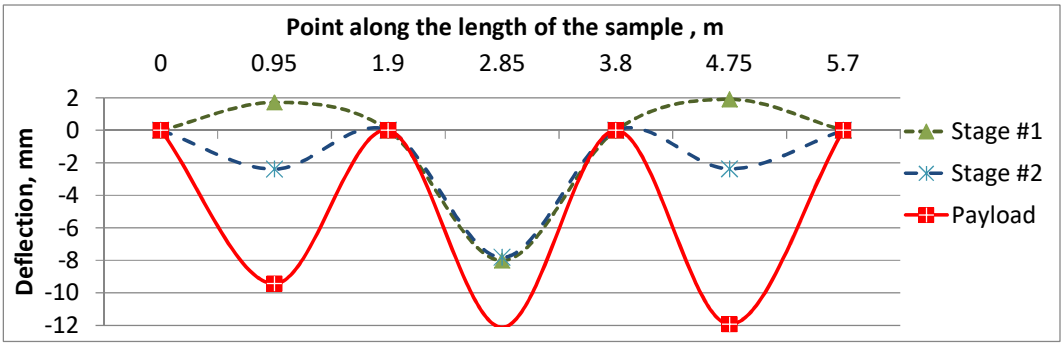

Figure 7 – Change of deflections along the length of the first sample 1,7-2,3-1,7 CRCS 0,53×6,0 at the end of two stages of concreting and at maximum payload

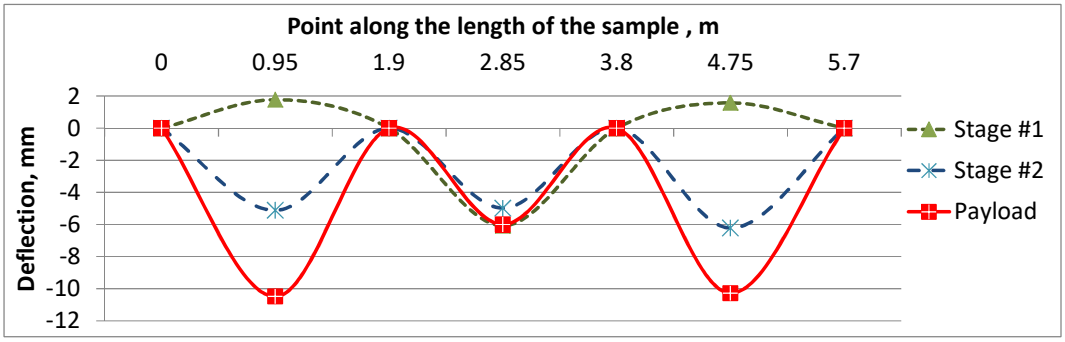

Figure 8 – Change of deflections along the length of the second sample 2,1-1,5-2,1 CRCS 0,53×6,0 at the end of two stages of concreting and at maximum payload

Conclusions

According to the results of tests of samples of reinforced concrete slabs to study the effect of the two-stage method of concreting monolithic slabs of reinforced concrete bent structures on the balance of the level of use of its load-bearing capacity, the following is:

– developed a two-stage method of concreting of continuous multi-span monolithic reinforced concrete slab on fixed formwork (the first stage – concreting of middle span; the second stage – concreting of extreme spans) allows to adjust deflections to balance the level of depletion in all bearing capacity of the slab;

– installation of concreting of the first stage (concreting of the middle span of the slab) outside the middle supports, allows to regulate the development of deflections in the extreme and middle spans by changing the stiffness of the cross section on the supports;

– the proposed method of uniform use of the bearing capacity of three spans can reduce deflections or increase the payload by 35%.

References

1. Гасенко А.В., Новицький О.П., Пенц В.Ф. (2021). Реконструкція багатоповерхових промислових будівель під доступне житло із використанням ресурсозберігувальних конструктивних рішень. *Вісник НУВГП, серія Технічні науки*, 2(94), 27-40 https://doi.org/10.31713/vt220214

2. Semko O.V., Hasenko A.V., Mahas N. N., Sirobaba V.O. (2018). Bearing Capacity and Deformability of Three-Component Steel Reinforced Concrete Constructions Made of Lightweight Concrete. *International Journal of Engineering & Technology,* 7(4.8), 53-57 https://doi.org/10.14419/ijet.v7i4.8.27213

3. Семко О.В., Гасенко А.В. (2006). Надійність стиснутих сталевих елементів з швелерів при корозійному зносі. *Металеві конструкції*, 11(3), 197-202

4. Semko O.V., Hasenko A.V. (2021). Classification of Self-stressed Steel-Concrete Composite Structures. *Lecture Notes in Civil Engineering,* 181, 367-374 https://doi.org/10.1007/978-3-030-85043-2_34

5. Arularasi V., Thamilselvi P., Avudaiappan S., Flores E.I.S., Amran M., Fediuk R., Vatin N., Karelina M. (2021). Rheological Behavior and Strength Characteristics of Cement Paste and Mortar with Fly Ash and GGBS Admixtures. *Sustainability*, 13(17). https://doi.org/10.3390/su13179600

6. Stelmakh S.A., Scherban E.M., Korobkin A.P., Tkacheva K.E., Osadchenko S.A., Kadrov A.A. (2018). Prescription and Technological Aspects of Manufacturing High-Quality Centrifuged Products and Structures from Heavy Concrete. *IOP Conf. Series: Materials Science and Engineering,* 905, 012060 https://doi:10.1088/1757-899X/905/1/012060

7. Чеканович О.М. (2013). *Напружено-деформований стан залізобетонних згинальних елементів, підсилених важільно-стрижневою системою* (дис. … канд. техн. наук), Сімферополь, Національна академія природокористування та курортного будівництва

8. Шагин А.Л., Избаш М.Ю., Шемет Р.Н. (2004). Оценка несущей способности двухпролетных сталежелезобетонных локально предварительно напряженных балок. *Науковий вісник будівництва*, 38, 81-89

9. Кінаш Р.І., Гладишев Г.М., Гладишев Д.Г. (1997). Розрахунок рами каркасу багатоповерхового будинку із неосьовою схемою ригелів. *Проблеми теорії і практики будівництва*, IV, 15-22

10. Storozhenko L., Yermolenko D., Gasii G. (2018). Investigation of the Deformation State of a Composite Cable Space Frame Structures with a Photogrammetric Method. *Intern. Journal of Engineering & Technology*, 7(3.2), 442-446 http://dx.doi.org/10.14419/ijet.v7i3.2.14568

11. Бібік Д.В., Семко О.В. (2010). Визначення внутрішніх зусиль у перерізі сталезалізобетонної балки з урахуванням стадійності виготовлення. *Строительство, материаловедение, машиностроение*, 56, 47-53

12. Storozhenko L., Gasii G. (2020). Experience and current issues of designing of steel and concrete composite structures of roof and floor systems. *Academic journal. Industrial Machine Building, Civil Engineering*, 2(55), 15-25 https://doi.org/10.26906/znp.2020.55.2337

13. Wright H.D., Evans H.R. & Harding P.W. (1987). The use of profiled steel sheeting in floor construction. *Journal of Constructional Steel Research*, 7(4), 279-295 https://doi.org/10.1016/0143-974X(87)90003-4

1. Hasenko A.V., Novytskyi O.P., Pents V.F. (2021). Reconstruction of multi-storey industrial buildings for affordable housing with the use of resource-saving design solutions. *Bulletin of NUVGP, series Technical Sciences*, 2(94), 27-40 https://doi.org/10.31713/vt220214

2. Semko O.V., Hasenko A.V., Mahas N. N., Sirobaba V.O. (2018). Bearing Capacity and Deformability of Three-Component Steel Reinforced Concrete Constructions Made of Lightweight Concrete. *International Journal of Engineering & Technology,* 7(4.8), 53-57 https://doi.org/10.14419/ijet.v7i4.8.27213

3. Semko O.V., Hasenko A.V. (2006). Reliability of compressed steel elements from channels at corrosion wear. *Metal structures*, 11(3), 197-202

4. Semko O.V., Hasenko A.V. (2021). Classification of Self-stressed Steel-Concrete Composite Structures. *Lecture Notes in Civil Engineering,* 181, 367-374 https://doi.org/10.1007/978-3-030-85043-2_34

5. Arularasi V., Thamilselvi P., Avudaiappan S., Flores E.I.S., Amran M., Fediuk R., Vatin N., Karelina M. (2021). Rheological Behavior and Strength Characteristics of Cement Paste and Mortar with Fly Ash and GGBS Admixtures. *Sustainability*, 13(17). https://doi.org/10.3390/su13179600

6. Stelmakh S.A., Scherban E.M., Korobkin A.P., Tkacheva K.E., Osadchenko S.A., Kadrov A.A. (2018). Prescription and Technological Aspects of Manufacturing High-Quality Centrifuged Products and Structures from Heavy Concrete. *IOP Conf. Series: Materials Science and Engineering,* 905, 012060 https://doi:10.1088/1757-899X/905/1/012060

7. Chekanovich O.M. (2013). *Stress-deformed state of reinforced concrete bending elements reinforced with a lever-rod system* (dis. … cand. tech. Sciences). Simferopol, National Academy of Nature Management and Resort Construction

8. Shagin A.L., Izbash M.Yu., Shemet R.N. (2004). Estimation of bearing capacity of two-span reinforced concrete locally pre-stressed beams. *Scientific Bulletin of Construction*, 38, 81-89

9. Kinash R.I., Gladyshev G.M., Gladyshev D.G. (1997). Calculation of the frame of a multi-storey building with a non-axial scheme of crossbars. *Problems of construction theory and practice*, IV, 15-22

10. Storozhenko L., Yermolenko D., Gasii G. (2018). Investigation of the Deformation State of a Composite Cable Space Frame Structures with a Photogrammetric Method. *Intern. Journal of Engineering & Technology*, 7(3.2), 442-446 http://dx.doi.org/10.14419/ijet.v7i3.2.14568

11. Bibik D.V., Semko O.V. (2010). Determination of internal forces in the section of reinforced concrete beam taking into account the stages of manufacture. *Construction, materials science, mechanical engineering*, 5647-53

12. Storozhenko L., Gasii G. (2020). Experience and current issues of designing of steel and concrete composite structures of roof and floor systems. *Academic journal. Industrial Machine Building, Civil Engineering*, 2(55), 15-25 https://doi.org/10.26906/znp.2020.55.2337

13. Wright H.D., Evans H.R. & Harding P.W. (1987). The use of profiled steel sheeting in floor construction. *Journal of Constructional Steel Research*, 7(4), 279-295 https://doi.org/10.1016/0143-974X(87)90003-4

CONTENTS

ЗМІСТ